The Functional Morphology of the Primate Zygomatic Arch

In Relation to Diet

by

Hallie Margaret Edmonds

A Dissertation Presented in Partial Fulfillment
of the Requirements for the Degree
Doctor of Philosophy

Approved June 2017 by the
Graduate Supervisory Committee:

Kaye Reed, Chair
Gary Schwartz
Chris Vinyard

ARIZONA STATE UNIVERSITY

August 2017

ABSTRACT

Craniofacial morphology in primates can vary on the basis of their diet because foods are often disparate in the amount and duration of force required to break them down. Therefore diet has the potential to exercise considerable selective pressure on the morphology of the masticatory system. The zygomatic arch is a known site of relatively high masticatory strain and yet the relationship between arch form and load type is relatively unknown in primates. While the relative position and robusticity of the arch is considered a key indicator of craniofacial adaptations to a mechanically challenging diet and central to efforts to infer diet in past species, the relationships between morphology and diet type in this feature are not well established. This study tested hypotheses using two diet categorizations: total consumption percent and food material properties (FMPs). The first hypothesis that cortical bone area (CA) and section moduli (bone strength) are positively correlated with masticatory loading tests whether CA and moduli measures were greatest anteriorly and decreased posteriorly along the arch. The results found these measures adhered to this predicted pattern in the majority of taxa. The second hypothesis examines complexity in the zygomaticotemporal suture as a function of dietary loading differences by calculating fractal dimensions as indices of complexity. No predictable pattern was found linking sutural complexity and diet in this primate sample, though hard object consumers possessed the most complex sutures. Lastly, cross-sectional geometric properties were measured to investigate whether bending and torsional resistance and cross-sectional shape are related to differences in masticatory loading. The highest measures of mechanical resistance tracked with areas of greatest strain in the majority of taxa. Cross-sectional shape differences do appear to reflect dietary differences. FMPs

were not correlated with cross-sectional variables, however pairwise comparisons suggest taxa that ingest foods of greater stiffness experience relatively larger measures of bending and torsional resistance. This study reveals that internal and external morphological factors vary across the arch and in conjunction with diet in primates. These findings underscore the importance of incorporating these mechanical differences in models of zygomatic arch mechanical behavior and primate craniofacial biomechanics.

DEDICATION

For my parents, Dr. Charles Edmonds and Mary Beth Edmonds, who taught me to always do the best that I can, and to “keep at it” no matter what.

ACKNOWLEDGMENTS

This dissertation would not have been possible without the support from my parents, friends, and colleagues. First and foremost, I would like to thank my committee members Gary Schwartz and Chris Vinyard for their time, training, and feedback and especially to my advisor and chair, Kaye Reed. Thank you for taking me on as a student, guiding me, and providing me with so much support.

I was fortunate to be able to use primate μCT scans provided by Chris Vinyard at NEOMED (NSF grant: BCS-0959438) and by Lynn Lucas and Lynn Copes at ASU. I sincerely thank these individuals for being so generous as to allow me to use these resources for my data collection. Thank you also to Chris Vinyard for allowing me to spend a summer at NEOMED to learn the ins - and - outs of 3D data visualization and data collection and for providing me the training that made this dissertation possible. The Elizabeth H. Harmon Research Endowment, SHESC Graduate Fellowship, and SHESC Research Grant provided funding for this project. Thank you also to Gary Schwartz and the SHESC Visualization Lab for allowing me to use the lab as my data collection headquarters.

I've had the pleasure of working with a host of wonderful graduate colleagues over the years and I thank them sincerely for making graduate school such a rich experience. Thank you to graduate students of both the past: Lynn Copes, Lynn Lucas, Theirra Nalley, Terry Ritzman, Laura Stroik, Amy Shapiro, Sam Russak, and present: Genevieve Housman, Neysa Gryder-Potter, Amanda McGrosky, Ignacio Lazagabaster, Irene Smail, Ellis Locke, & John Rowan for providing me help, support, and many laughs along the way. To my officemates, thank you for your patience, expertise, and many

hours of chit-chatting to help make grad school more enjoyable; thank you Lynn Lucas and Halszka Glowacka. To my cohort of wonderful, supportive people, I appreciate your support more than you probably know: thank you Halszka, E. Susanne Daly, Maria Nieves-Colón, and Kathleen Paul.

Outside of school I was fortunate to have an army of wonderful friends, near and far, who supported me every step of the way. To Mary Valderhaug and Krista Zegura, thank you for always believing I could do this, and for the years and years of constant encouragement. You are two of my greatest friends, and I cannot thank you enough. To the dynamic dancing duo, Lisa (Juliet) Hill and Andrea Alden, thank you for your support in and out of the studio; you are two of the most fantastic people I know. To BFF, my home away from home and purveyor of so many wonderful people and memories, thank you to all my fellow dance and fitness enthusiasts for your unbridled support and encouragement: Candace Johnson, Lisa Hunter, Holly Faeth, Mar Mancha, Bryn Chafin, Meg Mercanti, Danielle Hensley, Becca McCarthy, Callie Alden, Tamsin Foucrier, Tamara Huth, Gina Waters, Heeyoung Lee, Michaela Bloom and many more!
To my Uncle Randy Armenta, Aunt Barb Armenta, and Aunt Glee McCauley, thank you for your endless support and encouragement through the years. To my parents, thank you for giving me the support to pursue this degree; you are my heroes and I dedicate this work to you. Finally, a thank you to my two steadfast companions, Huxley and Shivapithecat, for the countless hours of "assistance" rendered during the writing of this dissertation.

TABLE OF CONTENTS

Page

CHAPTER Page

LIST OF TABLES

Table Page

LIST OF FIGURES

Figure Page

Figure Page

Figure Page

CHAPTER 1: INTRODUCTION

Craniofacial morphology in primates can vary on the basis of their diet because foods are often disparate in the amount and duration of force required to break them down. As a group, primates have significant dietary variability as compared to other mammals and the differences in primate masticatory complexes are hypothesized to map onto variances in food acquisition and processing (Bouvier and Hylander, 1982; Beecher et al., 1983; Anapol and Lee, 1994; Constantino, 2007; Yamashita et al., 2008a;b). As an integrated complex, the different parts of the face must co-exist in a relatively constrained space within the skull, while meeting all of the mechanical demands imposed by mastication (Kay, 1975; Constantino, 2007; Lucas et al., 2008). These mechanical demands span a broad range: from material properties of foods, to frequency and force of muscle activation and gape, to overall skull form and robusticity. Ultimately, these spatial and biomechanical constraints on bony morphology must be balanced against muscle orientation and efficient bite force production to enable efficient chewing performance and avoid tooth/bone failure or dislocation of the temporomandibular joint (Greaves, 1985; Spencer, 1995; 1999). Internally, the density and composition of facial bones are expected to vary in predictable ways according to the types of forces passing through them, just as cross-sectional shape and overall morphological form is predicted to be influenced by the types of loads experienced to maintain structural integrity and avoid failure. While the relationships between masticatory loading and bone response is central to our efforts to infer diet and dietary adaptation in extinct species, the relationships between diet type and a key masticatory feature of craniofacial complex, the

zygomatic arch, is not well established even though this feature is continually invoked as a hallmark of adaptation to a mechanically resistant diet.

Current understandings of craniofacial adaptation in relation to feeding derive from the creation of testable hypotheses from mechanical models and the rigorous testing of those questions using comprehensive, comparative studies. Food consumption is a combination of the muscular activation necessary to generate bite forces at a particular point along the tooth row and the subsequent repeated chewing bouts necessary to fully ingest the object; therefore, an attachment site for a major masticatory muscle is expected to experience varying magnitudes of loading in accordance with the food being processed because of the habitual nature of chewing. This study evaluates new data on bone cross-sectional properties and mechanical behavior in conjunction with primate dietary data to test specific hypotheses about the nature of interplay between zygomatic arch morphology, a feature which serves to anchor the masseter muscle, in relation to diet within an evolutionary context.

One of the most highly strained regions of the skull is the zygomatic arch, a bilaterally present bone feature comprised of the temporal process of the zygomatic bone and the zygomatic process of the temporal bone. The zygomatic arch serves as the attachment for the deep and superficial masseter muscles, which function as primary jaw adductor muscles. Geometrically, the arch resembles a beam with two fixed ends that is subjected to varying degrees of tension, compression, and shear as well as combinatory loading that includes parasagittal bending and torsion. Some of the earliest work on zygomatic arch mechanics centered on *in vivo* strain data collection at three discrete points along the zygomatic arch using strain gauges (Hylander and Johnson, 1997).

Importantly, these initial findings revealed that strain was not uniform along the zygomatic arch in that anterior sections (presumably due to the attachment of the masseter muscles) experienced relatively higher strain magnitudes than posterior portions. Within the fossil record, the relative positioning and robusticity of the arches have been interpreted as clear signals of adaptation to the consumption of mechanically resistant (i.e., hard and/or tough) foods, however the relationship between dietary loading and bone morphology in this region is not clear. Beyond the gross, observational level of arch form in terms of relative positioning on the skull and its relative robusticity, the nature of bone loading and response in terms of internal architecture and external shape is not clear in primates. Studies have suggested a link between zygomatic arch form and masticatory loading but have rarely tested the nature of this link in primates (but see Iwasaki, 1989; Hylander and Johnson, 1997).

With the use of micro-computed tomography (μCT) scans of primate skulls from a broad taxonomic sample of primates, this study investigated whether zygomatic arch morphology, in terms of internal architecture and cross-sectional form, reflected known strain patterns and if zygomaticotemporal sutural complexity varied in accordance with diet type. These comparisons were performed intraspecifically, interspecifically, and by diet type. By tracking how biomechanically relevant variables of bone structure change along the arch, this study tests whether the arch is uniformly constructed, which provides a solid foundation for a more complete understanding of arch morphology in relation to loading.

Research that studied the plasticity of this region in model organisms such as pigs (*Sus scrofa* Franks et al., 2016) and rabbits (*Oryctolagus cuniculus* Franks et al., 2016)

determined that animals fed strictly hard or soft diets resulted in differences in bone density and remodeling rates. This has been extended to experimental studies on primates, such as baboons (Corruccini and Beecher, 1984), squirrel monkeys (Bouvier and Hylander, 1982; Corruccini and Beecher, 1982; Beecher et al., 1983), and macaques (Iwaksai, 1989), in which feeding on hard objects was found to increase bone density compared to individuals who consumed soft foods. This finding suggests a greater frequency of remodeling events or possibly greater osteogenesis per event; resulting in greater bone growth and maintenance in individuals fed hard diets, as compared to those fed only soft foods (Bouvier and Hylander, 1981; Lieberman et al., 2004) and supports the assumed link between diet type and craniofacial morphology. My study tests the hypothesis that differences in diet type (and therefore differences in force magnitudes) translate into differences in zygomatic arch bone morphology by calculating a series of biomechanically relevant variables that quantify bone response to loading and comparing those values among taxa of different dietary groups. The expectation is that taxa that primarily consume hard and/or tough foods should have relatively greater measures of bone subperiosteal area, cortical area, and increased resistance to bending and torsional forces compared to taxa that consume soft or exudate foods.

Furthermore, this study examines whether measures of bone cross-sectional properties match existing *in vivo* strain distributions, and whether the extent to which these properties pattern relates to differences in diet type in a taxonomically diverse primate sample. These properties include measures of total area and cortical area, in which relatively large amounts of cortical area are expected to deposit in areas of increased loading, as well as measures of section moduli (bone strength), resistance to

bending and torsional forces, and bone cross-sectional shape. This study also quantifies the complexity of the single suture on the arch, the zygomaticotemporal suture, within the context of arch mechanics and it's biomechanical relevance to models of zygomatic arch functional morphology. Each part is tested within the context of primate diet type as defined by total consumption percent of a particular food item and food material properties (FMPs) data. To test these questions, this study is divided into three separate, but logically connected, hypotheses and results.

A comprehensive review of the vast literature and existing experimental work pertaining to craniofacial form and function is synthesized and presented in Chapter 2. Chapter 3 focuses on the quantification and comparison of zygomatic arch cross-sectional total area, cortical area, and section moduli (bone strength) measures in the study sample in relation to diet. In Chapter 4 the hypothesis that zygomaticotemporal sutural complexity tracks with diet type is tested using cross-sectional images of the zygomatic arch at the suture midpoint and two different dietary schemes. Chapter 5 provides the results of the third hypothesis, which examines cross-sectional shape and resistance to bending and torsional forces throughout the zygomatic arch. Chapter 6 describes and summarizes the important results, discusses the importance of the work to feeding biomechanics and primate craniofacial adaptation and offers possibilities for future research.

CHAPTER 2: BACKGROUND

Numerous lines of research suggest that significant selection pressures deriving from the necessity of efficiently process dietary items have shaped craniofacial morphology in the primate lineage. With regard to studying the effects of diet type on craniofacial morphology, research has often examined features such as the teeth and mandible to understand the complex interplay of masticatory loading and bone response. Yet the zygomatic arch, which is functionally linked to the mandible via the masseter muscle, and whose activation powers chewing bouts, remains a relatively understudied, yet highly relevant masticatory feature. This study examines the functional morphology of the primate zygomatic arch from the perspective of internal architecture, sutural complexity, and external cross-sectional shape to determine whether the arch's bony morphology reflects experimentally obtained strain measures as they pertain to dietary loading, as well as the relationship between bone morphology and differences in diet type.

EXPERIMENTAL RESEARCH

First models of masticatory performance

Models of masticatory performance can generally be divided into two main types. The first approach examines questions regarding force generation (Bakke and Michler, 1991; Antón, 1994:1999; Christiansen and Wroe, 2007; Clausen et al., 2008; Lucas, 2012) in which studies focus on quantifying the amount of force produced at a given point (e.g. bite force) within the oral cavity. Identifying loads at different locations indicates how much force one area of bone experiences relative to another, and helps trace patterns of high versus low force areas within the craniofacial complex.

The second type of model examines stress resistance; which examines the potential for the bone or bony feature to resist forces (Bouvier and Hylander, 1996; Bright and Gröning, 2011; Chalk et al., 2011; Lucas, 2012). These studies rely on measuring bone surface strain and estimating stress to explain how bone structure and its properties react to an applied load (Endo, 1965, 1973; Herring and Mucci, 1991; Spencer, 1995; Herring and Teng, 2000; Herring et al., 2005; Lucas, 2012) which in turn aid in the interpretation of the potential adaptive value of the feature. This second type of research has been conducted on many non-human primates and comprises a large amount of the literature on this topic (Bouvier and Hylander, 1981,1994; Hylander, 1984, 1986; Rubin, 1984; Herring and Mucci, 1991; Hylander and Johnson, 1992,1997; Spencer, 1995; Liu and Herring, 2000; Mulder et al., 2007; Koyabu and Endo, 2009).

Generally speaking, many studies do not subscribe to only one of these perspectives, but instead employ a combination of both (e.g., Picq and Hylander, 1989; Oberheim and Mao, 2002; Ravosa, 2000; Preuschoft and Witzel, 2005; Ravosa et al., 2009). Historically, some of the first studies on skull morphology assumed that any given force that contacted bone would spread evenly across its surface (Endo, 1966). Based on this premise, all parts of the skull were expected to be uniform in their bone density. Later experimental work revealed that this is not the case, but rather that there are areas of the facial skeleton that have relatively more bone present than the rest of the skull, suggesting that forces are distributed unevenly in these areas (Endo, 1966; Hylander et al., 1991; Hylander and Johnson, 1992, 1997) and that the skull is therefore not a homogenous structure.

The first model examining facial architecture in relation to masticatory force resistance came from Görke in 1904. His work envisioned the face being constructed from three vertical columns (Fig. 1). According to this model, facial strains increased as the bite point moved anteriorly; thus biting on the anterior teeth (with the accompanying high strains) would be resisted by the midline vertical column that passed through the nasal aperture and between the orbits (Görke, 1904; Endo, 1965,1966). The two remaining lateral columns would resist biting on the posterior teeth. This arrangement of the two lateral columns was used to explain why the inferior portions of the zygomatic arch were denser as a means to resist the forces of the masseter muscle during mastication.

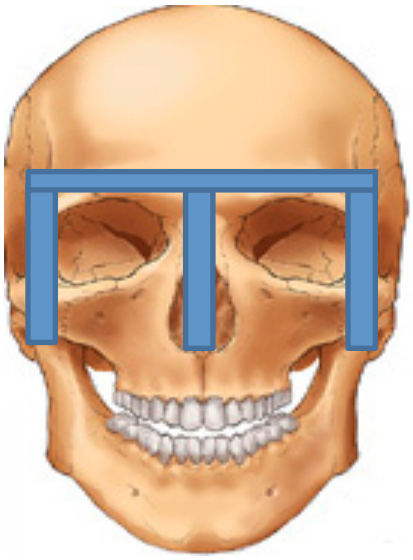

Fig. 1 Görke's model of facial architecture. Figure adapted from Endo, 1966.

In the following decades of research more models emerged. Among these was Richter's (1920) "watchtower model" (Fig. 2) which elaborated on Görke's model by incorporating additional horizontal beams in the supraorbital torus and alveolar margin that connected these beams with a series of struts (Richter, 1920; Endo, 1966). This organization creates a frame structure composed of additional horizontal and diagonal beams; features Görke's model did not include.

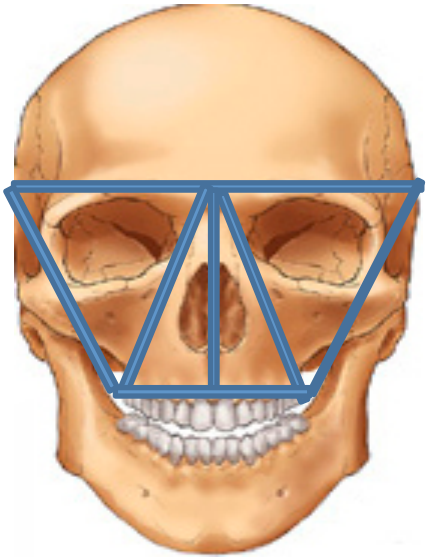

Fig. 2 Richter's model of facial architecture. Figure adapted from Endo, 1966.

Bluntschli (1926) proposed a model that incorporated pillars for support in the face. In this model, three paired struts originate from the alveolus and extend to the rest of the face while a single column resides in the midline of the face (Endo, 1966). Horizontal struts would then pass across these paired struts in the region of the lateral orbital margin, zygomatic arch, and infraorbital margin. However, this model was not well supported by empirical evidence and was eventually disregarded (Endo, 1966).

These early models were mainly theoretical and lacked experimental validation. In later decades, experimental work showed that these models did not accurately account for how the facial skeleton was dispersing or resisting forces (Benninghoff, 1925; Endo, 1966). Several decades later, Endo (1966, 1972) like Richter, proposed that the facial skeleton was best characterized as a frame, based on *in vitro* strain gauge analyses taken from gorilla and human skulls (Fig. 3). As in previous models, Endo characterized the alveolar region and supraorbital torus as a pair of parallel beams. In Endo's model, the masticatory muscles exert an inferior, vertical pull the face while the bite point exerts a superior and medial pull on the face. When combined, these produce compressive forces in the facial skeleton (Endo, 1966).

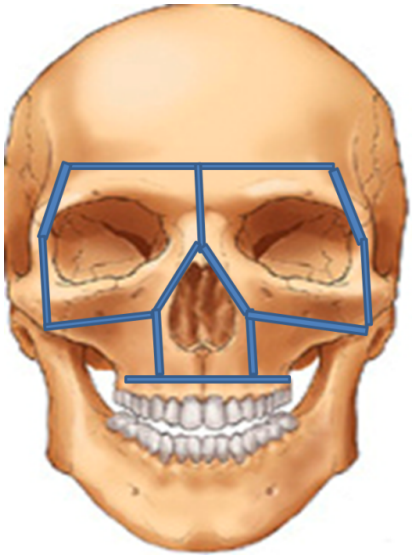

Fig. 3 Endo's 'rigid frame' model. Figure adapted from Endo, 1966.

These early ideas illustrate how difficult it is to model the distribution of stresses and stress resistance across the face because it is a complex anatomical region comprised of many fused parts. During these early years, empirical data were not available and

these types of models were constructed primarily from x-ray photographs (Endo, 1966). Current models continue to acknowledge that part of the difficulty in rendering accurate depictions derives from the variety of stresses encountered and the complex architecture of the bony features that comprise the face (Endo, 1973; Hylander and Johnson, 1992; Christianson and Wroe, 2007; Curtis, 2011).

Traditionally, denser and thicker areas of bone were associated with locations of high stress because bone mass tends to increase in the presence of higher loads (Görke, 1904; Bluntschli, 1926; Roberts and Tattersall, 1974). Early work in masticatory mechanics assumed that the skull experienced uniform and high levels of loading during mastication (Hylander and Johnson, 1997). Under this assumption all the bones of the facial skeleton should be equally optimized to resist strain caused by mastication (Hylander et al., 1991; Hylander and Johnson, 1997). However, this is not the observed trend throughout the skull. Masticatory strain varies in magnitude and depends on the types of foods consumed (Bouvier and Hylander, 1981, 1982; Daegling, 1993; Wright, 2005; Constantino, 2007). Because of this amount of variation, it is unlikely that all bones of the face are optimized solely for resisting chewing forces (Hylander et al., 1991, 1997) or that all diet types produce the same levels of bone density.

Facial loading

Banri Endo performed some of the earliest work that experimentally tested the nature of stress (force per unit area experienced by a material) and strain (amount of deformation experienced by a material) as they are produced during mastication (Endo, 1965, 1966). Using an apparatus meant to mimic the loading conditions of mastication,

he determined that facial strains shifted according to the location of the bite point (Endo, 1965). The axis of the principal strains (which represent the maximum and minimum stretches of a volume) appeared to be dependent on the location of the bite point. The highest principal strains were also found in areas closest to the bite point (e.g., portion of the maxilla closest to the loaded tooth, origin site of the masseter on the zygomatic arch and infero-lateral aspect of the orbit) (Endo, 1965). Throughout a chewing cycle, the bite point will move throughout the mouth and therefore subject the facial skeleton to a range of different principal strains depending on the location of the bite point and the resulting bite forces that are generated (Endo, 1965).

In addition, different facial features are subjected to varying force magnitudes that consequently leads them to undergo some form of loading (Endo, 1965). The post-orbital septum and zygomatic arch undergo parasagittal bending, shear (two materials pushing in opposite directions of one another) and torsional (twisting) forces (Hylander, 1986; Hylander et al., 1991; Herring et al., 1996; Ross, 2001; Lieberman et al., 2004) whereas the mandibular corpus is subjected to lateral transverse bending (wishboning), in addition to parasagittal bending and torsion (Hylander 1979, 1985, 1988; Daegling and Hylander, 1997; Lieberman et al., 2004). It is these load types (i.e., bending, torsion, and shear), which contribute primarily to models of facial loading during mastication (Ross, 2001; Lieberman et al., 2004), as they generally constitute the dominant loading regimes. In contrast to the high force zones observed in the post-orbital septum and zygomatic arch, the portions of the mid (region from the inferior part of the maxilla to the inferior portion of the orbits) and upper face (portion superior to the base of the orbit) experience relatively lower magnitude forces and do not appear to possess any consistent patterns of

high force like those observed in the lower portion of the face (Hylander et al., 1991; Hylander and Johnson, 1992, 1997; Lieberman et al., 2004).

One of the continuing problems that require addressing within comparative cranial biomechanics is how to identify the relationships between primate facial morphology and site-specific strain distributions. The majority of primate studies examining craniofacial stress and strain have focused on groups of anthropoid primates and have shown that a steep strain gradient exists from the lower part of the face (at the level of the occlusal plane) towards the mid and upperface (Hylander et al., 1991; Hylander and Johnson, 1992; Ross and Hylander, 1996; Ross and Metzger, 2004; Lieberman et al., 2004). However, the nature of the relationship between stress and strain profiles and the morphology of the facial skeleton continues to challenge researchers particularly in the context of dietary evolution. Furthermore, the biological architecture and functionality of specific and highly strained bone regions, such as the zygomatic arch, continue to challenge existing models of craniofacial performance. While the craniofacial complex is often discussed as a single functional unit, it is composed of 27 different bony parts that are different shapes and consequently subjected to varying force magnitudes. The space of the skull is finite which requires all of the parts to fit together in a functionally efficient and, ultimately, adaptive way.

Bone response to loading

Teeth and associated cranial fragments are some of the most commonly preserved skeletal elements preserved in the fossil record and reveal important information about the individual to which they belonged (Kay, 1975; Lucas et al., 1985; Lucas et al., 1986;

Teaford and Ungar, 2000; Lucas, 2004). While teeth offer some of the most direct evidence of diet, other parts of the cranium also are impacted by feeding behavior and can offer valuable insight into the diet mechanics of that individual. These major functional parts include the muscle attachment sites for the major masticatory muscles and specific bony areas that experience high amounts of loading as a result of feeding. During a given feeding episode, muscle recruitment patterns and resulting force potentials will cause the underlying cranial bone to react differently depending on how those forces are directed through the cranium (Mulder et al., 2007). Ultimately, the goal is to model these factors so that predictions can be made about how forces are generated, how they dissipated, and how the morphology responds. One way to accomplish this is through biomechanical models.

There are two major components that are necessary in the creation of a biomechanical model for some element of the body. First, there is a theoretical model that describes how a system operates under experimental conditions and secondly there is a mechanical model, which is usually simple, and is developed to capture how this system works in reality. In biology, mechanical models are useful because they can simplify a complicated system in terms of basic physics. However, caution should be exercised when it comes to relying on a model to explain all aspects of a biological system. A model can only be as accurate as the number of variables it can capture and accurately characterize. Typically, models are created based on some predictions grounded in a theoretical framework. To determine whether the model accurately captures the workings of the system it wants to describe, it must be accompanied by rigorous empirical testing.

In terms of biomechanical models, bone is a difficult material to model (Strait et al., 2008). The elastic properties of bone vary from area to area on the skull, making it difficult to construct a single model that subsumes all parts of the skull (Peterson and Dechow, 2003; Wang and Dechow, 2006; Strait et al., 2008). An example of this is the supraorbital torus versus the postorbital bar in macaques. The latter is about 51% stiffer (resistant to bending) than the former, indicating differences in the mechanical properties of adjacent cranial features. In general, bone is also anisotropic, meaning that its' materials are arranged in different directions (Strait et al., 2008). However, the craniofacial complex has many areas that are orthotropic, that is, wherein the bone has each of its three axes exhibiting its own material properties (Strait et al., 2008). The shape of the bone exerts a considerable influence on the orientation of the axes and complicates the construction of the model (Lanyon and Rubin, 1984; Antón, 1994; Bouvier and Hylander, 1996; Wang and Dechow, 2006; Strait et al., 2008). In previous studies that have examined the orientation of the axes in cortical bone, two of the three axes are parallel to the surface whereas the third is normal to the surface (Strait et al., 2008). However, much of the bone in the skull is curved which causes the axes to vary depending on the degree of curvature. This is an important consideration when trying to formulate a mechanical model of the skull.

One of the most well-known feeding models comes from Greaves (1985) who modeled the skull as a simple cylinder that twists along a 45 degree axis during feeding (Ross, 2009). This model hypothesizes that the global strains produced by mastication will affect the local environment of the circumorbital region (specifically the postorbital bar) (Ross, 2009). This model has received mixed support given Hylander et al. (1991)

found no support for the skull twisting like a cylinder. Ross and Hylander (1996) also examined the strain measures in the circumorbital region of *Aotus* but found that there was no consistent support for the skull twisting like a cylinder (Ross, 2001, 2009). *Otolemur* appeared to have some twisting in the postorbital region, suggesting further investigation of other strepsirrhines was required to determine if this was consistent throughout the clade. To further test whether haplorhines and strepsirrhines exhibit clade specific patterns, additional haplorhine (*Papio, Aotus* and *Macaca*) and strepsirrhine (*Eulemur*) specimens were measured. The skull of *Eulemur* did not act like a twisting cylinder, thus providing no support for a strepshirrhine specific pattern. Instead, *Eulemur's* pattern of strain actually resembled those of *Macaca, Papio* and *Aotus* (Ross, 2009). Based on these results, there appears to be some degree of twisting of the braincase relative to the facial skeleton in these primate taxa, which is consistent with findings in previous works (Ravosa et al., 2000a; Ross, 2001; 2009). This twisting is affecting the loading regime of the postorbital bar, but differences in the bar's geometry produce varying amounts of strain (Ross, 2001; 2009).

Hylander & Johnson (1992) measured strain along the postorbital bar of macaques to determine the strain environment during feeding bouts on various food types. They found that strain levels on the postorbital bar were intermediate between the dorsal interorbital area and the zygomatic arch. The amount of strain experienced was not equivalent bilaterally because the relative amount of muscle activation (i.e., the levels of masseter and temporalis recruitment) depends on whether the muscles are on the working (chewing side) or balancing (non-chewing side) of the skull. Therefore, the strain relationships were different between the working and balancing sides of the skull.

This is significant for the circumorbital region; especially for a feature like the anterior root of the zygomatic arch because it serves as the attachment point for the powerful masseter muscle (Hylander and Johnson, 1997; Rafferty et al., 2000; Witzel et al., 2004; Kupczik et al., 2007). Specifically, the high strains of the anterior portion of the zygomatic arch were higher on the working side than on the balancing side (Hylander & Johnson, 1992).

Masticatory strain

By definition, strain is a tissue property of bone and is a measure of the relative amount of deformation a material undergoes. Formally, this is calculated as the change in length divided by the original length (Nordin and Frankel, 2012). Mastication causes physiological deformations of the face as a result of a combination of forces produced by the muscles and teeth. Accurately mapping and measuring surface bone and sutural strains caused by mastication are key factors for assessing the mechanical environment of the skull (Bright and Gröning, 2011). One of the most common ways to study the masticatory system involves collecting *in vivo* or *in vitro* data to assess masticatory function during chewing (Hylander, 1986; Hylander et al., 1991; Daegling, 1993; Hylander and Johnson, 1997; Dechow and Hylander, 2000; Ravosa et al., 2000a; Vinyard et al., 2008). Both of these techniques rely on strain readings taken from strain gauges.

In vivo studies are valuable because they directly measure strains as they actively pass across the bone surface; however some researchers have raised questions about the ability of this technique to capture non-uniform strain distributions (Dumont et al., 2005; Wroe et al., 2007). *In vivo* is helpful because it allows live strain recordings to be taken,

however there are limits to how the gauges may be placed so as not impede the activity in the body part of interest. *In vitro* work is useful for testing hypotheses about strain patterns during biting and chewing but is limited because it cannot capture real masticatory behaviors as it is highly simulated (Rayfield, 2011). For instance, changes to the elastic properties of bone and tissues can occur as a result of preservation or from the process of being harvested from the individual. This is especially problematic for fossil taxa, as the precise material properties of the bone and the contribution of soft tissue cannot be known (Rayfield, 2011). Also, the rates at which the bone and tissue are loaded must be taken into account (Wang et al., 2008). Strain gauges can be problematic because there is a limit to the number that can be applied in a given space and they can be difficult to apply (Dumont et al., 2005; Rayfield, 2007; Wroe et al., 2007). As long as appropriate measures are taken to adjust for these factors during an experiment, the results should remain accurate (Wang et al., 2008).

Initially, it was expected that all regions of the facial skeleton would experience similar amounts of strain. This expectation is founded in the notion that bone mass reacts to specific loads and is optimized to resist those loads (Bouvier and Hylander, 1981; Lanyon and Rubin, 1984; Hylander and Johnson, 1992). Specifically, this prediction stated that an increase in bone mass would be stimulated in the presence of high magnitude, cyclical loading, while decreased loading would result in reduced bone mass (Hylander and Johnson, 1992). A bone's response to loading has often been defined as a "functional adaptation" (Hylander and Johnson, 1992; Lanyon and Rubin, 1985) and is hypothesized to restrict bone strain magnitudes to a small range of values (also known as the optimal strain environment) (Lanyon and Rubin, 1985; Hylander & Johnson, 1992).

This assumption served as the basis for previous studies that operated under the expectation that the facial skeleton experienced uniform strain distributions. However, the available *in vivo* data suggest that there is a large degree of variation in the functional strain magnitudes throughout the facial skeleton (Hylander et al., 1991; Hylander and Johnson, 1992). Based on these observations, it is unlikely that all facial bones are specifically structured to maximize strength and minimize bone tissue (Hylander and Johnson, 1992).

While the mandible is expected to endure high masticatory forces because of its involvement in every chewing bout, the zygomatic arch is also found to consistently bear relatively high loads across primates. This is supported by the findings of previous work on primates such as chimpanzees (*Pan troglodytes*) and macaques (*Macaca fascicularis*) (Hylander, 1997; Ravosa et al., 2000a; Ross and Metzger, 2004; Wroe et al., 2007). The zygomatic arch has an increasing amount of stress towards its anterior portion related to the activation of the masseter muscle during chewing activity (Hylander 1997; Wroe et al 2007). During mastication, the working side zygomatic arch strains are larger anteriorly than posteriorly (Hylander and Johnson, 1992) which is presumably due to the attachment of the masseter muscles at the anterior portion of the arch, and which is responsible for the presence of relatively high strain magnitudes. In contrast to the zygomatic arch, which bears some of the highest strains of the face, the browridge region in some species of primates had much lower strains present overall despite being notably more robust in its bony morphology (Hylander and Johnson, 1992). Hylander (1992) has argued that an area with a greater concentration of bone does not necessarily correlate with experiencing large routine cyclical loads associated with mastication or incisal

biting. Alternatively, these areas that are fortified with more bone may be some type of adaption to resist structural failure due to relatively infrequent non-masticatory external loads (Hylander and Johnson, 1992). Based on the strain data, if all the bony areas of the face have been optimized to resist masticatory forces, then each region of the face should vary in the amount of bone it possesses (Hylander and Johnson, 1992). Because there is a wide range of variation in the magnitude of strains across different regions of the face, it is not likely that all the facial bones are structured to maximize their strength against masticatory loading with the lowest amount of bone possible.

Within the realm of primate craniofacial biomechanics, *in vivo* studies provide the foundation for current, comparative studies being done and are particularly relevant for matching real-time strain loading with the underlying bone morphology. For the purposes of the current study, previous *in vivo* work on the zygomatic arch in primates provided the basis for making predictions concerning if and how the arch's morphology tracked given the experimentally collected strain measures by Hylander and Johnson in a 1997 study. As noted previously, strain gauges collect strain measures in discrete locations, making total strain coverage of a structure more difficult to obtain. Thus, the current *in vivo* data available for the zygomatic arch stem from strain gauges placed at three points along the zygomatic arch corresponding to anterior, mid-zygomaticotemporal suture, and posterior regions (Hylander and Johnson, 1997). This provides an important baseline upon which to make predictions about the underlying bony morphology, but it leaves much of the arch's remaining structure unaccounted for. While this current study does not collect in vivo data, it does expand the number of regions along that arch that are

sampled and evaluated in the context of mechanical performance to determine whether significant variation exists in closely adjacent bone regions along the zygomatic arch.

Masticatory muscle anatomy and function

Testing hypotheses about the biomechanics of feeding requires a consideration of masticatory muscle morphology, orientation, and how each contributes to the system's overall efficiency (Adams, 1918; Taylor and Vinyard, 2008; Vinyard and Taylor, 2010). In the last few decades, the number of studies utilizing *in vivo* methods (e.g., Hylander, 1984, 1985; Hylander and Johnson, 1994, 1997; Ross and Hylander, 2000; Vinyard et al., 2005; Wall et al., 2006) have provided some of the best data on the ways primates recruit their masticatory muscles and how those recruitment patterns translate to internal loads that are resisted by the masticatory apparatus (Taylor and Vinyard, 2008).

The underlying musculoskeletal morphology plays an important role in the proficiency and performance of the system. Previous studies have investigated hypotheses concerning muscle positioning and the resulting mechanical advantage of the complex (Biegert, 1963; Hylander, 1975, 1979; Ravosa, 1990; Anapol and Lee, 1994; Spencer, 1999; Williams et al., 2002; Vinyard et al., 2003; Wright, 2005; Vinyard and Taylor, 2010). In general, mammals possess a masticatory muscle scheme comprised of the masseter, temporalis, and medial and lateral pterygoid muscles (Roberts and Tattersall, 1974; Greaves, 1995; Taylor and Vinyard, 2008; Ravosa et al., 2010). The superficial and deep masseter muscles, along with the temporalis muscle, power mastication through a coordinated series of actions, which function to adduct and retrude the mandible.

The superficial masseter, which originates on the inferior, medial border of the zygomatic arch, has a strong vertical force component that when contracted results in the jaw being adducted (Hylander et al., 2005). The muscle fibers pass inferiorly and anteriorly to eventually insert onto the ramus of the mandible. The deep masseter is located posteriorly and deep to the superficial masseter and attaches along the medial border of the zygomatic arch. It is also smaller than the superficial masseter and its fibers pass inferiorly and posteriorly which eventually insert onto the coronoid process of the mandible. The deep masseter has a more medial force component when it is activated during mastication, which results in adduction and transverse movement of the mandible (Hylander et al., 2005). The medial pull of the deep masseter also exerts shear forces on the zygomatic relative to the squamosal suture. From the lateral side of the arch, these shearing forces would appear as tensile forces as well (Herring and Mucci, 1991). In all, the masseter pulls the zygomatic bone anteriorly, inferiorly, and medially (Herring and Mucci, 1991).

Work on the masseter muscles of pigs found muscle fibers had varying orientations and that not all fibers are simultaneously recruited (Herring and Mucci, 1991). Instead, groups of muscle fibers are recruited which alter the fine action of the masseter, and other muscles, during mandibular movement (Herring et al., 1979; Herring and Mucci, 1991). These differences in muscle fiber recruitment should affect strain patterns on the zygomatic arch and other bones. The temporalis, the other important jaw adductor, originates on the temporal, frontal and sphenoid bones and sweeps inferiorly to pass between the medial portion of the zygomatic arch and the skull. The anterior muscle

fibers are more vertically oriented whereas the posterior fibers run more horizontally (Cachel, 1979; Ross, 1995; Vinyard and Taylor, 2010).

The amount of force a muscle can produce is dependent on several different factors. Internally, muscle force potentials are reliant on which motor units are firing and for how long they fire. An important mechanical aspect associated with muscle force includes the length of the moment arm of a muscle and its cross-sectional area (Hylander, 1975;Weijs and Hillen, 1985; Anapol et al., 2008). Internal fiber architecture is a critical factor that determines the ability of the muscle to produce force and excursion during contraction (Powell et al., 1984; Wall et al., 2008; Vinyard and Taylor, 2010). Within the muscle itself, the individual fibers and motor units are responsible for its regular functioning (Herring et al., 1989,1991; Vinyard et al., 2008). Muscle is highly organized and composed of a hierarchy of structures (Lieber and Friden, 2000). At the smallest scale of the hierarchy is the sarcomere, which is composed of small myofilaments known as actin and myosin (Taylor and Vinyard, 2008). The manner in which the thin actin and thicker myosin fibers cross one another enables the muscle to contract (Powell et al., 1984; Lieber and Friden, 2000; Taylor and Vinyard, 2008). Within a given muscle, the fiber composition can vary throughout; this variation can also extend across individuals and species (Vinyard et al., 2008).

The arrangement of the fibers is important because it affects the force-generating potential of a muscle (Lieber and Friden, 2000; Vinyard and Taylor, 2010). The fibers can run along the muscle in different ways and this can influence the physiological cross-sectional area of the muscle. Myofibrils, which are rod-shaped muscle units composed of long proteins, are arranged in parallel formations whereas sarcomeres are oriented

longitudinally (Taylor and Vinyard, 2008). The arrangement of the myofibrils dictates the distance a muscle fiber can travel and is a measure of its contraction velocity. Both fiber diameter and length affect the function of the muscle fiber. For instance, the shortening or lengthening of a muscle fiber is dictated by fiber length whereas fiber diameter modulates how much force can be produced (Taylor and Vinyard, 2008).

Parallel and pinnate fiber muscles have different functional capabilities, which are reflected in the actions of the muscles. Pinnation results in an increase in the number of fibers packed together and which affects the muscle's force potential (Antón, 1999). Pinnate muscle fibers tend to be relatively shorter in length and are oriented at an angle relative to the force-generating axis; thus enabling a larger number of fibers to be packed together (Vinyard and Taylor, 2010). When a greater number of serially arranged sarcomeres (functional units of contraction) are present, a muscle is capable of shortening, or lengthening over a greater distance (Williams and Goldspink, 1978; Taylor and Vinyard, 2008; Vinyard and Taylor, 2010). Based on this observed relationship, fiber length is proportional to muscle excursion, and as Vinyard and Taylor (2010) argue, also proportional to extension contraction velocity.

Muscle force

Accurate models of muscle activity depend on estimates of muscle force magnitude and direction (Antón, 1999). A muscle fiber's diameter and alignment, relative to the force-generating axis, influences the maximum force generated during muscle contraction (Vinyard and Taylor, 2010). Depending on the angle of orientation of the fiber to the force-generating axis, some force potential can be lost. However, in spite

of force loss the muscle can compensate by packing more fibers together in a given area and increasing the cross-sectional area of the muscle. The directions of these muscle fibers vary within a single muscle across all muscles in the body and across species (Taylor and Vinyard, 2008). Because of these differences in orientation, using muscle mass is not an accurate measure for the force potential a muscle can produce.

Using a simple muscle area measurement to approximate muscle force is not entirely accurate. An example formula for simple muscle area (Ikai and Fukunaga, 1968; Perry and Wall, 2008) is as follows:

$$\text{Area} = \text{muscle mass} / (\text{average fiber length} \times \text{muscle density}) \quad (1)$$

Typically, muscle mass has been employed as a major determinant of muscle force. However, this has been shown to be inaccurate (Perry and Wall, 2008). Much of the muscle's mass is composed of sarcomeres held within muscle fibers and any additional fiber length (which would increase the muscle area) does not confer any extra muscle force (Perry and Wall, 2008).

A more accurate means of quantifying a muscle's force potential is to measure its physiological cross-sectional area (PCSA). Using PCSA as a proxy for muscle force is an improvement over previous estimates that used only gross muscle mass or size (Perry and Wall, 2008; Taylor and Vinyard, 2008). The formula for calculating PCSA is as follows (Anapol and Barry, 1996; Antón, 1999; Lieber and Friden, 2000; Taylor and Vinyard, 2008; Eng et al., 2013):

$$\text{PCSA} = \text{Muscle mass (gm)} \times \cos\theta / l_f\,(\text{cm}) \times 1.0564\ \text{gm/cm}^3 \quad (2)$$

Here, muscle mass in grams and the angle of pinnation, (θ), is the angle measured between the fiber orientation and line of action of the muscle (Anapol and Barry, 1996).

l_f is the fiber length and 1.0564 gm/cm^3 is the specific density of muscle (Murphy and Beardsley, 1974). The PCSA of a given muscle is a measure of the cross-sectional area of the fibers that compose the muscle and is thus proportional to the maximum force a muscle can generate (Powell et al., 1984; Antón, 1999). Muscles with greater PCSA are predicted to be relatively larger than those with smaller cross-sectional areas and exert greater amounts of force during muscle contraction.

For estimates of the superficial masseter muscle, the longest fibers are likely along the anterior portion of the muscle meaning that the PCSA based on the fiber lengths of the superficial masseter would yield a lower estimate for the overall masseter PCSA (Antón, 1999). While estimates for PCSA from muscle architecture are important for physiological studies, these analyses have been limited to only a few animals; fiber length measurements are even more limited (Antón, 1999). Additionally, PCSA estimates are more accurate when variables such as relative and absolute muscle mass (Demes et al., 1986; Demes et al., 1988; Antón, 1990; 1994; 1999) are included.

Previously, researchers utilized jaw-muscle electromyography (EMGs) taken from primates to understand muscle recruitment and timing during chew cycles. Timing is important because it reflects when the muscle reaches peak activity, how long that activity is sustained, and in what order the muscles are recruited (Hylander et al., 2005; Wall et al., 2009; Vinyard and Taylor, 2010). As such, the levels of stress and strain are expected to reflect the rise and fall of this activity. The present understanding of primate mastication and its relationship to jaw morphology has been greatly advanced by descriptions of jaw muscle activation (Hylander et al., 1987, 2000, 2005: Hylander and Johnson, 1994; Vinyard et al., 2005, 2006, 2007; Vinyard and Taylor, 2010).

Specifically, recording the levels of muscle recruitment of the working side (chewing side), versus the balancing (non-chewing side) of the jaw has highlighted differences in activity patterns and has been an essential part of current models of masticatory performance.

Comparisons between the working versus balancing sides of the jaw have provided ratios that can be used for measuring the relative recruitment of each side and, by extension, assessing the relationship between muscle activity and muscle architecture (Vinyard and Taylor, 2010). The relationships between muscle activity and muscle architecture has important bearing on the morphology of the bones. Some of the variation in bony morphology could reflect differences in muscle activity and architecture across groups. Within Primates, differences in jaw muscle activity are informative for understanding the variation in jaw muscle form across primate groups.

The types of relationships linking muscle activation and bone form have important applications within primate comparative work, especially with regard to masticatory mechanics and the evolution of its functional parts. Not surprisingly, differences between the masticatory muscle size, morphology, and composition have been observed in different primate groups such as platyrrhines and hominoids (Cachel, 1984; Taylor and Vinyard, 2009; Vinyard and Taylor, 2010: Vinyard et al., 2011). It is clear that primates exhibit a wide range of variation in their masticatory systems. In addition, food mechanical properties, bite location, and muscle orientation influence the complex nature of this system (Throckmorton and Throckmorton, 1985; van Eidjen, 1991; Spencer, 1995; Taylor et al., 2008; Vinyard et al., 2008) and are discussed in detail in the following sections.

The Jaw as a Simple Lever

To understand the application of mechanical terms to the body requires a discussion of lever systems and their components. In physics, a moment or torque refers to the tendency of a force to rotate an object about an axis or fulcrum and is calculated as "force x distance" (Nordin and Frankel, 2012) and a moment arm is the distance (d) from an applied load to the fulcrum. In anatomy, several parts of the body are modeled according to three different types of levers known as: 1st, 2nd, or 3rd class lever systems. Regardless of the type of lever, all are based on combination of a fulcrum or joint, an applied force, and resistance (Nordin and Frankel, 2012).

Classically, the jaw has been theoretically modeled as a third class lever (Hylander, 1975; Greaves, 1978; Smith, 1978; Spencer, 1995,1999; Perry and Wall, 2008) and the simple lever model is the most basic model used to interpret the biomechanics of chewing. According to this model, the masticatory adductor muscles (the temporalis, deep and superficial masseters, and medial pterygoid muscles) apply a superiorly directed force on the mandible, which is counteracted, by the downward reaction forces at the bite point and temporomandibular joints (TMJs). To quantify this, the muscle moment arm is measured as the perpendicular distance from the muscle force to the fulcrum (TMJ). The resistance moment arm (labeled the bite force moment arm in this model) is the distance from the resistance force (the bite point on the tooth row) to the fulcrum (TMJ).

Under the principle of static equilibrium, the equation for calculating bite forces and joint reaction forces at any given bite point is:

$$Bb + Jj + Mm = 0 \quad (3)$$

where B is the bite force magnitude, J is the joint reaction force, and M is the muscle resultant. Similarly, b,j, and m are their respective moment arms. When the fulcrum is placed at the TMJ, the moment arm j equals zero because no torque is generated by J. This model is routinely used to calculate bite forces and joint reaction forces at any bite point along the tooth row (Gysi, 1921; Bramble, 1978; Greaves, 1978; Smith, 1978; Hylander, 1985; Spencer, 1995).

Bite Force

As models of bite force production have noted, the location of the bite point along the tooth row changes the possible bite force that can be produced. The placement of the bite point relative to the muscles and temporomandibular joint affect its overall bite force potential (Spencer and Demes, 1993; Spencer, 1995,1998,1999). Modeled as a third class lever system, the bite point represents the point of loading on the lever, the (TMJ) temporomandibular joint is the fulcrum and the masticatory muscles produce the force (Spencer, 1995,1998). Whether the bite point is moved anteriorly or posteriorly changes the resulting bite force because it alters the distance (i.e., moment arm) from the TMJ. As the bite point is moved more anteriorly from the TMJ, the jaw moment arm increases resulting in a lower bite force. If the bite point is moved posteriorly (towards the TMJ), the moment arm is decreased and the resulting bite force increases (Spencer, 1995). The tooth morphology of each region of the mouth affects how much force is generated at a particular bite point (Spencer, 1995; Serra and Manns, 2013). The teeth with the largest occlusal surfaces in the posterior part of the mouth are the important sites for high bite

force production. Being able to produce bite forces sufficiently high enough to process foods of different material properties is important, particularly to individuals who ingest mechanically challenging foods.

Within the craniofacial system, leverage is defined as the ratio of the distance from the jaw joint (TMJ) to the point of application of a load (i.e. piece of food) (Rentes et al., 2002). Bite force is exerted by the adductor muscles of the mandible and regulated by the muscular, dental, and skeletal system (Rentes et al., 2002). There are also complex responses in the periodontal tissues, mandibular joint capsules, and motorneurons that have long been recognized as a means to ensure bite forces are not too high (Lund and Lamarre, 1974: Hannam, 1976). Like any other biomechanical system, bite force increases in response to the stresses of chewing (Eng et al., 2013). Over time, constant chewing results in an increase of masticatory muscle functional capacity and cross-sectional area as the muscles become better conditioned with repeated use (Rentes et al., 2002). In addition, longer durations of chewing are required to process a difficult food material, and an increased amount of tooth surface area or thicker enamel is necessary (Bakke et al., 1991; Ingervall and Minder, 1997). Within mammals, tooth morphology (especially in the molar region) reflects diet specializations (Spears and Crompton, 1996: Evans et al., 2007; Smits and Evans, 2012). For instance, thinly enameled molars can wear in such a way as to create new shearing crests which are helpful for a diet requiring large amounts of crushing and grinding (Kirk and Simons, 2001).

There are also data that suggest stress and strain change depending on the bite point. For example, stress and strain levels of the skull were observed to be slightly higher in unilateral molar biting on the balancing side than on the working side using a

Finite Element Analysis (FEA) simulation (Wroe et al., 2007). However, this result is contrary to past empirically derived results, which found the working side masseter indeed exerts more force than the balancing side (Hylander, 1997; Wroe et al., 2007).

Jaw muscle EMG data from *Lemur catta* during chewing revealed a relatively high working to balancing side (W/B) ratio in the deep masseter muscle activation that is similar to that observed in galagos, but unlike those seen in haplorhines (Vinyard et al., 2006). This activity suggests that haplorhines are using relatively more force during chewing with their BS deep masseter muscle than strepsirrhines (Vinyard et al., 2006). Though EMG data on W/B ratios within strepsirrhines are relatively limited, the available data suggest that within Primates there are different patterns of muscle recruitment during chewing which translate into different patterns of strain experienced by their facial skeletons. Therefore, the primate facial skeleton can experience variation in the magnitudes of masticatory force between the working and balancing sides during a single chewing bout. This exposes the bony morphology to variable levels of force instead of purely static loading.

The results of Wall et al. (2008) also suggest that the production of high bite forces is not only a function of muscle recruitment but also of the type of muscle fiber contained in the muscle belly. Type II fibers are found in higher proportions in the superficial part of the muscle than in the deeper portion (Wall et al., 2008). Type II fibers are responsible for rapid force production and are necessary for high bite forces (Herring et al., 1979; Wall et al., 2006; Wall et al., 2008). Research between baboon and macaque males and females was done to determine if sex differences in muscle fiber type or composition exist. In both cases, male baboons and macaques possess more type II fibers

in the superficial portion of the muscle as compared to the deeper sections (Wall et al., 2006, 2007, 2008). In addition, fiber size in females was smaller than males in both cases suggesting that sexual dimorphism is present in these and other dimorphic primate taxa (Wall et al., 2006, 2007, 2008). While differences in chewing forces between human males and females have been studied, it is not known whether all sexually dimorphic primates exhibit similar trends of fiber type.

Sexual dimorphism in the masticatory complex

Sexual dimorphism within the masticatory complex could impact the magnitude of the chewing forces that can be produced (Sciote et al., 2003; Daniels et al., 2008). In humans, changes in the amount of bite force an individual can exert are affected by the onset of puberty. Typically, female humans undergo puberty before males, and are the first to see increases in their bite forces. Males, however, achieve greater overall bite forces on average despite undergoing puberty later. It is unclear whether this pattern is consistent across all primates, but these patterns may exist in primate species that have marked sexual dimorphism. In the studies using mice, no significant difference in masticatory muscle function between the sexes was found (Daniels et al., 2008). However, mice are not very dimorphic so this result is not unexpected. However, differences in muscle fiber type and organization between sexes may impact the rate at which muscles contract and produce force (Daniels et al., 2008).

Sutures

A unique feature of the bones of the skull is the presence of sutures that run between the plates of the cranium. These sutures are places of bone deposition and growth and can influence the orientation, shape, and size of the cranium (Rayfield, 2005; Wang et al., 2008). While cranial sutures are classified as synarthroses, meaning they are "unfused, fibrous, and relatively immobile contact points" (Rayfield, 2005, p.349), they may actually be sites of cranial bone mobility (Kokitch, 1992; Perrson, 1995; Rayfield, 2005). This is further supported by the work of Herring et al. (2001), which noted that across vertebrates there is observable cranial flexibility at suture sites.

Cranial and facial sutures are composed of soft connective tissue that interlocks between the perimeters of bones (Mao, 2002). Based on their construction, forces that pass across the skull are experienced differently depending on whether they are passing across the solid bone or a suture. Because sutures are essentially joints between bones, they can transmit and absorb stresses that are produced from activities such as mastication (Mao, 2002; Wang et al., 2008). The manner in which forces pass across sutures affects the growth and physiology of bone and its associated tissues and is an important factor for constructing models of bone force (Mao, 2002).

Sutural morphology can vary a great deal depending on how straight or curved, or long or short, the suture is as it affects how it is able to resist forces (Herring, 1972; Wang et al., 2008). Quantifying the biomechanical nature of sutures is difficult because they can vary so much within an individual (Wang et al., 2008). A key aspect of suture morphology is the degree of interdigitation, which has been shown to correlate with the amount of mechanical loading experienced by the suture (Byron, 2009). Areas that

experience higher instances of force or greater degrees of force are expected to have relatively more complex sutures (Herring and Mucci, 1991; Rafferty and Herring, 1999; Byron et al., 2004; Rayfield, 2005; Byron, 2009). Greater amounts of interdigitation enable a bone to resist greater magnitude forces such as bending or torsion (Wang et al., 2008). In long-term experiments performed in rhesus macaques, devices that delivered static forces were attached to the skull to study how the bone and sutures would react (Mao, 2002). This study found tensile and compressive forces were created in both anterior and posterior directions along the bone and sutures (Mao, 2002). The presence of these forces promoted suture growth at both the nasofrontal and pre-maxillomaxillary sutures, suggesting both tensile and compressive forces help induce bone growth (Mao, 2002). Similar bone responses have been observed in the periosteal and endocortical bone growth in long bones (Rubin and Lanyon, 1984; Mosely and Lanyon, 1998; Mao, 2002).

When any force is applied to a bony suture, a mechanical stress is created, and this is measurable as sutural strain (Herring et al., 1996; Hylander and Johnson, 1997; Mao, 2002). Microstrain forces induced by tension or compression likely affect sutural growth (Mao, 2002; Mao et al., 2003) leading to increased interdigitation (or in some cases overlap) that allows for a certain degree of flexibility. The bones of the cranium are relatively stiff and inelastic compared to the flexibility of the sutures that run between them (Byron, 2009). Because of this arrangement, when loads are applied to the skull it reacts as a series of pieces rather than one solid structure (Herring and Teng, 2000; Byron, 2009). With the presence of these more elastic structures (sutures) bordering relatively inelastic structures (bone), the cranium is able to absorb an increased amount of force as compared to a completely solid structure that would have had to be thickened in

order to combat increased loading as a result of feeding (Rayfield, 2005; Byron, 2009). This supports the notion that sutures are important functional components of cranial bone construction and should be accounted for in models of chewing mechanics because they are mechanically relevant to the structure's performance.

The hypothesis that greater suture complexity is present in species that rely on mechanically resistant (both tough and hard) foods was tested on *Sapajus* (formerly *Cebus) apella,* a non-human primate that exhibits a robust dental, cranial, and mandibular profile (Byron et al., 2006; Wang et al., 2008; Byron, 2009). Compared to other species of cebids, *S. apella* feeds on hard seeds that require greater relative bite forces and more chewing cycles (Byron, 2009). Based on these characteristics, their cranial sutural complexity is expected to be greater than other cebids that do not rely on such mechanically challenging foods (Wang et al., 2008; Byron, 2009). The relatively increased sagittal complexity exhibited in *S. apella* compared to non-apelloid species (*C. albifrons, C. capuchinus, C. olivaceus*) was interpreted as a reflection of the increased reliance on hard and tough foods present in *S. apella* relative to the other species. These findings are compelling because they indicate sutural complexity may represent a non-dental morphological correlate that may be compared across primates of varying diet type.

DIET CATEGORIES

Within the realm of primate feeding ecology, non-human primates are often grouped as either frugivores, folivores, or insectivores. However, within each of these broad dietary categories lies a plethora of variation including graminivory (grasses), granivory (seeds), gummivory (tree exudates), nectivory (nectar), and faunivory (animals

and/or insects) (Kay, 1973; Lambert, 2010). There is no clear consensus on how to define the mechanical implications of these dietary categories, making it difficult to compare the results of studies especially when different sets of criteria are used (Lambert, 2010). The majority of primate taxa are not exclusive to any single dietary category but usually consume a variety of foods (Kay, 1973; Lambert, 2010; Pickett et al., 2012). Because of this, matching a specific morphology or set of morphologies with a specific food in extant species can be difficult. Different diets require different morphologies so as to best process those foods.

With these broad dietary categories, the functional demands of different foods are variable, especially in terms of their mechanical properties, total chewing time, and the quantity of consumed food necessary for the individual to meet its nutritional requirements (Kay, 1973). Because of this, specific morphological features associated with mastication (i.e. teeth, mandible, and other craniofacial features) are assumed to be adapted in a way that helps the individual to best process their respective food choices.

The force requirements to break down food can vary greatly and the expectation is that with more resistant (i.e., food material that resists deformation and/or crack propagation) foods, the facial skeleton will be exposed to increased stress and strain during feeding. In species that are specialized to accommodate a highly resistant diet, the facial skeleton is predicted to be buttressed to resist those forces, especially in areas that experience elevated stresses. Food fragmentation is measured according to the material properties of food, which include: toughness, hardness, and Young's modulus (stiffness) (Lucas and Pereira, 1990; Constantino, 2007;Yamashita et al., 2009). Tough foods, which are usually highly fibrous, require longer feeding times because they are more difficult to

fracture and are sometimes not preferred (Hill and Lucas, 1996; Ang et al., 2008; Lucas et al., 2012). In contrast, hard objects tend to be brittle because they break into small pieces at high stresses (Lucas et al., 2000; Yamashita, 2008a). These distinctions in food material type suggest specific anatomical domains associated with mastication (e.g., teeth, mandible, and zygomatic arch) are assumed to be adapted in ways that allow the individual to best process the foods on their menu. For instance, possible morphological adaptations include enlarged, molarized premolars (Hylander, 1988; Daegling and Grine, 1991; Teaford and Ungar, 2000) thick enamel (Grine and Martin, 1988; Lucas et al., 2008) both of which are found in species of *Paranthropus.*

Previous experimental work has noted that the amount of strain in the circumorbital region (i.e., the post orbital bar, dorsal orbital region and zygomatic arch) changes depending on how mechanically challenging the foods being processed are (Hylander, 1997; Wroe et al., 2007). Evidence from Finite Element Analysis (FEA) highlights a similarity in the stress and strains between both sides as increasingly tough foods are processed (Wroe et al., 2007). Early *in vivo* work by Hylander (1997) also supports this conclusion. In experimental work with macaques and baboons, Hylander and Johnson (1992) found that during the mastication of an almond, the strains of the zygomatic arch were much larger than in the dorsal interorbital region. Similarly, during the mastication of an apricot, zygomatic arch strains were larger than strains in the dorsal interorbital area and the postorbital bar (Hylander and Johnson, 1992). Diet type is also predicted to affect soft tissue structures such as the PSCA of the jaw adductor muscles (Perry and Wall, 2008).

Food material properties (FMPs)

The physical properties of food are understood in terms of their size and shape (external factors) and the nature of their material composition (internal factors) (Strait, 1997; Lucas, 2004; Yamashita, 2008a;b). Because a food item needs to be broken down for consumption, understanding the physical composition of different foods involves elements of fracture mechanics; specifically the extent to which a dietary item is stiff or compliant, soft or hard, tough or brittle (Lucas et al., 2000; Wood and Schroer, 2012). The internal factors that govern food fragmentation include strength, toughness, and deformability (Lucas et al., 1986b; Lucas, 2004) and it is these factors that influence the morphological components that function to fracture the food item. To understand the relationships between an applied force, material deformation, and fracture (failure) of a food item, one examines a load/deformation plot (Figure 4).

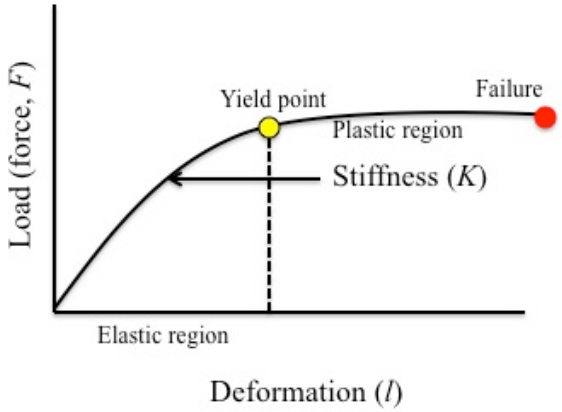

Fig. 4 Hypothetical load vs. deformation curve. Elastic region denotes the loads in which a material will return to its original state. The yield point (yellow dot) indicates the load at which the material begins to deform. The plastic region indicates the loads that permanently deform the material. Failure (red dot) indicates the point at which the material can no longer resist loading. Stiffness (K) is the slope along the line and toughness is calculated based on the area under the curve.

Within the realm of biomechanics, stiffness (K) is a measure of the change in force divided by the change in deformation for a material when it is under some external load. Stiffness is measured within the elastic region of a load-deformation curve (Yamashita, 2008a).

With respect to ingested food items, the equivalent relationship in a stress (σ)-strain (ε) curve is Young's modulus (*E*), which is a scaled version of stiffness of a particular food item (Figure 5). Young's modulus is calculated as the slope of the elastic region in a stress – strain curve.

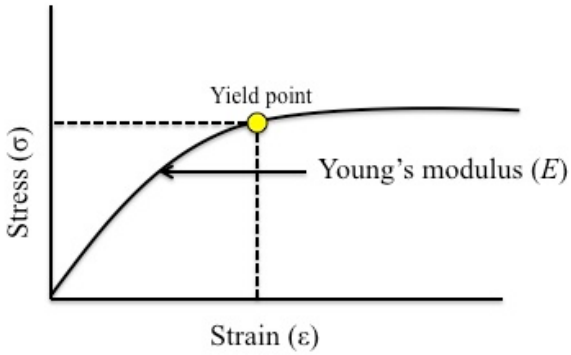

Fig. 5 Stress – strain curve with Young's modulus. Yellow dot indicates the point past which the material is permanently deformed.

In general, stiff materials under high stress undergo low levels of strain (Wood and Schroer, 2011; Nordin and Frankel, 2012) while a material that experiences low stress and high levels of strain is a compliant material (the opposite of a stiff material). These characteristics are sometimes translated in the primate dietary ecology as the relative "hardness" or "softness" of a food item. Hardness is the extent to which a material resists deformation in the plastic and elastic regions (Lucas et al., 2000). This is typically

measured by the degree to which a material resists indentation. A soft material easily deforms and is therefore easily indented (Wood and Schroer, 2011).

Another key food material property, particularly with regard to primate dietary mechanics, is toughness (*R*) which describes a material that is compliant yet difficult to fracture. In practical terms, toughness is defined in two ways that both describe how a solid material resists the propagation of cracks (Lucas et al., 2008; 2012). First, toughness is a measure of the amount of work required to fracture a (food) material's surface (Lucas et al., 2000,2012; Wood and Schroer, 2011). This value for toughness (R) is measured in Joules per meter squared (J m^2) and is calculated as the area under a given a load/deformation curve of a material (Yamashita, 2008b; Lucas et al., 2012). The second definition of toughness describes the effect of cracking on the stress field of the material that has linear elastic behavior. Calculated as (*T*) it is the measure of combining the average stress experienced by the material and the square root of crack length. This value provides the critical measure for the instance when stress is high enough to propagate and/or extend a crack (Lucas et al., 2012).

In a tough food, a high amount of force (i.e., bite force) must be applied to effectively fracture the material. Highly fibrous foods tend to be tough, and for primates, a food of this quality is not preferred (Lucas et al., 2012). A brittle object, which lacks toughness, requires only small amounts of energy to fracture (Lucas et al., 2000; Yamashita, 2008b). Nuts are examples of hard objects that tend to be brittle because they break into small pieces at high stresses. There would be no plastic deformation, suggesting these pieces could, theoretically, be put back together to construct the original nut. This is not characteristic of soft objects, like leaves, which fracture at low stresses

and do not break in a way that allows them to easily reconstruct the original leaf. Soft objects, for this reason, tend to be tough (Wood and Schroer, 2011).

The ways foods fragment is complex and many of the factors are difficult to measure, particularly in the wild. A common way to measure fragmentation is through toughness and stiffness. These two factors capture how a plant's construction can deter herbivores from consuming it (Agrawal et al., 1998; Lucas et al., 2000; Lucas, 2004; Yamashita, 2008b). Stress-limited foods are characteristically brittle and break apart when sufficient force is applied to them. This plant type relies on the consumer not being able to generate sufficient chewing forces to break it down (Yamashita, 2008b). In contrast, displacement limited plants rely on the inability of the herbivore to induce enough strain on the plant to cause it to fracture (Agrawal et al., 1998; Yamashita, 2008b). These include tough foods. These distinctions in food material type are important for understanding how the teeth must function to efficiently break down different food types with varying force requirements. While there is great interest in this field, more information about the relationship between the food properties and microstructure and how these interface with mastication is still needed (Lucas et al., 2012). If these relationships are better understood, then the ways tooth macro- and microwear are interpreted can be improved in living and fossil primates.

DIETARY DIFFERENCES IN RELATION TO FACIAL MORPHOLOGY

Understanding the ways in which masticatory forces are resisted is crucial for modeling facial growth. While genetic and environmental factors exert considerable influence on facial growth, it is also important to consider how mechanical factors

associated with mastication shape growth and the resulting morphological forms that manifest in the craniofacial complex. A large literature exists concerning the effects of craniofacial morphology and diet type, and the breadth of experimentally obtained evidence suggests a strong link between these elements across mammals.

Most of the models of facial growth in relation to masticatory loading are derived from experimental studies performed on non-human anthropoid primates and mammals (Lieberman et al., 2004a; Wall et al., 2008; Ross et al., 2009; Perry and Hartstone-Rose, 2010). For example, a study by Koyabu et al. (2009) examined the differences in craniodental morphology between two sympatric species of tree squirrels (*Callosciurus erythraeus* and *Dremomys rufigenis*) finding that while both species prefer the same fruits and insects, only *C. erythraeus* incorporated tree bark and hard seeds into its' diet. As expected, *C. erythraeus* possessed cranial features that would aid in resisting increased masticatory loading and higher bite force production required for hard-seed feeding (Koyabu et al., 2009). These features include a more robust zygomatic arch to resist increased forces from masseter muscle activation, greater temporalis and masseter muscle leverage during incision and a relatively wider interorbital region as compared to *D. rufigenis* (Koyabu et al., 2009). That study's findings suggest that the differences in craniofacial morphology between these squirrel species is functionally linked to the differences in their diets. Experimental work on rats determined that those that were fed soft foods had smaller muscle attachment sites smaller jaw adductor muscles and decreased overall facial height (Kilidaris et al., 1986; Engström et al., 1986; Yamada and Kimmel, 1991; Lieberman et al., 2004a). As expected, the associated strain magnitudes on the mandible, decreased in soft food eaters. Work by Lieberman et al. (2004a)

investigated the effects of food material property type in relation to growth in rock hyraxes (*Procavia capensis*) given their similarities in strain distributions to the non-human primate skull. Their findings support the hypothesis that masticatory strains follow a gradient in which the highest strains occur near sites of occlusion and masticatory muscle insertion but decrease when moving dorsally on the skull (Lieberman et al., 2004a). These conclusions also agree with the strain patterns observed in primates (Hylander and Johnson, 1992; Hylander and Ravosa, 1992; Ross and Hylander, 1996).

Within the work done on primates there have been numerous studies directed at answering questions concerning the effects of hard versus soft diets in primates such as baboons (Corruccini and Beecher, 1984) and squirrel monkeys (Bouvier and Hylander, 1982; Corruccini and Beecher, 1982; Beecher et al., 1983). In each case, the individuals who chewed on harder foods exhibited taller palates, thicker mandibular corpora, and faces that were taller and wider. In contrast, those raised on soft diets possessed several abnormal features including crowded teeth, malocclusion and narrowed maxillary arches, all of which are indicators of abnormal growth (Lieberman et al., 2004a). One way to explain how different growth trajectories manifest between these broad diets due to the rate at which the Haversian systems (the fundamental units of bone) are remodeling. Individuals who feed on harder foods may be experiencing higher rates of remodeling (or more remodeling events) which result in greater bone growth and maintenance as compared to those fed only soft foods (Bouvier and Hylander, 1981, 1996; Lieberman et al., 2004a). This suggests that the portions of the face impacted by increased masticatory loading have greater bone response throughout the course of growth and development.

In addition to the size of facial features, the internal bone architecture and degree of mineralization has been altered in cases of reduced forces applied to features such as the mandible (Tanaka et al., 2007) and zygomatic arch (Franks et al., 2016). It is hypothesized that low magnitude forces will result in lower bone remodeling rates, whereas high magnitude forces would require higher bone remodeling rates to ensure the bone will not fail (Tanaka et al., 2007). Tanaka et al. (2007) compared mandibular cortical and trabecular bone mineralization and determined that rats fed hard pellets had lower degrees of mineralization than those fed soft pellets. With a soft diet, less muscle force is required to power the masticatory muscles, which causes the bone to resorb. The rates of new bone formation decrease, causing the bone to become more mineralized. In trabecular bone, the deeper portions of the bone have higher mineralization than more superficial zones (Mulder et al., 2007). The extent to which is a bone is mineralized has an affect on its stiffness. Bone with high mineralization is generally stiff and brittle with a lower threshold to failure (Mulder et al., 2007). At a bone's surface, the trabecular bone (which is less mineralized) would be more compliant and therefore less stiff. This makes bone capable of resisting higher strains over a period of time (Mulder et al., 2007).

Certain primate taxa stand out morphologically because of their specialized diets, and because of specified feeding behaviors that required adaptations of the skull. These morphologies are notable because they appear to be adaptations for specific diets. Cebids, especially *S. apella*, have served as test subjects for studies interested in trying to identify features associated with a hard object diet (Byron, 2009; Lieberman et al., 2004a). Among the factors that seem to relate to hard-object feeding is an orientation of the mandibular ramus in a more vertical plane, a more anteriorly placed temporalis

muscle, and a shift of the root of the zygomatic bone to a more anterior position. *Pithecia,* a group known to consume seeds as a major portion of their diet, relied on their post-canine dentition to produce enough force to break through the seed and process it (Happel, 1982; Martin et al., 2003; Lieberman et al., 2004a).

In addition to the work on food material properties, several studies have examined the relationships between strain magnitudes and nutrition (Moore, 1965; Kilidaris, 1989; Kilidaris et al., 1992; Lieberman et al., 2004a). While the material properties of a food require certain levels of force production, the nutritional content of the food can also affect the growth of some bony features. Studies done on rats revealed that diets lower in calcium had smaller mandibles in terms of their overall dimensions as compared to rats that had low calcium content and soft foods had mandibles that were smaller in vertical height and smaller in condyle size (Lieberman et al., 2004a). From this, it appears that differences in strain and calcium content create changes in the jaw size as compared to differences in strain magnitude alone, which resulted in changes of jaw shape (Lieberman et al., 2004a). These types of data support hypotheses about the influence of food material properties on facial form.

The patterns and relationships linking morphology and diet in extant groups provide researchers with a frame within which to understand similar morphologies in fossil specimens. Using the knowledge accrued from the studies performed on primate taxa and their diet specializations allows hypotheses about similar specializations in past taxa. Once aspects of diet can be identified, other aspects of their life, activities, and behavior can be inferred.

THE ZYGOMATIC ARCH

Previous studies of zygomatic arch morphology have typically focused on only a few mammalian species including pigs (Herring and Mucci, 1991; Herring et al., 1996; Freeman et al., 1997; Teng et al., 1997), macaques (Hylander and Johnson, 1997) and chimpanzees (Witzel et al., 2004) and used small sample sizes making it a relatively under-studied feature of the primate cranium. During a chewing bout, the masseter muscles are activated causing the arch to twist along its long axis resulting in eversion of the superior border and inversion of the lower border of the arch (Hylander and Johnson, 1997). In previous experimental studies on pig and macaque zygomatic arches the contraction of the masseter affected strain distribution causing disproportionate amounts of strain to accumulate anteriorly along the arch as well as producing high concentrations of bending and shearing forces at the anterior portion of the arch (Herring and Mucci, 1991; Hylander et al., 1991a,b; Herring et al., 1996; Freeman et al., 1997; Hylander and Johnson, 1997; Rafferty et al., 2000; Witzel et al., 2004). The vertical component of the masseteric force bends the arch in the parasagittal plane, which is considered to be the dominant loading regime experienced by the bony arch (Hylander and Johnson, 1997). Furthermore, experimental work on chimpanzees (*Pan troglodytes*) and macaques (*Macaca fascicularis*) shows the zygomatic arch experiences some of the highest strains in the face (Hylander and Johnson, 1997; Ravosa et al., 2000a,b; Ross and Metzger, 2004).

The form of the zygomatic arch is unique compared to other cranial bones, and is typically modeled as a curved beam with two fixed ends (Hylander and Johnson, 1997; Kupczik et al., 2007). However, modeling the zygomatic arch in this way is difficult, as

it tends to oversimplify the overall form. Because of variation in loading experienced during mastication, the arch does not experience uniform loads throughout a single chew cycle. In addition, the presence of a suture on the bone affects the dispersion of forces along the arch over time (Hylander and Johnson, 1997). The zygomatic arch is bent laterally in the middle and medially at both ends (Oberheim and Mao, 2002). This construction causes the zygomatic arch to experience tensile forces along its inferior margin and compressive forces on the superior margin (Witzel et al., 2004).

While modeling the zygomatic arch as a curved beam has heuristic value, such a model fails to incorporate the non-uniform strain distributions and the effects of high magnitude strains on the bone. In addition, the presence of a suture between bones affects the load distribution along the arch throughout growth (Herring and Mucci, 1991; Hylander and Johnson, 1997; Curtis et al., 2014). Zygomatic arch form is intriguing from a biomechanical perspective because structures in tension are more likely to fail than those in compression, and as the bony anchor for the masseter muscle, bone failure would prove detrimental to an individual's ability to masticate, and therefore cause a severe fitness cost.

Additionally, the zygomaticotemporal suture along the arch is impacted by mechanical stress, which affects its ontogeny and function. Sutural anatomy has been used to predict the magnitude of loading, though interpreting the type of load (i.e., compression or tension) is not easily determined from the sutural morphology (Herring, 1972; Jaslow, 1990; Hylander and Johnson, 1997; Mao, 2002; Mao et al., 2003; Rafferty et al., 2003; Rayfield, 2005; Kupczik et al., 2007). Herring and Mucci (1991) examined the zygomatico-temporal suture of pigs and found the vertical portion of the suture

experienced tension (and some shear) while the horizontal portion was loaded in compression. Importantly, the intrasutural fibers appear to differ between the two loading types with the fibers running obliquely between the interlocking laminae in compression and directly between the bones in tension (Herring and Mucci, 1991). This supports the utility of using intrasutural fiber orientation to trace functional stress in cranial bones (Prahl-Andersen, 1968; Herring and Mucci, 1991).

The bony morphology of the zygomatic arch is expected to respond to the high masticatory forces generated by mastication but it is unclear whether this response would change the external cross-sectional shape, internal cortical bone distribution, or both. Despite the extensive work performed on the primate craniofacial skeleton, the influences that may pattern variation (both intra- and inter- specifically, and by diet) in zygomatic arch form remain relatively unclear.

FOSSIL HOMININS

The relationships between masticatory function and force resistance have important evolutionary implications for primate craniofacial form. Studies of masticatory performance are important for quantifying differences among extant groups, which then can be applied to the fossil record of hominin evolution. When fossil specimens with robust morphologies are uncovered the assumption is that those individuals primarily relied on mechanically challenging foods. However, this generalization has some exceptions such as *Paranthropus boisei* (Ungar et al., 2008). For this fossil species, the robust morphology may reflect an adaptation for the consumption of occasional fallback foods rather than preferred foods based on the dental microwear signal (Ungar et al.,

2008). This raises questions about how to interpret robust morphologies in the fossil record, especially among other lines of evidence such as microwear and isotopic analyses.

Determining the diet of early hominins is an important part of the foundation of paleoanthropology and remains a highly debated issue because many lines of evidence do not agree on what extinct taxa were feeding on. Using what is known about the feeding behaviors and morphology of living taxa helps researchers explain the variation in cranial morphology in fossil hominins. Taking a dietary perspective offers other ways of examining extinct taxa beyond just the foods they were eating. For instance, understanding the hominin facial form is an important starting point for creating hypotheses about their radiation across Africa and the foods that they were relying on (Cerling et al., 2011; Dominy et al., 2008; Daegling et al., 2011; Lee-Thorp et al., 2010; Wood and Schroer, 2012).

There are several features of the skull that suggest these fossil taxa had different dietary specializations. Models of masticatory performance based on extant primates help reconstruct the diets of extinct taxa such as *Australopithecus* and *Paranthropus* (DuBrul, 1977; Rak, 1983; Lucas et al., 1985; McCollum, 1994; Wood and Lieberman, 2001; Macho et al., 2005; Daegling et al., 2011; Balter et al., 2012; Wood and Schroer, 2012; Daegling et al., 2013). The craniofacial morphologies of these groups are complex and there are some striking differences between the craniodental features of these taxa tied to their dietary choices. However, *Australopithecus* and *Paranthropus* pose many challenges to those interested in reconstructing their diet and interpreting their

morphology because different lines of evidence have led researchers to conflicting conclusions.

Upon its discovery, *Paranthropus* was characterized as a strict herbivore whereas *Australopithecus* was a more generalized feeder (Broom, 1946; Robinson, 1954a,b; 1956; DuBrul, 1977; Rak, 1983). In *Paranthropus*, the possession of robust craniodental characteristics, which include an anteriorly thickened hard palate, thickly enameled teeth, tall mandibular ramus and flaring zygomatic arches, suggested it was specialized for a diet requiring high magnitude forces (Broom, 1950; Robinson, 1954b; Grine, 1986; Wood and Lieberman, 2001; Ungar et al., 2008). However, the craniodental features within australopiths (i.e., the marked anterior placement of the zygomatic roots along with some mediolateral expansion of the face and reduced prognathism) suggested a diet that did not require high magnitude forces and was more in line with omnivory (DuBrul, 1977; Rak, 1983). The features of *Paranthropus* seem to allude to some degree of dietary specialization for tough and/or hard foods (DuBrul, 1977; Wood and Lieberman, 2001; Wood and Strait, 2004; Wood and Constantino, 2007; Cerling et al., 2011; Daegling et al., 2011).

Paranthropus boisei, an East African hominin, had a relatively large and thick mandibular corpus, large and low-cusped postcanine teeth and cranial features that suggest the presence of large temporalis muscles (Rak, 1983; Lucas et al., 1985; Grine, 1986; Grine and Kay, 1988; McCollum, 1994; Cerling et al., 2011; Ungar and Sponheimer, 2011). Rak (1983) provided one of the earliest evaluations of the craniofacial features in *Paranthropus* by applying Endo's (1966) frame model of the face to hominoids. Under Endo's model, the highest masticatory stresses should reside in the

supraorbital region bringing Rak (1983) to conclude that the robust australopiths evolved a face that minimized the effects of these forces through increased facial height and elongated malar regions in relation to greater bizygomatic breadth. However, subsequent analyses (Picq and Hylander, 1989; Hylander et al., 1991; Ravosa, 1991) found that Endo's model did not agree with the results from their experimental work, bringing Rak's conclusions into question (McCollum, 1994). Experimental evidence has revealed that masticatory strains have limited impact on the browridge region (Hylander et al., 1991; McCollum, 1994). Clearly facial development is dictated by a host of factors and is not simply a product of mechanics; however the masticatory apparatus must meet the mechanical demands imposed on it throughout development. The nature of this relationship remains unclear and requires further study.

Diet of Paranthropus

One of the most studied and continually debated cases of specialized masticatory loading revolves around interpretations of the craniofacial and craniodental morphology of *Paranthropus*. These taxa possess several features pinned as adaptations for producing high bite forces and resisting high magnitude strains (Strait et al., 2008; Daegling et al., 2011). Specifically, these individuals had large, thickly enameled cheek teeth, molarized premolars, more anteriorly placed zygomatic root and well-developed muscle attachment sites for the masseter and temporalis muscles which would aid in resisting bending and torsion forces experienced during feeding (Rak, 1983,1985; McCollum, 1994; Strait et al., 2008; Daegling et al., 2011).

Durophagy, or hard-object feeding, is used by some living primate groups, such as mangabeys, as an alternative dietary strategy (McGraw et al., 2012) during times of resource scarcity. Because hard-object feeding serves as a fallback food in some extant groups, some researchers have argued that it could also be used by fossil hominins during times of resource scarcity or when preferred foods are unavailable (Daegling et al., 2011).

Feeding on large, hard objects has been suggested to explain premolar adaptations in fossil hominins such as *Paranthropus* (Strait et al., 2008). Accompanying this diet type is the necessity of generating high bite forces, as well as a concomitant increase in the maximum distance individuals could open their mouth (i.e., gape) to accommodate the size of the food. Thus, gape is an important mechanical constraint of the masticatory complex (Perry & Hartstone-Rose, 2010; Daegling et al., 2011). Gape is multifaceted as it is affected by factors such as location and morphology of the jaw adductor muscles and the height of the teeth (Herring & Herring, 1974; Hylander, 1979a; 2009; Perry & Hartstone, 2010).

If the food item were large relative to the individual's oral cavity, it would be difficult for that individual to open their mouths enough to situate the item comfortably on the post-canine teeth (Strait et al., 2008). In anthropoids that consume large objects, such as fruit, they first use their incisors to take bites out of the object to reduce it to more manageable-sized pieces (Ungar, 1994; Strait et al., 2008). However, if the food was too resistant to process with the incisors, then the premolars could be used to produce higher bite forces that then would allow the food to be fully processed. Because premolars are located more mesially in the mouth, they do not require the same degree of gape as compared to molars. The premolars could then be capable of breaking off a piece of the

food or at least propagating cracks in the food item so that it can eventually be consumed (Strait et al., 2008). This has been argued for the diet of *Paranthropus boisei*, given the low amount of microwear on the incisors (Ungar and Grine, 1991; Strait et al., 2008).

However, gape is difficult to determine in the fossil record because of how much constraint soft tissues (specifically, the adductor muscles) influence the bone (Daegling et al., 2011). In the absence of soft tissue and/or large canines, gape is impossible to reconstruct in the fossil record (Daegling et al., 2011). In fossil hominins, gape to accommodate canine size is likely not a selective force on their morphology. Based on the suite of adaptations possessed by *Paranthropus*, the consumption of small, hard objects was identified as an important component of their diet (Jolly, 1970; Grine, 1981; Strait et al., 2008); however this conclusion is not entirely supported biomechanically.

Biomechanical models constructed in several studies have not found small, hard objects to be a source of higher magnitude premolar loading (DuBrul, 1977; Smith, 1978; Greaves, 1978; Spencer, 1995, 1998) given that biting on premolars produces bite forces almost equivalent to that of molar biting but with higher resulting strains. There would be no advantage to chewing a small, hard object on the premolars: thus, no specialization for premolar loading would be necessary (Strait et al., 2008).

Finite-element modeling performed on *Australopithecus africanus* has suggested that hard-object feeding, using their premolars, was part of their overall feeding strategy (Strait et al., 2009). It is plausible that *A. africanus* had a relatively gape, which would confer more muscular mechanical advantage but would limit the size of the object that could be processed orally (Daegling et al., 2011). To bypass this constraint on object size, *A. africanus* could have used extraoral processing to reduce the food's size

(Daegling et al., 2011). This type of behavior is observed in chimpanzees (*Pan troglodytes*) and mangabeys (*Cercocebus atys*) (Boesch and Boesch, 1982; Daegling et al., 2011). However, wear patterns observed in consistent hard-object feeders, such as sooty mangabeys, does not support hard-object feeding in *A. africanus* (Daegling et al., 2011). This is due to dissimilarities between the cranial features of *A. africanus* and extant hard-object feeders, as well as inconsistencies in the microwear signals of these groups.

While disagreement concerning early hominin diets continues, if hard-object feeding was a significant part of fossil hominin diets then placing high loads on the premolars and being able to produce the high magnitude bite forces would likely be required (Grine, 1986; Strait et al., 2008; Grine et al., 2010; Daegling et al., 2011). One way the facial skeleton has been hypothesized to accommodate increased loading is through evolving more anteriorly placed zygomatic roots and anterior pillars, which are features found in *Australopithecus* and *Paranthropus* (Rak, 1983; Daegling et al., 2011). The anterior pillars of *Australopithecus africanus* have been interpreted to as forms of facial buttressing necessary for the consumption of hard objects (Rak, 1983). However, extant primate species, such as sooty mangabeys, utilize hard objects but lack the facial buttressing of *A. africanus* (Singleton, 2004; Daegling et al., 2011). Because they do not share similar cranial features with earlier hominins, making inferences from such diet comparisons is tenuous.

PREDICTIONS

The masticatory complex has been subjected to different selection pressures over the course of evolution. As a whole, the different parts of the face must exist in a

relatively constrained space on the skull. The mechanical demands of chewing vary depending on the material properties of the food, muscle activation and gape. Internally, the density and composition of the bone is also expected to vary according the types of force passing through the face. In addition, this dissertation will be able to comment on the influence of hard-object feeding in relationship to zygomatic arch morphology, which will inform on current understandings of this dietary strategy in living and extinct priamtes. The following are a set of predictions addressing these points with respect to zygomatic arch form in primates with the intention of generating new insight regarding craniofacial dietary adaptation and reconstruction in fossil hominins.

Cross-sectional shape, cortical bone, and diet

Features that are subjected to higher magnitude loading, such as the zygomatic arch and inferior circumorbital region, are expected to exhibit reinforced bone architecture; a pattern that has been observed in many primate taxa. The consumption of less mechanically resistant foods would require lower magnitude forces as compared to those required of more resistant foods. In primates, this is the difference between soft, fleshy ripe fruits as compared to hard nuts or seeds. The forces required for processing resistant foods are higher than those of less resistant foods. Thus, the morphology associated with mastication in hard-object feeders should exhibit adaptations for resisting high magnitude loads, including larger masticatory muscles that are positioned more anteriorly, larger bone cross-sectional areas (CSA) and/or increased bone density.

One of the most notable adaptations of the haplorrhine skull is the presence of post-orbital closure. Many have argued that this feature is representative of a

major morphological shift to accommodate larger chewing muscles (Cartmill, 1970,1972,1980). If true, this suggests other features in this area may have undergone some additional selection to accommodate higher magnitude loads. The zygomatic arch may have a functional role in resisting masticatory forces associated with particular diet because it serves as the attachment site for the masseter muscle. In addition, the temporalis muscle passes between the arch and the lateral part of the cranial vault. Changes to the morphology zygomatic arch may confer some mechanical advantage in terms of force production. For instance, a taller, wider or denser zygomatic arch may be able to support a larger masseter muscle that would be required to exert high magnitude forces.

In the following studies, cross-sectional shape in relation to bone mechanical behavior is investigated to determine whether different masticatory induced load types (bending and torsion) are uniformly experienced along the arch or whether they follow the known strain distribution. In addition, specific cross-sectional shapes and their ability to best resist bending or torsional loads are quantified and compared intraspecifically, interspecifically, and by diet type.

Stress Resistance

It is well established that bone responds to different loads in a way that allows it to resist applied forces and avoid failure. Studies that have quantified bone stress note than an increase in cortical bone is a response to high stress (Bouvier and Hylander, 1981; Wang and Dechow, 2006). Areas of the face that experience high stress should therefore exhibit greater amounts of cortical bone and those that experience less stress should have

relatively less cortical bone. In primates, and other mammals, the areas that experience the greatest amount of stress, such as the zygomatic arch, are expected to exhibit some architectural response, either by exhibiting a more robust form or changing the internal architecture by way of increasing bone density or cortical area (Chamay and Tschantz, 1972; Bouvier and Hylander, 1981, 1996; Beecher et al., 1983; Martin and Burr, 1989; Antón, 1994; Hylander and Johnson, 1997; Mulder et al., 2007; Kupczik et al., 2009). While the strain profile of the zygomatic arch has been examined in past studies, its morphology and shape in relation to the stress profiles have not been well understood. Its unique structure and position relative to the masseter and temporalis muscles makes it a good candidate for looking at the relationship between masticatory stress and bone. It is not clear whether the morphology of the zygomatic arch, which is highly variable across primate taxa (both living and extinct), is a product primarily of function, phylogeny, or some combination of both. The unique form of the arch also calls into question the role of shape in strain resistance and the impact of the feature's location relative to other structures (e.g., the lateral portion of the orbit and the tooth row). In the following studies, the expectation is that areas of greatest cortical bone concentration and measures of bone strength will correspond to the areas of greatest strain in the zygomatic arch.

Sutural Complexity

Given the findings observed in cebids, the expectation is that sutural complexity will be greater in primate taxa that consume mechanically resistant diets. In particular, given that hard-object consumption in *S. apella* suggests that the high magnitude loads associated with fracturing a hard object necessitate increased bite forces and high facial

strains, the expectation is that hard-object consumers will exhibit relatively more complex sutures than taxa with less resistant diets.

Diet

The above predictions are couched within larger questions that relate to linking specific aspects of craniofacial morphology with diet in primates. To quantify these relationships, two different dietary schemes are employed: total reported consumption percents for food items, and food material properties (FMPs) data. Using this comparative approach to examine arch cross-sectional variables and sutural complexity provides an opportunity to test the duality of these approaches and make determinations about how to improve dietary categorization for future studies.

CHAPTER 3: ZYGOMATIC ARCH CORTICAL AREA AND DIET IN PRIMATES

3.1 Abstract

The influence that various types of ingested foods have on the form (size and shape) of specific features of the masticatory system is an area in which many questions remain unanswered. The bony zygomatic arch, the focus of this study, is directly linked to the masticatory system because it serves as the anchor for the masseter muscle, a primary muscle of chewing and source of masticatory force. However, the influence of diet and the forces associated with different diet types on the arch's internal bone architecture is not well understood across haplorhine primates. Despite the breadth of work centered around the craniofacial complex and biomechanics of mastication, there is a need for further investigations into the functional relationships between specific bony features that experience high strains, (e.g., the zygomatic arch), and the masticatory forces generated by different diets (e.g., mechanically resistant versus non- mechanically resistant) across non-human primates.

A hypothesis and series of predictions assessing diet in relation to variability in cortical area distributions and values of section moduli (measures of bone strength) throughout the zygomatic arch were tested in a sample of haplorhine primates. Cortical area and measures of section moduli appear to track with the known masticatory strain distribution along the zygomatic arch. Pairwise comparisons between closely related taxa of different diets reveals significant differences in anterior cortical area and section moduli values. These results imply that differences in masticatory loading due to diet manifest in the zygomatic arch's internal bone structure.

3.2 Introduction

Craniofacial morphology and diet type are intricately linked. Different foods have variable functional demands, especially in terms of their mechanical properties, total chewing time, and the quantity of food an individual must consume to meet its nutritional requirements (Kay, 1973). The force requirements to break down food can vary greatly (Lucas and Luke, 1984; Kinzey and Norconk, 1990; Lucas et al., 2008, 2012; Taylor et al., 2008; Reed and Ross, 2010). More mechanically challenging foods (i.e., those that resist deformation and/or crack propagation) should expose the facial skeleton to increased *stress* (defined as the amount of force per unit area) and *strain* (defined as the amount of deformation as a result of stress). As a result, primate species that feed on resistant diets should possess buttressed facial skeletons that act to resist those forces.

Investigating the relationship between dietary loading and bone response is a critical part of understanding the morphology of the cranium. The zygomatic arch must resist repetitive masticatory forces given that feeding is a routine behavior that involves habitual loading of the face (Hylander et al., 1991a,b; Hylander and Johnson, 1992, 1997). It is imperative that the zygomatic arch, a known site of high masticatory strains, be examined in order to understand the effects of different loads on a specific portion of the primate cranium.

Research on the craniofacial skeleton and the biomechanics of mastication have revealed that the primate cranium experiences varying amounts of stress and strain during feeding (e.g., Hylander, 1979b, 1984; Hylander and Johnson, 1997; Dechow and Hylander, 2000; Ravosa et al., 2000b). To understand how different masticatory stresses and strains influence craniofacial form, a consideration of the individual components of

the face, and in particular, those regions that experience the greatest masticatory loading is required. Thus, studies that investigate the effects of processing different diet types (and therefore different force magnitudes) on specific parts of the facial skeleton (e.g., Spencer, 2003; Wright, 2005; Terhune, 2011) are an essential part of understanding masticatory biomechanics in living primates and in the rendering of accurate dietary reconstructions in extinct taxa.

Internally, the density and composition of facial bones are expected to vary in predictable ways according to the types of forces passing through them. In a structure like the skull, the degree of bone stiffness and flexibility affects how the bone responds to masticatory strains (Dechow and Hylander, 2000; Wang et al. 2006). In discussions of bone strain and bone loading, it is important to note that "high strain" is not equivalent to "high loading" in all instances. While high loading (i.e., high magnitude external force applied to bone) does elevate strain (i.e., increase the displacement of bone material), high strains may also appear in regions that are structurally less strong. Strain data collected *in vivo* presumably derive from bone regions that are already adapted to their habitual loading environment. Thus, bone regions that consistently experience high strains are assumed to have greater bone stiffness. Furthermore, areas with high bone stiffness will resist strain more than those with high flexibility (Dechow and Hylander, 2000). Cortical bone density is used as evidence of bone response to variations in strains and stress (Hylander, 1979a,b, 1985; Ohman et al., 1997; Hylander et al., 1998; Demes et al., 2000; Daegling, 2002a), thus providing morphologists with a means of gauging the extent to which forces can be resisted; higher densities of cortical bone are believed to signal higher loading.

It is well established that bone responds to loading by increasing bone formation (Currey, 2003; Rantalanien et al., 2011; Mantila Roosa et al., 2012) and that levels of bone mass are maintained through repeated loading (Lanyon and Rubin, 1984; Rubin and Lanyon, 1984). Within the realm of masticatory biomechanics, experimental studies have detailed the effects of hard versus soft diets in primates such as baboons (Corruccini and Beecher, 1984) and squirrel monkeys (Bouvier and Hylander, 1982; Corruccini and Beecher, 1982; Beecher et al., 1983) and found that feeding on hard objects increases bone density. This suggests a greater frequency of remodeling events (or possibly greater osteogenesis per event); resulting in greater bone growth and maintenance in individuals fed hard diets, as compared to those fed only soft foods (Bouvier and Hylander, 1981; Lieberman et al., 2004a). While these studies highlight the localized effects of a soft versus hard diet on bone, these data suggest that diet type directly influences bone remodeling and that the portions of the face that are affected by increased masticatory loading exhibit a greater bony response. Based on this experimental work, an underlying assumption of comparative morphology studies is that skeletal elements reflect their force environment *in vivo* (Daegling, 2002a).

Attachment sites for the masticatory muscles show increased bone mass as a reflection of the increased loads they experience during activation. In the last few decades, a number of studies utilizing *in vivo* methods (e.g., Hylander, 1984, 1985; Hylander and Johnson, 1994, 1997; Ross and Hylander, 2000; Vinyard et al., 2005; Wall et al., 2006; Taylor and Vinyard, 2008) have provided some data on the ways primates recruit their masticatory muscles and how those recruitment patterns translate to internal loads that are resisted by the bones of the masticatory apparatus. However, this approach

has not been applied to investigate the morphology of an area that routinely experiences high strain due to mastication: the zygomatic arch.

Previous studies of zygomatic arch morphology have focused on only a few mammalian species including pigs (Herring and Mucci, 1991; Herring et al., 1996; Freeman et al., 1997; Teng et al., 1997), macaques (Hylander and Johnson, 1997) and chimpanzees (Witzel et al., 2004). This limited taxonomic breadth, in combination with these studies' small sample sizes, makes the zygomatic arch a relatively under-studied feature of the primate cranium.

Early experimental work found that the zygomatic arch experiences a non-uniform strain distribution; the anterior portion experiences greater strains than the posterior portion (Herring and Mucci, 1991; Hylander et al., 1991a,b; Herring et al., 1996; Freeman et al., 1997; Hylander and Johnson, 1997; Rafferty et al., 2000; Witzel et al., 2004). Studies of pig (*Sus scrofa domesticus*) and macaque (*Macaca fascicularis*) zygomatic arches revealed that masseter muscle contraction affected strain distribution along the arch and produced high concentrations of bending and shearing loads at the anterior portion of the arch (Herring and Mucci, 1991; Herring et al., 1996; Hylander and Johnson, 1997). Furthermore, experimental work on chimpanzees (*Pan troglodytes*) and macaques showed that the zygomatic arch experiences some of the highest strains in the face (Hylander and Johnson, 1992,1997; Ravosa et al., 2000a,b; Ross and Metzger, 2004). Based on these strains, the internal bone architecture is expected to reflect these loading regimes, but it is unknown whether the internal architecture indeed correlates with experimentally obtained strain patterns.

From a biomechanical perspective, zygomatic arch form is intriguing because structures in tension are more likely to fail than those in compression (Wood, 1971), and as the bony anchor for the masseter muscle, bone failure would prove detrimental to an individual's ability to masticate. Despite the extensive work performed on the primate craniofacial skeleton, the influences that may pattern variation (both intra- and inter-specifically, as well as by diet) in zygomatic arch form remain relatively unclear. An understanding of the internal architecture of the zygomatic arch in relation to diet has untapped value in the realm of masticatory biomechanics for both living and extinct taxa, not only from the perspective of comparative morphology, but also in the creation and validation of Finite Element Models (FEM), and the reconstruction of diet.

3.3 Materials and Methods

3.3.1 *Study Sample*

MicroCT scans (voxel range 7.94-30.0 voxels/mm) of skulls from 11 primate species (*n*=77 individuals; Table 1) were selected from skeletal and cadaver collections at Arizona State University and Northeast Ohio Medical University (NEOMED). Species were selected to obtain a sample that spanned a variety of diet types and were assigned to a dietary category based on a diet profile constructed from published data on specific foods consumed and the mechanical properties of those foods. Only adult, wild specimens without pathology were included to control for influences resulting from captivity and/or disease. A summary of the number of males and females for each species is shown in Table 1.

Table 1. Study sample composition

Taxon	**Female, *n***	**Male, *n***	**Unknown, *n***	**Total, *n***
Gorilla gorilla	9	-	-	9
Piliocolobus badius	4	3	-	7
Alouatta caraya	2	3	1	6
Pan troglodytes	8	-	-	8
Cercopithecus mitis	8	-	-	8
Ateles geoffroyi	-	-	8	8
Callicebus moloch	-	7	-	7
Cebus capucinus	5	-	4	9
Pithecia pithecia	1	1	1	3
Sapajus apella	1	3	2	6
Callithrix jacchus	-	-	6	6
Total	38	17	22	**77**

3.3.2 *Dietary categories*

A species' designation as a "tough feeder," "hard feeder," "soft feeder," or "exudate feeder" was based on total consumption of 55% or more of a particular food type deemed as tough, hard, soft, or exudate based on its mechanical properties. Because this study examined the effects of presumed variation in masticatory loads on the bony morphology of the zygomatic arch, "exudate feeder" remained distinct from "soft feeder" as each of these food types differ in their material properties and time required for mastication (Norconk et al., 2009). In instances where two or more primary food types are consumed (e.g., tough and soft), the species' diet characterization was assigned based on the food type with the highest consumption percent (Table 2).

3.3.3 *Hypothesis*

The hypothesis that cortical bone area (CA) is positively correlated with elevated masticatory loading regimes experienced in the zygomatic arch during feeding

was tested in this study. Increased cortical bone concentrations are known to track with areas of greater loading (Hylander and Johnson, 1997) and to provide increased axial strength. Thus, areas of higher loading in the zygomatic arch are expected to possess increased cortical bone concentrations. Because *in vivo* data on macaques (Hylander and Johnson, 1997) document zygomatic arch strains to be highest anteriorly and lowest posteriorly, it is expected that the relative amount of cortical bone as a function of cross-sectional area be relatively largest anteriorly and smallest posteriorly. With regard to diet, haplorhines who feed on resistant diets likely experience relatively higher strains along their arches. Therefore, it is expected that resistant-object feeders exhibit relatively greater amounts of CA compared to closely related non-resistant feeders. Because the anterior portion of the arch experiences the largest loads *in vivo* during feeding, all comparisons were focused on this region. Finally, the greatest measures of the section moduli (Z_x and Z_y) are predicted to occur anteriorly given loading is greatest in this region. As a measure of cross-sectional strength (Ruff, 2000; 2008), section moduli values should be greatest in areas of increased loading as compared to regions of decreased loading

Table 2. Study sample dietary categorizations

Taxon	% Fruits	% Leaves	% Seeds	% Other	Dietary designation	References
Gorilla gorilla	15.3	61.1			tough	Rothman et al. (2007)
Piliocolobus badius	7.1	60.7	30.8	1.4 (flowers)	tough	Hayes et al. (1996)
Alouatta caraya	24	76	0	1	tough	Zunino and Rumiz (1986)
Pan troglodytes	64	16	3	2 (flowers)	soft	Conklin-Brittain et al. (2006)
Cercopithecus mitis	54.6	18.9	2.5	3.7 (flowers), 16.8 (insects)	soft	Jaffe and Isbell (2011)
Ateles geoffroyi	82.2	17.2		1	soft	Terhune (2011)
Callicebus moloch	54	28			soft	Hohmann (2009)
Cebus capucinus	68	0.4		0.3 (flowers), 31.3 (other)	soft	Chapman and Fedigan (1990)
Pithecia pithecia	27.8	7.1	60.6	2.2 (flowers)	hard	Norconk (1996), Terhune (2011)
Sapajus apella	53.9*	6.3	16	11.1 (flowers)	hard	Galetti and Pedroni (1994)
Callithrix jacchus	24			42 (exudates), 29 (animal prey)	exudate	Smith and Smith (2013)

*The fruit consumption of *S. apella* includes hard fruits *Cariniana legalis*, *Hymeneae courbaril*, and *Metrodoria stipularis* (see Galetti and Pedroni,

3.3.4 *Data Collection*

Bones under loading have been characterized by beam models (Ohman, 1993; Ruff, 2000), which enable estimates of cross-sectional strength and resistance to bending and torsion to be calculated. Within the cranium, the anthropoid mandibular symphysis has been modeled as a curved beam (Hylander 1984,1985) in which higher concentrations of cortical bone developed lingually to offset the effects of bending forces during chewing. Given the structure and orientation of the zygomatic arch on the skull, a beam model is appropriate, but more complicated because it requires the considerations of a *curved* beam undergoing combinatory loading as a result of mastication. Using a model of a hollow, circular beam for the zygomatic arch requires the collection of data on internal bone organization relative to total cross-sectional area.

Three-dimensional (3D) models of primate skulls were constructed from microCT scans from existing collections at ASU and NEOMED using Amira 3D visualization software (FEI Visualization Sciences Group). Once created, each skull model was placed in the Frankfort horizontal position to standardize their orientation. Using the 3D models of each skull, five locations along the zygomatic arch were identified and resliced along the long axis of the arch using Amira's "obliqueslice" tool. This generated the necessary cross sections at each slice location for analysis. The five slice locations chosen were based on previous work (Hylander and Johnson, 1992) that placed strain gauges at the anterior, midsuture, and posterior areas on a macaque zygomatic arch (Figure 6). This present study incorporated two additional locations (anterior to the suture and posterior to the suture) to provide more coverage of the arch and to determine if these intermediate areas are markedly different from the initial three locations. Arch cross-sections were

extracted, exported and then analyzed with the MomentMacroJ v1.4 program (Ruff, 2006) for ImageJ (http://www.hopkinsmedicine.org/FAE/mmacro.htm). In short, this macro generated estimates of total subperiosteal area, cortical area, the distribution of bone around both the x- and y-axes, and variables describing the tendency of the bone to resist bending forces in the transverse and sagittal planes.

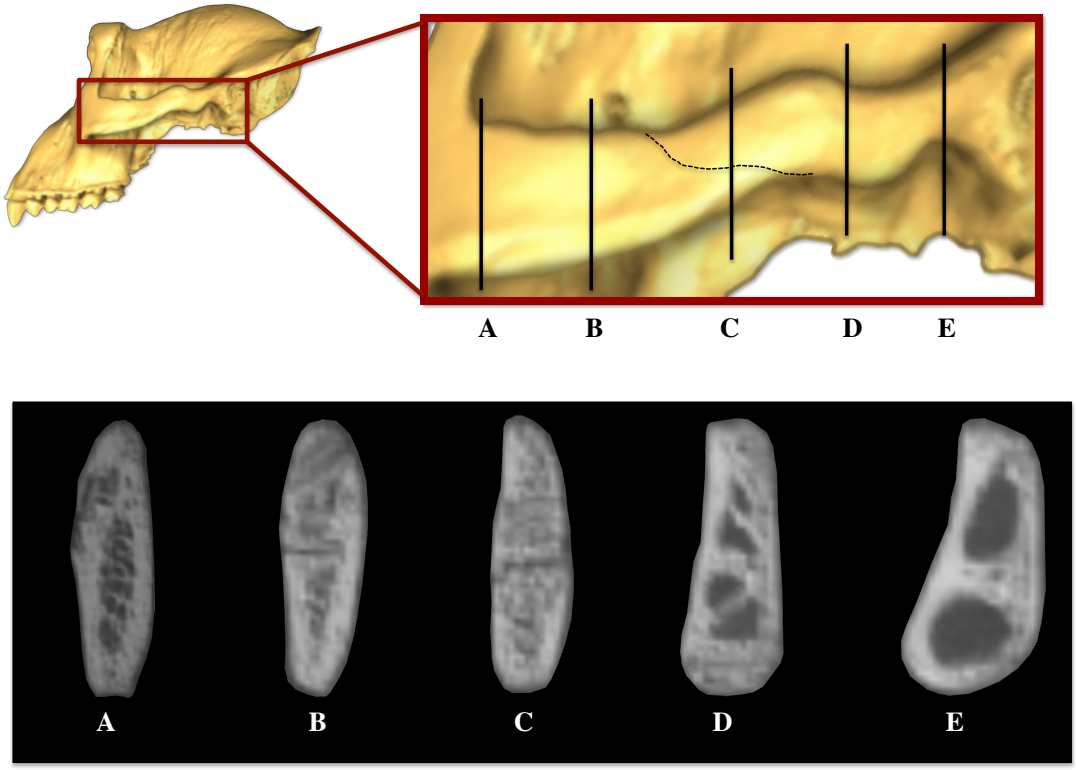

Figure 6. Schematic of five arch slice locations taken on *Gorilla gorilla* specimen. Top: Slice locations (A-E) along zygomatic arch represent (from left to right): anterior, anterior suture, midsuture, posterior suture, and posterior regions. Suture is indicated by the dotted line. Bottom: Resulting cross-sectional images for each slice location.

Using this protocol, four variables were collected on each arch cross-section using the above protocol: cortical area (CA), total subperiosteal area (TA), section modulus about a transverse axis (Z_x), and the section modulus about a superoinferior axis (Z_y) (see Fig. 7 for descriptions). Internal bone architecture, specifically cortical bone distribution, was examined at each of the five arch locations to determine if cortical bone varies by arch location. In response to the range of strains experienced by the arch during mastication, CA is expected to be greater in areas of higher strain (i.e., anterior zygomatic region) and relatively lower in low strain areas (i.e., posterior zygomatic arch). The CA of each cross-section was measured from the cross-sectional slices using Amira. For both the x- and y-axis of each cross-section, the section modulus (Z), a direct measure of the strength of a beam, or in this case, a bone, was measured (O'Neill and Ruff, 2004; Ruff, 2008). Ratios of cortical area to total area (CA/TA) were then calculated to quantify cortical distributions relative to total area at each arch location. Descriptive statistics for CA, TA, and CA/TA ratios are available in Table 3.

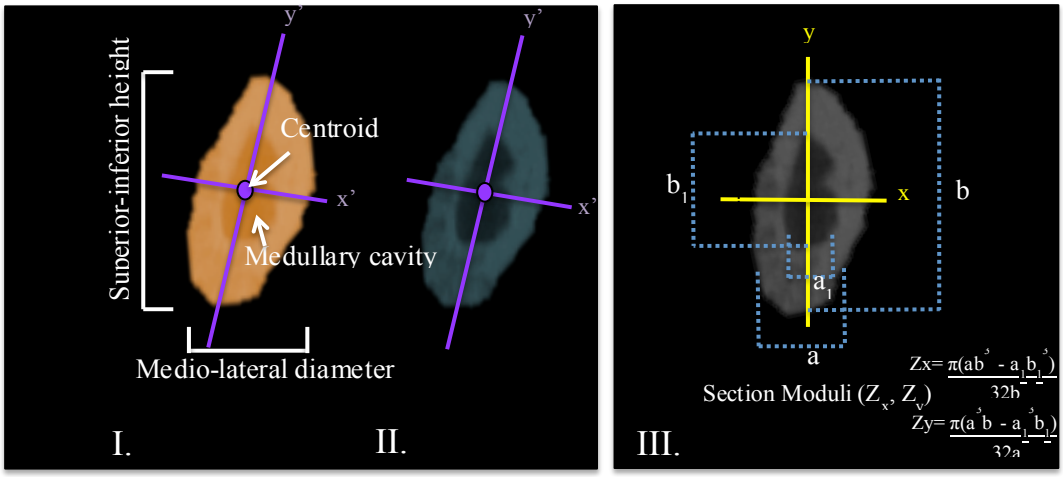

Image: Anterior zygomatic arch cross section of *Sapajus apella* with illustrated examples of biomechanical measures (I) Total subperiosteal area (TA) highlighted in orange. (II) Cortical area (CA) highlighted in blue. The x' and y' axes are the major and minor principal axes, respectively. (III) Illustration of the section moduli (Z_x and Z_y) of a cross-section. Axes x and y are parallel and perpendicular to the horizontal plane. Z_x is measured about the x-axis, whereas Z_y is measured about the y-axis.

Variable	Description[1]
TA	Total subperiosteal area
CA	Cortical area
CA/TA	Amount of cortical bone relative to total subperiosteal area
Z_x	Section modulus about x-axis (I_x/max y radius) measures stiffness about x-axis
Z_y	Section modulus about y-axis (I_x/max x radius) measures stiffness about y-axis

[1]Descriptions taken from momentmacro (NIH image) from www.hopkinsmedicine.org

Figure 7. Biomechanical variables characterizing zygomatic arch cross-sectional form measured from momentmacro readout through ImageJ. The top image illustrates the variables in relation to the cross-sectional image.

Table 3. Species means and standard deviation values for Total Area (TA), Cortical Area (CA), and CA relative to TA (CA/TA)

Taxon	Variable	A	AS	M	PS	P
Gorilla gorilla	TA	35.4558 (7.6452)	33.9513 (13.9263)	32.7179 (14.955)	33.9217 (11.8898)	47.3352(23.1717)
	CA	33.2888(6.2423)	30.0088(9.8665)	28.4458(12.1981)	29.2105(9.9822)	39.7464(15.0996)
	CA/TA	0.9465 (0.0646)	0.9051 (0.0774)	0.88525(0.09275)	0.7822(0.2905)	0.87182(0.0962)
Piliocolobus badius	TA	9.5169(2.6766)	8.9248(2.9359)	7.6469(3.0921)	6.5498(3.0921)	7.9936(2.7698)
	CA	8.6858(1.9292)	8.0636(2.1348)	6.7655(2.7602)	5.9607(2.7876)	7.2460(2.7301)
	CA/TA	0.9258(0.0655)	0.9220(0.0794)	0.9023(0.1031)	0.9347(0.0949)	0.9042(2.2766)
Alouatta caraya	TA	17.9162(10.0091)	12.7031(9.0816)	13.1634(8.7146)	13.9633(7.3909)	14.6163(8.8477)
	CA	15.9154(8.2826)	10.873(7.2456)	11.4542(7.0470)	11.3390(5.5901)	11.4734(6.7075)
	CA/TA	0.9040(0.0413)	0.8892(0.0932)	0.8942(0.0538)	0.8388(0.0914)	0.0823(0.0727)
Pan troglodytes	TA	14.1422(6.0882)	10.2142(2.2671)	9.05415(1.7012)	8.3603(2.37052)	9.7225(4.1521)
	CA	13.7577(6.0391)	9.9518(2.4441)	8.6951(1.8089)	8.0561(2.3479)	9.5102(4.0399)
	CA/TA	0.9684(0.0668)	0.9718(0.06985)	0.96069(0.0763)	0.9634(0.0644)	0.9734(0.0433)
Cercopithecus mitis	TA	11.3276(4.2234)	8.6506(3.7805)	4.4172(2.1963)	4.3253(1.0926)	5.5412(2.3757)
	CA	9.3961(2.8491)	7.2054(2.7926)	3.9598(1.7053)	3.8287(0.9299)	4.4078(1.3943)
	CA/TA	0.8490(0.09377)	0.8663(0.1106)	0.9176(0.0725)	0.8893(0.0800)	0.8528(0.1958)
Ateles geoffroyi	TA	4.9899(1.3993)	3.9661(1.6237)	3.2569(1.0066)	3.6914(1.3270)	4.9183(1.1081)
	CA	5.0596(1.7361)	4.0455(1.5447)	3.1717(0.6384)	3.4569(1.1327)	4.7939(1.2732)
	CA/TA	1.0216(0.2550)	1.0770(0.4345)	1.0590(0.3774)	0.9979(0.2727)	1.0123(0.3746)
Callicebus moloch	TA	4.6458(2.2393)	3.1897(1.1292)	2.4181(0.8477)	2.7749(0.6517)	2.4365(1.2645)
	CA	4.1835(1.9605)	3.0291(1.0419)	2.2166(0.9831)	2.3611(0.4592)	2.1304(1.0443)
	CA/TA	0.9132(0.0783)	0.9534(0.0272)	0.9000(0.1604)	0.8818(0.1912)	0.9010(0.0959)
Cebus capucinus	TA	5.5315(1.5828)	4.4209(2.1652)	3.0914(1.4048)	2.9101(0.7358)	2.6486(0.7921)
	CA	5.0310(1.5953)	3.9588(2.0772)	2.7643(1.1104)	2.7707(0.6665)	2.4159(0.6302)
	CA/TA	0.9078(0.0632)	0.8913(0.0527)	0.9119(0.0636)	0.9547(0.0442)	0.9229(0.0703)
Pithecia pithecia	TA	2.3444(0.0823)	2.1195 (0.9272)	0.3239(0.1306)	0.5347(0.1876)	0.50022(0.1889)
	CA	2.2893(0.7643)	2.0157(0.9057)	1.8075(0.4937)	2.889(0.8132)	2.6213(0.7583)
	CA/TA	0.9802(0.0192)	0.9468(0.0159)	0.8367(0.0919)	0.8250(0.1208)	0.8150(0.1728)
Sapajus apella	TA	7.7627(1.1625)	4.1549(0.5941)	3.3613(0.5902)	3.0082(0.5687)	3.4289(0.8065)
	CA	6.5799(0.9523)	3.4156(0.5022)	2.8602(0.3341)	2.6583(0.4380)	3.2014(0.7312)
	CA/TA	0.8503(0.0610)	0.8248(0.0675)	0.8605(0.0913)	0.8882(0.07224)	0.9351(0.0477)
Callithrix jacchus	TA	1.0742(0.1287)	0.9240(1.2162)	0.8032(0.1821)	0.7404(0.2735)	0.9552(0.3870)
	CA	1.0359(0.1075)	0.8814(0.1946)	0.7431(0.1528)	0.6932(0.2536)	0.8351(0.3071)
	CA/TA	0.9665(0.0398)	0.9577(0.0494)	0.9310(0.05144)	0.9455(0.0865)	0.8894(0.0938)

3.3.5 *Data analysis*

Because this study's primary focus is to quantify cortical bone distributions, and to compare those distributions by arch region, species, and diet type, these analyses concentrated on the five previously mentioned variables. In species that have males, females, and/or unknown individuals present, each sex was compared intraspecifically for each variable to determine if there were any significant effects of sex. All comparisons found no significant differences. Therefore, males, females, and unknown individuals for each species were analyzed together.

All data were log transformed in order to meet assumptions of normality and homogeneity of variance. Log transformed cortical area (CA) measurements were compared using a mixed effects analysis of variance (ANOVA) to address whether cortical bone distributions were greatest anteriorly and lowest posteriorly. A Bonferroni correction was applied to account for multiple comparisons. Post-hoc paired *t*-tests comparing log transformed cortical area distributions between location pairs (e.g., anterior v. anterior suture, anterior v. midsuture, etc) throughout the arch were performed on all significant results. To compare the amount of cortical area (CA) relative to total area in a particular location, a ratio of cortical area/total area (CA/TA) was calculated and compared between regions. Because the uncorrected CA/TA ratios did not meet the statistical assumptions for normality, a log-transformed ratio of logCA/logTA was generated for each species so that pairwise comparisons between taxa of different diets could be performed. The transformed CA/TA ratios in anterior regions were compared among diet types using pairwise comparisons between closely related taxa of differing diet to determine if primates who fed on resistant food items possessed more CA as compared to non-resistant feeders. A multivariate analysis of variance (MANOVA) was performed along with pairwise comparisons on measures of Z_x and Z_y for all taxa to determine if section moduli values were greatest anteriorly as compared to posteriorly. All calculations were performed in the software program R studio (RStudio Team, 2015)

3.4 Results

Log transformed measures of CA at each arch location were analyzed using a mixed effects ANOVA. The ANOVA compared log transformed CA measures by

location within a species. The results of the mixed-effects ANOVA revealed significant differences across arch locations for every taxon except *Callithrix jacchus* (see Table 4).

Table 4. ANOVA results for logCA distributions across arch locations

Taxon	**Result**
Gorilla gorilla	**S** (F=3.826, p=0.0119)
Piliocolobus badius	**S** (F=5.525, p=0.0027)
Alouatta caraya	**S** (F=4.227, p= 0.0122)
Pan troglodytes	**S** (F=6.761, p=0.0006)
Cercopithecus mitis	**S** (F=14.85, p=0.0000)
Ateles geoffroyi	**S** (F=2.974, p=0.0364)
Callicebus moloch	**S** (F= 15.76, p=0.0007)
Cebus capucinus	**S** (F=50.44, p=0.0000)
Pithecia pithecia	**S** (F=6.41, p=0.0129)
Sapajus apella	**S** (F=36.97, p=0.0000)
Callithrix jacchus	**NS** (F=2.087, p=0.1230)

The results of post-hoc paired *t*-tests comparing log transformed cortical area distributions between location pairs (e.g., anterior v. anterior suture, anterior v. midsuture, etc) throughout the arch are listed in Table 5. Tough food consumers showed no significant results, which indicates that the CA in anterior, middle, and posterior portions of the arch are not significantly different from one another. Soft food consumers showed significant differences primarily in their anterior v. midsuture, anterior v. posterior suture, and anterior v. posterior regions comparisons. This indicates that soft food consumers have significantly different amounts of cortical area from anterior to posterior regions. *Sapajus apella,* a hard-object feeder that also consumes fruit, yielded significant differences ($p<0.001$) in CA amounts in all anterior comparisons, similar to soft food consumers. In contrast, *Pithecia pithecia,* showed no significant differences in cortical bone area by region, which is more similar to the distributions observed in tough feeders.

Table 5. Anterior logCA paired *t*-test results*

Taxon	A v. AS	A v. M	A v. PS	A v. P	AS v. M	AS v. PS	AS v.P	M v. PS	M v. P	PS v. P
Gorilla gorilla	0.1085	0.136	0.1404	0.3162	0.3659	0.7069	0.0537	0.5588	0.0166	0.0068
Piliocolobus badius	0.1572	0.0279	0.022	0.137	0.0297	0.0395	0.3233	0.0904	0.4178	0.0355
Alouatta caraya	0.0124	0.0121	0.0388	0.0646	0.7408	0.8674	0.9053	0.8394	0.8286	0.9189
Pan troglodytes	0.0489	0.0244	**0.0009**	**0.0024**	0.0445	0.5438	0.4425	0.2144	0.8877	0.3076
Cercopithecus mitis	0.0374	**0.0004**	**0.00003**	**0.0027**	**0.0006**	**0.002**	0.1028	0.8491	0.4638	0.3143
Ateles geoffroyi	0.108	0.0292	0.115	0.8517	0.321	0.5438	0.2208	0.6297	0.0261	0.0591
Callicebus moloch	0.0419	**0.0006**	0.0235	**0.0039**	0.0253	0.131	0.0203	0.3434	0.4837	0.2537
Cebus capucinus	0.0253	**0.0007**	**0.0005**	**0.0001**	**0.0011**	0.0205	**0.0001**	0.6074	0.1485	0.0347
Pithecia pithecia	0.4372	0.0522	0.1754	0.3022	0.7719	0.0869	0.1251	0.0195	0.0214	0.0273
Sapajus apella	**0.0017**	**0.0001**	**0.00003**	**0.0016**	0.0408	0.0441	0.3138	0.241	0.3077	0.1054
Callithrix jacchus	0.2144	0.0341	0.0517	0.2483	0.3619	0.3164	0.9951	0.6381	0.4365	0.1416

***Bolded** values are significant after Bonferroni correction

To determine whether CA was relatively greater anteriorly than posteriorly, ratios of cortical area/total area (CA/TA) were calculated and averaged by species and then compared across arch regions. It was predicted that the areas of greatest masticatory loading (i.e., anterior portions of the arch) should exhibit greater amounts of cortical bone relative to posterior portions as a reflection of masticatory strain distribution. Of the 11 taxa compared, 8 yielded their highest CA/TA ratios in anterior and/or anterior suture locations (see Table 3). Tough food consumers all possessed their absolute highest CA/TA ratios in their anterior arch sections. Soft consumers in general varied in which regions had the greatest proportion of cortical area with three of the five taxa, (*Ateles geoffroyi, Callicebus moloch,* and *Pan troglodytes*), yielding their greatest CA/TA ratios in anterior and/or anterior suture locations. Unexpectedly, *Sapajus apella* exhibited its greatest CA/TA ratios in posterior portions as did *Cebus capucinus*. Box plots of anterior CA/TA ratios for each taxa are shown in Figure 8.

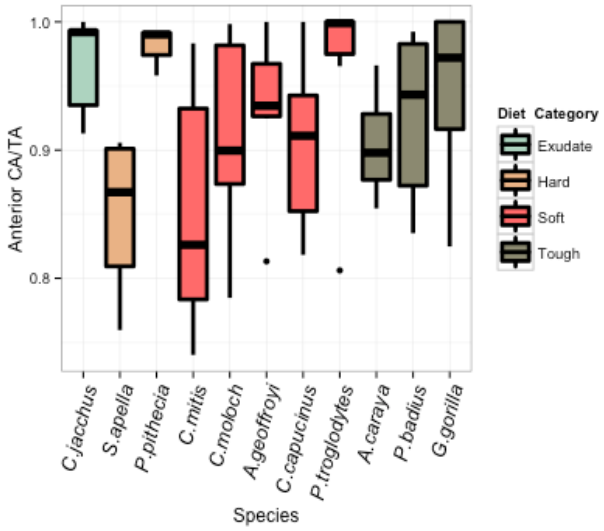

Figure 8. Box and whisker plot of anterior CA/TA measures for all study taxa grouped by diet category

Pairwise comparisons between closely related taxa of different diets were performed on log-transformed variables of CA, section moduli (Z_x and Z_y), and CA/TA for anterior arch regions (Table 6). Significant differences ($p \leq 0.01$) in logCA measures were found in every comparison except when exudate consumer *Callithrix jacchus* was compared to hard-object consumer *Pithecia pithecia* ($p=0.056$). All pairwise comparisons on $\log Z_x$ were significant except in the comparison between *Cebus capucinus* and *Sapajus apella*. Comparisons using $\log Z_y$ were significant except in the pairings of *Callithrix jacchus* and *Pithecia pithecia, Sapajus apella* and *Piliocolobus badius*, and *Sapajus apella* and *Alouatta caraya*. In contrast, no comparisons for logCA/TA were significant except for the comparison of *Sapajus apella* and *Cebus capucinus* (Table 6).

Table 6. Results of pairwise comparisons on anterior regions

#	Comparison	Diet group	Variable	Results
1	*C. jacchus v. P. pithecia*	exudate v. hard	logCA	(*t=3.7459, p*=0.0561)
2			$\log Z_x$	(*t=5.3337, p*=0.0131)
3			$\log Z_y$	(*t=1.0988,* NS)
4			logCA/TA	(*t=-0.5645,* NS)
5	*C. jacchus v. C. moloch*	exudate v. soft	logCA	(*t=6.7387*, *p*=0.0003)
6			$\log Z_x$	(*t=11.2983, p*<0.0001)
7			$\log Z_y$	(*t=7.5328, p*<0.0001)
8			logCA/TA	(*t=2.6816,* NS)
9	*S. apella v. P. badius*	hard v. tough	logCA	(*t=2.6868, p*= 0.0220)
10			$\log Z_x$	(*t=2.834, p*=0.0165)
11			$\log Z_y$	(*t=0.2107,* NS)
12			logCA/TA	(*t=1.0554, p*=0.0230)
13	*S. apella v. C. capuchinus*	hard v. soft	logCA	(*t=-2.6768, p*=0.0120)
14			$\log Z_x$	(*t=-1.8756,* NS)
15			$\log Z_y$	(*t=-3.3841, p*=0.0049)
16			logCA/TA	(*t=1.0554*, NS)
17	*C. jacchus v. A. caraya*	exudate v. tough	logCA	(*t=12.3468, p*<0.0001)
18			$\log Z_x$	(*t=12.9412, p*<0.0001)
19			$\log Z_y$	(*t=8.8365, p*<0.0001)
20			logCA/TA	(*t=-0.4733*, NS)
21	*S. apella v. A. caraya*	hard v. tough	logCA	(*t=3.5844, p*=0.0124)
22			$\log Z_x$	(*t=5.0185, p*=0.0017)
23			$\log Z_y$	(*t=1.3214, p*=NS)
24			logCA/TA	(*t=3.0235*, p=0.0213)
25	*A. caraya v. A. geoffroyi*	tough v. soft	logCA	(*t=4.4399, p*=0.0019)
26			$\log Z_x$	(*t=5.3665, p*=0.0005)
27			$\log Z_y$	(*t=3.2114, p*=0.0090)
28			logCA/TA	(*t=-0.821*, NS)
29	*G. gorilla v. P. troglodytes*	tough v. soft	logCA	(*t=5.7426, p*=0.0002)
30			$\log Z_x$	(*t=4.9465, p*=0.0009)
31			$\log Z_y$	(*t=4.7355, p*=0.0005)
32			logCA/TA	(*t=-0.0537,* NS)

To address prediction three, measures of bone cross-sectional strength, Z_x and Z_y, were compared by arch region intraspecifically, interspecifically, and by diet type. When compared by arch location, the highest values of Z_x appeared in anterior cross-sections

across all taxa (see Appendix A for descriptive statistics for section moduli measures, Z_{max}, Z_{min}, and Theta values; Tables SM1 and SM2). Similarly, Z_y was also highest in all anterior cross-sections except for *Gorilla gorilla* whose greatest values were found in posterior regions. Across diet types, hard and tough food consumers exhibited the greatest anterior Z_x values compared to soft and exudate consumers, with the exception of *Pan troglodytes*. MANOVA analyses of these variables were performed on each species to test for differences in mean values. A Bonferroni correction was applied to account for the multiple comparisons. The results of the MANOVA found varying results among different diet types (Table 7). In general, tough food consumers showed significant differences in midsuture - posterior and posterior suture - posterior comparisons. Soft food consumers showed a greater spread in values, in which anterior - posterior/posterior suture and midsuture - posterior portions were significantly different from one another. Both *Ateles geoffroyi* and *Pan troglodytes* yielded no significant differences. Hard-object consumer *Sapajus apella* showed significant differences in all anterior v. midsuture and anterior v. posterior comparisons. In contrast, *Pithecia pithecia* exhibited no significant differences among regions. *Callithrix jacchus* showed significant differences in anterior - posterior, and midsuture - posterior comparisons. Pairwise comparisons of anterior Z_x regions in taxa of different diet types revealed significant results ($p \leq 0.01$) in all comparisons except *Sapajus apella* and *Cebus capuchinus* (see Table 6).

Table 7. MANOVA Results* on Z_x and Z_v

Taxon	A v. AS	A v. M	A v. PS	A v. P	AS v. M	AS v. PS	AS v. P	M v. PS	M v. P	PS v. P
Gorilla gorilla	NS	NS	0.017	0.0262	NS	NS	NS	NS	NS	NS
Piliocolobus badius	NS	NS	0.0497	0.0275	NS	NS	**0.0005**	NS	**0.0007**	**0.0018**
Alouatta caraya	NS	NS	NS	0.0092	NS	NS	0.0084	NS	**0.0001**	**0.0005**
Pan troglodytes	NS	NS	0.0346	NS	NS	NS	NS	NS	NS	NS
Cercopithecus mitis	NS	**0.0018**	**0.00008**	**<0.000**	**0.0089**	**<0.000**	**0.0003**	NS	**0.0078**	NS
Ateles geoffroyi	NS	NS	NS	NS	NS	NS	NS	NS	0.0241	0.0423
Callicebus moloch	NS	0.0345	**0.0059**	**<0.000**	NS	0.0366	**0.0001**	NS	**0.0002**	**0.0034**
Cebus capucinus	0.0423	**0.0002**	**<0.000**	**0.0001**	NS	NS	**0.0018**	NS	**0.0002**	**0.0001**
Pithecia pithecia	NS	NS	NS	NS	NS	NS	NS	NS	0.0201	NS
Sapajus apella	**0.0003**	**<0.000**	**<0.000**	**0.0001**	NS	0.0133	NS	NS	NS	NS
Callithrix jacchus	0.0349	0.0204	0.0216	**0.0014**	NS	0.0131	**0.0001**	0.0022	**<0.000**	0.0106

***Bolded** values are significant after Bonferroni correction

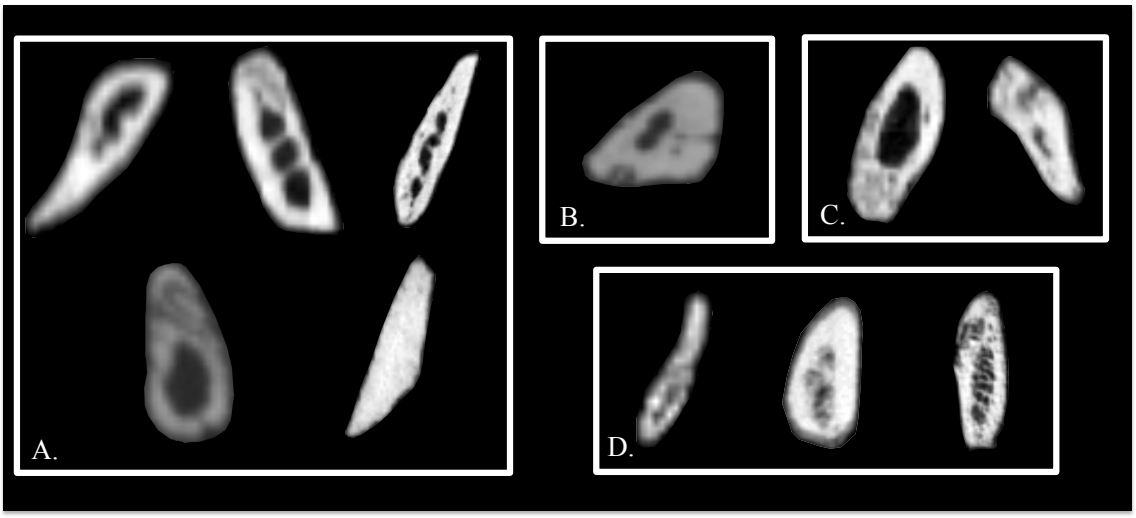

Figure 9. Anterior cross-sectional images for all study taxa, grouped by diet category. A. Soft consumers (top row, L to R): *Ateles geoffroyi*, *Cercopithecus mitis*, *Callicebus moloch* (bottom row, L to R): *Cebus capucinus*, *Pan troglodytes*. B. Exudate consumer *Callithrix jacchus*. C. Hard consumers (L to R): *Sapajus apella*, *Pithecia pithecia*. D. Tough consumers (L to R): *Alouatta caraya*, *Piliocolobus badius*, *Gorilla gorilla*. Note that images are sized similarly for the purposes of illustration.

3.5 Discussion

The strength of a bone is a function both of the CA present and how cortical bone is distributed around the centroid of the axis (Stock and Shaw, 2007). When viewed in cross-section, one can observe differences in the deployment of CA at various points along the zygomatic arch (Figure 9). Quantifying these differences and linking them with diet is an important step towards understanding how internal bone structure resists external masticatory loading. The hypothesis that the internal architecture of the arch, namely CA and section moduli (Z_x and Z_y) values, is patterned based on known strain distributions was supported in the majority of taxa tested. The greatest amounts of cortical area relative to total area were found in anterior or anterior suture regions in 8 of the 11 taxa tested. Unlike other taxa, *Cebus capuchinus*, *Sapajus apella,* and

Cercopithecus mitis exhibited their greatest CA distributions in posterior suture and posterior arch portions. One reason some species did not follow the expected pattern may be related to interspecific differences in strain distributions. In both *Sapajus apella* and *Cebus capuchinus* the highest relative amounts of cortical bone appear in posterior and posterior suture regions while *Cercopithecus mitis* yielded its greatest values in midsuture and posterior suture sections. The published values on zygomatic arch strains in primates have primarily been limited to studies on macaques (e.g., Hylander and Johnson, 1997), a group not included in the present study. Because strain gradients may be species specific, CA is likely best examined in concert with documented strain measures for a particular species.

Tough food consumers (*Piliocolobus badius, Gorilla gorilla,* and *Alouatta caraya*) all contained their highest CA/TA ratios in their anterior regions. For these taxa, loading associated with a tough diet generates greater CA amounts in anterior regions relative to the rest of the arch. *Callicebus moloch*, a soft food consumer that also ingests leaves in varying amounts (23-66% (Müller, 1996)), also had its greatest amounts of CA in anterior regions. Given the range of tough food consumption reported for this species, it is possible that masticatory loading associated with such a diet is sufficient to yield CA amounts more similar to strict tough food consumers than soft food consumers. Taylor et al. (2008) notes that material properties of a food, rather than consumption percent, may explain the patterning of such variables. In this case, the toughest food consumed may influence how much CA is maintained at a specific location along the arch.

In contrast, the apparent lack of a pattern among soft food consumers with respect to the location of their greatest CA/TA ratios along the arch may be due to a combination

of other factors that influence load resistance. The magnitude of the loads produced by processing soft foods may not be sufficient for the generation and maintenance of more bone in certain regions relative to other areas. If a primate consumes more mechanically challenging foods (e.g., leaves and/or nuts, seeds) on a seasonal basis then relatively high amounts of cortical bone may not be continuously maintained. The type of load (i.e., bending, torsion, shear) experienced during chewing varies and may be due in part to the nature of the foods being processed. Preliminary analyses of arch form in a group of haplorhines have shown that resistant feeders (hard and/or tough feeders) have arch cross-sections that are shaped differently than non-resistant feeders at different points along the arch (Edmonds, 2015). This suggests the dominant loading type varies across these taxa, which likely influences the internal bone architecture. Because loading in this region is so different than loading in the postcrania, the threshold for increased bone maintenance in anterior regions, despite being the site of the attachment for the masseter, may not be met. Other factors such as zygomatic arch cross-sectional shape and/or positioning on the lateral portion of the cranium should be taken into consideration for future analyses as they may play a large role in mediating masticatory loading. Non-mechanical factors such as sexual dimorphism may also contribute to some differences in the arch's morphology.

In vivo studies of primates chewing on various types of foods suggest that the activation of the deep and superficial masseter muscles subjects the anterior portion of the zygomatic arch to a vertical force component and (to a lesser degree) a medial force component. Together, these actions induce relatively high instances of parasagittal

bending. To combat these bending forces, increased strength in the superoinferior direction would be necessary.

The section moduli measures, Z_x and Z_y, quantify the bending tendency of a cross-section about both the transverse and sagittal planes. In this study, the highest measures of Z_x (i.e., the measure of axial strength about a transverse axis – x in Fig 2. III) occurred anteriorly in every species, thus indicating that this region was the most strengthened relative to the other portions of the arch. Similarly, Z_y (i.e., the measure of axial strength about a superoinferior axis – y in Fig. 2. III) was greatest anteriorly in all species except *Gorilla gorilla*. These results support the prediction that measures of axial strength, about both the superoinferior and transverse axes, are greater in anterior regions than in posterior regions in all study taxa.

Pairwise comparisons between closely related taxa with, different diets yielded significant differences in anterior logZ_x measures in all pairs but one comparison. Notably, the comparisons between a hard-object feeder *Sapajus apella* and tough food consumer *Piliocolobus badius* were significantly different ($p=0.016$) as well as between *Sapajus apella* and soft food consumer *Cercopithecus mitis* ($p=0.003$). This suggests hard-object feeders may have significantly different Z_x measures, and therefore their zygomatic arches are "strengthened" differently than both tough and soft feeders.

When Z_x and Z_y are compared intraspecifically, Z_x values are greater than Z_y values at each zygomatic arch region within each species. This suggests parasagittal bending forces are greater than transverse bending. The presence of lower Z_y values relative to Z_x values overall may be due to the fact that the zygomatic arch is a curved beam-like structure, and is thus inherently bent about the transverse x-axis. In addition,

the attachment location and subsequent activation of the masseter muscles does not generate force vectors that would cause significant bending in the transverse plane.

3.6 Conclusions

Cortical area has been hypothesized to track with loading, and the results of this study found the majority of taxa adhere to this pattern. Cortical area alone, however, does not capture the complete picture. Incorporating measures of arch strength provides a way to quantify which region is most fortified against an applied load. While CA may not always be greatest anteriorly, the relative strength of the arch is greatest at the anterior portions. Intuitively, this makes sense given the attachment of the masseter muscle and in light of the observed strain values in experimental studies, which demonstrate that the anterior zygomatic arch routinely experiences the greatest masticatory strains. Broadly speaking, these results support the notion that internal bone architecture patterns with masticatory strain values.

Primates vary greatly in their dietary breadth. As such, consideration of the effects of different diets on craniofacial morphology is critical. An important distinction within the food material properties literature is the dichotomy between the effects of hard-object consumption and tough food consumption and how the nature of those diets manifests in the bony morphology (Spencer, 2003; Wright, 2005; Yamashita, 2008b). Studies on primate mandibular morphology have not found adaptations that distinguish the effects of a hard versus a tough diet (Hylander, 1988; Daegling and Grine, 1991; 2007) suggesting that there is not a single mandibular form necessary to process those diets (Daegling et al., 2011). However, the significant differences in the pairwise

comparisons between “hard” and “tough” feeders with respect to CA and Z_x suggests that zygomatic arch morphology may detect dietary signals and help to disentangle these diet types.

Notably, the “hard-food consumer versus tough food consumer” debate still surfaces frequently in paleoanthropology when assessing the diets of the *Paranthropus* species (Wood and Strait, 2004; Ungar, 2011). Previous work on *Paranthropus boisei* has suggested it subsisted on tough foods (Dubrul, 1977), while others have proposed it consumed hard foods (Peters, 1987) or just consumed greater quantities of food (Walker, 1981). A distinctive feature shared by the *Paranthropus* species is their wide, flaring, and anteriorly placed zygomatic arches. This has been widely accepted as an indicator of dietary specialization yet a critical examination of the internal architecture of their arches has not been carried out. Furthermore, measures of paranthropine CA, TA, and section moduli (to the extent they are preserved) would provide novel insights into the mechanical behavior of their arches and how they differ from other primates, both living and extinct.

CHAPTER 4: ZYGOMATICOTEMPORAL SUTURAL COMPLEXITY IN RELATION TO DIET IN PRIMATES

4.1 Abstract

Cranial sutures are primarily composed of complex, collagenous fibers that serve as joints between the bones of the skull. Cranial suture complexity, defined as the degree of interdigitation of these collagenous fibers, is thought to vary in relation to the mechanical demands of the skull. These sutures link bones together, allowing movement between parts of the skull during growth, while also serving to help dissipate stress generated by mastication. However, sutures presumably create areas of potential weakness in the presence of high loads. To combat this weakness, increased interdigitation of the bones is thought to minimize and/or mitigate these loads. The zygomatic arch experiences considerable masticatory loading during feeding and the zygomaticotemporal suture, the single suture on the arch, is assumed to experience similar loads. Previous work shows increased sagittal sutural complexity tracked with mechanically resistant diets in *Cebus* but this pattern has not been shown to extend to other cranial sutures. If greater loading promotes increased sutural complexity, then other sutures in the masticatory complex (e.g., zygomaticotemporal suture) are predicted to also reflect differences in diet type. This study employed two different dietary schemes, total consumption percent and food material properties (FMPs) data, to investigate the relationship between sutural complexity and diet type in primates. The results indicate that neither dietary approach was a good predictor for sutural complexity in this primate sample. These results suggest that the zygomaticotemporal suture is not sensitive to the

effects of dietary loads and/or the magnitude of loading experience is not sufficient to catalyze significantly increased sutural complexity in this region.

4.2 Introduction

One of the critical components underlying the biomechanics of the craniofacial system is an understanding of the role of cranial sutures during dynamic loading. Cranial sutures are composed of collagenous connective tissue fibers that interlock neighboring edges of bones together. These complex, fibrous structures function as joints between bones of the skull (Moss, 1957; Koskincn et al., 1976, Johansen and Hall, 1982; Kokich, 1986; Jaslow, 1990; Burn et al., 2010; Di Ieva, 2013) and function to prevent the cranial bones from separating during loading. Specifically, sutures mediate the effects of bone deformation during instances of cyclic loading from muscle activity, cranial distortion during birth, and traumatic impacts (Mao et al. 2003) as well as mechanical stress transmission (Moss, 1957; Maloul et al., 2013).

In humans, sutures are relatively simple at birth and are composed of straight edges that interlock to varying degrees (Jaslow, 1990). Postnatally, sutures are characterized as relatively simple, flat joints with some degree of patency. In contrast, the sutures in an adult are characterized by relatively greater degrees of interdigitation and interlocking bony projections that typically fully fuse by late adulthood (Rice, 2008; Maloul et al., 2013). The degree of patency in a suture has been experimentally shown to affect the local strain environment of the suture (Behrents et al., 1978; Herring and Mucci 1991; Herring and Teng, 2000) since more patent sutures offer greater flexibility than more fused sutures. As such, the relative stiffness or rigidity of cranial sutures changes in

response to the needs of craniofacial development (Weidenreich, 1941; Moss & Young, 1960; Moss, 1969; Moss and Salentijn, 1969; Enlow and Hans, 1996; Mooney et al. 2002; Richtsmeier et al., 2006; Sardi et al., 2007; Cray et al. 2011) and mastication (Herring and Mucci, 1991; Herring, 1993, 2008; Herring and Teng, 2000; Herring et al., 2001; Mao, 2002; Fong et al., 2003; Byron et al., 2004a, 2008; Alaqeel et al., 2006; Wu et al., 2007; Yu et al. 2009) throughout ontogeny leading to differences in the potential to resist loading as well. A key difference between these two factors is that neurocranial expansion terminates at adulthood while masticatory loading and suture closure persists throughout the life of the individual (Meindl and Lovejoy, 1985; Cray et al., 2008; 2010).

Localized, elevated strain levels have been identified over sutures in numerous *in vivo* and *in vitro* strain gauge studies (e.g., Behrents et al., 1978; Smith and Hylander, 1995; Herring and Mucci, 1991; Herring, 1993; Jaslow and Biewener, 1995; Rafferty and Herring, 1999; Herring and Teng, 2000; Sun et al., 2004; Shibazaki et al., 2007; Wang et al., 2008) indicating sutures are mechanically relevant to models of the cranium. In adults, the cranium is modeled as a static and stable body whose sutures act as shock absorbers that dissipate stresses transmitted through the skull (Buckland-Wright, 1978; Herring and Mucci, 1990, Byron et al., 2004a; Herring and Teng, 2000; Jaslow, 1990b; Jaslow and Biewener, 1995; Pritchard et al., 1956; Rafferty et al., 2003; Rayfield, 2004, 2005; Byron, 2009; Maloul et al., 2013). While it is known that cranial sutures form even in the absence of muscle activity (Persson, 1983), many studies have supported the hypothesis of Moss (1957) which proposed that sutural morphology and interdigitation are secondary responses to extrinsic forces and that sutures disturb local strain flow (Wang et al., 2010).

By increasing the degree of complexity (i.e., interdigitation), the suture is able to absorb more energy by virtue of increasing the surface area across which collagen fibers of different bones attach (Jaslow, 1990; Nicolay and Vaders, 2008). The nature of the fiber's orientation better adapts the structure to resist either tensile or compressive loads. Obliquely attached fibers are able to resist compressive forces (Rafferty and Herring, 1999) as well as accommodate stresses emanating from different directions (Jaslow, 1990; Rafferty and Herring, 1999; Byron et al., 2004, Nicolay and Vaders, 2008). In contrast, the cruciate or perpendicular arrangement of "butt-ended" sutures are associated with tensile resistance (Herring and Teng, 2000). Thus, the relative increase in interdigitation through growth is presumed to be directly linked to the magnitude of mechanical loads imposed on the cranium (Masler and Schour, 1951, Moss 1957, Oudhof 1982; Jaslow, 1990) and the orientation of the sutural fibers are indicative of the load type experienced.

Under these assumptions, previous studies have investigated the relationship between suture morphology and response to loading during the functioning of the craniofacial complex in instances such as rooting in pigs and peccaries (Herring, 1972), head butting in sheep (Jaslow, 1989), competitive horn sparring in goats (Jaslow and Biewener, 1995) and antler use in white-tailed deer (Nicolay and Vaders, 2006). Using goats (*Capra hircus*), Jaslow (1990) identified several key findings regarding the response of cranial sutures to three point bending loads: energy absorption by sutures was positively correlated with increased sutural complexity, such that greater interdigitation enabled more bending strength. Maloul et al. (2013) also found this to be true in the cranial sutures of humans. While sutures alone are generally not as strong as pure cranial

bone (which is likely due to the collagenous component of the suture), highly interdigitated sutures were found to resist bending loads to the same extent as pure bone when loaded slowly (Hubbard et al., 1971; Jaslow, 1990). Importantly, cranial bone with sutures was found to absorb more energy than bone without sutures, which further reinforces the mechanical importance of their presence on the cranium (Jaslow, 1990).

Studies in the last decade have used fractal analysis as a meanigful tool for quantifying the complexity of natural structures, such as sutures, because natural structures are typically complex, and irregularly shaped (Long, 1985; Slice, 1993; Monterio and Lessa, 2000). Put simply, the fractal dimension (D) is calculated as a measure of suture complexity or interdigitation. A suture that is more interdigitated (deviates from a straight line), or more complex, results in larger fractal value compared to a suture that is relatively less interdigitated (Monterio and Lessa, 2000).

Within primates, the primary source of mechanical loading in the skull is related to mastication and the loading associated with triturating different types of food items. In addition, ingestive biting, accessing hard objects, and breaching the coatings of foods are also sources of loading in the skull. One of the contributing factors to masticatory loading is related to bite force, which is proportional to recruitment and size of the masticatory muscles. Experimental studies have detailed a linear relationship between temporalis muscle activation and bite force using electromyographic (EMG) measurements (Van Eijden, 1990; Van Eijden et al., 1990). To examine the extent to which muscle recruitment impacted sutural morphology, Byron et al. (2004a) employed myostatin-deficient mouse models to study the effects of increased temporalis muscle mass, and therefore increased stress, on the sagittal suture. This study found that

increased temporalis muscle size induced larger tensile loads on the sagittal suture during activation, which contributed to instances of greater sutural complexity and waveform formation in the sagittal suture (Byron et al. 2004a). This result has been confirmed in other studies as well (Herring and Teng, 2000; Mao, 2002, Lieberman et al., 2004a) suggesting that increased masticatory muscle recruitment induces bone loading to the extent that sutural interdigitation increases in response. Thus, in instances where mechanically resistant food items are consumed, the concomitant increase in masticatory muscles recruitment presumably leads to increased sutural complexity as well.

Beyond model organisms in experimental settings, species of caiman (*Caiman*) that consume hard foods have been found to possess more complex cranial sutures than those of congeners (Monteiro and Lessa, 2000). Specifically *C. latirostris*, a type of Caimen that consumes gastropods with hard shells, possessed the largest fractal measures in the suture between the maxilla and nasal bones; an area that is important for maintaining stability and functional integrity of the skull during feeding (Monterio and Lessa, 2000). One possible functional interpretation is that because this species possesses a relatively broad snout, and consumes hard-shelled mollusks, the skull experiences high shearing loads during each bite necessitating increased sutural formation to resist these loads (Monterio and Lessa, 2000). A similar phenomenon has been observed in primates, in which Byron (2009) noted that cranial suture complexity in cebids varied such that the hard-object feeder *Sapajus apella* possessed more complex sagittal sutures than other closely related taxa *Cebus albifrons*, *Cebus capucinus*, and *Cebus olivaceus*. Coupled with their robust mandibular morphology, these results suggest that the presence of relatively more complex sutures in the *S. apella* cranium is a result of relatively higher

jaw muscle activity and increased chewing forces as compared to other cebids (Byron, 2009). It is also important to note that the ingestive behaviors of these taxa are also key sources of loading in their cranium and may be more important than masticatory forces alone. Fractal measures of cranial sutures in mammals generally exceed the values found in reptiles based on the global shape differences in the skull and differences in dental morphology and bone architecture. Furthermore, the effect of suture morphology and patency has been found to alter strain levels in lizards (Moazen et al., 2008) but not to the same extent in primates (Wang et al., 2010), suggesting that suture morphology may be more important in animals with relatively more patent sutures or greater suture to bone volume (Curtis et al., 2013). Despite these differences, the consumption of hard objects appears to instigate increased sutural complexity in both groups.

In a comparative study of chimpanzee (*Pan troglodytes*) and gorilla (*Gorilla gorilla*), ectocranial suture activity, defined as the relative amount of bone formation due to osteoblast and osteoclast activity, differs between these two closely-related taxa resulting in differential timing of sutural closure (Cray et al., 2011). Compared to other extant hominoids, gorillas possess a more robust masticatory complex characterized by the presence of large temporalis and masseter muscles and a pronounced sagittal crest (Shea, 1983). Previously, Cray et al. (2010) found a strong relationship between suture activity and dental eruption in hominoids such that suture activity generally terminates after the emergence of the third molar. When this was investigated in gorillas however, suture activity was found to initiate earlier in ontogeny as compared to both *Pan* and *Homo*. This suggests that the larger masticatory muscles (Hylander, 1979a; Shea, 1983, 1985; Taylor, 2002, 2006; Taylor et al., 2008), early ingestion of mechanically resistant

foods (Nowell and Fletcher, 2008), and resulting mechanical loads in gorillas leads to increases in ectocranial sutural activity earlier in ontogeny (Cray et al., 2011). These studies broadly suggest that masticatory muscle size and contractile force affects sutural morphology and that sutural complexity and the mechanical loading environment are functionally linked.

An important area to consider in terms of suture morphology and masticatory loading is the zygomatic arch because it is such a highly strained environment on the macaque skull (Hylander and Johnson, 1997) and presumably across all primates as well, though only a limited amount of *in vivo* data on zygomatic arch strains exists for these taxa. The zygomatic arch experiences considerable masticatory loading during feeding and the zygomaticotemporal suture, the single suture on the arch, is assumed to experience similar loads. The zygomatic arch resembles a beam with two fixed ends, which bears an off-center load (due to the origin of the deep and superficial masseter muscles) and has been modeled as such in experimental studies (Hylander and Johnson, 1997; Kupczik et al., 2007). The primate zygomatic arch has been shown to experience a range of strain magnitudes, with the highest strains occurring anteriorly and then decreasing posteriorly (Hylander and Johnson, 1997). Hylander and Johnson (1997) noted that modeling the zygomatic arch as a beam did not take into account the presence of the zygomaticotemporal suture. However, given the potential mechanical benefit of the suture to dissipate loads across the bone surface, it is prudent to investigate the biomechanical significance of this feature to improve current models of zygomatic arch bone behavior.

Many studies have approached questions concerning the impact of sutures in a wide breadth of both living and extinct taxa using finite element analysis (FEA) (Rayfield, 2004, 2005; Kupczik et al., 2007; Wang et al., 2007, 2008, 2010, 2012; Farke, 2008; Moazen et al., 2009; Fitton et al., 2009; Jasinowski et al., 2010), yet FEA often yields conflicting results concerning the influence sutures have on local and global aspects of the skull (see Kupczik et al., 2007 and Wang et al., 2012). With respect to the zygomatic arch, previous studies have assessed the mechanical role of the zygomaticotemporal suture using finite element models of primate crania to incorporate the presumed effect of the suture on strain dispersal along the arch (Kupczik et al., 2007; Wang et al., 2012). While both studies conducted their analyses using macaque crania, they found contrasting results. Wang et al. (2012) found that the zygomaticotemporal suture responded similarly to loading in both static and dynamic scenarios but had little effect in mediating global strain patterns, whereas Kupczik et al. (2007) found sutures have an effect on the global strain environment of the skull. A critical difference between the studies of Kupczik et al. (2007) and Wang et al. (2012), was that the former used the skull of a juvenile (*Macaca fascicularis*) whereas the latter used an adult (*Macaca mulatta*) cranium. Experimental studies on pig crania have demonstrated that cranial sutures disperse facial strains under dynamic loading (Herring & Teng, 2000; Rafferty et al., 2003) and furthermore that the polarity and degree of strain in some cranial sutures change with age (Sun et al., 2004). If this is the case in primates, then juveniles with more patent sutures likely experience higher bending moments as compared to adults with relatively stiffer (more mineralized) sutures (Kupczik et al., 2007). There are also marked dietary differences between these two primate taxa. Though phylogenetically

similar, the diets are quite different: *Macaca mulatta* consumes high levels of leaves and buds (84.4%, see Goldstein and Richard, 1989) compared to *Macaca fasciularis,* which primarily consumes fruits (66.7-87%, see Wheatley, 1980; Yeager, 1996). A diet composed of primarily tough or hard foods as opposed to soft foods imposes different mechanical demands on the bone and presumably contributes to differences in sutural morphology. Given the wide dietary range found in primates, it is unclear whether diet influences sutural morphology in the zygomaticotemporal suture to the degree that it can be detected across primates of different dietary profiles. Thus, a biomechanical understanding of cranial sutures is important for elucidating the manner in which forces are dispersed through bone, how differences in suture architecture affect how masticatory strain levels, and the nature of the interplay between diet and bone response.

In this study, I quantify zygomaticotemporal sutural complexity using a broad, comparative sample to determine if sutural complexity is related to differences in primate diets. This study uses fractal geometry, a common method that is useful for examining the two-dimensional nature of sutures (Long, 1985; Hartwig, 1991; Long and Long, 1992; Monteiro and Lessa, 2000; Skrzat and Walocha, 2003a,b; Lynnerup and Jacobsen, 2003; Yu et al., 2003; Byron et al., 2004a; Byron, 2006) to quantify suture complexity in the zygomaticotemporal suture in relation to its masticatory loading environment. Using this approach, this study will provide a novel perspective from which to examine the interplay of primate diet and zygomatiotemporal sutural response on the zygomatic arch.

4.2.1 *Predictions*

The hypothesis that I test here is that the distribution and magnitude of masticatory strain affects the complexity of the zygomaticotemporal suture such tha high forces transmitted across the suture require greater sutural complexity. Increased sutural complexity is observed in some primates (e.g., *Sapajus apella*) that consume mechanically challenging food items as compared to other congeners (Byron et al., 2006; Wang et al., 2008). Therefore, I predict that (1) more complex sutures characterize taxa with diets consisting principally of mechanically resistant (specifically tough and/or hard) foods compared to those consuming less mechanically resistant foods overall, and (2) that primates with diets consisting of high toughness (*R*) or high Young's modulus (*E*) possess more complex sutures than those consuming foods with low toughness or low Young's modulus. Toughness is defined as a material's resistance to the propagation of a crack (Lucas and Pereira, 1990; Lucas et al., 2000, 2011) and Young's modulus, also known as the elastic modulus, is the ratio of stress (force per unit area) to strain (deformation) and is a measure of a material's ability to resist elastic deformation (Gordon, 1978; Williams et al., 2005). The higher the value of Young's modulus, the harder that material is.

4.3 Materials & Methods

4.3.1 *Study sample*

MicroCT (μCT) scans (voxel range 7.9-30.0 voxels/mm) of skulls from 43 species (N=349, Table 8) were selected from scan collections housed at Arizona State University and Northeast Ohio Medical University (NEOMED). Only adult, wildshot

specimens without pathology were included to control for influences from captivity and/or disease. In species where equal numbers of males and females were available, preliminary comparisons were performed to determine whether there was an effect of sex. Because no significant differences were found the sexes were grouped together for the purpose of analysis in this study.

Table 8. Study sample

Species	**Males**	**Females**	**Unknown**	***n***
Alouatta caraya	2	2	1	5
Alouatta palliata	-	-	12	12
Aotus trivirgatus	3	6	3	12
Ateles geoffroyi	-	5	14	19
Cacajao rubicunda	1	1	-	2
Callicebus moloch	12	2	1	15
Callithrix argentata	6	1	-	7
Callithrix humeralifera	2	2	-	4
Callithrix jacchus	1	1	1	3
Cebus capucinus	-	5	5	10
Cercocebus torquatus	8	2	-	10
Cercopithecus mitis	-	12	-	12
Chiropotes albinasus	-	1	-	1
Chiropotes satanas	-	-	1	1
Colobus polykomos	2	10	-	12
Erythrocebus patas	2	2	1	5
Gorilla gorilla	-	10	-	10
Hylobates lar	-	18	-	18
Lophocebus albigena	6	2	2	10
Macaca fascicularis	2	9	1	12
Macaca fuscata	2	-	-	2
Macaca mulatta	2	-	2	4
Mandrillus sphinx	-	-	2	2
Macaca sylvanus	8	-	-	8
Mandrillus leucophaeus	3	1	1	5
Miopithecus talapoin	4	1	1	6
Nasalis larvatus	-	12	-	12
Pan paniscus	1	2	-	3
Pan troglodytes	-	12	2	14
Papio anubis	8	3	1	12
Piliocolobus badius	4	6	1	11
Pithecia monachus	1	1	3	5
Pithecia pithecia	2	1	-	3
Pongo pygmaeus	-	3	-	3
Presbytis hosei	1	3	2	6
Presbytis rubicunda	2	5	4	11
Saguinus oedipus	6	5	-	11
Saimiri oerstedii	3	2	-	5
Saimiri sciureus	4	1	1	6
Sapajus apella	7	9	1	17
Symphalangus syndactylus	1	-	-	1
Theropithecus gelada	-	-	2	2
Trachypithecus cristatus	-	20	-	20
Total				**349**

*Indicates taxa for which food material properties (FMP) data were available

4.3.2 *Dietary categorization*

A twofold approach was used to categorize the taxa into dietary categories. The first approach used published data on dietary preference to assign each species to a dietary category on the basis of food mechanical properties. Following the methodology of Muchlinkski (2010) a species' designation as a "tough feeder," "hard feeder," "soft feeder," or "exudate feeder" was based on total consumption of 50% or more of a particular food type (as measured from time spent feeding on an item) deemed as tough, hard, soft, or exudate based on its material properties. Because this study examined the effects of presumed variation in masticatory loads on the bony morphology of the zygomatic arch, "exudate feeder" remained distinct from "soft feeder" as each of these food types differ in their material properties and time required for mastication (Norconk et al., 2009). In instances where two or more primary food types are consumed (e.g., tough and soft), the species' diet characterization was assigned based on the food type with the highest consumption percent (See Appendix B, Table SM1 for species' reported dietary consumption percents and dietary categorizations).

The second dietary approach was used to divide a subset of the total study sample (species $n = 9$, Table 9) using specific food material properties (FMPs) data collected on foods consumed by those species in the field (Venkatamaran et al., 2014; Coiner-Collier et al., 2016). Specifically, these recorded material properties are toughness (R), and Young's modulus (E). Because material properties data were not available for all taxa included in this study, the second dietary approach and its associated analyses will be limited to these nine primate species. For the purposes of comparison, "high" toughness measures and "high" Young's modulus measures were determined as follows: based on

the available FMPs data, taxa were divided based on whether their mean fracture toughness values are greater or equal to 700 Jm^{-2} and those that are less than 700 Jm^{-2}. For the purposes of this study, those that exceed 700 Jm^{-2} are considered to have a high toughness diet. For example, the seed shells of *Mezzetia parviflora* consumed by orangutans range from 1,204 to 3,113 Jm^{-2} (Lucas, 1989; Lucas et al., 1991) while apple pulp is much lower, averaging about 663 Jm^{-2} (Williams et al., 2005). To define the threshold for high Young's modulus values, taxa consuming foods with mean Young's modulus measures of $\leq$10 MPa are considered to be of "low" Young's modulus values. The include foods like carrots (average 6.86 MPa) or pear skins (average 5.80 Mpa) (Williams et al., 2005). Taxa consuming foods with values of $\geq$90 MPa or more are considered to have "high" Young's modulus values. These include foods such as cherry pits (average 189.48 Mpa) or prune pits (average 325.40 Mpa) (Williams et al., 2005).

Table 9. Sub-sample of taxa and their reported FMPs values

	Reported Average Food Material Properties (FMPs) values	
Species	**Mean fracture toughness, R (Jm^{-2})**	**Young's Modulus, E (MPa)**
Alouatta palliata[1]	529.2	-
Callithrix jacchus[1]	1651	198.4
Chiropotes satanas[1]	846.7	95.67
Pan troglodytes[1]	505.8	1.028
Piliocolobus badius[1]	538.4	9.110
Pithecia pithecia[1]	856.7	111.4
Pongo pygmaeus[1]	2743	4.011
Sapajus apella[1]	666.4	91.87
Theropithecus gelada[2]	2686	-

[1] Fracture toughness and Young's Modulus data from Coiner-Collier et al. (2016)

[2] FMP data from Venkataraman et al. (2014)

4.3.3 *Data Collection*

The use of high-resolution microCT (μCT) scans to collect data on trabecular and cortical bone across humans and animals has grown immensely in the past years (Bouxsein et al., 2010) and has become a standard means of collecting comparative morphological data. MicroCT scans possess greater resolution than standard CT scans in that microCT scans decrease the thickness of each virtual cross-section (commonly referred to as "slices") from about 1mm to approximately 10μm (Mittra et al., 2008). This serves to increase the total number of slices generated per specimen and increases the number of pixels in each slice, which enables fine bone features to be identified, and accurately measured (Peyrin et al., 1998; Ding et al., 1999; Laib et al., 2000). For the purposes of examining sutural morphology, microCT scans are necessary in order to achieve precise and accurate measures of the suture's pattern and ensure no damage befalls the specimen.

Scans of primate skulls were used to construct 3D models of the cranium using Amira (FEI Visualization Group, 2016). Once constructed, the skull model was oriented in Frankfurt horizontal to standardize cranial position during virtual sectioning. Once oriented, the Amira "slice" feature was used to pass a vertical plane along the zygomatic arch (Fig. 10). Once positioned at the midpoint of the zygomaticotemporal suture, a "slice" was captured. This midsuture slice was collected on each specimen and then exported to ImageJ (Schneider et al., 2012) for fractal analysis. Each cross-section is saved as an 8-bit image and the "adjust" feature is used to improve the contrast of the image in prepration for highlighting the suture. For each image, FracLac (Karperien,

2013) for ImageJ was used to generate measures of fractal dimension (D_f), lacunarity (λ), and prefactor lacunarity (PΛ) using the box counting (or grid) method.

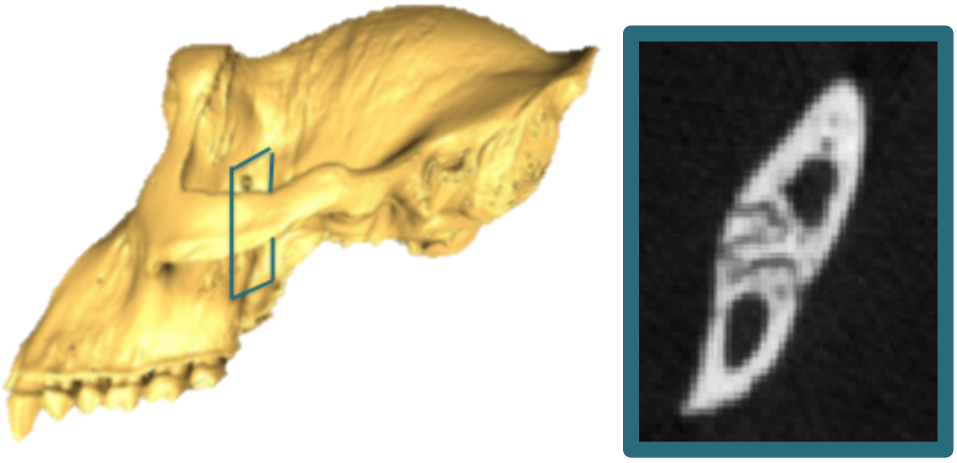

Figure 10. Midsuture cross-sectional image collected from model of *Gorilla*

4.3.4 *Fractal dimensions*

Fractal dimensions (D_f) are a measure of a shape's self-similarity with increasing magnification (or scale) (Byron et al., 2004a; Karperien et al., 2013). Generally speaking, the more complex the pattern, and the greater the scale, the higher the fractal dimension. This method was developed by Benoit Mandelbrot and has been successfully used to characterize the geometry found in Nature (Mandelbrot 1967, 1977; Monteiro and Lessa, 2000; Jaslow, 1990; Long and Long, 1992; Nicolay and Vader, 2006). Fractal analysis quantifies the complexity of a pattern by assigning a unit-free measure ranging between one and two dimensions (1.0-2.0) (Byron et al., 2004a). The fractal dimension (D_f) is calculated as:

$$N_\varepsilon = \varepsilon^{Df} \quad (4)$$

$$Df = \frac{lnN_\varepsilon}{ln\varepsilon} \quad (5)$$

where the number of sampling elements (N_ε) is equal to the scale (ε) raised to the power of D_f. Specifically for this study, the box-counting method was used to measure the fractal dimension (D_B) for each specimen. This method is common for calculating fractal dimensions because of its simplicity and computability (Li et al., 2009). The approximation (D) of a D_B is estimated from the limit as scale decreases:

$$D_B = \lim_{\varepsilon \to 0} \frac{logN\varepsilon}{\log\varepsilon} \quad (6)$$

where *N* is the number of sampling elements (i.e., boxes) at a particular box size that contain meaningful foreground pixels in a box counting scan, ε is the scale, and Df finds the slope of the regression line for the data. Simply stated, the box-counting method covers the image in a series of non-rotating grids and then counts how many of the boxes are inhabited by the pattern (Smith et al., 1996; Fig. 11). Each series of boxes is characterized by a box size and the number of boxes necessary to cover the structure of interest and is recorded as a function of box size.

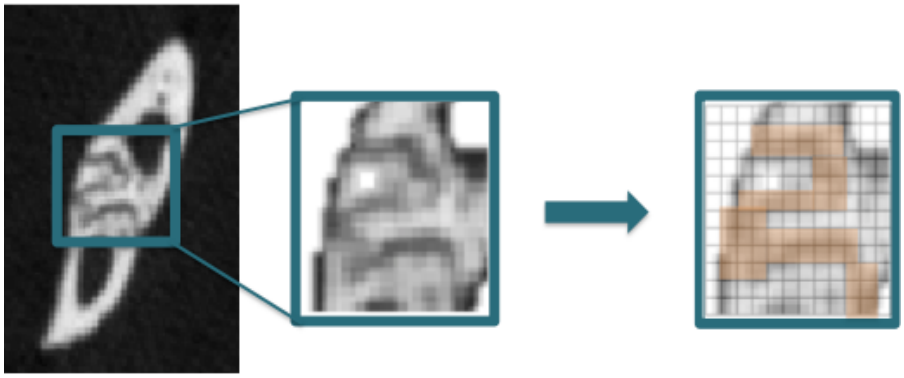

Figure 11. Example of grid overlay used in the box counting method used on each cross-sectional image.

This process is iterative as the grid is refined with smaller and smaller boxes (Fig. 12). The log of the number of boxes inhabited by the structure is then multiplied by the length

of a box edge and plotted against the log length of a box edge for each series of differently-sized boxes (Smith et al., 1996).

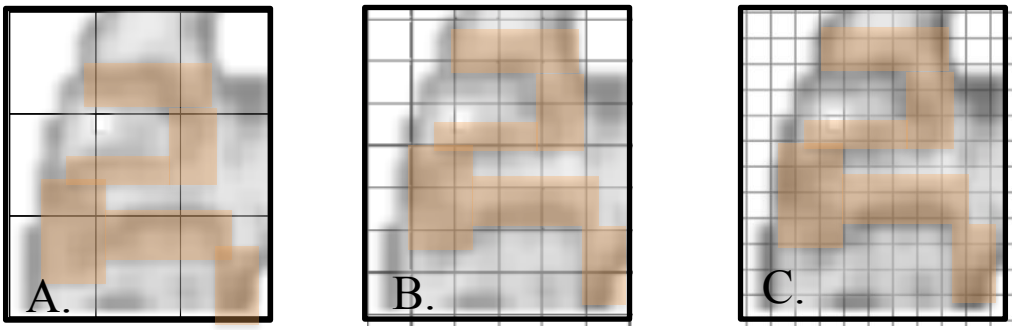

Figure 12. Examples of varying grid sizes overlaying an image. Box size decreases as scale increases. A. Grid with low scale, larger box size B. Grid with higher scale and smaller box size C. Grid with high scale, small box size

FracLac infers a scaling rule for each pattern by taking measurements over many box sizes and approximating the log-log relationship from the slope of the regression line for the data. Given that this method can be sensitive to the structure's location on the grid, each image was measured three times and averaged in order to obtain the most accurate fractal dimension measure.

Because the arch cross-sectional images are grayscale, it is important to ensure that only the meaningful parts of the pattern are recognized. To address this, the intensity (*I*) is quantified for each image. *I* is calculated as:

$$I_{i,j,\varepsilon} = maximum\ pixel\ intensity\ \delta I_{i,j,\varepsilon} - \ minimum\ pixel\ intensity\ \delta I_{i,j,\varepsilon} \quad (7)$$

This is used in the calculation of the fractal dimension by using box counting (D_B), from the log-log regression line of the sum of all $I_{ij\varepsilon}$ (intensity) vs ε (scale). For more information about box counting algorithms see Mandelbrot (1983) or Ristanovic et al. (2009).

Lacunarity (λ) derived from Latin, *lacuna*, meaning gap or hole (Mandelbrot, 1982) is a scale-dependent measure of the texture of a fractal based on the number of gaps and rotational and translational invariance in the structure (Plotnick et al., 1993). Prefactor lacunarity, PΛ, is a type of lacunarity that measures the heterogeneity dependent on where a grid series is placed and is affected by image size. The difference between these two measures (that is lacunarity and prefactor lacunarity) is one of scale; there is a λ measure for each size of the sampling unit, whereas Λ is usually an average of overall sizes used to sample an image. Biologically, lacunarity is a measure of the "roughness" of sutures based on the spatial distributions of the gaps in the suture (Cordeiro et al., 2016). Thus, this is a measure that quantifies how space is filled and is a reasonable means by which to measure sutures in terms of gap distribution (Cordeiro et al., 2016) and is also useful for discerning amongst patterns sutures that have similar fractal values.

Linear measures of total arch height and traced measures of sutural path length were taken to generate a ratio of traced length to total height following a modified version of the method from Jaslow (1990). Using ImageJ, the straight-line tool was used to measure the vertical distance of the cross-section of the image, and then the freehand tool was used to trace along the entire suture path (Fig. 13).

A series of three-dimensional (3D) anatomical landmarks were collected across the skull (18 landmarks) including 4 landmarks across the zygomatic arch (see Fig. 14). In the absence of body mass estimates for these taxa, geometric means of skull size and zygomatic arch size were calculated from these landmarks to serve as a proxy for size in comparative analyses.

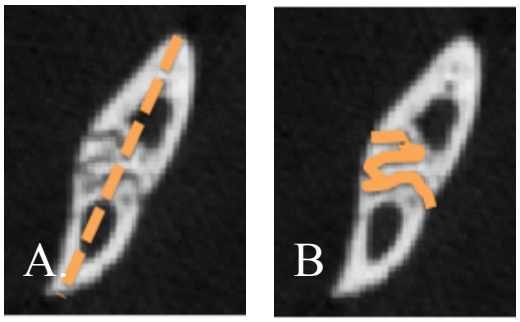

Figure 13**.** Linear measures taken in ImageJ to calculate suture path length: A. vertical height (dashed line) and B. traced suture path length (solid line)

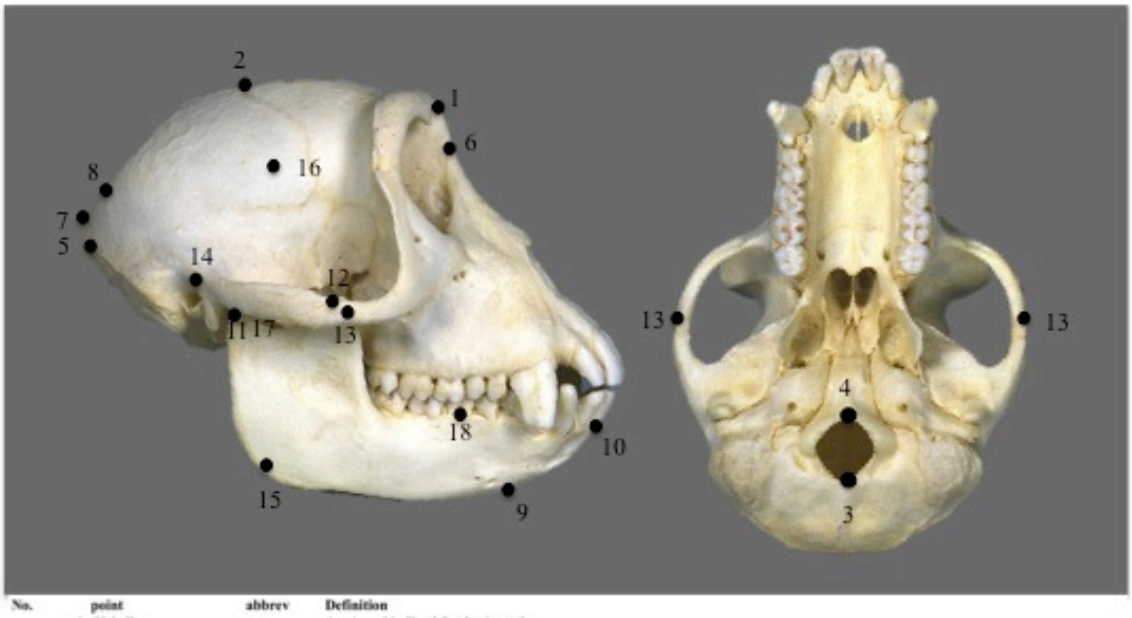

No.	point	abbrev	Definition
1	Glabella	g	As viewed in Frankfurt horizontal
2	Bregma	b	Junction of coronal and sagittal sutures, on sagittal crest if necessary
3	Opisthion	o	Posterior most point of formen magnum
4	Basion	ba	anterior most point of foramen magnum
5	Inion	i	Most posterior point of cranium, when viewed in the Frankfurt horizontal, be it on sagittal/nuchal crest or not.
6	Nasion	n	Fronto-nasal suture in midline
7	Opisthocranion	op	The most posteriorly protruding point on the back of the braincase, located in the mid-sagittal plane.
8	Lambda	l	The point where the two branches of the lambdoidal suture meet with the sagittal suture.
9	Gnathion	gn	The lowest point on the inferior margin of the mandibular body in the mid-sagittal plane.
10	Infradentale	id	The midline point at the superior tip of the septum between the mandibular central incisors.

BILATERAL (right/left)

No.	point	abbrev	Definition
11	Zygo-max inferior	zmi	Anteroinferior point of zygomaticomaxially suture, in anterolateral view.
12	Zygo-temp superior	zti	Superior point of zygomatico-temporal suture on lateral face of zygomatic arch.
13	Zygion	zy	The most laterally positioned point on the zygomatic arches.
14	Auriculare	au	The point on the lateral aspect of the root of the zygomatic process at the deepest incurvature.
15	Gonion	go	The point on the mandible where the inferior margin of the mandibular corpus and the posterior margin of the ramus meet.
16	Euryon	eu	Instrumentally determined sctocranial points on opposite sides of the skull that form the termini of the line of greatest cranial breadth.
17	Condylion laterale	cdl	The most lateral point on the mandibular condyles.
18	First mandibular molar	M1	Position of the first mandibular molar.

Figure 14. Cranial landmarks taken on each specimen to determine the geometric mean for skull size and zygomatic arch size. Descriptions from Buikstra and Ubelaker (1994).

4.3.5 *Statistics*

Shapiro-Wilk Tests and Levene's Tests were used to determine if the variables met the assumptions of normality and homogeneity of variance. Variables were log transformed to meet these assumptions. The variables for complexity, lacunarity, prefactor lacunarity, and relative suture path length were compared by diet type using two diet categorization schemes with Analysis of Variance (ANOVA) and post-hoc Tukey-HSD tests. Student's *t*-tests were used for comparing sample means. Pairwise comparisons between closely related taxa were also performed for each variable using two-sample *t*-tests. The significance level for all tests was set at $\alpha < 0.05$. A Bonferroni-Holm correction for multiple comparisons was also applied (Holm, 1979).

All variables were log-transformed in order meet assumptions of normality and homogeneity of variance. To first examine the effect of size on sutural complexity, the geometric mean for skull size and zygomatic arch size were compared. To compare these variables, a Reduced Major Axis (RMA) regression was used to determine whether the difference between the variables had an isometric or allometric relationship (Warton et al., 2006; Smith, 2009). The expected slope of isometry for skull size and zygomatic arch size for these data was 1.0. To compare skull size and logged measures of complexity (D), lacunarity (λ), prefactor lacunarity ($P\Lambda$), and sutural path length, Ordinary Least Squares (OLS) regressions were used to determine whether skull size affected complexity in addition to diet (Smith, 2009). Descriptive statistics for all variables are available in Appendix B, Table SM2.

Phylogenetic Generalized Least Squares (PGLS) Regressions were also used to account for the influence of phylogeny in the data. Consensus trees for the entire study

sample as well as the subsample were obtained from the 10KTrees database (http://10ktrees.nunn-lab.org/, Arnold et al., 2010). Because not all the species in this study were available in the 10KTrees database, published phylogenetic positions and divergence dates for *Chiropotes albinasus*, *Presbytis rubicunda* and *Presbytis hosei* were acquired from the literature (Finstermeier et al., 2013) and added to the final consensus tree. Given that this study tested hypotheses using two different dietary schemes and not all taxa have available FMPs data, the initial consensus tree containing 43 species was trimmed to include only the 9 species for which FMP data were available.

Principal Coordinate Analysis (PCoA) was performed to visualize the data and determine whether diet groups (as determined by traditional dietary categories or food material properties) diverge from one another and to determine the dissimilarity among groups. In this type of analysis, distances between samples are used to calculate positions in the multidimensional framework.

All analyses were performed using the R Statistical Programming Language version 3.1.0 (http://www.R-project.org/) (R Development Core Team, 2014). Packages APE (Paradis et al., 2004) and caper (Orme et al., 2013) were used for PGLS. To test the hypotheses that total consumption percent, FMP, and variables of complexity are related, PGLS regressions incorporating an interaction between FMPs and total consumption percent were performed. If the interaction was not significant then the models were run again without the interaction.

4.4 Results

4.4.1 *Size and sutural complexity*

The results of the RMA regression of skull size regressed on zygomatic arch size found a significant, positive relationship between the size variables (R^2=0.895, slope= 2.609, CI= 2.170, 2.933, p<0.000) indicating that the relationship between skull size and arch size is positively allometric. Zygomatic arch size, relative to skull size, is greater than would be expected under an isometric relationship. The results of the OLS regression of log skull size and log complexity values (logD) yielded a significant relationship (R^2= 0.168, slope= 0.180, CI=0.359,1.724, p=0.003) (Table 10; Fig. 15). Average log size of the zygomatic arch and log complexity were also significantly correlated (R^2=0.171, slope=0.069, CI= 0.024, 0.115, p=0.003), indicating both scale relatively equally to sutural complexity (Fig. 15). Measures of skull size and logged values of lacunarity as well as logged values of prefactor lacunarity were not significantly correlated. Suture path length was correlated with both the geometric mean of skull size (R^2=0.139, slope=0.714, CI=0.197, 1.230, p=0.007) and zygomatic arch size (R^2=0.107, slope=0.245, CI=-.194.7, -134.3, p<0.000) (Fig. 15). See Table 10 for the results of all OLS regressions.

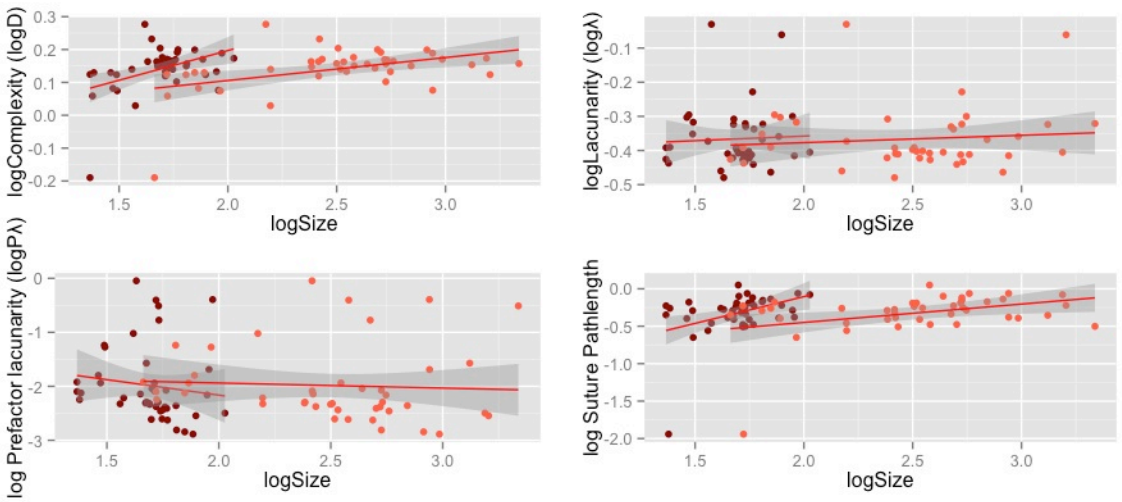

Figure 15. OLS Regressions of skull size (dark red) and zygomatic arch size (light red) with logged complexity (D) and suture path length measures

Table 10. Results of RMA regressions with geometric mean of skull size and zygomatic arch size

Skull size	Dependent variable	R^2	slope	CI	*p*
	log complexity (D)	0.168	0.180	0.359, 1.724	**0.003**
	log lacunarity (λ)	0.006	-0.598	-1.329, 0.132	0.106
	log prefactor lacunarity (PΛ)	-0.006	-0.570	-1.910, 0.767	0.393
	log suture path length	0.139	0.714	0.197, 1.230	**0.007**
	log Young's modulus (E)	0.874	-325.2	-466.9, -183.6	**0.001**
	log toughness (R)	0.160	0.710	-0.32, 1.75	0.148
Zygomatic arch size	log complexity (D)	0.171	0.069	0.024, 0.115	**0.003**
	log lacunarity (λ)	-0.006	-0.120	-0.407, 0.166	0.402
	log prefactor lacunarity (PΛ)	-0.021	-0.093	-0.610, 0.423	0.715
	log suture path length	0.107	0.245	0.044, 0.447	**0.018**
	log Young's modulus (E)	0.970	-164.7	-194.7, -134.3	**<0.000**
	log toughness (R)	0.001	597.5	-807.7, 2002	0.348

Phylogenetic Generalized Least Squares (PGLS) regressions were performed on the data to determine the evolutionary association between the sutural complexity values, diet consumption percent, and FMP data. The GenBank consensus tree from 10KTrees was used to estimate the phylogenetic relationships and divergence dates for the primate species. Pagel's lambda was calculated as a quantitative measure of phylogenetic signal in the data (Nunn, 2011). These models resulted in a maximum-likelihood estimate of 0 for Pagel's lambda indicating a low phylogenetic signal in the residual errors for the traits. Under these models, dietary designations using total consumption percent and food material properties, were not good predictors of lacunarity, prefactor lacunarity, or sutural path length.

4.4.2 *Sutural complexity (D_B)*

Box and whisker plot showing average complexity values for each dietary group is in Figure 16. Hard-object consumers possessed the largest complexity measures on average. ANOVA analyses with posthoc Tukey HSD tests were performed on taxa organized in the traditional dietary groups of "tough", "hard", "soft", and "exudate" to determine the degree of variation between dietary groups as well as within dietary groups. ANOVA results on log transformed complexity (logD) compared among dietary categories found no significant differences (F= 2.192, p=0.088; Table 11).

Table 11. ANOVA results between dietary category for measures of complexity and its associated variables

Variable	***F***	***P***
Complexity (D_B)	2.192	0.088
Lacunarity (λ)	0.023	0.995
Prefactor lacunarity (PΛ)	1.247	0.293
Sutural path length	11.04	**<0.000**

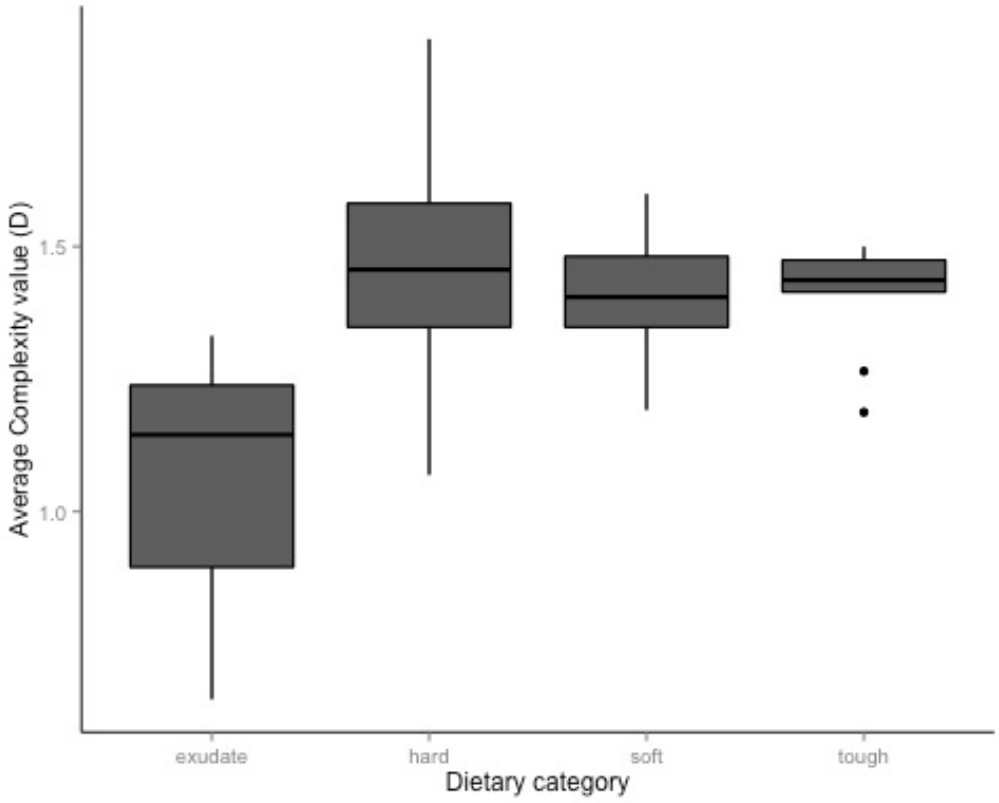

Figure 16. Box and whisker plot of average zygomaticotemporal sutural complexity values by diet type

ANOVA analyses were also performed on each dietary group to determine the variance in complexity within each dietary category. Tough consumers were found to be significantly different in complexity (F= 2.65, p=0.012) as were soft consumers (F= 2.212, p=0.002). Exudate consumers were not significantly different from one another, nor were hard-object feeders (Table 12). Comparisons between raw complexity values and diet type shows hard-object consumers generally possess greater complexity measures on average, followed by tough consumers, soft consumers, and exudate consumers, but no comparisons were significantly different.

To examine whether differences in sutural complexity measures between closely related taxa based on total consumption percent of a particular food item existed, pairwise comparisons were performed on 17 pairs of species (Table 13) using logged complexity values. All comparisons were not significant except for the one comparison between *Theropithecus gelada*, a tough food consumer, and *Papio anubis*, a soft (and sometimes hard) food consumer (p= 0.033).

Table 12. ANOVA results within dietary category for measures of complexity and its associated variables

	Diet category			
Variable	**Tough**	**Hard**	**Soft**	**Exudate**
Complexity (D_B)	***F*= 2.46, *p*=0.012**	*F*=0.555, *p*=0.698	***F*=2.212, *p*=0.002**	*F*=0.401, *p*=0.540
Lacunarity (λ)	***F*= 2.23, *p*=0.023**	***F*= 9.145, *p*<0.001**	***F*=36.36, *p*<0.001**	*F*=0.863, *p*=0.373
Prefactor lacunarity ($P\Lambda$)	***F*=30.36, *p*<0.001**	***F*=6.066, *p*<0.001**	***F*=5.573, *p*<0.001**	*F*=1.358, *p*=0.269
Sutural path length	***F*=9.145, *p*<0.001**	*F*=1.711, *p*=0.158	***F*=4.605, *p*<0.001**	***F*=640.8, *p*<0.001**

Bolded values significant after Bonferroni-Holm correction

Table 13. Results of pairwise comparisons using two-sample *t*-tests comparing logD values

Comparison	***t***	**df**	***p***
G. gorilla (T) v. *P. troglodytes* (S)	1.71	14.4	0.11
G. gorilla (T) v. *P. pygmaeus* (S)	-1.84	8.59	0.09
M. fascicularis (S) v. *M. mulatta* (T)	0.59	7.42	0.56
L. albigena (H) v. *C. torquatus* (S)	-1.78	10.5	0.10
A. palliata (T) v. *A. geoffroyi* (S)	0.37	20.1	0.71
P. pithecia (H) v. *P. monachus* (S)	-1.84	1.21	0.28
M. talapoin (S) v. *E. patas* (S)	0.36	5.80	0.72
P. anubis (S) v. *T. gelada* (T)	8.11	1.48	**0.03**
P. badius (T) v. *C. polykomos* (T)	-0.44	16.2	0.66
T. cristata (T) v. *P. hosei* (T)	0.61	7.64	0.56
T. cristata (T) v. *P. rubicunda* (H)	1.45	11.3	0.17
G. gorilla (T) v. *H. lar* (S)	-0.70	12.5	0.49
C. jacchus (E) v. *S. oedipus* (S)	-1.56	9.72	0.15
S. sciureus (S) v. *S. oerstedii* (S)	-0.77	6.91	0.46
S. sciureus (S). *A. trivirgatus* (S)	-1.75	3.44	0.16
S. apella (H) v. *C. capucinus* (S)	0.53	21.5	0.59
N. larvatus (T) v. *P. rubicunda* (H)	-0.22	10.7	0.82

T= tough consumer; S= soft consumer, H= hard-object consumer; E= exudate consumer

4.4.3 *Lacunarity*

For lacunarity, λ, which describes the texture or heterogeneity of the fractal, ANOVA and post-hoc Tukey HSD tests were performed to assess the degree of variation in fractal texture across diet groups. Logged lacunarity ANOVA comparisons between dietary groups found no significant differences (F=0.016, p=0.995). Similar to the results of logged complexity (logD), when separated by dietary group, significant differences within groups were found in soft feeders and tough food consumers (Table 12). Hard-object consumers and exudate consumers had no significant differences within their group members. These results suggest that there is relatively higher instances of heterogeneity in soft and tough consumers overall, and more homogeneity in hard-object and exudate consumers.

4.4.4 *Prefactor lacunarity*

The results of ANOVA comparisons between dietary groups found no significant differences (F=1.24, p=0.293). Similar to the results found within dietary groups with respect to complexity and lacunarity (Table 12), soft and tough consumers yielded significant results (Table 12). Interestingly, hard-object consumers were also significantly different (Table 12), although they were not in previous tests of lacunarity and sutural complexity. Exudate feeders were not significantly different from one another. These results suggest that for this measure of lacunarity, there is varying heterogeneity in the fractal measures in all diet categories except exudate consumers.

4.4.5 *Suture path length*

Relative suture path length was calculated for each specimen using linear measures of vertical arch height and the total traced path length of the suture on the bone. ANOVA comparisons between dietary groups found significant differences between exudate consumers and all other dietary categories (F=11.04, p<0.000; Fig. 17). Post-hoc Tukey HSD tests found exudate consumers to be significantly shorter in pathlength comparison to tough, soft, and hard-object consumers (p<0.000, Table 9). In addition, comparisons between soft and tough consumers were also significant with tough consumers being longer than soft consumers in pathlength (p=0.010).

ANOVA results for comparison within traditional dietary categorization found significant results within tough, soft, and exudate consumers (Table 12). Hard-object consumers did not yield significant results. Pairwise comparisons of closely related taxa from different diets were performed and seven pairs of taxa yielded significant results ($p\leq$

0.030, Table 10). Path length and logged complexity values were compared to determine whether longer path lengths were also more complex. OLS regression on complexity and path length found no relationship between the variables (p=0.08).

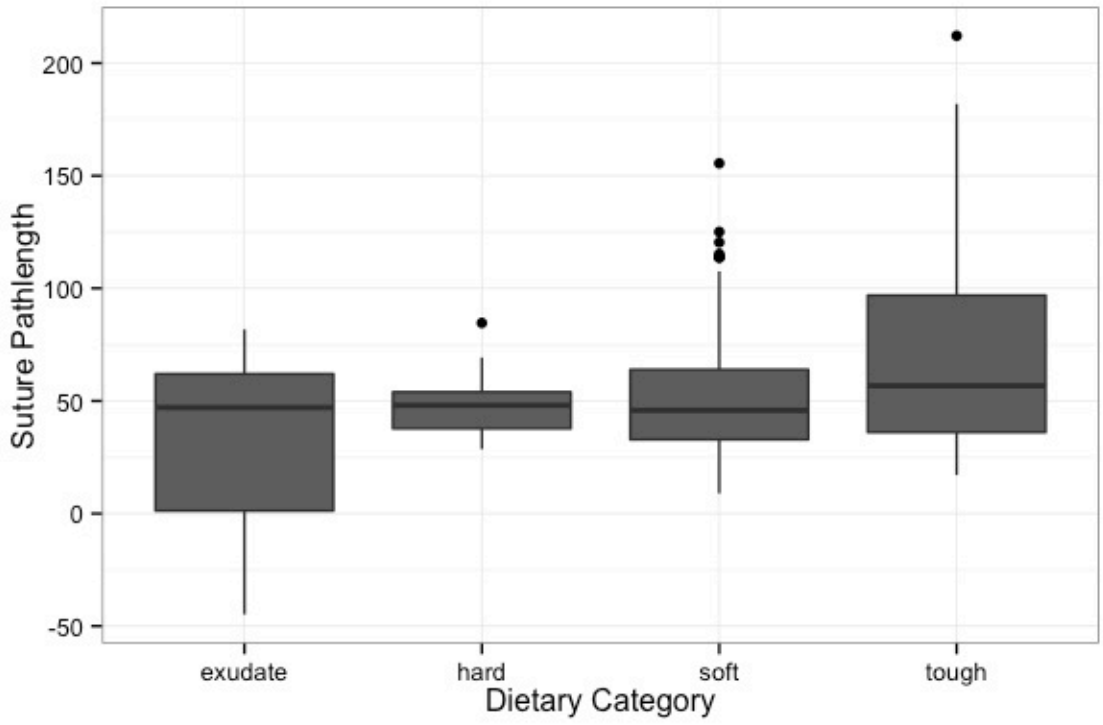

Figure 17. Box and whisker plot of zygomaticotemporal suture path length measures by traditional dietary category.

Table 14**.** Post-hoc Tukey HSD Tests on suture pathlength

Comparison	Tough	Soft	Hard	Exudate
Tough	---	**0.010**	0.381	**<0.000**
Soft	**0.010**	---	0.999	**<0.000**
Hard	0.381	0.999	---	**<0.000**
Exudate	**<0.000**	**<0.000**	**<0.000**	---

4.4.6 *Sutural complexity and diet: Total consumption percent of food type*

A series of Phylogenetic Generalized Least Squares (PGLS) regressions conducted using the consensus tree of all study taxa and which included measures of size, total consumption percent of a food type, and measure of complexity, found total consumption percent to be a poor predictor of complexity (Appendix B; Table SM3). All models generated a maximum-likelihood estimate of 0 for lambda indicating a low phylogenetic signal in the data. One contributing factor to this result is the relatively low number of species with FMPs data available (n=9); ideally PGLS regression recommends that sample size considerably exceed the number of predictors (Mundry, 2014).

4.4.7 *Sutural complexity and diet: Food material properties (FMPs)*

A Phylogenetic Generalized Least Squares (PGLS) regression was calculated on the subsample of species for which FMP data were available. None of the overall models, which included complexity, lacunarity, prefactor lacunarity, and suture path length, mean toughness (R) and mean Young's modulus (E) values, were significant. All models generated a maximum-likelihood estimate of 0 for lambda indicating a low phylogenetic signal in the data (Appendix B; Table SM3).

Individual OLS regressions of food materials properties (FMP) and size found a significant relationship between Young's modulus and skull size (Table 15; Fig. 18) as well as Young's modulus and zygomatic arch size. These regression results suggest that larger taxa consume foods of less hardness than smaller-bodied taxa. It is important to note that these data were only available for a relatively small number of species, and that the measures of Young's modulus only represent the hardest foods consumed, not the

most commonly consumed foods. For instance, *Callithrix jacchus* consumes bark and cambium of trees, which yielded average *E* measures of 113.0-282.9 MPa (Correa et al., 2000) even though the primary foods consumed for these taxa are exudates. These values even exceed some seed tissues consumed by *S. apella* (114.3 MPa, see Coiner-Collier et al., 2016). No relationship between toughness and skull size or toughness and zygomatic arch size was found. No relationship between Young's modulus and toughness was found. Lacunarity and mean toughness were significantly correlated (Table 15). No relationship was found between lacunarity and Young's modulus. Neither prefactor lacunarity nor suture path length was correlated with toughness or Young's modulus.

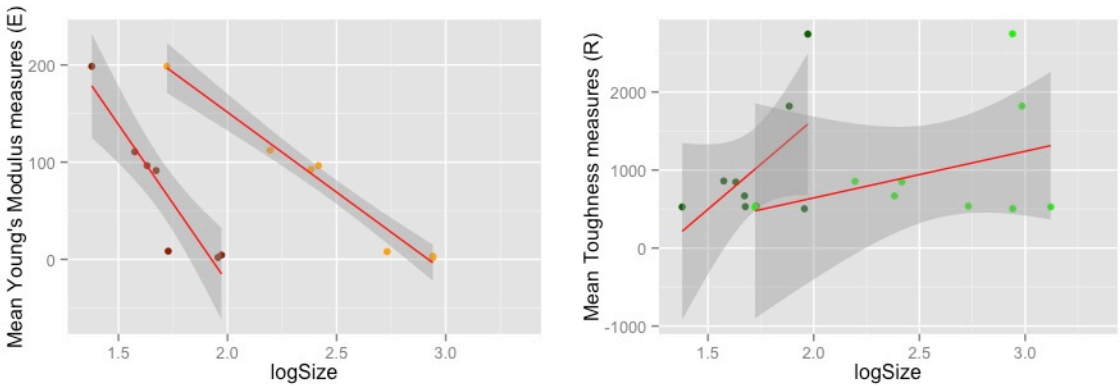

Figure 18. OLS regression of logged average values for Young's Modulus and logged geometric mean for skull size and logged lacunarity and mean toughness measures. Dark red is skull size, orange is zygomatic arch size; dark green is skull size and light green is zygomatic arch size.

Table 15. OLS regressions results for with FMPs and complexity measures

Toughness (*R*)	**Dependent variable**	***r***	**slope**	**CI**	***p***
	log complexity (D)	0.07	1.95	-1.65, 5.56	0.24
	log lacunarity (λ)	0.43	-0.22	-0.41, -0.02	**0.03**
	log prefactor lacunarity (PΛ)	-0.06	0.07	-0.16, 0.31	0.48
	log suture path length	0.01	0.17	-0.22, 0.56	0.33
Young's Modulus (*E*)	log complexity (D)	-0.13	-3.21	-18.50, 12.07	0.61
	log lacunarity (λ)	0.02	0.39	-0.55, 1.34	0.33
	log prefactor lacunarity (PΛ)	-0.15	-0.17	-1.19, 0.84	0.67
	log suture path length	0.08	-0.67	-2.05, 0.70	0.26

Results of the Principal Coordinates Analysis (PCoA) on both FMPs and traditional dietary groupings were performed to visually assess the data and to also quantify the dissimilarity between groups. PCoA results for the traditional dietary categories found a combined 69.46% of the variation captured by the first two coordinate axes (Fig. 19). Visually, tough consumers and soft consumers cluster separately from one another with only slight overlap. Exudate consumers fall within the distribution of soft consumers, while only some hard-object consumers (*Sapajus apella* and *Chiropotes satanas*) overlap with soft consumers. All other hard-object consumers clustered separately from soft, exudate, and tough consumers.

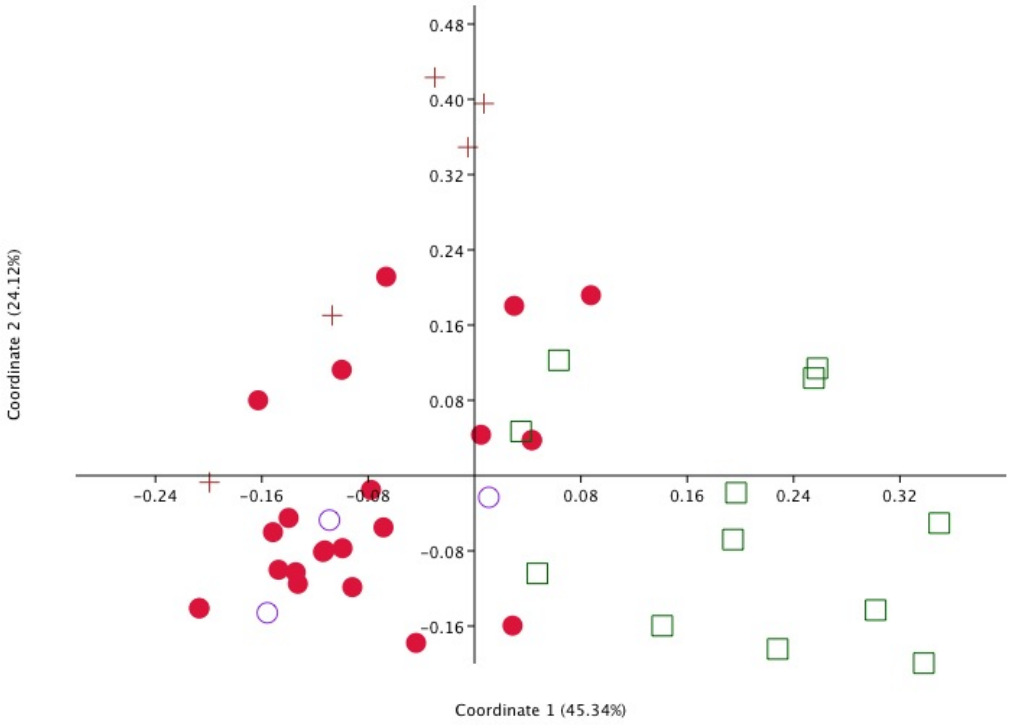

Figure 19. Principal Coordinates Analysis (PCoA) plot of complexity measures and size using traditional dietary categories. Filled circle= soft consumers, open circles=exudate consumers, open squares= tough consumers, plus=hard-object consumers.

PCoA plots were generated for both toughness and Young's modulus measures in relation to measures of sutural complexity. With regard to toughness, approximately 87.69% of the variation was accounted for in the first two principal coordinates. In this plot, tough consumers were relatively closely clustered overall, though tough consumer *Alouatta paliatta* clustered more closely to *Pan troglodytes* (a soft consumer) and *Pithecia pithecia* (a hard consumer) than it did to any other tough consumer (Fig. 20). Similarly, *S. apella* grouped more closely with *Callithrix jacchus,* the sole exudate consumer, and *P. troglodytes* than with hard-object consumer *Chiropotes satanas* or *Pithecia pithecia*. *Chiropotes satanas*, separated from all other dietary groups as did *Pongo pygmaeus.*

For measures of Young's modulus, the first two principal coordinates account for 80.40% of the variation observed. PCoA plots generated for Young's modulus measures in relation to suture complexity measures yielded a different clustering pattern than was observed in toughness measures (Fig. 21); generally speaking, taxa with similar primary dietary types grouped more closely together and there is relatively less overlap between groups as well.

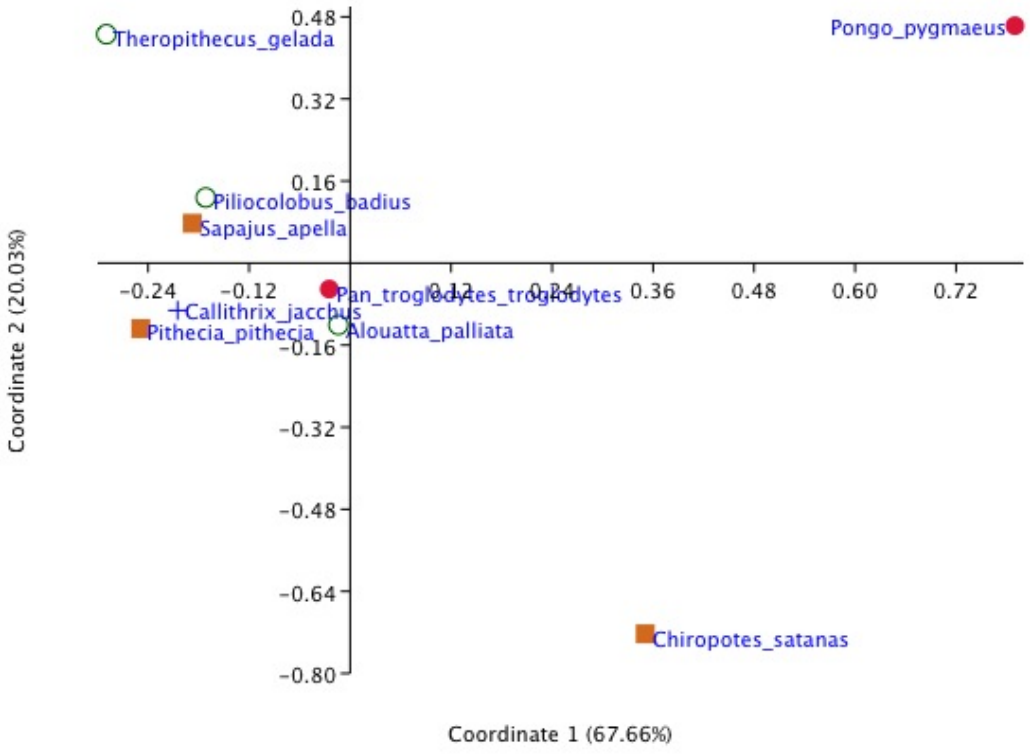

Figure 20. Principal Coordinates Analysis (PCoA) plot of sutural complexity and size with measures of fracture toughness (*R)*. Key: filled square = hard-object consumer; filled circle = soft consumer; open circle = tough consumer; plus = exudate consumer

Overall, the results for Young's modulus measures in relation to complexity has taxa with relatively higher Young's modulus values (i.e., values above 90 MPa) clustering together above the second coordinate axis with the exception of *Pongo pygmaeus*. In the toughness plot however, the taxa with the relatively highest toughness measures (i.e., values greater than 700 Jm^{-2}) separate farther from other groups regardless of diet type. However, *C. jacchus* and *P. pithecia* cluster more closely together than to any other group. In the Young's modulus PCoA plot, the taxa that consume primarily

tough foods clustered closer together than to any other group. In addition, *P. troglodytes* and *Pongo pygmaeus*, which are both categorized as soft consumers, separated less than in the toughness plot, and plotted within the same quadrant to the exclusion of all other taxa. Hard-object consumers *S. apella* and *P. pithecia* plotted more closely to exudate consumer *C. jacchus*, than hard-object consumer *C. satanas*. *C. satanas* remained separated from other hard-object consumers in both the Young's modulus plot and toughness plot.

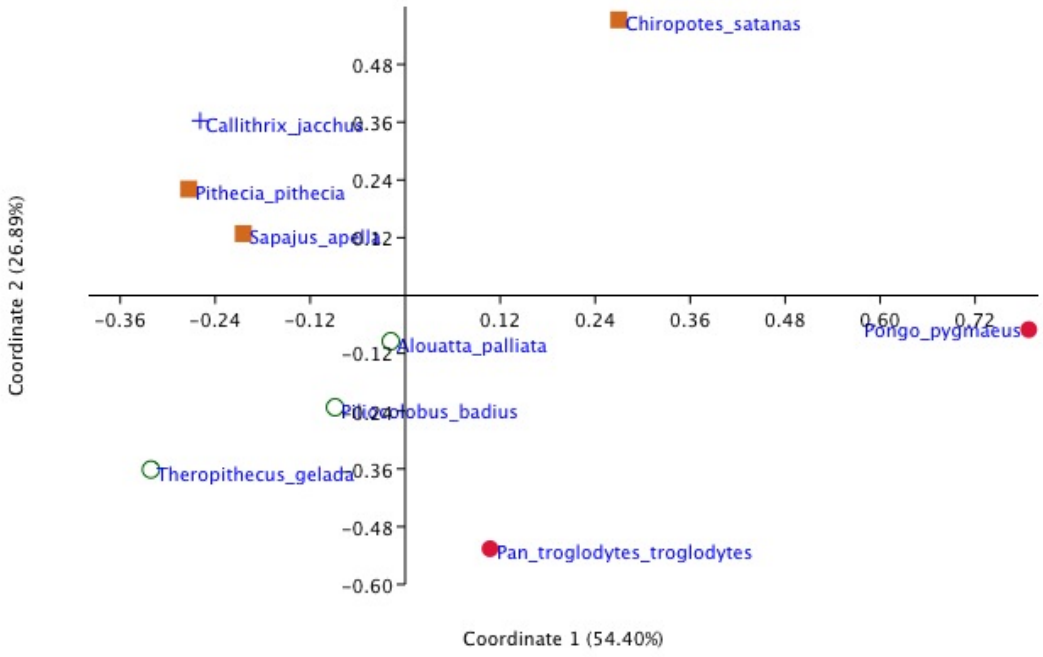

Figure 21. Principal Coordinates Analysis (PCoA) plot of sutural complexity and size with measures of Young's modulus (*E*). Key: filled square = hard-object consumer; filled circle = soft consumer; open circle = tough consumer; plus = exudate consumer

4.5 Discussion

One of the key functions of cranial sutures is their role in the transmission and dissipation of mechanical loads experienced during mastication (Herring, 1972). If this is the case, then suture morphology should reflect the loading environment to which it is subjected (Rafferty and Herring, 1999). Previous work in primates by Byron (2009) determined that dietary signals were detectable in the sagittal sutures of cebids, and that the relative increased interdigitation observed in *Sapajus apella* compared to other closely related cebids was attributable to the consumption of hard objects. Thus, this study sought to extend this reasoning to the zygomaticotemporal suture in order to test whether sutures in other highly loaded areas of the cranium respond to differences in strain magnitude.

The results of this study do not support the predictions that increased sutural complexity (in the form of increased interdigitation) is found (1) in taxa consuming a mechanically resistant diet (tough and/or hard) as compared to those with less mechanically resistant diets or (2) in taxa that consume foods with higher toughness and/or Young's Modulus values. Broadly speaking, both total consumption percent and FMPs data appear to be poor predictors of complexity in the zygomaticotemporal suture in this sample of primates. The lack of differences between dietary groups as well as in pairwise comparisons between closely related taxa support the idea that differences in sutural complexity are not driven by diet, in terms of total consumption percent or FMPs, in this sample.

It is notable however that across the study sample as a whole, the raw complexity measures were on average greatest in hard-object consumers, followed by tough

consumers, soft consumers, and exudate consumers (Fig. 7). While this does not directly support the study's hypotheses in a statistical sense, it may broadly suggest that feeding on hard or tough foods may be an indirect contributor to sutural complexity through the resulting masticatory strains produced during the oral processing of these foods. While this study did not find direct support for the hypothesis that dietary type catalyzes an increased sutural response, it does not discredit the notion that morphological complexity is in part related to diet, and that in this region of the skull, sutural morphology may be relatively conserved regarding the extent to which that morphology can vary. Furthermore, the lack of support for the hypothesis may derive from the relatively low variation in complexity across the entire primate sample, given complexity values are generally constrained to values between 1 and 2.

The overall shape of the zygomatic arch, compared to other cranial bones joined by sutures is also notably different; as a beam-like structure fully suspended in space from the skull, the presence of high loading will presumably cause it to behave differently as compared to the large, rounded, bony plates between which the sagittal, or coronal sutures run. Furthermore, the zygomaticotemporal suture appears on a bone that directly experiences high forces due to the direct attachment of powerful masticatory muscles and other fascia, which generate high magnitude and opposing forces along the length of the zygomatic arch (Eisenberg and Brodie, 1965; Preushoft and Witzel, 2004; Rodriguez-Vegas and Casado Perez, 2004; Curtis et al., 2011; Curtis et al., 2014). Burn et al. (2010) found that regardless of diet, cranial suture in pigs were thicker and less interdigitated than facial sutures, and that relative interdigitation can vary within sutures as well. If this is the case in primates, then the low variance in interdigitation

observed between groups may be because masticatory strain doesn't appear to significantly affect suture form and the variation observed within dietary groups may be due to species specific patterns unrelated to masticatory loading.

Sutural complexity in the mid-palatal sutures of two species of colobus monkeys (*Colobus polykomos* and *Procolobus badius*) have been previously quantified using fractal analysis to determine whether differences in the dietary composition of these sympatric primates manifested in the relative interdigitation of the mid-palatine suture (Hotzman, 2004). This study found no significant differences between these taxa with respect to mid-palatal suture complexity, which is consistent with the findings of the zygomaticotemporal suture in the present study. Hotzman (2004) found that the average fractal measure in *C. polykomos* (D=1.18) was slightly, though not significantly, greater than in *P. badius* (D=1.13) which may be attributable to the relatively higher consumption of the particularly hard African oil bean (*Pentaclethra macrophylla*) in *C. polykomos* as compared to *P. badius*. In spite of this key dietary difference, the consumption of this seed likely does not generate enough force to cause more stress in this portion of the palate (Hotzman, 2004). The current study also executed pairwise comparisons of fractal values between specimens of *C. polykomos* and *P. badius* but found no significant differences between these taxa, and determined that overall, their zygomaticotemporal suture complexity values are relatively the same (D=1.46 and D=1.47 respectively). This further suggests that dietary loading is not sufficient to catalyze significant variation in suture morphology and that the extent to which sutural morphology can be modified is relatively restricted in particular portions of the masticatory complex. In the zygomatic arch (and palate) architectural differences in the

amount and composition of bone that exist between the forces generated at various bite points in the tooth row may disrupt the masticatory forces generated during chewing, and therefore reduce the magnitude of the loads at the suture sites. However, without *in vivo* strain data, bite force measures, or estimates of muscle activation, this remains speculative at best.

The zygomatic arch is known to experience a range in strains along its long axis with the highest loads occurring anteriorly and decreasing posteriorly (Hylander and Johnson, 1997). Because the entire arch does not bear uniformly high magnitude loading, increased zygomaticotemporal sutural complexity may not be necessary. Alternatively, because sutures could be places of potential structural weakness, particularly under high loading, it may not be selectively advantageous to allow highly flexible or pliant sutural phenotypes in a highly strained area because bone failure would result in severe fitness consequences. Therefore, the range of sutural values may be constrained as a protective measure to ensure structural integrity.

4.5.1 *Complexity measures and diet*

This study found that zygomaticotemporal sutural complexity is related to both skull size and zygomatic arch size in primates, and suggests that generally, larger individuals exhibit greater sutural complexity in this region than do smaller individuals. However, size alone only explains a small portion of the variation observed. Suture path length and complexity were also not related, indicating that larger zygomatic arches do not necessitate more complex suture morphology. For measures of complexity, lacunarity, and prefactor lacunarity, no significant results were found between dietary

groupings, but significant variation was observed within specific dietary groups (soft and tough). This suggests that the dietary groupings of "tough," "soft," "hard," and "exudate" are not the most informative way to categorize diet and may overlook some underlying patterning because they are too generalized. In addition, there is also the possibility that the size association found among the taxa may be a function of measurement scale or the resolution of the scans.

The significant findings within tough and soft consumers indicate that there is substantial variation within these two groups, which is unsurprising given they had relatively larger sample sizes than either the hard-object or exudate groups. The tough and soft consumer groups contained some of the largest bodied taxa overall (e.g., *G. gorilla*, *P. pygmaeus*, and *P. troglodytes*) and while complexity was correlated with size, size alone appears to account for only a small portion of the variation within these groups. Therefore the weak relationship between size and complexity leaves the majority of the variation unaccounted for. The relatively low variation observed in hard object and exudate is likely due to their relatively small sample sizes and more similar body sizes.

The results for pairwise comparisons between different dietary groups also supports the finding that dietary grouping on the basis of total consumption percent is not a good predictor for complexity. In this set of comparisons, only the pairing between *Theropithecus gelada* and *Papio anubis* was significant (p=0.030). There are several potential explanations for this result. First, given that geladas are specialized gramnivores with highly tough diets, and *Papio anubis* is a relative generalist that consumes a wide variety of foods, the dietary signal in this pairing may be more detectable because their

diets are more diametrically opposed as compared to taxa who have more similar diet compositions. Secondly, with respect to the bone morphology of the zygomatic arch, geladas appear to possess measures of bending and torsional resistance that are relatively greater in posterior portions than in anterior portions; a pattern that opposed what is typically observed in primates, including *P. anubis.* If this difference in bending and torsional resistance is due to the fact that masticatory strain measures are also greatest posteriorly as compared to anteriorly in this species, then that would potentially explain the significant differences between *T. gelada* and *P. anubis* because the concentrations of the highest strains would be positioned on opposite sides of the zygomaticotemporal suture in these taxa. Finally, the architectural differences in the skulls of geladas versus baboons may also contribute to the differences seen here; both are highly prognathaic compared to other primates and the relative activation of the masseter muscle when opening and closing the jaw during non-masticatory behaviors may subject the suture to a different series of strains. It would be interesting to investigate the relationships between these taxa further by way of masseter muscle activation and *in vivo* strain measurement along the zygomatic arch to determine whether geladas possess a species-specific pattern unique among other primates.

The results for lacunarity (relative "gappiness") and prefactor lacunarity (heterogeneity) concur with the findings for complexity with regard to dietary categorization on the basis of total consumption percent. These results indicate that for soft and tough consumers, the texture and fluctuation in the suture's path are greatest as compared to hard and exudate consumers. Both soft and tough feeders had significant variation in these measures indicating suture patterns with varying degrees of holes or

gaps persisted throughout both groups. In addition, the significant variability in the heterogeneity of the fractals in the soft and tough diet groups suggests that the suture path ungulates non-uniformly and that there is variation both intra-, interspecifically, and by diet type in these species. Given these variables are related to complexity, it logically follows that they pattern similarly to complexity in relation to the dietary groups. Moreover, both lacunarity and prefactor lacunarity do not appear to be related to traditional dietary categories in any predictable way nor do they appear to be related to any measures of size.

Suture pathlength was significantly related to both skull and zygomatic arch though the relationships are relatively weak (r^2= 0.139 and 0.107 respectively; Table 5). This suggests that on average, larger taxa have relatively greater path lengths, though this relationship is relatively weak. Suture path length and complexity, however, are not related suggesting that taxa with relatively longer sutures do not necessarily have more complex sutures. Surprisingly, suture path length was significantly different among dietary groups with exudate consumers possessing significantly different path length measures as compared to soft, hard, and tough consumers. Compared to the other groups, exudate consumers possessed the lowest complexity values as well as the relatively shortest path length values on average, which at least partially explains why they are so different from the lengths in other taxa. Soft and tough consumers were also found to have significantly different average path lengths, with tough consumers possessing the greatest path lengths on average among all taxa. Because path length was correlated with size, it is not surprising that tough consumers yielded the greatest path lengths since they contained some of the largest taxa in the sample.

An additional component to consider in future analyses is the potential effect of sexual dimorphism, specifically masseter muscle size, on sutural complexity. The lack of equal sex samples for each species in this study precluded the performance of extensive comparisons between males and females, particularly given the lack of male specimens representing the more dimorphic species such as *Gorilla gorilla* and *Pongo pygmaeus*. While this study did conduct preliminary comparisons between males and females in species where sample sizes were more equal, no significant differences were found. Sexual dimorphism in cranial sutures has been identified in sheep, where males were found to possess greater complexity in facial sutures (presumably from clashing horns) while females had greater complexity in their cranial sutures as compared to males (Jaslow, 1989). While primates do not engage in these types of traumatic behaviors, the degree of sexual dimorphism in the masticatory muscles may explain sutural complexity differences intraspecifically, particularly in highly dimorphic species such as gorillas, orangutans, or chimpanzees. Given the developmental differences in sutural growth and fusion observed in gorillas and chimpanzees, a consideration of the effect of diet and masticatory muscle size on suture formation would improve our understanding of cranial suture ontogeny.

4.5.2 *Hard-object feeding and sutural complexity*

The effect of hard-object feeding is of great import and debate in paleoanthropology given its implications for extinct hominin diets and associated craniofacial adaptations in both *Australopithecus* and *Paranthropus* (Jolly, 1970; Grine, 1981; Rak, 1983; Kay, 1985; Lucas et al., 1985; Hylander, 1988; Teaford and Ungar,

2000; Strait et al., 2009; Daegling et al., 2011). To understand these effects, extant primate models are critical because they provide a comparative foundation in which both their morphology and behavior can be observed and then applied to the fossil record.

The *Pitheciinae* are distinct among living primates because of their reliance on hard seeds, immature fruits, and possession of specially adapted dentition (e.g., procumbent, high crowned lower incisors, large canines, specialized premolars) and deep jaws (Ayres, 1989; Norconk et al., 1998; Boubli, 1999), which allows them to process these foods. Comprised of three genera (*Chiropotes*, *Cacajao*, and *Pithecia*) these taxa consume fruit, and in particular hard and immature seeds to varying degrees, although during resource stress they are known to increase their reliance on hard seeds (Ayres, 1989; Martin et al., 2003). These taxa are all predispersal seed predators (Janzen, 1971) that consume fruit encased in a hard pericarp that is pierced using their procumbent incisors (Kinzey, 1992). These types of fruits typically have softer seeds, which are easily masticated on the molars once the hard pericarp is pierced (Martin et al., 2003).

Sapajus apella also consumes hard objects, though not to the extent of the pithecids. A significant aspect of *S. apella*'s consumption of hard objects (such as palm nuts) is the manual manipulation of the hard husks (Peres, 1991) and their thickly-enameled molars that crush hard food items. Compared to the pithecids, which use their anterior dentition to open the hard pericarp, *S. apella* relies on the power of its posterior dentition to puncture-crush the hard food (Martin el al., 2003). In both pithecids and *S. apella*, there is presumably high masseter recruitment with correspondingly high masticatory strain during feeding on these objects, which would theoretically create a mechanical environment forging the basis for increased sutural response.

When average fractal values (D) are compared across all study taxa, the highest averages values were indeed found in *Chiropotes albinasus* (D=1.894) and *Cacajao rubicundus* (D=1.705), both of which consume hard seeds and immature fruit, though *C. albinasus* consumes relatively fewer amounts of seeds (about 35.9%, see Ayres, 1989) as compared to *C. rubicunda* which consumes about 67% (see Ayres, 1989). *Chiropotes satanas*, also a routine hard-object consumer, possessed an average complexity value of 1.45, placing it below the averages of the other pithecids. In contrast, *S. apella*'s average complexity value of 1.45 places it within the same range as *C. satanas* but below the average for both *C. rubicundus* and *C. albinasus.* In both species of *Chiropotes* in this study however, the species is represented by a single datum point, which is used with caution in the interpretation of these results. For future study, it would be important to include larger sample sizes. For the purpose of the present study these results may indicate that the increased complexity in pithecids compared to *S. apella* may be a function of the differences in the portions of their diets dedicated to hard-object consumption. Dietary data on *Sapajus* indicates that approximately 12.5% of its diet is composed of hard seeds, while up to 75% of the diet is primarily fruit (Galetti et al., 1994) suggesting that the relatively infrequent consumption of these hard items compared to these other taxa does not lead to same degree of sutural complexity found in the pithecids.

Among the Cercopithecidae, *Cercocebus torquatus*, a thickly enameled, hard-object consumer possessed a higher complexity value (D=1.583) than *Lophocebus albigena* (D=1.476) a result that is unsurprising (and not statistically significant) given that *Cercocebus* consumes harder items on average that *Lophocebus*. Like the pithecids,

L. albigena populations in Kibale National Park, Uganda, are known to switch to eating seeds (which are presumed to have high hardness) and bark during periods of food scarcity (Lambert et al., 2004). Because hard seeds can serve as an important fallback food source, the ability to process such a food item would be advantageous, particularly during periods of extended resource scarcity.

Previous work has examined the craniodental features of *S. apella* in relation to other cebid species (e.g., Eaglen, 1984; Bovier, 1986; Cole, 1992; Daegling, 1992; Masterson, 1996; Wright, 2005) finding *S. apella* possesses clear morphological adaptations to hard-object feeding. When the complexity values of *S. apella* are compared to closely related *C. capucinus*, *S. apella* possesses only slightly more complex (D=1.45) zygomaticotemporal sutures compared to *C. capucinus* (D= 1.40) despite the marked craniofacial morphological differences found between these taxa. This finding is in contrast to that of Byron (2009a) who found sagittal sutural complexity was greater in *S. apella* compared to that of other capuchins. The relatively larger temporal area of *S. apella* (a proxy for the size of the temporalis muscle) compared to other cebids suggests that increased temporalis recruitment resulting from hard-object biting induces greater tensile loads on each side the sagittal suture, causing greater tensile loading along the bone edges, and consequently increasing sutural complexity (Byron, 2009a). In addition, the deep layer of the temporal fascia attaches along the medial surface of the arch and the superficial layer attaches to the lateral surface of the archwhich functions to resist the tension generated by the masseter muscle (Eisenberg and Brodie, 1965; Curtis et al., 2011).

In the case of the zygomaticotemporal suture, the relationship between the masticatory muscle (i.e., the superficial and deep masseter) and its resulting strain magnitudes and orientation relative to the zygomaticotemporal suture is different than that of the sagittal suture. Specifically, the masseter muscle takes its origin at the anterior portion of the zygomatic arch (and thus anteriorly to the zygomaticotemporal suture), which, upon activation, would presumably generate greater tensile loads along the zygomatic portion of the suture as compared to the temporal bone portion. Thus, unlike the sagittal suture, which experiences tensile loads emanating from the respective temporalis muscles on each side of the cranium, the zygomaticotemporal suture experiences strain only from the one side, consequently diluting the amount of strain experienced on the other side. This may make the suture less sensitive to the effects of high magnitude, obdurate feeding because the suture is not entrenched in a uniformly strained region. In the case of cebids, this may explain the differences in interdigitation found in the sagittal versus zygomaticotemporal sutures, if the strains on the zygomatic arch do not differ significantly between *S. apella* and *C. capucinus*. To more adequately test this, future work should consider collecting measures of masticatory muscle activation in concert with masticatory strains in both regions during feeding in this group.

The taxa with the lowest overall sutural complexity values were *Callithrix humeralifera*, (D= 0.646), and *Callithrix jacchus* (D=1.144), both of which are committed exudate consumers whose complexity measures support the initial prediction that less mechanically resistant diets result in less complex sutures. Surprisingly however, the two species of *Pithecia* (*Pithecia monachus* and *Pithecia pithecia*) also possessed relatively low complexity values overall (D= 1.37 and D=1.06 respectively) as compared

to other seed predators and the study sample as a whole. Like *Cacajao* and *Chiropotes, Pithecia* too exhibits clear craniodental adaptions for hard-object feeding (e.g., procumbent incisors, molarized premolars, low occlusal relief in the molars and premolars, see Ledogar et al., 2013). Yet, their low complexity values, particularly in *P. pithecia*, place them within the range of exudate consumers as opposed to other hard-object feeders. One possible explanation for the presence of craniodental adaptations to hard-object consumption in *P. pithecia* but low sutural complexity values rests not in the degree of suture interdigitation, but in the degree of overlap in the suture as a means of resisting tensile and shear forces generated during mastication.

In a 2014 study, Dzialo and colleagues examined the squamosal suture of *Paranthropus boisei* to determine whether its large and overlapping sutures were an adaptation to maintain sutural integrity during seemingly high magnitude masticatory forces and to prevent any separation of the bones. The high degree of squamosal suture overlap in *P. boisei* was first noted by Rak (1978) who predicted the potential failure of the squamosal suture in two ways: as being a consequence of high shearing forces derived from the inferior pull of the temporalis muscle on the parietal bone or from the inferior pull of the masseter on an anteriorly shifted, flaring zygomatic arch, which would rotate the temporal bone, causing it to separate from the parietal (Dvialo et al., 2014).

Using Finite Element Modeling (FEM), this study simulated the effect of static premolar biting on suture strength and integrity in models of *P. boisei* and *Pan troglodytes* (Dvialo et al., 2014). The peak von Mises and maximum principal stress results for this study found that an increase in suture size led to a decrease in stress on both the working and balancing side sutures. Furthermore, this study found that these

maximum principle stresses were consistently greater on the balancing side than on the working side, suggesting that the risk of suture failure is higher on the balancing side than on the working side (Dvialo et al., 2014). Shearing forces appeared to be the dominant force type experienced on both the working and balancing sides, and the increased thickness of the suture was necessary to avoid failure (Dvialo et al., 2014). In addition, increasing contact area effectively reduces shearing loads as shear resistance ability to a function of cross-sectional area. If relative suture volume and overlap do function to resist high magnitude strains independently of sutural complexity, then this could represent an alternative means to combat high masticatory strains. A valuable future study would be to quantify suture volume and overlap in extant hard-object consumers (such as the pithecids) to establish a baseline to which fossil taxa can be compared.

4.5.3 *Total consumption percent versus FMPs data*

One of the primary aims of this study was to determine whether food material properties data or total consumption percent was a better predictor of zygomaticotemporal sutural complexity in a diverse primate sample. The results for total consumption percent do not suggest that it is a good predictor of sutural complexity in the zygomaticotemporal suture in this primate sample. This study designated consumption percent using the protocol of Muchlinkski et al. (2010) in which a species' dietary designation was based on 50% or more consumption of a food item. Given the dietary shifts that can take place as a result of food availability, a species dietary category may technically shift depending on the time of year, particularly if a species transitions to the consumption of harder food items as a fallback strategy. For example, *Lophocebus*

albigena populations in Kibale National Park, Uganda, are known to switch to eating seeds (which are presumed to have high hardness) and bark during periods of food scarcity (Lambert et al. 2004). The utility of both FMP data and total consumption percent may be hampered when in isolation from other measures of primate diets. One of the disadvantages of categorization based on total consumption percent alone is the fact that cumulative measures of consumption do not account for the variation in food material properties that can occur within a single food item. Furthermore, the seasonal fluctuation and variation in local ecology complicates the issue when populations of the same species are compared. To account for these effects, it would be prudent to generate estimates of diet that weigh FMP measures by reported consumption percentages. Venkatraman et al. (2014) generated estimates of cumulative toughness in geladas that took measures of toughness (R) for a given food item multiplied by the percent the food item constituted in the diet. The result of these estimates for all food items were summed together, representing a weighted measure of the toughness that can be used for comparisons between groups across an annual dietary cycle. By extension, an analogous estimate for Young's Modulus (E) could be generated and used to more adequately quantify the variation in stiffness of various food items. Furthermore, the scale at which these cumulative, weighted measures are applied can also target questions concerning the relative differences in material property measures within a single food item. Plant tissues range from those that are easily processed to those that are more mechanically resistant and a primate ingesting that food may encounter a series of plant layers with markedly different processing requirements (Wright, 2004). For instance, the *Inga* fruit ingested by *P. pithecia* varies in toughness depending on the plant part; the endosperm has relatively

low toughness measuring about 182.1 J m^{-2} compared to the much tougher sections of the external woody tissues (4382.9 J m^{-2}) (See Table 5.3 in Wright, 2004). Thus, the toughness measures of this fruit fall within the range of many types of leaves, and would impose greater masticatory demands on the masticatory complex compared to less tough fruits. Given the complexity of primate feeding ecology, future studies would ideally be able to collate data on FMPs, total consumption percent, feeding times, and site-specific local ecology to craft a more comprehensive dietary profile.

The results for the FMPs comparisons indicate that mean measures of both toughness and Young's modulus have no relationship to zygomaticotemporal sutural complexity. With respect to size, no relationship was found between skull size or zygomatic arch and mean toughness, but a significant, negative relationship between skull size and mean Young's modulus was found in this sub-sample of primate taxa (Fig. 6). This result suggests that taxa of increasing skull size consume foods of decreasing hardness or stiffness; a finding also observed by Coiner-Collier et al. (2016) in their sample of primates. This result may be misleading given the difficulties in including the full spectrum of hard food items consumed by larger bodied taxa because of issues with FMP data collection in the field (see Coiner-Collier et al., 2016, p. 112). If complete dietary profiles could be constructed, particularly on these large-bodied taxa, then that would provide more information about this relationship and provide increased explanatory power.

Despite these issues, a notable strength of FMP data is its ability to differentiate between hard (using Young's modulus) foods and tough foods in a mechanical sense. Dietary comparisons are usually dichotomized into food categories of "hard versus soft"

or “mechanically challenging versus less mechanically challenging” as a means of characterizing the mechanical differences between the two categories. For example, previous work by Burn et al. (2010) examined the effect of a hard diet versus a soft diet on midline cranial sutures in pigs (*Sus scrofa*). Their results found subjects consuming hard foods had greater sutural thickness and greater interdigitation compared to those fed soft foods, but these relationships were not statistically significant (Burn et al., 2010). In contrast both tough and hard foods are commonly subsumed under the category of “mechanically challenging” which carries expectations about the durability of the food item, time necessary to process it, and the concomitant bite forces required to break it down. Hard foods and tough foods, however, differ in these regards. In this study, separation of tough consumers from hard consumers, as well as the inclusion of FMP data was meant to test whether differences between hard and tough consumers were detectable. Gorillas are known for consuming large quantities of tough food in contrast to orangutans, which generally consume fruits, as well as hard seeds (Vogel et al., 2008). This study found that average complexity measures of orangutans (D=1.54) were greater than that of gorillas (D=1.49) though these values were not significantly different. Similar to the findings of Burn et al. (2010), absolute differences in sutural interdigitation, albeit not statistically different, occur in individuals consuming different diets. Given that this study found hard-object consumers tend to have absolutely greater complexity values than closely related taxa suggests there may be an indirect effect on suture morphology connected to hard-object feeding.

Mechanically, the presence of the zygomaticotemporal suture on the zygomatic arch is important for the maintenance of arch architectural integrity because it allows for

relatively small levels of tensile and rotational freedom during instances of bending induced during mastication (Curtis et al., 2014). While a limited range of motion is necessary to accommodate the pull on the arch during mastication, too much instability has the potential to cause breakage or failure. The finding that sutural complexity was not significantly different across the taxa in this study may stem from the need to allow enough movement to adequately disperse forces impacting bone while simultaneously maintaining a safety factor that ensures the bone will not fail.

In addition to feeding, the ontogenetic nature of suture structure on the zygomatic arch reveals that suture complexity and stiffness increases with age. The study on Curtis et al. (2014) found that ontogenetic changes affected zygomaticotemporal sutural form in macaques of different ages. Despite the simple representation of this suture in models of the zygomatic arch, this study finds that significant increase in organized bone facets that interlock to minimize movement between the zygomatic and temporal bones during feeding (Curtis et al., 2014). Younger individuals have relatively more movement at this junction allowing the two bones to displace in the same direction along the bone plane whereas older individuals have relatively less movement due to the constraining nature of the increased suture interdigitation. Thus complexity appears to increase with age (Curtis et al., 2014). While this study was limited in sample size and only looked at a single macaque species, it would be interesting to expand this is future work through an examination of ontogeny in relation diet, particularly at the point when young individuals make the transition to a fully adult diet.

Finally, a key point accompanying the findings of this study concerns the use of fractals for quantifying complexity in a biological structure. Some have criticized the use

of fractals analysis on human cranial sutures (see Long and Long, 1992) because these suture forms were believed to violate the rule of "self-similarity" and were therefore not fractals despite yielding dimensions between 1 and 2 (Hotzman, 2004). Studies of human cranial sutural complexity that have employed the box counting method have demonstrated that these sutures indeed reflect self-similarity by plotting the logged number of squares with length *r* occupied by the suture against the logarithm of 1/*r*. Fraclac provides the log-log graphs for each analyzed suture and has shown a linear relationship between the points indicating that the sutures are self-similar and thus by definition considered fractal. However, one of the issues that arose was that some specimens that are exudate consumers yielded fractal values below 1, as fractal dimensions in nature are expected to exceed 1 (Long and Long, 1992). In this case, these exudate consumers can still generate fractal measures but may actually represent a nonfractal curve. In sutures generally, irregular curves are adaptive in resisting shear and compression (Herring, 1972), however mathematically they can become non-scaling (Long and Long, 1992). This means that as length N(r) increases (because r is smaller) a fractal dimension is still measured. High values of r generate a false fractal, while smaller values of r result in curves that are Euclidean in nature and yield values approximating 1 (Long and Long, 1992). In some human lambdoid sutures (Long and Long, 1992), the suture folds and extends back and forth in such a way as to create a wavelength with an r value that is relatively smaller, and thus superficially appears to be a fractal. It has been argued that there are distinctions within suture types such that sutures can be ordinary, irregular, waveform, or intricate (Long, 1985; Long and Long, 1992) depending on the extent to which the suture undulates to create elaborate,

interlocked bonds between bone or relatively low interdigitations that still provide adequate stiffness.

In the case of the zygomaticotemporal suture, it may be more appropriate to examine differences in sutural morphology with respect to suture type to determine whether the patterning of the convolutions is markedly different among taxa. Observationally, the sutures of exudate consumers appear to have sutures with relatively longer wavelengths (i.e., greater distance between peaks) and the amplitude of the peaks appear less wide relative to other taxa. In other words, the sutures appear relatively more linear with r lengths that are smaller, and therefore more Euclidean as compared to taxa with shorter wavelengths and larger amplitudes.

4.6 Conclusions

Modeling the biomechanical nature of the primate cranium has often focused on analyzing bone samples without accounting for the presence of cranial sutures and their role in strain dissemination. Despite the highly strained environment of the zygomatic arch, the degree of complexity in the zygomaticotemporal suture appears to have no relationship to food material properties data or total consumption percent in primates. The measures of sutural complexity observed here were generally highest in hard-object consumers but not statistically significant, which may suggest that hard-object feeding potentially indirectly influences sutural interdigitation through increased masticatory loading; however, more work in the future is required to test this more extensively. In addition, the degree of overlap in the zygomaticotemporal suture may have a greater functional role in dissipating strain experienced during feeding in this region of the skull

that the amount of interdigitation present. In addition, the composition of the sutural fibers themselves may reveal important information about the nature of the suture joints and their mechanical importance to the cranium. Thus further exploration of the mechanical factors that affect sutural morphology and the craniofacial complex as a whole are necessary for the improvement of models of feeding and for a comprehensive understanding of the biomechanics in this region.

CHAPTER 5: ZYGOMATIC ARCH CROSS-SECTIONAL GEOMETRY COMPARED WITH DIET IN PRIMATES

5.1 Abstract

Craniofacial morphology in primates is suggested to vary on the basis of diet because foods are often disparate in the amount and duration of force required to break them down. Therefore, diet has the potential to exercise considerable pressure on the morphology of the masticatory system. The zygomatic arch is a known site of relatively high masticatory strain and yet the relationship between arch form and load type is relatively unknown in primates. This study uses cross-sectional geometric properties to investigate the effects of different diet types (measured in terms of total consumption percent and food materials properties) on zygomatic arch form to determine whether measures of bone mechanical resistance and shape track with experimental strain patterns. Across the primate sample presented here, measures of maximum bending and torsion resistance were found to track with experimentally obtained strain patterns. Species who primarily consumed tough foods exhibited the greatest measures of bending and torsional resistance in the zygomatic arch compared to other dietary groups. The highest measures of bending resistance and torsional resistance were found in anterior regions in the majority of taxa regardless of diet type, which supports the prediction that zygomatic arch cross-sections reflect known strain distributions. Tough consumers generally possessed the highest measures of these variables compared to other diet groups, but no predictable pattern within any diet group emerged. Direct measures of toughness (*R*) and Young's modulus (*E*) were not found to correlate with cross-sectional geometric properties. Stress-limited and displacement-limited indices were also not

correlated. Pairwise comparisons between taxa do reveal that consumption of hard/tough items does suggest higher instances of bending and torsional resistance, however. Cross-sectional shape indexed by I_{max}/I_{min} determined there is shape variation throughout the zygomatic arch regions, but that no predicable pattern emerges. These results suggest that direct measures of resistance to bending and torsion are relatively predictable along the zygomatic arch, whereas measures of cross-sectional shape are less predictable. These findings support the hypothesis that the mechanical behavior of the arch reflects known strain patterns, that zygomatic arch bone cross-sectional form is complex, that simple beam models do not adequately explain the differences in cross-sectional shape, and that further study of bone form and dietary type in this region is necessary.

5.2 Introduction

The anatomy of the craniofacial complex is central to masticatory function across mammals, and adaptations within this complex enable individuals to access necessary food items. As a group, primates have significant dietary variability compared to other mammals and the differences in primate masticatory complexes are hypothesized to map onto variances in food acquisition and processing (Bouvier & Hylander, 1982; Beecher et al., 1983; Anapol & Lee, 1994; Lucas et al., 2008a,b; Yamashita, 2008b). Within mammals, experimental work has shown broadly that biting on mechanically challenging (i.e., tough or hard) foods leads to longer chewing durations and processing time, increased bite forces, increased jaw-adductor recruitment activity, and relatively higher levels of balancing-side jaw-muscle force activity (Herring and Scapino, 1973; Luschei and Goodwin, 1974; Weijs et al., 1989; Hylander et al., 1992). In the latter, differences

in jaw-muscle activity patterns ultimately affect the frequency and magnitude of bite force applied to food itemds, as well as the reaction forces experienced by masticatory features through the course of a chewing cycle (Franks et al., 2016).

Internally, the presence of elevated peak bone strain magnitudes and increased cyclical loading during the mastication of challenging (particularly obdurate) foods has been shown to induce increased cortical bone modeling and remodeling instances of masticatory elements in mammals (Beecher and Corruccini, 1981; Bouvier and Hylander, 1981; He and Kiliaridis, 2003; Lieberman et al., 2004a; Ravosa et al., 2007; Menegaz et al., 2009, 2010; Scott et al., 2014). In extant primate taxa that regularly consume hard or tough foods, more wide spread morphological adaption has been found to translate into robust features such as deeper mandibular corpora, differences in occlusal morphology (Degusta et al., 2003; Vogel et al., 2008; Ledogar et al., 2013), and increased enamel thickness (Dumont, 1995; Constantino et al., 2012) and these observations have been extended for use in the fossil record. In addition to those listed here, a key masticatory element hallmarked as an indicator of a mechanically challenging diet in fossil taxa, such as *Paranthropus,* is the relative positioning and robusticity of the zygomatic arch on the cranium. In the case of *Paranthropus,* the anterior positioning, coupled with the large degree of lateral flare and robust bone of the arch are perceived as evidence of increased mechanical advantage during chewing (Rak, 1983). However, despite the weight of this cranial feature in determining the diet of an individual, relatively little is known concerning the specific bone structural and mechanical elements of the zygomatic arch in relation to dietary loading in living primates especially given that the existing *in vivo* zygomatic arch strain data is primarily limited to macaques (e.g.,

Iwasaki, 1989; Hylander and Johnson, 1997). Without a sense of the extent that bone responds to masticatory loading in this region, accurate dietary assessments in fossil taxa cannot be made. This issue is further compounded because zygomatic arches in fossil hominin crania often are not adequately preserved, leaving only broken or missing portions of the arch exposed. Therefore, an understanding of zygomatic arch cross-sectional form in relation to dietary loading in extant primates arms future investigations with the tools to assess this feature in fossilized individuals, despite the presence of broken or damaged arches.

The zygomatic arch is particularly relevant to mammalian masticatory mechanics given its structural placement within the mammalian skull and because it serves as the anchor for the masseter muscle. *In vivo* bone strain data reveal that upon activation, the masseter exerts an inferiorly directed force that induces parasagittal bending on the zygomatic arch as well as a torsional force caused by the inferior, medial pull of the masseter on bone (Hylander and Johnson, 1997; Herring et al., 1996). Furthermore, the inferior pull of the masseter may also produce a mediolateral bending moment (Smith and Grosse, 2016). Given that the masseter attaches on the anterior portion of zygomatic arch, a steep strain gradient has been experimentally shown to exist along the length of the arch in cats (Buckland-Wright, 1978), pigs (*Sus scrofa*) (Herring et al., 1996, 2001; Marks et al., 1997; Herring and Teng, 2000; Rafferty et al., 2000, 2003), and macaques (*Macaca fascicularis*) (Hylander et al., 1991; Hylander and Johnson, 1997). In *Macaca* specifically, a strain gradient was observed in which strains were highest anteriorly and decreased posteriorly (Hylander and Johnson, 1997). The published max micro strain (γ-max in $\mu\varepsilon$) values for macaques indicates that strain is approximately three times higher

in anterior as compared to posterior sections (see Table 1 in Hylander and Johnson, 1997). Furthermore, mean anterior zygomatic arch micro strain values (985 με) greatly surpass strain measures in the upper face (98-216 με), and mandibular corpus (783 με) (Hylander, 1984; Hylander et al., 1991; Hylander and Johnson, 1997; Ravosa et al., 2010). Compared to other regions of the cranium, the peak strains experienced by the zygomatic arch are similar to, and even surpass, those of the mandible and maxilla, and far outstrip strains experienced in the circumorbital region (Frank et al., 2016). Given these observations, it follows that the zygomatic arch experiences some of the highest strains overall (Ross and Metzger, 2004) and that as the origin for the primary jaw adductor muscles, it serves a crucial role within the primate masticatory system.

The zygomatic arch is constructed from the zygomatic process of temporal bone and the temporal process of the zygomatic bone, and the two bones are joined at the zygomaticotemporal suture. The zygomatic arch's unique form, from a simple geometric perspective, is most similar to a hollow beam with two fixed ends. This model has been employed in previous work (Hylander and Johnson, 1997) and the application of beam theory has been used to elucidate the mechanical behavior of the arch under masticatory loading (e.g., Iwasaki, 1989; Smith and Grosse, 2016). Under such loading, the zygomatic arch in macaques has been found to bear high concentrations of compressive and tensile strains in its anterior portions (Hylander and Johnson, 1997), medial to the masseter muscle, and lateral to the tooth row (Pryor McIntosh et al., 2016). Principal strains are also directionally distinct between anterior and posterior positions along the zygomatic arch (Iwasaki, 1989). Within macaques, the tensile axis was close to vertical anteriorly, mirroring the orientation of the masseter muscle, while posteriorly the tensile

axis was almost horizontal (Iwasaki, 1989). This arrangement, however, is not unique to macaques as it has also been observed in pigs (Herring et al., 1996). Notably though, there is a contrast between pigs and macaques concerning where the greatest zygomatic arch strains are present. In pigs (and cats) the highest strains are found posteriorly, rather than anteriorly (Buckland-Wright, 1978; Herring et al., 1996).

The squamosal portion of the zygomatic arch in pigs (which comprises the posterior portion of the arch) experiences about twice as much strain on average (349 με) as the zygomatic bone (174 με) (see Table 2 in Herring et al., 1996) indicating that the strain pattern is reversed from that of macaques. These disparities are likely attributable to how the arch deforms under loading in each species. In pigs, the squamosal region experiences a degree of out-of-plane bending in the squamosal region causing the presence of high strains in the posterior region of the arch (Herring et al., 1996). Accordingly, the cross-sectional shape of the zygomatic arch of pigs is primarily flat, and bladelike, which effectively resists high parasagittal bending loads (Herring et al., 1996). In contrast, the activation of the masseter muscle in macaques results in anteriorly concentrated peak strains, leading to more in plane bending tendencies (Hylander and Johnson, 1997). Notwithstanding the differences in the locations of the highest strain values on the zygomatic arch in these species, it is notable that average strain measures on the arch exceed strain measures found in other masticatory elements in both of these mammalian taxa.

Early comparative work on zygomatic arch shape by Hollister (1917) argued that differences in diets between captive and wild lions (*Panthera leo*), resulted in observable shape differences in the arch; namely that wild lions displayed more mediolaterally broad

and robust sections that tapered to a point superiorly, while captive lions exhibited more blade-like sections that were relatively narrow and tall, tapering superiorly to a point that curves medially (see Figs. 1-2 in Hollister, 1917). Hollister (1917) argued that the inability for captive lions to hunt prey resulted in the "non-action" of the masseter muscles, which lead to a more blade-like arch cross-sectional shape in the captive lions, as compared to the more circular section in wild lions. Later studies of dietary effects on craniofacial bone morphology in non-carnivores (specifically primates) (i.e., Bouvier and Hylander, 1982; Corruccini and Beecher, 1982; Beecher et al., 1983; Corruccini and Beecher, 1984; Iwasaki, 1989) determined that the consumption of hard foods resulted in relatively greater bone density as compared to soft foods and also demonstrates the relative plasticity of the masticatory complex.

The plasticity of the zygomatic arch in rabbits and pigs was experimentally examined by Franks et al. (2016) to determine whether cortical bone or levels of biomineralization differed between dietary groups. While the pig sample was not significant (likely attributed to the sample size of 2 for each treatment and thus lack of statistical power) specimens in the rabbit sample that consumed more resistant foods exhibited relatively greater biomineralization in the superior and medial portions of the zygomatic arch as compared to those consuming a less resistant diet (Franks et al., 2016). As Franks et al. (2016) notes in their discussion, interpretations restricted only to the results for the cortical bone would incorrectly infer that the zygomatic arch does not undergo bone remodeling under higher magnitude dietary loading despite the presence of high strains. However, the increased biomineral response precipitated by differences in diet does support the argument that the zygomatic arch is part of the masticatory system

and that increased dietary loading translates to differential bony response (Franks et al., 2016). Beyond rabbits and pigs, a recent study of cortical bone distributions and section moduli (measures of bone strength) in the zygomatic in a sample of high order primates found that cortical area distributions generally tracked with areas of high strain in the zygomatic arch (Edmonds, 2016). More importantly, every species included in Edmonds (2016) exhibited their highest section moduli measures in anterior sections, further reifying the assumption that arch architecture and regions of greatest bone strength track with reported strain distributions. However, it is important to note that the relative scarcity of *in vivo* data on the zygomatic arch across primates makes these conclusions speculative at best. While there appears to be evidence of similar patterns in cortical bone distributions and bone strength measures in the zygomatic arch across various primate taxa, *in vivo* data are necessary to understand what types of loads are present and at what magnitudes.

If changes in dietary loading affect strain magnitude, do changes in bone cross-sectional geometry also alter strain distributions? Recent work by Smith and Grosse (2016) manipulated chimpanzee zygomatic arch cross-sectional shape using three forms (cylindrical, elliptical, and blade-like) to determine whether changes in shape altered strain distributions. Regardless of the cross-sectional shape, few regular strain patterns emerged (Smith and Grosse, 2016). While blade-like cross-sectional shapes were associated with elevated magnitudes of strain in the point where the postorbital bar meets the zygomatic arch (likely as a means of stiffening the arch in the parasagittal plane), strains were not reduced in the arch itself compared to cylindrical or elliptical shapes (Smith and Grosse, 2016). This suggests that in this model, cross-sectional shape did not

reduce the strain magnitudes within the arch body indicating that the arch does not conform to simple beam theory, which confirms the findings of previous studies (Herring et al., 1996; Teng et al., 1997; Rafferty et al., 2000). If the objective is to test for the effects of zygomatic arch cross-sectional shape on strain using computational models, it is difficult to make predictions without first knowing how shape patterns along the zygomatic arch and the extent to which those patterns differ intra-individually, taxonomically, or by diet type. In order to adequately model the effects of masticatory loading, bone shape needs to be assessed in conjunction with measures of load resistance, known strain data, and dietary composition across multiple regions along the zygomatic arch to establish a foundation upon which hypotheses can be tested within a broad, comparative framework.

The importance of the zygomatic arch within the masticatory complex is undisputed, yet it remains unclear how cross-sectional geometry relates to the masticatory loads experienced, whether shape patterning is predictable by diet type, or whether arch shape and/or load resistance remains relatively uniform along the zygomatic arch. An investigation into the specific biomechanics of the zygomatic arch by way of cross-sectional shape and direct measures of bending and torsional strength is an approach not yet conducted in primates, but one that has the potential to influence current knowledge on dietary loading in response to a specific bony feature and the mechanical and ultimately adaptive consequences of form within the masticatory complex. Furthermore, this study couches these questions within the context of dietary adaptation and evaluates the effects of two distinct dietary schemes when approaching such questions. It is clear that simple beam models are not adequate to address the mechanical behavior of the arch

and the mechanical response of the arch can change depending on whether it is on the working or balancing side of the skull. Furthermore, within a single chewing bout, the working and balancing sides alternate between the left and right zygomatic arches. Better characterizing the role zygomatic arches play in resisting loads associated with different diets offers an opportunity to test how a bony feature responds to differential loading from differing diets and further emphasizes the zygomatic arch as a functionally relevant structure to studies of craniofacial biomechanics and primate cranial evolution as a whole.

5.2.1 *Hypotheses*

In haplorhines, cross-sectional shape in the zygomatic arch is related to masticatory loading regimes experienced along the arch during feeding. It is difficult to predict specific loading regimes across most primates as we lack *in vivo* data on loading in the majority of species. Thus, I take an exploratory approach to examine the functional consequences of arch form across haplorhine primates, making comparisons intraspecifically, interspecifically, and by dietary preferences.

First, the ability to resist torsion (twisting) versus bending loads is predicted to vary with the ratio of bizygomatic arch width to biramus width across primates. This ratio should reflect the line of action of the masseter muscle relative to the arch, in the coronal plane. As this ratio of bi-zygomatic arch width to bi-ramus width is closer to 1.0 (i.e., a more vertically-oriented masseter muscle), bending resistance should increase resulting in a higher I_{max}/I_{min} ratio (i.e., an I_{max}/I_{min} ratio that deviates from 1.0). As the zygomatic arch becomes more flared, the masseter muscle line of action will generate

increased torsion of the arch resulting in a lower I_{max}/I_{min} ratio (i.e., a I_{max}/I_{min} ratio that approximates 1.0). Second, the greatest measures of torsional strength (the polar moment of inertia, J) and resistance to bending moments (I_{max}) are predicted to occur in the anterior cross sections of the zygomatic arch given the highest bending and torsional forces are generally concentrated anteriorly.

5.3 Materials and Methods

5.3.1 *Study sample*

Micro-computed tomography (μCT) scans (voxel range 7.94-30.0 voxels/mm) of skulls from 43 species (n=349, see Table 8) were selected from scan collections housed at Arizona State University and Northeast Ohio Medical University (NEOMED). Only adult, wildshot specimens without pathology were included to control for influences from captivity and/or disease. Because a disparate number of males and females were found in the majority of the study species, some taxa only have one sex represented. In species where equal numbers of males and females were available, preliminary comparisons were performed to determine whether there was an effect of sex. Because no significant differences were found between males and females, the sexes were grouped together for the purposes of analysis in this study.

5.3.2 *Dietary categorization*

A twofold approach was used to categorize the taxa into dietary categories. The first approach used published data on dietary preference to assign each species to a dietary category on the basis of food mechanical properties. Following the methodology

of Muchlinkski (2010) a species' designation as a "tough feeder", "hard feeder", "soft feeder", or "exudate feeder" was based on total consumption of 50% or more of a particular food type (as measured based on the cumulative time spent feeding on an item) deemed as tough, hard, soft, or exudate based on its mechanical properties. Because this study examined the effects of presumed variation in masticatory loads on the bony morphology of the zygomatic arch, "exudate feeder" remained distinct from "soft feeder" as each of these food types differ in their material properties and time required for mastication (Norconk et al., 2009). In instances where two or more primary food types are consumed (e.g., tough and soft), the species' diet characterization was assigned based on the food type with the highest consumption percent (Appendix B, Table SM1).

The second dietary approach was used to divide a sub-set of the total study sample (species $n = 9$, see Table 9) using specific food material properties data collected on foods consumed by those species in the field (Venkatamaran et al., 2014; Coiner-Collier et al., 2016). Specifically, these recorded material properties are "toughness" (R), and "Young's modulus" (E). Toughness is defined as a material's resistance to the propagation of a crack (Lucas et al., 1986, 2000, 2002, 2008; Lucas and Pereira, 1990) and Young's modulus, also known as the elastic modulus, is the ratio of stress (force per unit area) to strain (deformation) and is a measure of a material's ability to resist elastic deformation (Gordon, 1978; Williams et al., 2005; Lucas et al., 2008a; Coiner-Collier et al., 2016). The higher the value of Young's modulus, the harder the material is. These properties constitute the two main mechanical defenses of plants and possess different material construction and ecological functions (Lucas et al., 2000). Because materials properties data were not available for all taxa included in this study, the second dietary

approach and its associated analyses will be limited to these nine primate species. Because foods can possess overlapping values of both stiffness and toughness, measures of stiffness and toughness were used to calculate stress-limited ($[R^*E]^{0.5}$) and displacement-limited ($[R/E]^{0.5}$) fragmentation indices. These indices quantify the mechanical condition dictating the processing and breakdown of a food item due to its stiffness and toughness (Lucas, 2004; Williams, 2005).

5.3.3 *Image acquisition and analysis*

Micro-computed tomography (μCT) is a non-invasive imaging technique ideal for examining fine structures of bone, particularly in cases where specimens are delicate and fragmentary. Because μCT images are digital representations of the scan field divided into a finite number of pixels, it is important to maintain constant pixel size in order to standardize the resolution of the images (Carlson, 2005). Pixel length in a μCT image is calculated as the field of view (FOV) divided by the matrix size. Voxels, which represent the three-dimensional pixels in digital image data, are calculated as pixel area multiplied by slice thickness (Foley et al., 1990; Carlson, 2005).

For this study, microCT scans of primate skulls were used to construct 3D models of the cranium using Amira 5.6 (FEI Visualization Group, Burlington, Mass 2016). Once constructed, the skull model was oriented in Frankfurt horizontal to standardize the cranial position during sectioning. Once oriented, the Amira "slice" feature was used to pass a vertical plane along the zygomatic arch to capture cross-sectional images in the coronal plane in five locations: The anterior-most point of the zygomatic arch, anterior to the zygomaticotemporal suture, midway along the zygomaticotemporal suture

(midsuture), posterior to the zygomaticotemporal suture, and posterior-most point of the zygomatic arch (Fig. 22). These images were saved and exported as 2D TIFF files to ImageJ (Schneider et al., 2012).

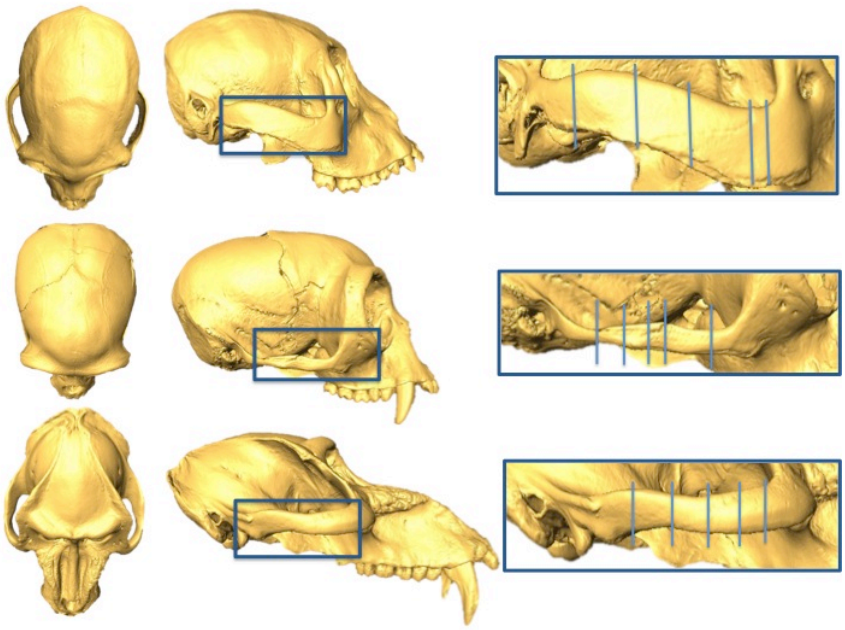

Figure 22. Sites of measurement for each arch location. The locations include: anterior-most point on the zygomatic arch ('Anterior'), anterior-most point of the zygomaticotemporal suture ('Anterior - Suture'), the midway point along the zygomaticotemporal suture ('Midsuture'), the posterior-most point of the zygomaticotemporal suture ('Posterior - Suture'), and the posterior-most point on the zygomatic arch ('Posterior').

To calculate cross-sectional geometric properties (e.g., areas, second moments of area, and polar moments of inertia) for bone cross-sectional images, the MomentMacroJ v1.4B (Ruff, 2006, http://www.hopkinsmedcine.org/fae/mmacro.html) macro for ImageJ was used. In ImageJ, each section was converted to an 8-bit gray scale image, and cropped to isolate the zygomatic cross-section (or region) of interest. Using the "threshold" option, the portions of bone in the cross-section are highlighted. This "thresholding" works by separating pixels that fall within a desired range of intensity

values from those that do not. Once the pixel intensities have been determined, the "wand tool" was used to outline the highlighted zygomatic arch section to be analyzed. Finally, the MomentMacro is selected, and the image's intensity values as well as its voxel size are entered to set the proper scale and ensure accurate calculation of the resulting biomechanical variables.

5.3.4 *Cross-sectional geometry*

With regard to craniofacial functional adaptation, bone response to mechanical loads is the crux of examinations of bone morphology in relation to the *in vivo* force environment. Since bone undergoes varying load types (e.g., bending, shear, torsion), cross-sectional geometric properties are expected to be influenced by the magnitude and types of loads experienced (e.g., Lanyon and Baggott, 1976; Lovejoy and Burstein, 1977; Ruff and Runestad, 1992; Trinkaus et al., 1994; Ruff, 2000; Daegling, 2002b; Lieberman et al., 2004b). Given the high peak strains reported in the aforementioned studies on the zygomatic arch during mastication, bone formation along the arch is expected to respond to the varying magnitudes and types of load induced during chewing.

Cross-sectional geometric properties of long bones have been used to make inferences about the magnitude and type of load experienced during use (Polk et al., 2002; Lieberman et al., 2004a; Patel et al., 2013). This perspective is based on the premise that bone cross-sectional geometry reflects bone functional adaptation to its loading environment (e.g., Wainwright et al., 1976; Ruff and Hayes, 1983; Ruff et al., 1984, 2006; Schaffler et al., 1985; Burr et al., 1989a; Trinkaus et al., 1991; Ruff and Runestad, 1992; Martin et al., 1998; Polk et al., 2000; Currey, 2002; Ruff, 2002; Habib

and Ruff, 2008; Shaw and Ryan, 2012). The use of these cross-sectional properties depends on the type of model used and the assumptions concerning how that model structure responds to loads. For bone, beam models are typically employed (Ohman, 1993; Ruff, 2000). Several beam models exist (i.e., circular, non-circular, solid, hollow etc.), but bone (e.g., long bone) is commonly modeled as a hollow, circular beam undergoing mechanical loading (Ruff and Runestad, 1992; Lieberman et al., 2004b). Using a beam model for the zygomatic arch is more complex because it requires considerations of the mechanical response of a *curved*, hollow beam subjected to combinatory loading as a result of chewing.

Previous experimental studies found that the unexpected strain characteristics of the zygomatic arch suggests it does not behave like a simple beam (Herring et al., 1996) but is rather much more complex in its mechanical behavior. This study uses cross-sectional geometric properties to examine the arch's tendency to resist parasagittal bending and torsional forces during mastication. These properties are informative about beam behavior, including those of a curved beam, and enable morphologists to be better characterize the geometric structure of the arch.

To quantify the relative strength of the bone and its ability to resist different load types (e.g., bending and torsion), specific cross-sectional geometric properties are calculated. Specifically, a series of variables reflecting biomechanical measures of resistance to bending (second moments of area, I), torsion (polar moment of inertia, J), and other loads are calculated from the amount and distribution of cortical and trabecular bone in a given cross section which elucidate the mechanical environment of that bony region (Schaffler et al., 1985; Polk et al., 2000; Daegling, 2002b).

Second moments of area (I) measure how material (i.e., bone) is distributed around a specified axis (Schaffler et al., 1985; Polk et al., 2000). Once I is calculated, the section modulus (Z) can be measured, which provides an approximation for a cross section's resistance to bending in a particular plane (Wainwright et al., 1976; Lieberman et al., 2004b). In addition to the measures themselves, estimates of body size (or skull size) are necessary to generate accurate interpretations of J and I (Polk, 2000). Common methods for estimating the cross-sectional shape of a bone include the measurement of second moments of area (I) about anatomical axes (anteroposterior [I_y] and mediolateral [I_x]) or maximum (I_{max}) and minimum (I_{min}) bending resistances about principle axes on cross-section (CT) images (Schaffler et al., 1985; Carlson, 2005: Patel et al., 2013; Fig. 23). In the latter, I_{max} is an approximation of maximum rigidity which is expected to reflect the magnitude of peak loads (Carlson, 2005).

Bending resistance

Second moments of area (I_x, I_y):

About transverse (I_x) & vertical (I_y) axis

Maximum & minimum resistance to bending (I_{max}, I_{min})

Torsional resistance

Polar moment of inertia (J) = I_{max} + I_{min}

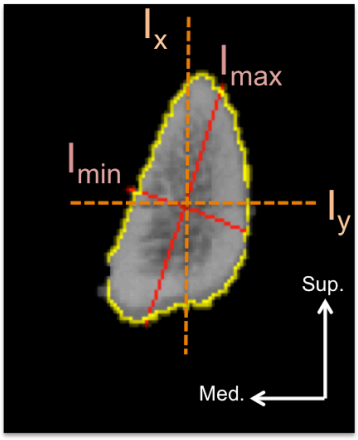

Figure 23. Schematic of cross-sectional variables that quantify bending and torsional resistance.

Ratios created from these variables (e.g., I_{max}/I_{min}) provide a biomechanically relevant index of cross-sectional shape where a ratio of 1.0 indicates axial symmetry (and

therefore a more circular section) and a ratio deviating from 1.0 indicates a more elliptically shaped section (Schaffler et al., 1985; Daegling, 2002b; Patel et al., 2013). An advantage of using shape ratios is that they do not require an estimate of body size and I_{max}/I_{min} does not require information about the anatomical orientation of the bone making it ideal for analysis of fragmentary shafts (Patel et al., 2013). In addition, Schaffler et al. (1985) proposed that the shape ratio I_{max}/I_{min} provided an appropriate measure for estimating locomotor type. For the purposes of this study, shape ratios about principal axes (I_{max}/I_{min}) are used to approximate cross-sectional shape.

This study quantifies and compares cross-sectional geometric properties (i.e., I_x, I_y, I_{max}, I_{min}, I_{max}/I_{min}, J) of the zygomatic arch across various locations to determine if arch cross-sectional shape varies intra-individually in relation to strain distribution, if cross-sectional shape varies interspecifically, and if it does, whether variation in cross-sectional shape is the result of differing diet types across primates. Because this approach has been primarily applied to long bones, this study takes a novel approach in the examination of bone cross-sectional shape and estimation of load resistance along the zygomatic arch to investigate relationships between masticatory loading and bone form.

5.3.5 *Resistance to bending & torsion*

Certain cross-sectional shapes are more conducive to resisting bending forces than others; and the zygomatic arch is known to experience both bending and torsional forces during mastication. In circular cross sections, second moments of area (I) measure the distribution of cortical area around a centroid, which provides an approximation of average bending resistance (rigidity) of a bone (Schaffler et al., 1985; Polk et al., 2000;

Holmes and Ruff, 2011). Minimum and maximum bending strengths (I_{min} and I_{max} respectively) along with I_x and I_y (second moments of area about the x- and y-axes) will be compared among slice locations to determine the relative bending resistance of the arch.

A circular bone cross section is most efficient for withstanding torsion (twisting) while oval sections are better suited to resist bending along its long axis. The ratio of I_{max}/I_{min} will be calculated for each slice location to quantify the circularity (or non-circularity) of a zygomatic cross section (Daegling, 2002b; Gosman et al., 2013; Patel et al., 2013). I_{max}/I_{min} values deviating from 1.0 are more elliptical (non-circular) whereas I_{max}/I_{min} values approximating 1.0 indicate a relatively round cross-section (Schaffler et al., 1985; Daegling, 2002b; Patel et al., 2013). I_{max}/I_{min} ratios deviating from 1.0 indicate increased resistance to bending as oblong, or oval, shapes are capable of resisting different types of bending forces (e.g., parasagittal or transverse bending) by aligning the longest diameter in the direction of the bending load. The polar moment of inertia (J) will be calculated as the sum of perpendicular second moments of area (Ruff and Runestad, 1992; Polk et al., 2000; Ruff, 2000; Stock and Shaw, 2007). This will serve as an estimate of torsional strength and bone rigidity. The regions of the zygomatic arch subjected to greater torsional loads are expected to have greater measures of J overall. Greater measures of J would suggest relatively round and rigid cross-sections as compared to parts of the arch that experience higher bending forces. In these high force areas, J should be lower.

The ratio of bizygomatic breadth to biramus breadth (BZBR) (which is distinct from the shape ratio I_{max}/I_{min}) should affect of the angle of the masseter and the resulting

pull on the zygomatic arch. Therefore taxa with more flared zygomatic arches (and thus greater bizygomatic breadth) are characterized by more angled masseter insertions, are therefore expected to possess more circular cross-sections given the masseter activation would induce a relatively greater torsional moment on the zygomatic arch. In contrast, taxa with less flared arches (and therefore more vertical masseter muscle orientations) should correspond to BZBR ratios approximating 1.0 and experience greater bending moments. To combat this, arch cross-sectional shapes are predicted to be elliptical.

5.3.6 *Statistics*

Statistical analyses included the calculation of descriptive statistics for each cross-sectional variable for each taxon in the study. Box-and-whisker plots were created to visually assess the data. Shapiro-Wilk Tests and Levene's Tests were used to determine if the variables met the assumptions of normality and homogeneity of variance; the data were log transformed to meet these assumptions. Variation in second moments of area about the x- and y- axes (I_x, I_y), maximum and minimum bending resistance (I_{max}, I_{min}), polar moment of inertia (J), and differences in cross-sectional shape (I_{max}/I_{min}) among five arch regions in the zygomatic arch were examined at three scales: intra-individually (comparing arch regions), intraspecifically, interspecifically, and by diet type. Analysis of Variance (ANOVA) and post-hoc paired *t*-tests and Tukey-HSD tests were used to compare the distribution of values for a specific variable within a taxon across different zygomatic arch locations (i.e., anterior, anterior suture, midsuture, posterior suture, and posterior regions) as well as to compare variances between dietary groups. Student's *t*-tests were used for comparing sample means. Interdietary and intradietary pairwise

comparisons between closely related taxa were also performed for each variable using Welch's two-sample *t*-tests. The significance level for all tests was set at $p < 0.05$. A Bonferroni-Holm correction for multiple comparisons was also applied (Holm, 1979). Pearson product moment correlations were performed between I_{max}/I_{min} ratios and FMP data as well as between I_{max}/I_{min} ratios and reported total consumption percent data. Bizygomatic breadth to biramus width (BZBR) ratios were calculated and compared to approximate the angle of the masseter (masseter line of action) in relation to zygomatic arch cross-sectional shape.

Phylogenetic Generalized Least Squares (PGLS) and multiple regressions were used to account for the influence of phylogeny in the data. (PGLS) Regressions were also performed on each variable in relation to two proxies for size: skull size and zygomatic arch size. Consensus trees for the entire study sample as well as the subsample were obtained from the 10KTrees database (http://10ktrees.nunn-lab.org/, Arnold et al., 2010). Because not all the species in this study were available in the 10KTrees database, published phylogenetic positions and divergence dates for *Chiropotes albinasus*, *Presbytis rubicunda* and *Presbytis hosei* were acquired from the literature (Finstermeier et al., 2013) and added to the final consensus tree. Given that this study tested hypotheses using two different dietary schemes and not all taxa have FMP data available, the initial consensus tree containing 43 species was trimmed to include only the 9 species for which FMP data were available (Fig. 24).

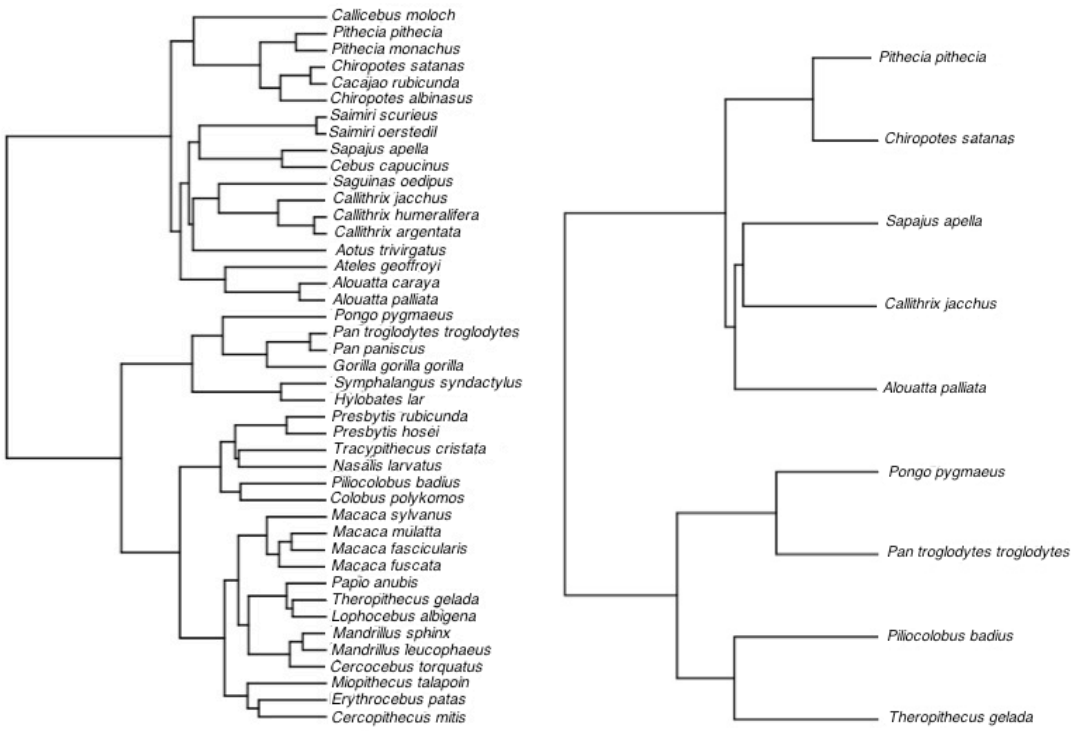

Figure 24. Consensus trees created from 10KTrees database: Tree containing all study species (left), and trimmed tree (right) containing nine species for which FMP data were available.

All analyses were performed using the R Statistical Programming Language version 3.1.0 (http://www.R-project.org/) (R Development Core Team, 2014). Packages APE (Paradis et al., 2004) and caper (Orme et al., 2013) were used for PGLS. To test the hypotheses that total consumption percent, FMPs, and variables of cross-sectional geometry are related, PGLS regressions incorporating an interaction between FMPs and total consumption percent were performed. If the interaction was not significant then the models were run again without the interaction.

5.4 Results

Descriptive statistics (Appendix E, Table SM1) and results of statistical comparisons of zygomatic arch cross-sectional shape are provided in Tables 16-22. Anterior cross-sectional images for each species are shown in Figures 25a-25d and grouped by dietary category. The following section details the results for comparisons of cross-sectional geometric variables in relation to arch location, size (skull size and zygomatic arch size) and diet type.

Phylogenetic Generalized Least Squares (PGLS) Regressions were conducted on each cross-sectional variable in relation to two measures of size (skull size and zygomatic arch size) in anterior regions to account for the effects of phylogeny on the data. Size and scaling adjustments were not made. For every model, the interactions did not approach significance, requiring that models be re-run without the interaction (Table 16). The results found no relationships between size estimates and measures of I_{min} and I_{max}/I_{min} ratios. Positive relationships were observed in all models I_x, I_y, I_{max}, and J; however the individual correlations with each size proxy are not significant.

Table 16. PGLS Results for size in relation to cross-sectional variables*

Independent variable	*t*	Slope	*p*
A. Anterior I_x and size (skull size and zygomatic arch size) (F=12.42, r^2= 0.722, p=0.019, Pagel's lambda= 0.150)			
logAverage skull geometric mean (logAvGM)	1.352	4.984	0.247
logAverage zygomatic arch geometric mean (logAvZGM)	-0.147	-0.243	0.889
B. Anterior I_y and size (skull size and zygomatic arch size) (F=20.07, r^2= 0.909, p=0.008, Pagel's lambda= 0.054)			
logAverage skull geometric mean (logAvGM)	-0.166	-0.554	0.868
logAverage zygomatic arch geometric mean (logAvZGM)	-0.081	-0.162	0.935
C. Anterior I_{max} and size (skull size and zygomatic arch size) (F=6.176, r^2= 0.721, p=0.019, Pagel's lambda= 0.012)			
logAverage skull geometric mean (logAvGM)	0.518	1.393	0.235
logAverage zygomatic arch geometric mean (logAvZGM)	0.020	-0.197	0.853
D. Anterior I_{min} and size (skull size and zygomatic arch size) (F=1.445, r^2= 0.129, p=0.337, Pagel's lambda= 0.064)			
logAverage skull geometric mean (logAvGM)	-0.47	-2.664	0.662
logAverage zygomatic arch geometric mean (logAvZGM)	0.852	2.314	0.441
E. AnteriorI_{max}/I_{min} and size (skull size and zygomatic arch size) (F=1.532, r^2=0.433, p=0.320, Pagel's lambda= 0.297)			
logAverage skull geometric mean (logAvGM)	-0.773	-1.66	0.443
logAverage zygomatic arch geometric mean (logAvZGM)	-0.845	-1.100	0.403
F. Anterior J and size (skull size and zygomatic arch size) (F=12.33, r^2= 0.790, p=0.019, Pagel's lambda= 0.091)			
logAverage skull geometric mean (logAvGM)	1.289	4.192	0.266
logAverage zygomatic arch geometric mean (logAvZGM)	-0.087	-0.135	0.934

* Models including interactions were run first; if the interaction term did not approach significance, the result without the interaction is presented. All of the results presented here are those without interaction.

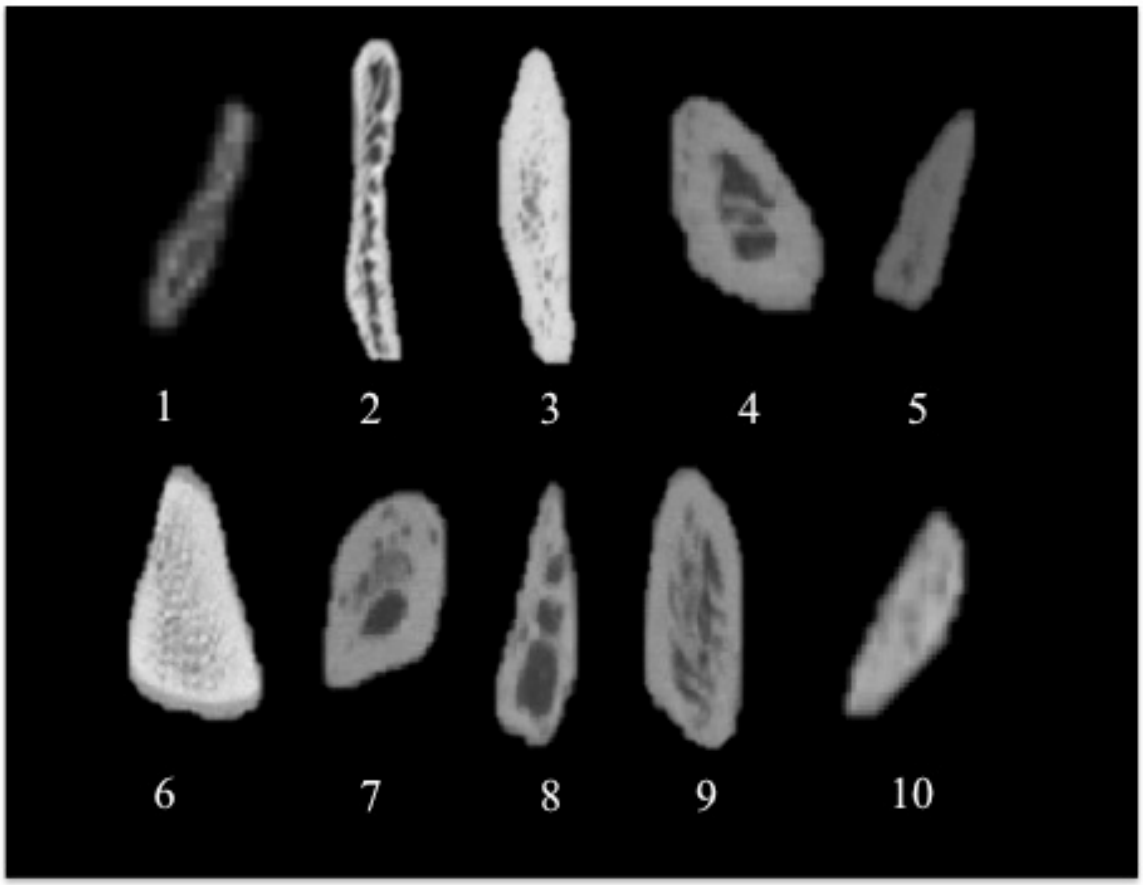

Figure 25a. Anterior arch cross-sectional images for all tough consumers. Images are not to scale. From top, left: 1. *Alouatta caraya*, 2. *Alouatta palliata,* 3. *Gorilla gorilla,*4. *Macaca mulatta,*5. *Piliocolobus. badius*. From bottom, left: *6. Theropithecus gelada,*7. *Trachypithecus cristatus,* 8. *Nasalis larvatus,*9. *Colobus polykomos,* 10. *Presbytis hosei*

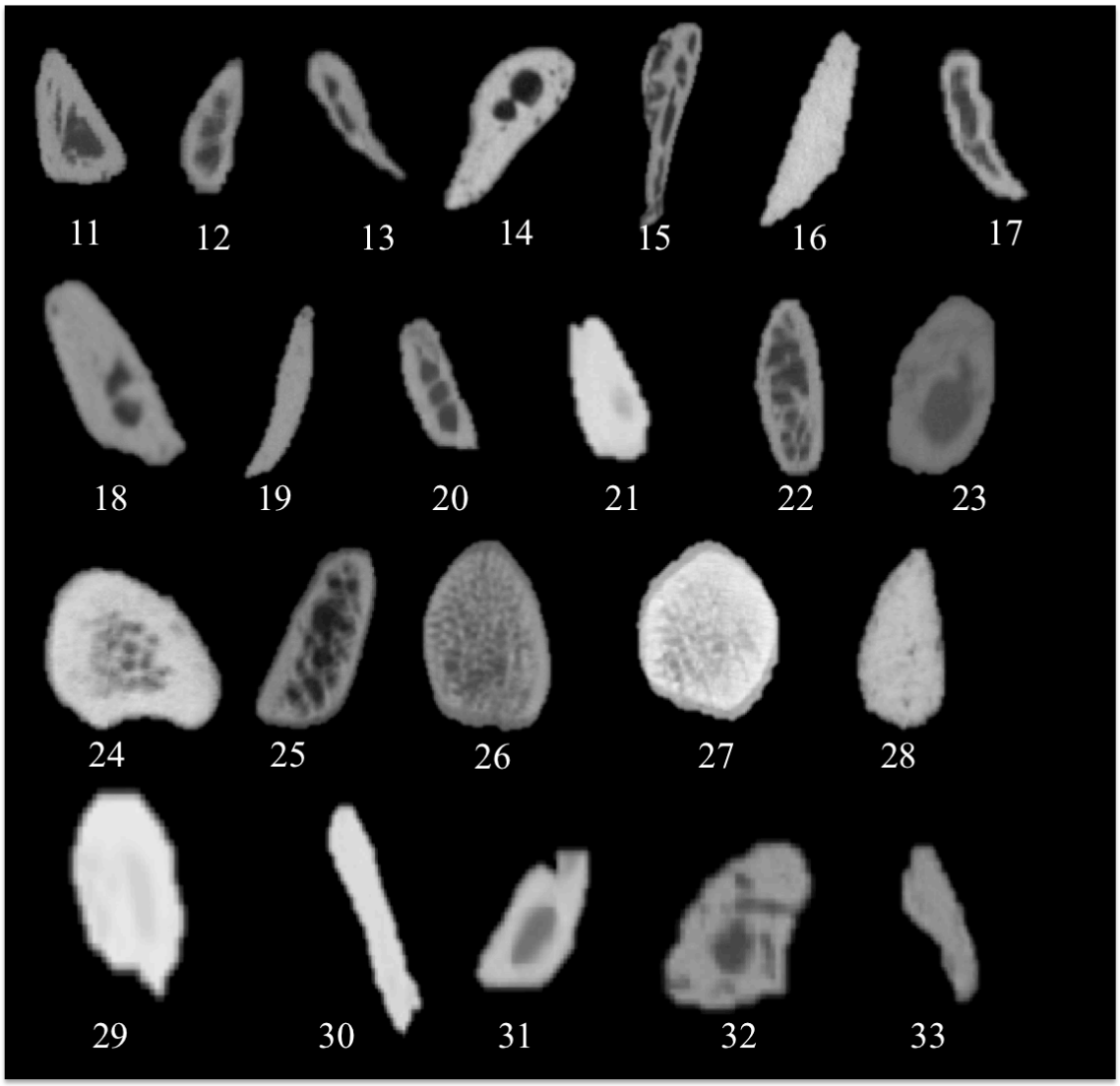

Figure 25b. Anterior arch cross-sectional images for all soft consumers. Images are not to scale. From top, left: 11. *Erythrocebus patas,* 12. *Hylobates lar,* 13. *Aotus trivirgatus,* 14. *Ateles geoffroyi,* 15. *Callicebus moloch,* 17. *Pan troglodytes,* 17. *Pithecia monachus,* 18. *Cebus capucinus,* 19. *Pan paniscus,* 20. *Cercopithecus mitis,* 21. *Miopithecus talapoin,* 22. *Cercocebus torquatus,* 23. *Lophocebus albigena,* 24. *Papio anubis,* 25. *Macaca fasicularis,* 26. *Mandrillus leucophaeus,* 27. *Mandrillus sphinx,* 28. *Pongo pygmaeus,* 29. *Saguinas oedipus,* 30. *Saimiri oerstedii,* 31. *Saimiri sciureus,* 32. *Chiropotes satanas,* 33. *Symphalangus syndactylus*

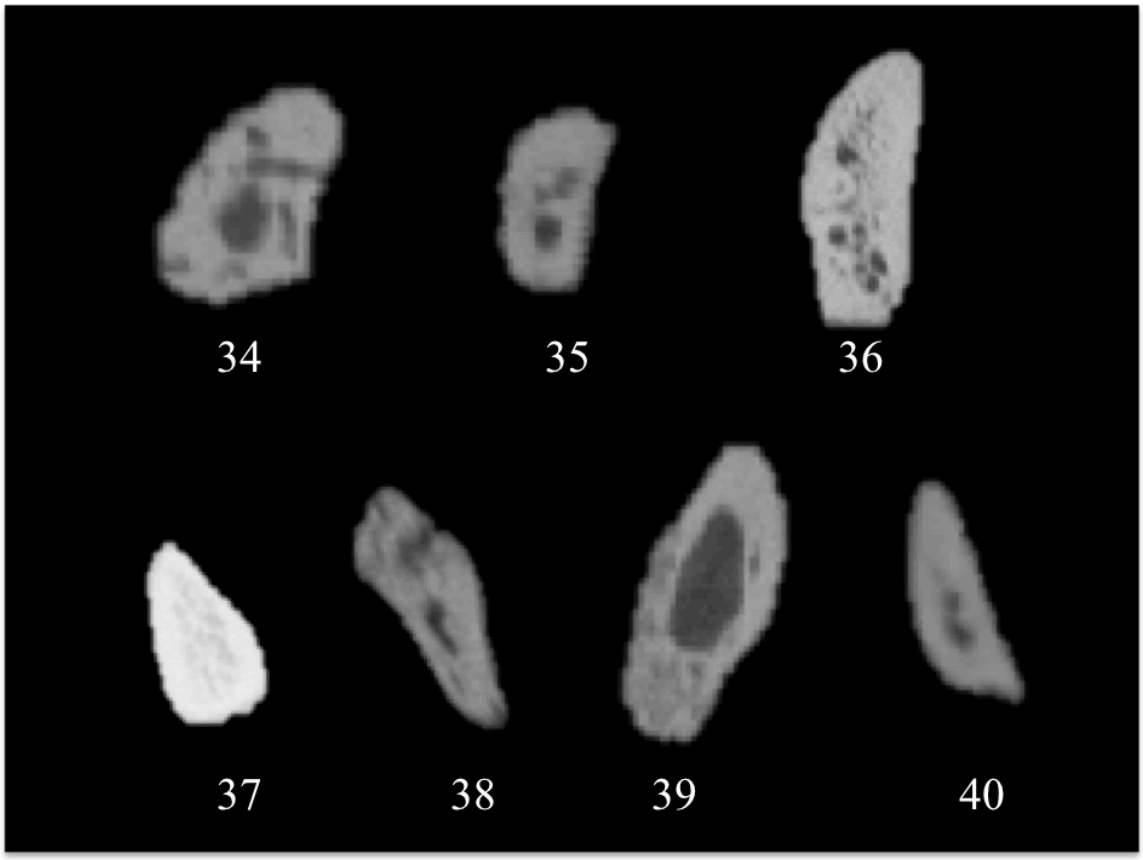

Figure 25c. Anterior arch cross-sectional images for all hard-object consumers. Images are not to scale. From top, left: 34. *Chiropotes satanas*, 35. *Cacajao rubicunda*, 36. *Macaca fuscata*, 37. *Macaca sylvanus*, 38. *Pithecia pithecia,* 39. *Sapajus apella,* 40. *Presbytis rubicunda*

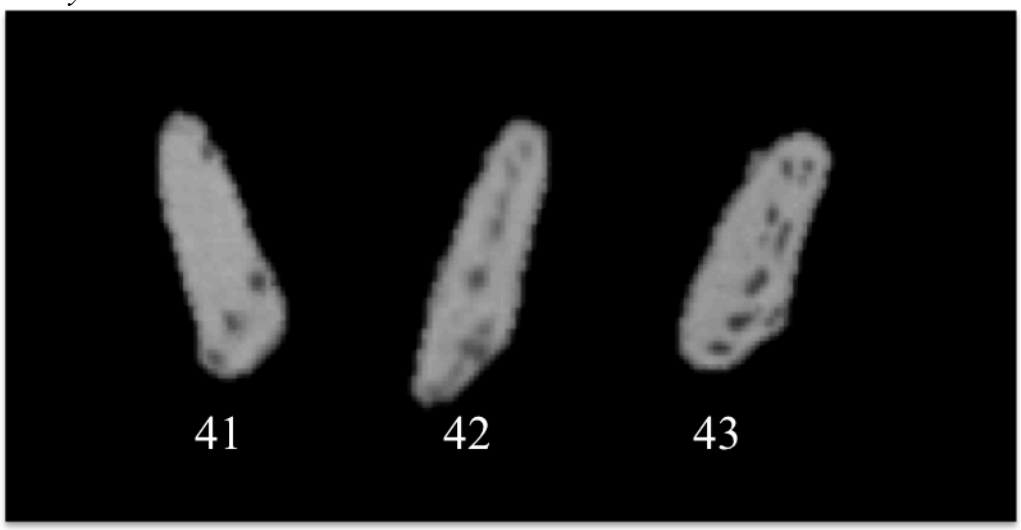

Figure 25d. Anterior arch cross-sectional images for all exudate consumers. Images are not to scale. From left: 41. *Callitrhix jacchus*, 42. *Mico argentata,* 43. *Mico humeralifera*

5.4.1 *Comparisons by dietary group*

ANOVA comparisons were first conducted on the four dietary groups to determine the extent to which each biomechanical variable varied across each arch region. Posthoc Tukey HSD tests were performed on significant results in order to determine which dietary groups varied at a given zygomatic arch region. The findings of these ANOVA analyses (see Table 17) determined that measures of second moments of area about the x-axis (I_x), and polar moment of inertia measures (J) were significantly different in all arch regions among all dietary groups. Maximum bending tendency (I_{max}) measures were significant in all regions except anterior sections whereas minimum bending tendencies (I_{min}) and second moments of area about the y-axis (I_y) were significantly different only in anterior and anterior-suture sections. Post hoc TukeyHSD tests found that tough consumers and exudate consumers were significantly different ($p<0.05$) from one another in each of these comparisons (Appendix D, Tables SM1), which is probably due to size. No other dietary group was significantly different in any comparison.

To assess the amount of variation within each dietary group with respect to each biomechanical variable and arch region, ANOVA analyses (Appendix D, Table SM2) were conducted within each diet group (tough, soft, hard, exudate) and posthoc Tukey HSD tests were used to evaluate significant results. The results for these ANOVA analyses found that all variables (I_x, I_y, I_{max}, I_{min}, J) and arch regions were significantly different in soft consumers and tough consumers at all locations except in midsuture I_{max}/I_{min} measures in tough consumers. Hard-object consumers and exudate consumers both exhibited significant differences in measures of I_x, I_{max}, and J, but both were not

significantly different with respect to I_{max}/I_{min} ratios. Intraspecific comparisons for each variable are reported in Appendix D, Table SM3.

Table 17. ANOVA results across dietary groups

Variable	Anterior	Anterior suture	Midsuture	Posterior suture	Posterior
$\log I_x$	F=3.650, p=0.020	F=4.829, p=0.005	F=3.192, p= 0.034	F=3.507, p=0.024	F=3.659, p=0.020
$\log I_y$	NS	F=3.425, p=0.026	NS	NS	NS
$\log I_{min}$	F=2.421, p=0.025	F=3.113, p=0.037	NS	NS	F=3.017, p=0.041
$\log I_{max}$	NS	F=4.805, p=0.006	F=3.315, p=0.029	F=3.637, p=0.020	F=3.605, p=0.021
I_{max}/I_{min}	NS	NS	NS	NS	NS
logJ	F=3.382, p= 0.027	F=4.574, p=0.007	F=3.082, p=0.038	F=3.479, p=0.024	F=3.522, p=0.023

Paired *t*-tests performed on significant comparisons in tough consumers found that *A. palliata, G. gorilla*, and *C. polykomos* were consistently different from other taxa in measures of I_x, I_{max}, and J (Appendix D, Table SM4). In contrast, within soft consumers, most taxa differed from one another in some comparisons, but no single species was consistently different in all comparisons. Within hard consumers, the species that constantly differed from other species was *Macaca fuscata*. Among exudate consumers, *C. jacchus* and *C. argentata* were significantly different in comparisons of I_x, I_{max}, and J. In sum, these results indicate there is broad variation within soft and tough food consumers with respect to biomechanical variables across different arch regions. Significant variation is also present in hard-object and exudate consumers, though to a lesser degree. Hard-object and exudate consumers were not found to have significant variation in arch cross-sectional shape between arch regions unlike tough and soft food consumers. The results of intraspecific comparisons (Table H, Table SM1) determined that the majority of taxa varied in one or more of the biomechanical variables measured across arch regions. The following sections detail the results for each variable as well as the results for post-hoc analyses.

5.4.2 *Bending resistance about the x - and y - axes (I_x and I_y)*

Across the 43 taxa included in this study, the largest measures of I_x occurred in anterior or anterior suture regions in all taxa except *Pongo pygmaeus*, *Macaca sylvanus* (highest in midsuture regions), *Pithecia pithecia, Pithecia monachus* (highest in posterior suture regions), *Theropithecus gelada*, *Mandrillus leucophaeus* (highest in posterior regions) (Appendix C, Table SM1). Paired *t*-test comparisons between the sites of highest

bending and the predicted sites of highest bending (anterior regions) were not found to be significantly different. This was also true for I_y measures, in which all taxa possessed their highest values in anterior or anterior suture sections except for *Pithecia pithecia* (highest in posterior suture regions) *Gorilla gorilla*, *Theropithecus gelada*, *Chiropotes albinasus*, *Mandrillus leucophaeus*, *Presbytis rubicunda* (highest in posterior regions). Paired t-test comparisons between predicted areas of highest I_y measures and observed highest I_y measures for these taxa found significant differences for *G. gorilla* (t=0.556, p=0.001) alone. *C. albinasus* and *M. sylvanus* could not be compared because the sample size was not sufficient to meet the assumptions of the *t*-test.

Across all dietary groups, tough consumers on average possessed the highest bending resistance moments (see Figs. 26a & 26b). In taxa categorized as tough consumers, ANOVA results determined that all species yielded significant variation in bending measures except for *Macaca mulatta*, and I_x measures in *G. gorilla* and *T. gelada* (Appendix D, Table SM3).

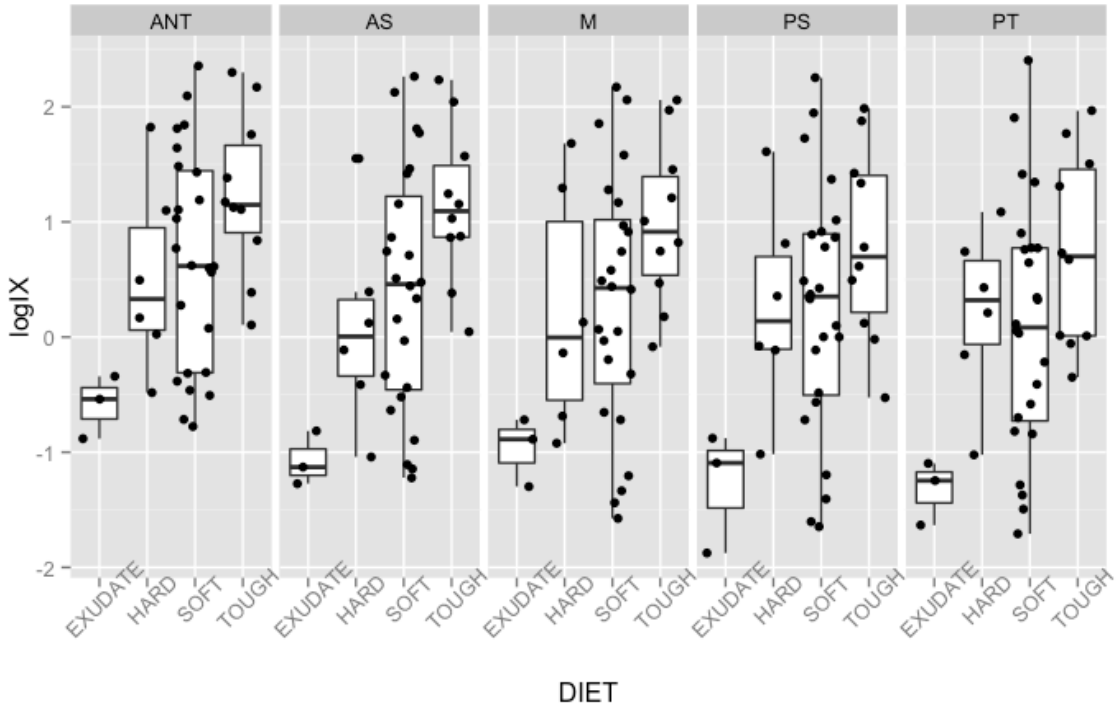

Figure 26a. Box and whisker plots of measures of bending resistance about the x-axis (I_x) for each dietary group across all arch regions. ANT= anterior arch sections, AS= anterior suture sections, M= midsuture, PS= posterior suture, PT= posterior arch.

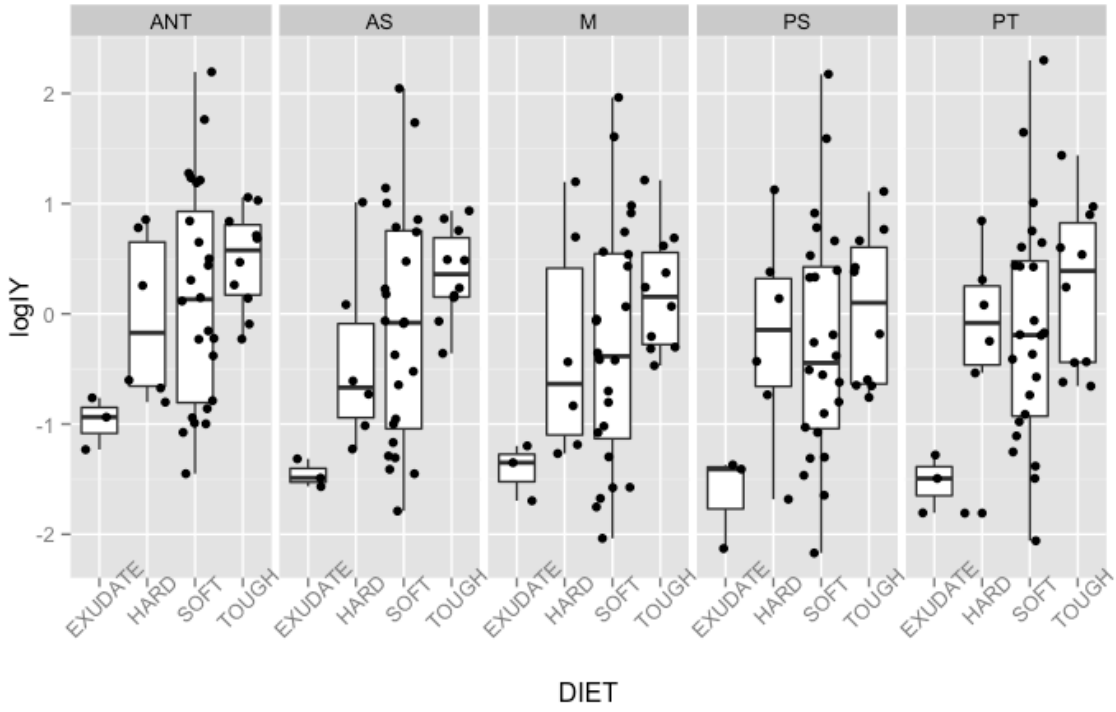

Figure 26b. Box and whisker plots of measures of bending resistance about the y-axis (I_y) for each dietary group across all arch regions. ANT= anterior arch sections, AS= anterior suture sections, M= midsuture, PS= posterior suture, PT= posterior arch.

Paired *t*-tests performed between all possible arch region comparisons determined that measures of I_x and I_y were significantly different in comparisons of anterior sections versus midsuture and anterior sections versus posterior regions. Both *G. gorilla* and *P. badius* did possess significantly different comparison in anterior versus posterior measure in I_y, but none in I_x (Appendix D, Table SM4). Of the ten species designated as tough consumers, eight possessed significant differences in one or more comparison of arch regions in I_x and I_y. More specifically, within the taxa that possessed differences in second moments of area, the majority had bending resistance measures that are significantly different in anterior regions of the zygomatic arch as compared to other regions (see Appendix D, Table SM4).

In soft consumers, ANOVA results found significant variation in bending measures in all taxa except *Pongo pygmaeus*, *Presbytis rubicunda*, and *Saimiri scurieus*. Because of issues with sample size, *Chiropotes albinasus*, and *Symphalangus syndactylus* could not be evaluated using an ANOVA. In the remaining taxa, measures of I_x and I_y were significantly different in anterior regions compared to other regions in the majority of soft consumer comparisons. Generally speaking, the significant differences among arch regions are concentrated in comparisons of anterior regions with other regions (e.g., midsuture, posterior-suture, and posterior). However, paired *t*-tests between locations arch region pairs (Appendix D, Table SM4) found the majority of soft consumers possessed significant differences throughout the arch, including in adjacent areas. For example, *Lophocebus albigena* and *Macaca fascicularis*, exhibited significant comparisons in adjacent arch regions (e.g., anterior vs. anterior suture, anterior versus midsuture etc) as well as in comparisons of anterior arch sections to other sites. It is notable that in ten of the twenty-four species classified as soft consumers, significant differences between adjacent regions (i.e., anterior vs. anterior-suture, anterior-suture vs. midsuture, midsuture vs. posterior suture, or posterior-suture vs. posterior) were found. This suggests that areas intermediate to the primary three regions traditionally examined (namely anterior, midsuture, and posterior) possess significantly different bending resistance potentials.

In contrast, ANOVA results for hard-objet consumers found no significant differences among arch regions except in *Sapajus apella, Pithecia pithecia*, and *Macaca fuscata*. Paired *t*-test results, however, rendered no significant differences among arch regions in these taxa except for *S. apella* (Appendix D, Table SM4) whose significant

comparisons were between anterior sections and all other arch regions. In exudate consumers, ANOVA results found significant results for all species, but only *Callithrix argentata* yielded significant differences by arch region in I_x. No significant differences were found with respect to I_y. Arch region comparisons determined that anterior versus anterior suture, posterior suture, and posterior measures were significantly different as well as between midsuture versus posterior regions in this sample of exudate consumers.

5.4.3 *Maximum and minimum bending tendencies (I_{max} and I_{min})*

Maximum bending resistance measures were greatest in anterior (or anterior suture) sections in all taxa except *M. sylvanus* (highest in midsuture sections) *P. monachus*, *P. pithecia* (highest in posterior suture sections) *T. gelada*, *C. albinasus*, *M. leucophaeus* (highest in posterior sections). Paired *t*-test comparisons between areas of observed highest I_{max} values compared to predicted areas of highest I_{max} values found no significant differences between sites. *C. albinasus* and *M. sylvanus* could not be compared because the sample size was not sufficient to meet the assumptions of the *t*-test.

When average anterior I_{max} values were compared across dietary groups, tough consumers yielded the highest average values followed by soft consumers, hard-object consumers, and exudate consumers (Figs. 26c & 26d). Similar to the findings for I_x and I_y, ANOVA comparisons among tough food consumers found significant differences in maximum and minimum bending tendencies in all taxa except *G. gorilla*, *M. mulatta*, *P. badius*, and *T. gelada* (Appendix D, Table SM3).

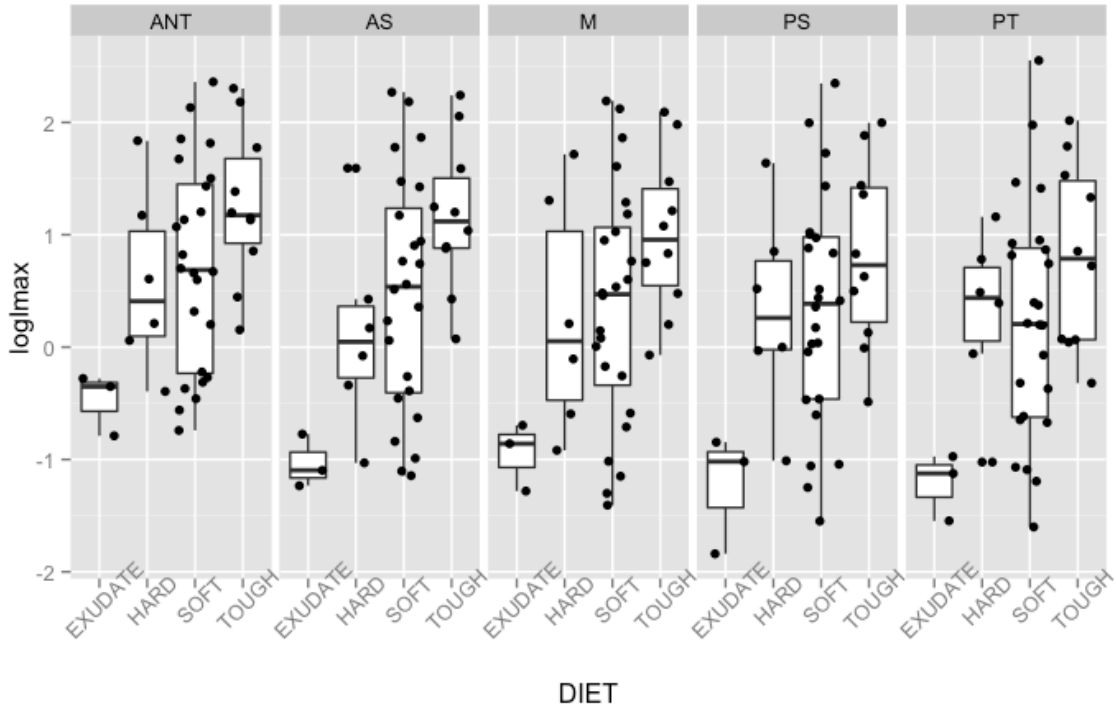

Figure 26c. Box and whisker plots of measures of maximum bending resistance (I_{max}) for each dietary group across all arch regions. ANT= anterior arch sections, AS= anterior suture sections, M= midsuture, PS= posterior suture, PT= posterior arch.

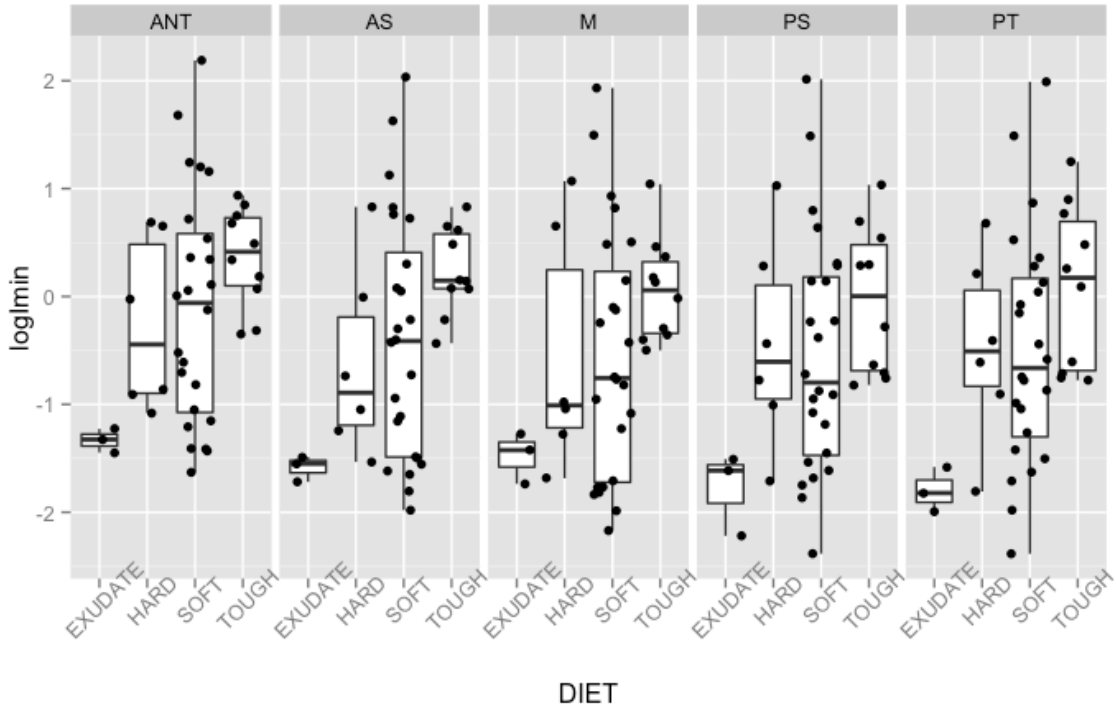

Figure 26d. Box and whisker plots of measures of minimum bending resistance (I_{min}) for each dietary group across all arch regions. ANT= anterior arch sections, AS= anterior suture sections, M= midsuture, PS= posterior suture, PT= posterior arch.

Post hoc comparisons found seven of the ten total tough consumer species yielded significant differences between anterior or anterior suture regions and midsuture, posterior suture, and/or posterior regions (Appendix D, Table SM4). Four taxa exhibited extensive differences in maximum and minimum bending tendencies across all regions of their zygomatic arch: *Alouatta palliata*, *Colobus polykomos*, *Nasalis larvatus*, *Trachypithecus cristatus*. Similar to the results for I_x and I_y, the significant differences in maximum bending resistance in these taxa demonstrate that adjacent regions can yield significantly different bending resistance potentials.

ANOVA results for sixteen of twenty-four species of soft consumers found significant differences among arch regions (Appendix D, Table SM3). Post-hoc tests

revealed that arch regions varied significantly by location and that while anterior regions were generally significantly different from posterior regions, midsuture and posterior regions were also found to differ from one another in several taxa such as in *Cebus capucinus*, *Cercocebus torquatus*, *Cercopithecus mitis*, and *Lophocebus albigena*.

The extent to which specific regions differed from one another varied extensively throughout this dietary group. Some species, such as *Miopithecus talapoin*, possessed a single significant comparison between two arch regions with respect to I_{max} measures, while other species possessed significant differences in most (almost all) arch comparisons (e.g., *Lophocebus albigena*, *Cercopithecus mitis*) for I_{max}. It is notable that in every species that possessed a significant comparison or comparisons among arch regions, anterior sections were found to consistently differ from posterior sections.

ANOVA results for hard-object consumers found significant variation in I_{max} measures in about half the species (*P. pithecia, S. apella, and M. fuscata*). Comparisons with hard-object consumers found all species possessed their largest measures I_{max} in anterior regions except in two taxa *Macaca sylvanus (*greatest in midsuture sections) and *Pithecia pithecia* (greatest in posterior suture sections). As noted previously for I_x and I_y, the differences between the regions of observed highest I_{max} values and predicted highest I_{max} values were not significantly different from one another. Posthoc analyses on significant results found that only *S. apella* exhibited statistically significant differences in I_{max} and I_{min} measures across zygomatic arch regions. Specifically, these differences occurred in comparisons of anterior sections to all other arch regions.

All ANOVA results for exudate consumers were significant indicating significant variability in maximum bending resistance. I_{min} measures were also significant for this

group except for in *Callithrix humeralifer* (ANOVA F= 3.537, p=0.061). All exudate consumers possessed their absolute highest I_{max} measures in anterior sections as well. Posthoc comparisons revealed that only *C. argentata* had statistically significant differences in anterior I_{max} values compared to other regions.

In sum, the results for both second moments of area and maximum bending resistance indicate that the majority of primates, regardless of dietary type, possess the highest bending resistance in anterior portions of the zygomatic arch. This supports the hypothesis that arch cross-sectional geometry with respect to bending resistance reflects the same gradient observed in previous strain studies.

5.4.4 *Resistance to torsion (J)*

Measures of the polar moment of inertia (J) were compared across arch regions to determine differences in resistance to torsion and overall rigidity at varying arch locations. The expectation was that similar to I_{max} measures, torsional resistance would be greatest anteriorly compared to posteriorly because torsional loads derived from mastication concentrate anteriorly. The greatest measures of J co-occurred in the same regions where I_{max} was also greatest, indicating that the regions of highest bending resistance are also most resistant to torsional forces as well (Appendix C, Table SM1). Among dietary groups, tough consumers had the highest J measures on average, followed by soft consumers, hard-object consumers, and exudate consumers; the same result also noted with regard to I_{max} (Fig. 26e). Measures of J were also significant across arch regions both within and between all dietary groups (Tables 16 and 17).

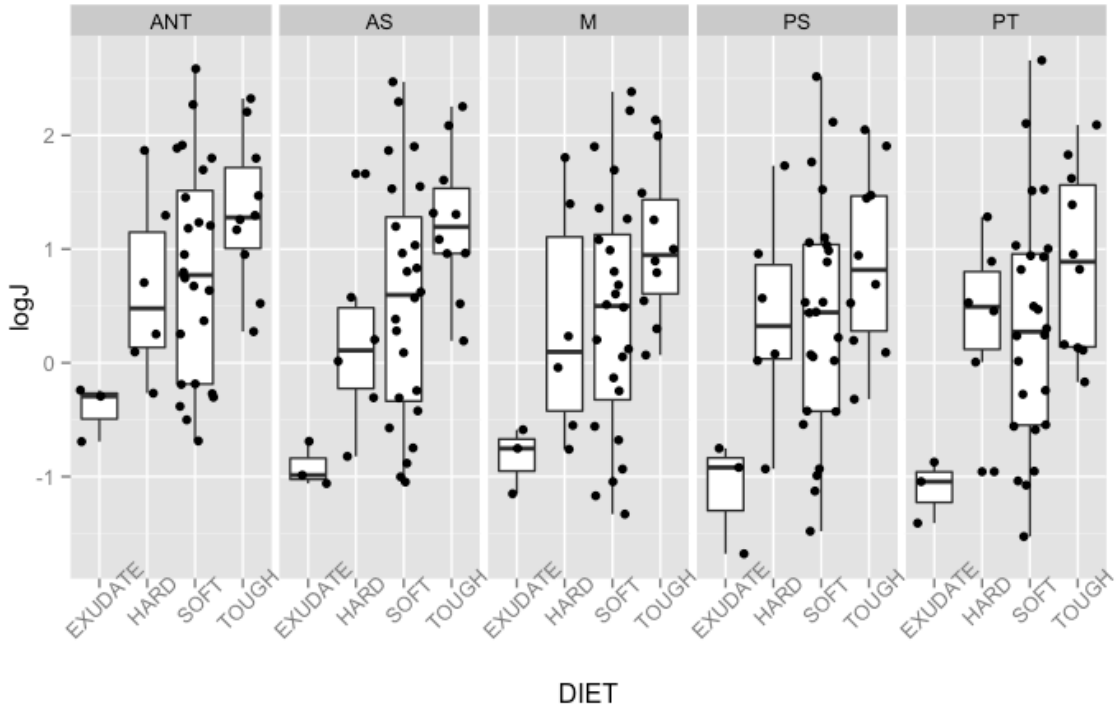

Figure 26e. Box and whisker plots of measures of torsional resistance (J) for each dietary group across all arch regions. ANT= anterior arch sections, AS= anterior suture sections, M= midsuture, PS= posterior suture, PT= posterior arch.

Within tough consumers, *T. gelada* was the only species to have its highest J values in posterior regions, as opposed to anterior or anterior suture regions, which typified all other tough consumers. The second highest measures of J for this species, however, occurred in anterior measures. While posterior measures were absolutely larger, the differences between anterior arch regions and posterior regions for geladas are not significant (see Appendix D, Table SM4). Given the small sample size for *T. gelada* in this study, it would be interesting to investigate these patterns in a larger gelada sample to determine whether this pattern of arch mechanics is specific to this species.

Among soft food consumers, all taxa possessed their highest measure of J in anterior regions with the exception of *M. leucophaeus*, *C. albinasus*, and *P. monachus*

which all possessed their greatest resistance to torsion in posterior or posterior suture regions. As in the case of the second moments of area as well as maximum bending resistance values, the relatively high posterior and posterior suture measures observed the these taxa were not significantly different from measures of J in anterior sections. ANOVA results for each species revealed that approximately of the taxa classified as soft consumers did not possess significant differences among arch regions with regard to torsional resistance, indicating relatively uniform resistance to torsional loads throughout the arch. Posthoc analyses on significant results found that taxa varied in terms of which arch regions were significantly different. For instance, *Lophocebus albigena* possessed significant differences in torsional resistance in every arch comparison while *Ateles geoffroyi* possessed only a single significant comparison between anterior and midsuture regions. Additionally, significant comparisons are not relegated to those that include anterior regions and a more posterior region. Unlike the findings for bending resistance in soft consumers, anterior measures, while absolutely greater on average, are not consistently different from other arch regions in this group.

ANOVA results both within and between hard-object consumer and exudate consumers found significant differences in each group (Appendix D, Table SM2 and Appendix D, Table SM3). All hard-object consumers as well as exudate consumers possess their highest values of J within anterior regions. Paired *t*-tests determine that *S. apella* as the only hard-object consumer to possess any significant differences in arch regions with respect to measures of J. In addition, these are the same arch location pairs that were significantly different in response to I_{max} measures as well. With respect to exudate consumers, paired *t*-test results found *C. argentata* to be the only taxon with

significant comparisons between anterior and more posterior locations. *C. jacchus* though also possessed a single significant comparisons between anterior suture regions and posterior regions (Appendix D, Table SM4; t=15.30, p=0.004). Of all the variables tested on this species in particular, this was the only significant comparison that appeared.

In sum, the results for torsional measures, suggest that like bending resistance, resistance to torsional forces is also on average greatest in anterior arch sections compared to other regions and therefore supports the prediction that torsional loads are greatest anteriorly as compared to other regions.

5.4.5 *Shape ratio comparisons I_{max}/I_{min}*

The ratio I_{max}/I_{min} serves as an indicator of whether a bone section is more circular or elliptical in shape. Sections with a ratio approximating 1.0 are more circular and are thus better suited for resisting torsional forces, while sections with ratios deviating from 1.0 are elliptical in shape and best for bending resistance along the long axis of the section. Thus, sections with greater measures of J (resistance to torsion) are predicted to correspond to arch regions in which I_{max}/I_{min} ratios approximate 1.0. In contrast, sections with relatively lower measures of J, and therefore I_{max}/I_{min} ratios deviating from 1.0, are expected to be more elliptical in shape and thus more resistant to bending. ANOVA results for comparisons among dietary groups found no significant differences between groups. However, ANOVA tests conducted within dietary groups found significant differences between arch regions in tough consumers and soft consumers, but not in hard or exudate consumers (Table 17 and Appendix D, Tables SM1).

Ratios were compared across arch locations based on the degree to which the ratio deviated from 1.0. By measuring the deviation of the ratio from 1.0, it was possible to determine the extent to which the cross-section was elongated into an elliptical form. In other words, the more distant the ratio was from 1.0, the more elliptical the cross-sectional shape of the arch. Generally speaking, arch cross-sections in zygomatic arch regions across the majority of the study taxa possess one or more region that is generally elliptical in shape (i.e., a ratio deviating by more than 0.1 from 1.0), suggesting that these arch sections are best constructed to resist bending rather than torsional forces and that this is likely the primary load type experienced (Fig. 26).

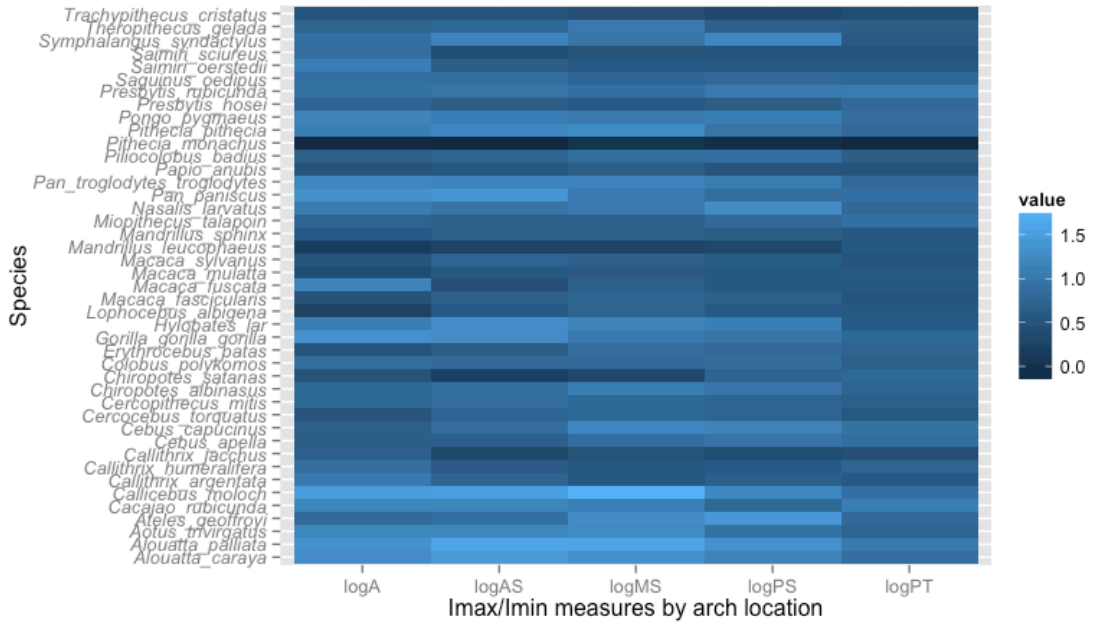

Figure 27**.** Heatmap of I_{max}/I_{min} ratios by species. Darker values indicate relatively more circular regions while lighter values indicate relatively more elliptically shaped sections. Abbreviations: logA= logged anterior values, logAS= logged anterior suture values, logMS= logged midsuture values, logPS=logged posterior suture values, logPT= logged posterior values.

Of the 43 total species included, 18 exhibited one or more arch region whose ratio deviated less than 0.1 from 1.0, indicating a relatively more circular (rather than

elliptical) arch cross-section. Notably, of these 18 species only one taxon, *Presbytis rubicunda*, exhibited consistently relatively circular cross-sections across all of its arch regions. This is reinforced by the lack of significant differences in shape ratio across regions, suggesting a relatively uniform cross-sectional shape along the arch. *Nasalis larvatus* possessed circular sections in three arch regions (anterior, anterior suture, and midsuture). Within *N. larvatus*, paired *t*-test comparisons of I_{max}/I_{min} ratios found anterior suture versus posterior suture, midsuture versus posterior suture, and posterior suture versus posterior sections to be significantly different, indicating that the presence of distinct cross-sectional shape in regions in close proximity. Across the study sample, a species' most circular arch cross-sections generally occurred in posterior regions, indicating that torsional forces may be the more dominant load type in posterior sections as compared to other regions. Otherwise, the overwhelming cross-sectional shape observed throughout all taxa was elliptical.

Within tough consumers, intraspecific ANOVA comparisons for *A. caraya, G. gorilla, N. larvatus, P. badius, T. cristatus* all yielded significant results for I_{max}/I_{min} ratios across arch regions (Appendix D, Table SM2). Posthoc comparisons determined that of these taxa, *A. caraya*, *G. gorilla*, and *T. cristatus* yielded significant differences in comparisons of anterior versus posterior arch sections, while all other significant comparisons were restricted to comparisons in the midsuture, posterior suture, and posterior portions of the arch. Taken together, the results for tough consumers indicate that anterior sections have less shape variation than posterior sections.

Intraspecific ANOVA comparisons within soft consumers revealed that nine species yielded significant differences in shape ratios, of which all had at least one

significant comparison between an anterior or anterior suture and a more posterior cross-section location (Appendix D, Table SM3). Of all the variables compared across this dietary group, I_{max}/I_{min} measures appear to be the least variable not only along the arch but within and across species as well.

Interspecific ANOVA results for hard-object consumers were not significant with respect to I_{max}/I_{min} ratios. The sole intraspecific ANOVA comparison that rendered a significant result was for *S. apella*. Paired *t*-test results of arch region pairs in this diet group similarly found no significant differences between regions except in *S. apella.* Like taxa in both the tough and soft consumer groups, *S. apella* possessed significant differences in I_{max}/I_{min} ratios in multiple arch region comparisons indicating that this species possesses significant variation throughout its arch. In exudate consumers, interspecific ANOVA results were not significant, and intraspecific results were significant only for *C. argentata*. Paired *t*-test results for this species found anterior regions to be significantly different in comparison to midsuture, posterior suture, and posterior arch sections (Appendix D, Table SM4).

In sum, these results suggest that I_{max}/I_{min} ratios do not follow a pattern of predictability akin to those observed in I_{max} and J measures, however, the results across all dietary groups indicate that anterior consistently manifest as regions that are significantly different in shape as compared to other regions.

5.4.6 *Bizygomatic breadth and biramus breadth (BZBR) ratios in relation to cross-sectional shape*

Within the study taxa, those with BZBR ratios closest to 1.0 (i.e., more vertical masseter muscles) were *H. lar*, *C. jacchus,* and *C. humeralifera* (Appendix D, Table

SM5). The cross-sectional shapes of their arch sections were compared to determine whether these taxa indeed possessed more elliptically shaped cross-sections. Comparisons of their I_{max}/I_{min} ratio reveals these taxa did not have significantly more elliptically shaped arch sections compared to other taxa in the sample.

The taxa that on average did possess the most elliptically shaped arch sections were *Mandrillus leucophaeus* (I_{max}/I_{min} ratios 0.17-0.62), and *Pithecia monachus* (I_{max}/I_{min} ratios -0.16-0.01). In taxa with more angled masseters, the expectation is that the increased angle induces greater torsional loads on the arch than would be present if the masseter remained more vertically oriented. Taxa with BZBR values deviating most from 1.0 (i.e., more angled masseters and I_{max}/I_{min} ratios approximating 1.0) were predicted to have the relatively roundest cross-sections were *Macaca sylvanus*, *Theropithecus gelada*, and *Alouatta caraya*. However, when I_{max}/I_{min} ratios were compared across the study taxa, the roundest sections appeared in *Presbytis rubicunda* and *Nasalis larvatus.* In these taxa, the masseter is flared relative to some taxa in this sample, is not significantly more flared overall. This suggests that the presence of more circular cross-sections is not directly predictable from the angle of the masseter.

Ratios of BZBR were calculated (Appendix D, Table SM5) compared to measures of J and I_{max}/I_{min} for each arch location across species using Ordinary Least Squares (OLS) Regressions (Table 18).

Table 18. OLS results for Bizygomatic-Biramus breadth (BZBR) ratios, torsional resisitance (J), and cross-sectional shape (I_{max}/I_{min})

Arch Location	Comparison	intercept (95% C.I.)	slope (95% C.I.)	r^2	*p*
Anterior	log J ~ BZBR	-0.541 (-5.1207, 4.024)	1.263 (-2.509, 5.035)	-0.022	0.811
	log J ~ logI_{max}/I_{min}	0.188 (-0.621, 0.998)	0.662(-0.061, 5.035)	-0.018	0.640
	BZBR~ logI_{max}/I_{min}	1.071 (-0.391, 2.535)	-0.304 (-2.076, 1.466)	-0.021	0.729
Anterior Suture	log J ~ BZBR	7.589 (3.954, 11.223)	-8.534 (-12.933, -4.134)	0.254	**<0.000**
	log J ~ logI_{max}/I_{min}	0.118 (-0.435, 0.673)	0.502 (-0.023, 1.028)	0.060	0.060
	BZBR~ logI_{max}/I_{min}	2.158 (-0.254, 4.571)	-1.557 (-4.477, 1.363)	0.003	0.288
Midsuture	log J ~ BZBR	8.018 (4.502, 11.532)	-9.158 (-13.413, -4.903)	0.298	**<0.000**
	log J ~ logI_{max}/I_{min}	0.186 (-0.289, 0.662)	0.299 (-0.077, 0.677)	0.036	0.116
	BZBR~ logI_{max}/I_{min}	2.370 (-1.045, 5.786)	-1.718 (-5.852, 2.416)	-0.007	0.406
Posterior Suture	log J ~ BZBR	8.535 (5.154, 11.914)	-9.867 (-13.958, -5.776)	0.351	**<0.000**
	log J ~ logI_{max}/I_{min}	0.079 (-0.829, 0.988)	0.405 (-0.652, 1.463)	-0.009	0.443
	BZBR~ logI_{max}/I_{min}	1.274 (0.026, 2.522)	-0.570 (-2.080, 0.939)	-0.010	0.450
Posterior	log J ~ BZBR	8.585 (5.261, 11.908)	-9.989 (-14.012, -5.965)	0.365	**<0.000**
	log J ~ logI_{max}/I_{min}	0.221 (-0.858, 1.301)	0.193 (-1.295, 1.683)	-0.022	0.794
	BZBR~ logI_{max}/I_{min}	1.002 (0.114, 1.890)	-0.376 (-1.450, 0.698)	-0.012	0.483

Surprisingly, no significant correlations were found in anterior arch regions, however significant negative correlations ($p<0.000$) were found between measures of J and BZBR breadth in anterior suture, midsuture, posterior suture, and posterior regions (Table 18). These results indicate that as measures of torsional resistance increase, BZBR ratios are decreasing. Lower BZBR ratios indicate a greater disparity in the distances spanning the zygomatic roots and mandibular width, and thus lower ratios indicate the presence of relatively more flared zygomatic arches. Therefore, as zygomatic arches become more laterally flared, torsional resistance appears to increase, which supports the hypothesis that a more diagonally oriented line of action of the masseter results in greater torsional moments.

Under condition of high torsional loads, measures of I_{max}/I_{min} approaching 1.0 (indicating a circular cross-sectional shape) were predicted to correlate with BZBR measures that are less than 1.0 (indicating a more flared zygomatic arch). The results of OLS regressions found a relatively weak, negative correlation among that data in all regions except anterior suture, but the results were not significant. I_{max}/I_{min} appear to have no significant relationship to measures of BZBR in this sample and thus do not support the hypothesis that relative flare (quantified as BZBR) is correlated with zygomatic arch cross-sectional shape.

ANOVA comparisons of ratios of bizygomatic breadth to biramus breadth across dietary groups revealed significant differences between the groups (ANOVA, F= 4.46, p=0.008). Post hoc Tukey HSD tests found significant differences in comparisons of exudate consumers and hard object consumers (Table 19; p=0.007), exudate consumers and soft consumers (p=0.049), and exudate consumers and tough consumers (p=0.013).

Table 19. Tukey HSD results for Bizygomatic-biramus (BZBR) ratios across dietary groups

Comparison	Tough	Soft	Hard	Exudate
Tough	---	0.644	0.927	**0.013**
Soft	0.644	---	0.355	**0.045**
Hard	0.927	0.355	---	**0.007**
Exudate	**0.013**	**0.045**	**0.007**	---

No significant differences were found in the remaining comparisons. These results suggest that exudate consumers are significantly different from all other dietary groups in their ratio of bizygomatic breadth to biramus breadth, whereas tough, soft, and hard are not significantly different from one another.

5.4.7 *Pairwise comparisons*

Pairwise comparisons of anterior measures of I_x, I_y, I_{max}, J, and I_{max}/I_{min} were conducted on pairs of closely related taxa from different diet types using Welch's two-sample *t*-tests. Because masticatory loading is hypothesized to be greatest anteriorly, comparisons were concentrated in this region. Seven of 13 comparisons found significant differences ($p<0.05$) in one or more variables (Appendix D, Table SM6 and Figs. 27a-27m) though no singular pattern emerged. Of these pairs, the comparisons between *Ateles geoffroyi* (a soft food consumer) and *Alouatta palliata* (a tough food consumer) rendered significant differences in every cross-sectional variable ($p<0.000$).

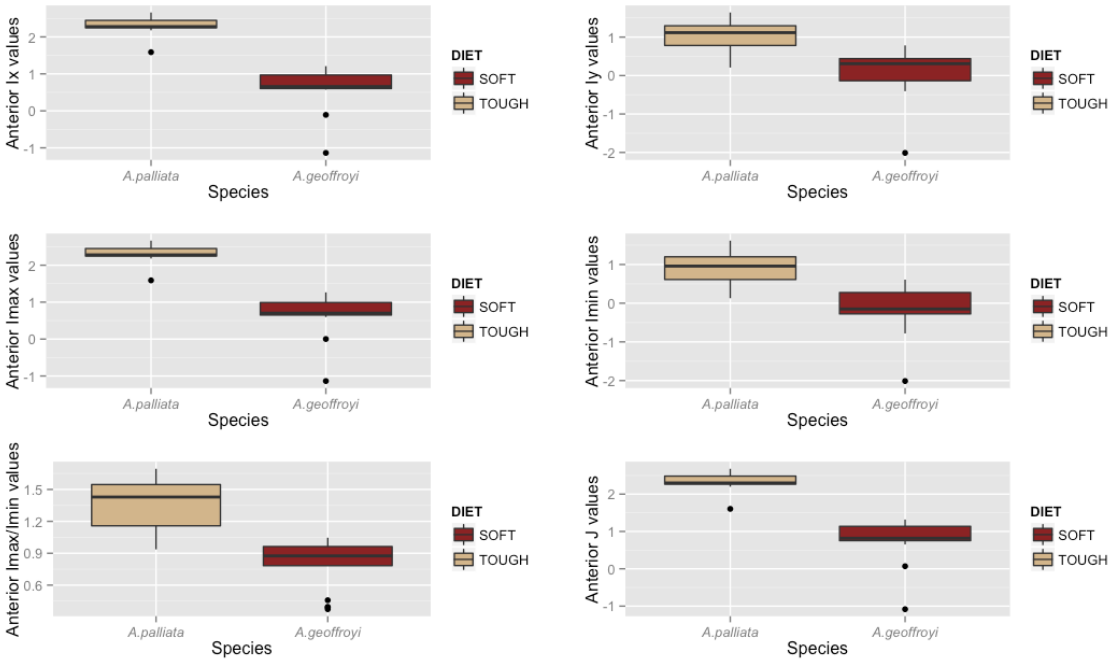

Figure 28a. Boxplots of pairwise comparisons between *A. palliata* and *A. geoffroyi* for each biomechanical variable.

Other comparisons between soft and tough consumers (e.g., *Pan troglodytes* & *Gorilla gorilla*, *Macaca fascicularis* & *Macaca mulatta*) also yielded significant differences (p=0.02, and p<0.04 respectively) in cross-sectional variables. Specifically, *P. troglodytes* and *G. gorilla* were significantly difference in I_{max}, J and I_x, while *M. fascicularis* and *M. mulatta* were significantly different in measures of J, I_x, and I_y. Comparisons between other soft food and tough food consuming taxa did not yield significant differences. For instance, comparisons of *T. gelada* and *Papio anubis* were not significantly different for any cross-sectional variable and neither were the comparisons between *G. gorilla* and *P. pygmaeus* despite the differences in their diets.

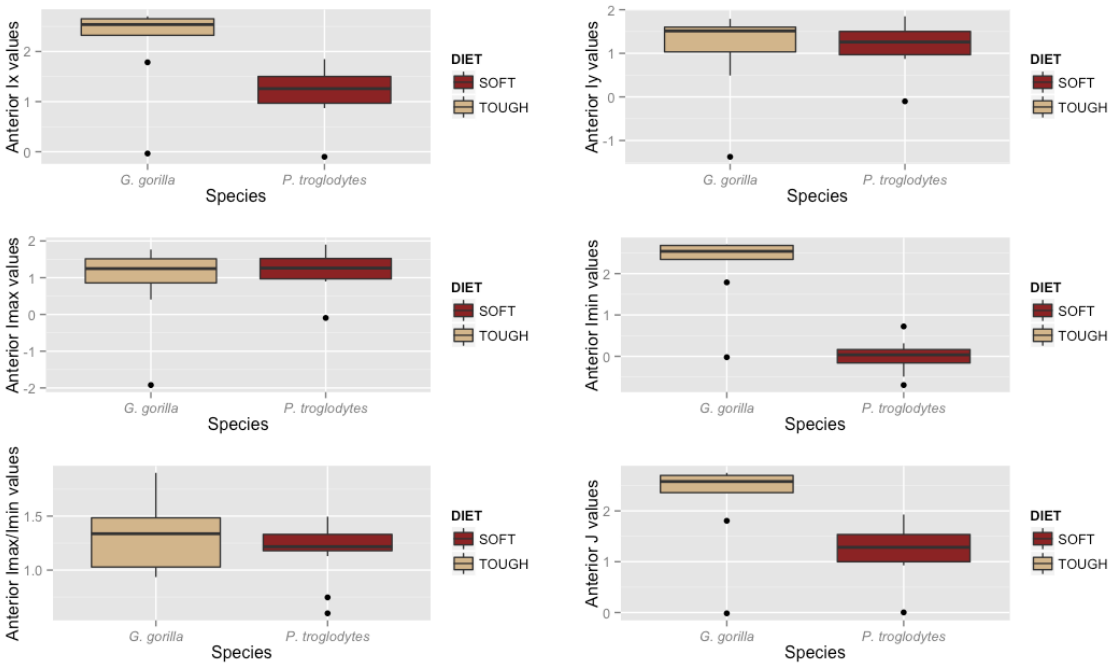

Figure 28b. Boxplots of pairwise comparisons between *G. gorilla* and *P. troglodytes* for each biomechanical variable.

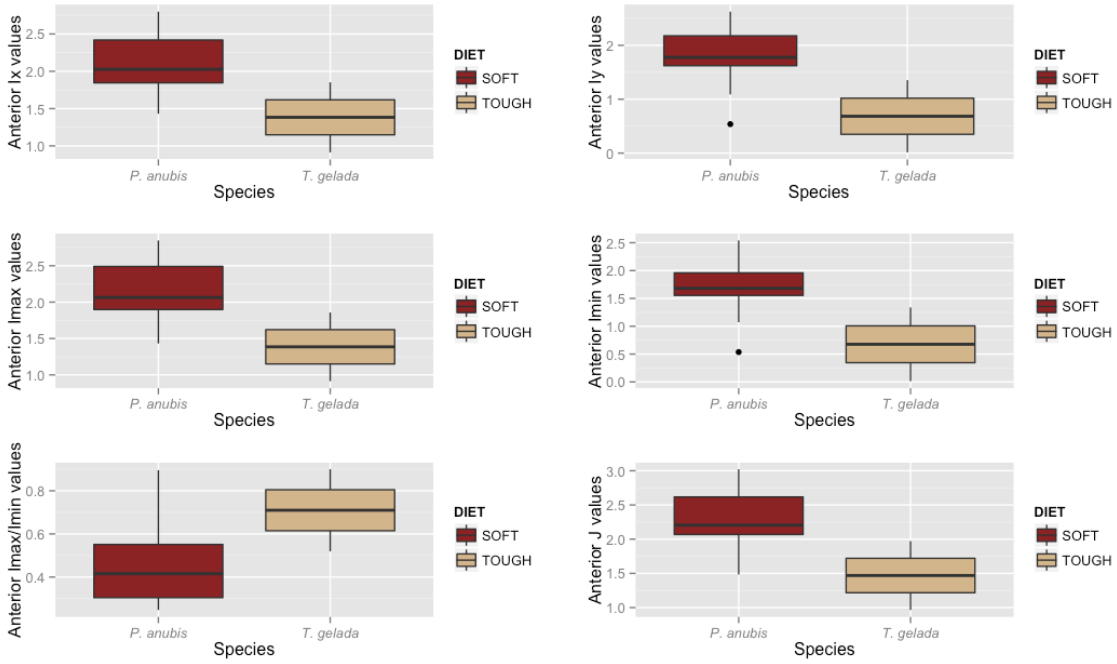

Figure 28c. Boxplots of pairwise comparisons between *P. anubis* and *T. gelada* for each biomechanical variable.

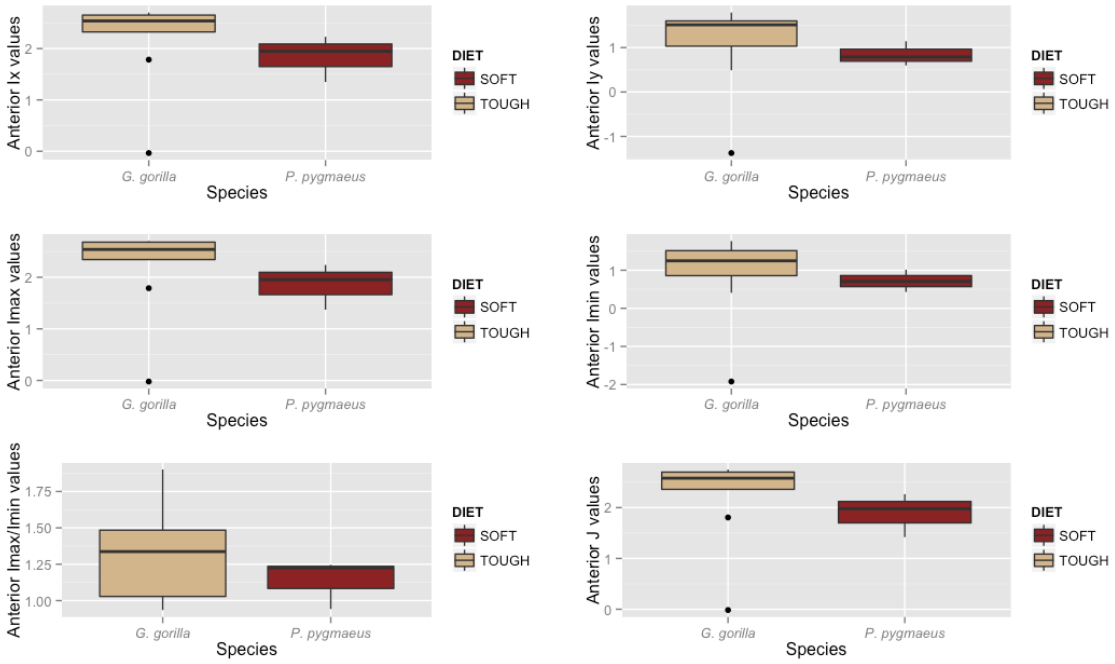

Figure 28d. Boxplots of pairwise comparisons between *G. gorilla* and *P. pygmaeus* for each biomechanical variable.

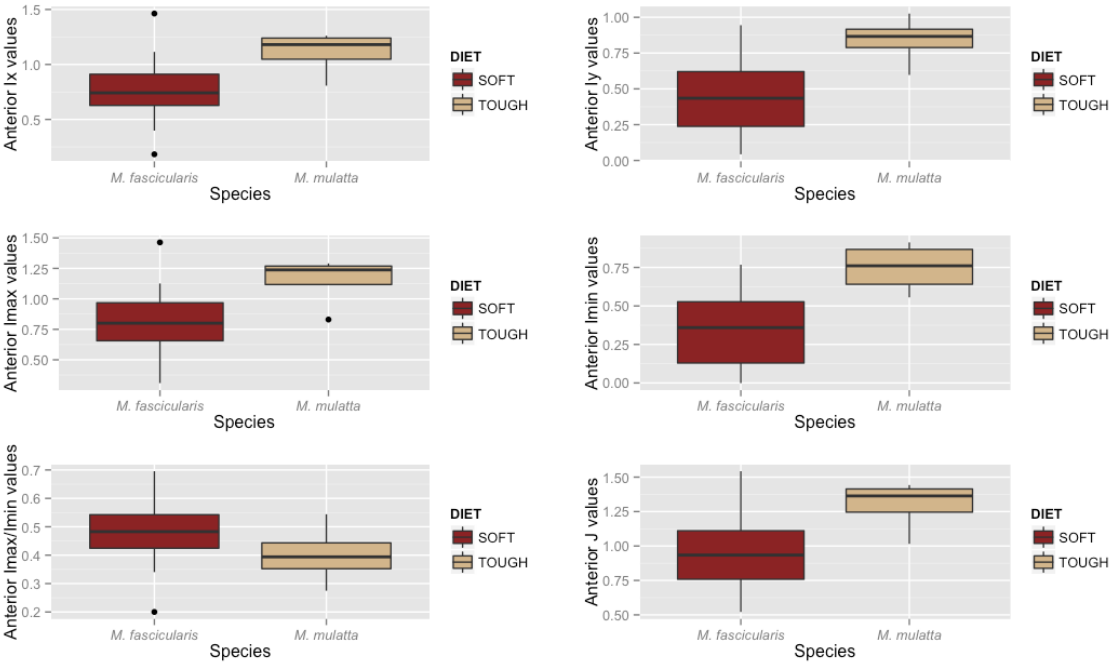

Figure 28e. Boxplots of pairwise comparisons between *M. fascicularis* and *M. mulatta* for each biomechanical variable.

Comparisons between exudate consume *Callithrix jacchus* and soft consumer Saguinas oediupus found no significant differences between taxa, though *S. oedipus* possessed higher average values for each variable. Among all comparisons, the result for anterior Imax/Imin values is most marked in this taxa pair, suggesting that cross-sectional shape is different in these taxa; specifically it appears that *S. oedipus* has relatively rounder secitions compared to the more oval-shaped sections of *C. jacchus*. Comparisons between *Saimiri scurieus* and *Saimiri oerstedii* found *S. oerstedii* consisitenly exhibited relatively higher values on average for each variable. The differences are not significant, which is not surpising given the overall dietary similarity between these species.

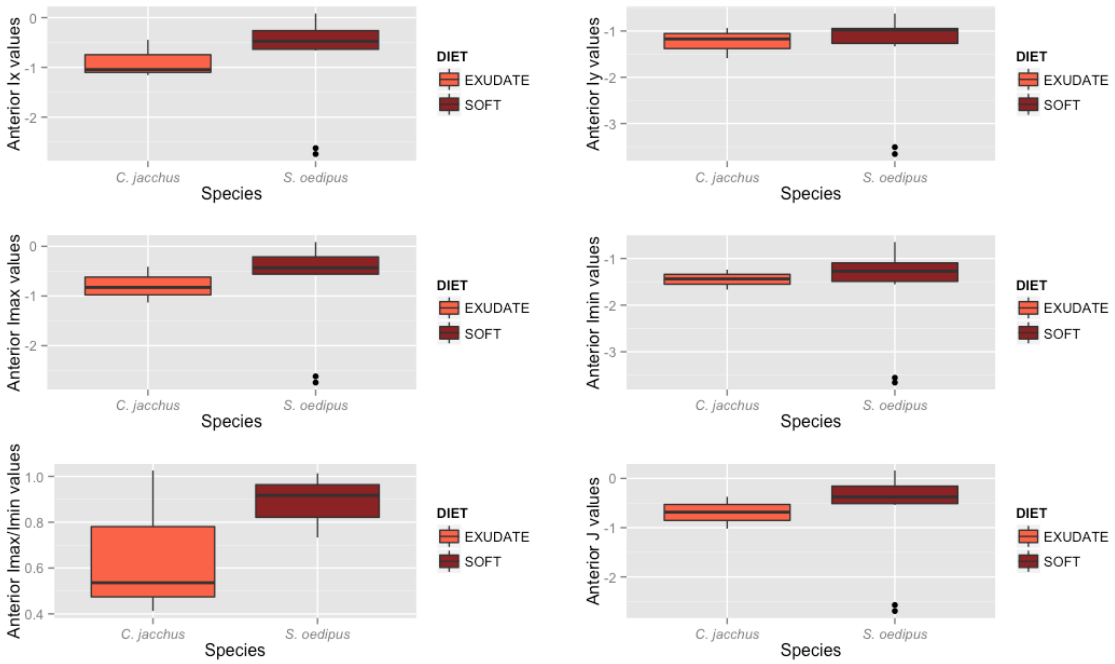

Figure 28f. Boxplots of pairwise comparisons between *C. jacchus* and *S. oedipus* for each biomechanical variable.

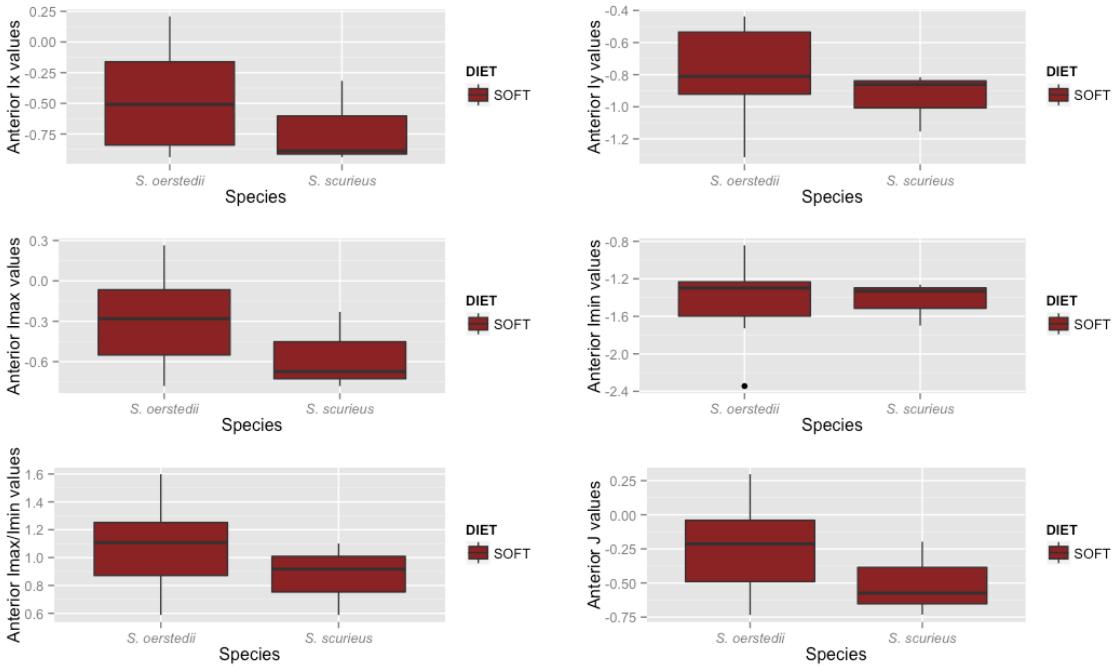

Figure 28g. Boxplots of pairwise comparisons between *S. oerstedii* and *S. scurieus* for each biomechanical variable.

Comparisons between taxa consuming hard objects and soft foods also yielded significant differences. *Pithecia monachus* and *Pithecia pithecia*, both members of the pithecids though the former generally consumes more fruits, were found to differ in their measures of I_{max}, I_x, and I_{max}/I_{min} measures. *Macaca fasicularis* and *Macaca fuscata* varied in their measures of I_{max}, J, and I_x finding that hard-object consumer *M. fuscata* was significantly greater than soft consumer *M. fasicularis* in measures of I_{max}, J, and I_x. Surprisingly, the comparisons between hard-object consumer *Sapajus apella* and soft consumer *Cebus capucinus* found relatively similar values for each variable on average. While the differences between these taxa were not significant, *C. capucinus* possessed slightly higher values on average. The morphological similarity between this pair may be due in part to the preoral preparation of hard objects by *S. apella*.

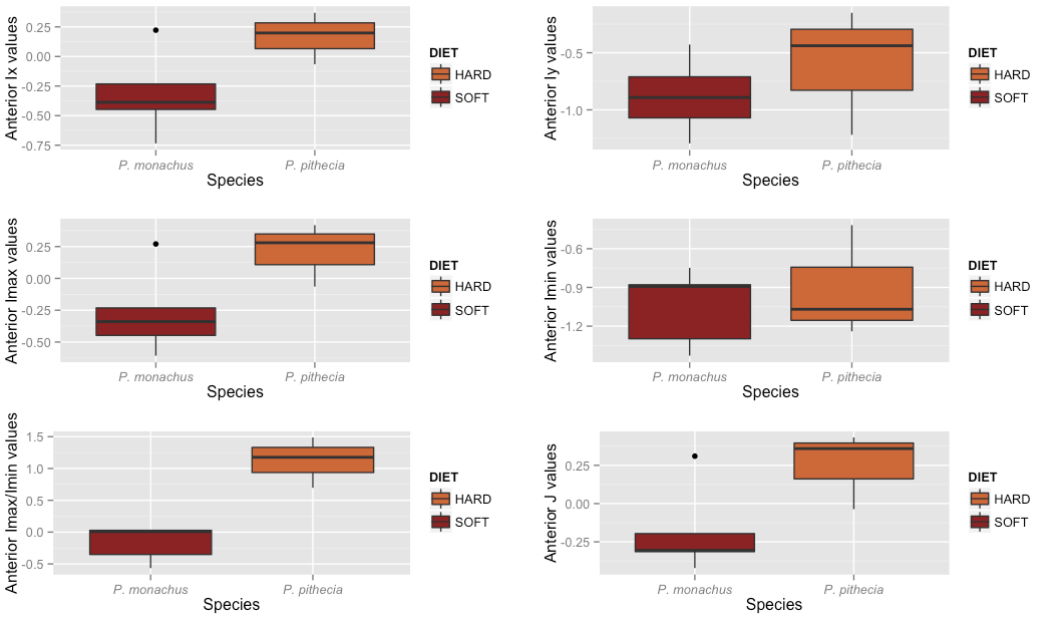

Figure 28h. Boxplots of pairwise comparisons between *P. monachus* and *P. pithecia* for each biomechanical variable.

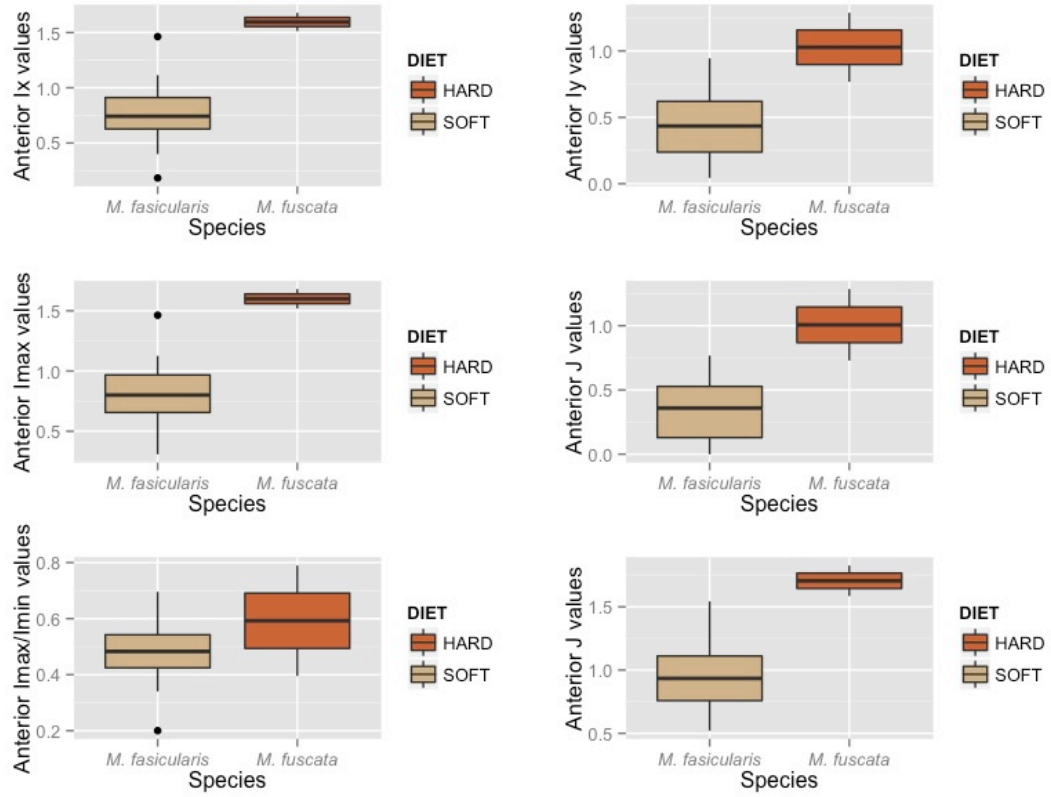

Figure 28i. Boxplots of pairwise comparisons between *M. fasicularis* and *M. fuscata* for each biomechanical variable.

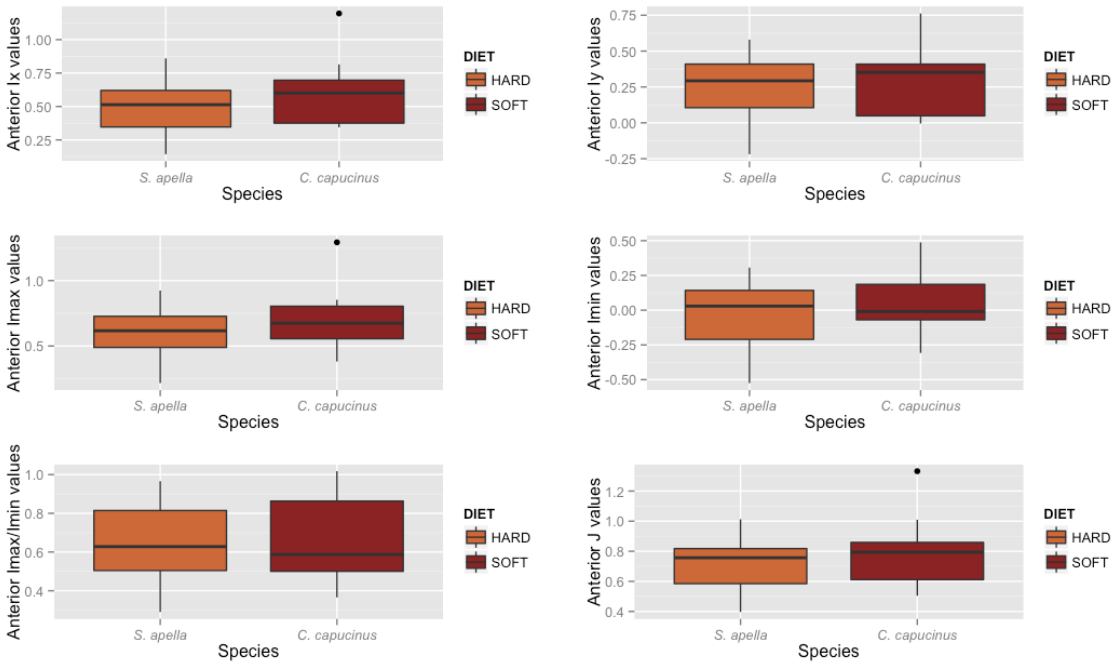

Figure 28j. Boxplots of pairwise comparisons between *S. apella* and *C. capucinus* for each biomechanical variable.

Lophocebus albigena and *Cercocebus torquatus*, both classified as soft consumers in this study, were also compared. This comparison yielded differences in I_{max}/I_{min} indicating these taxa, while similar in many aspects of bending and torsional resistance, varied in shape. When I_{max}/I_{min} is compared in anterior regions for this pair, *C. torquatus* is relatively more circular than *L. albigena*. While the diet of these taxa is primarily fruit, both also consume hard seeds to different extents: 20% in *C. torquatus* (see Mitani, 1989) and 29-36% in *L. albigena* (see Ham, 1994; Poulsen et al., 2001). However, the seeds consumed by *C. torquatus* tend to be harder than those consumed by *L. albigena*. Thus, the higher I_{max}/I_{min} value observed in *C. torquatus* may indicate that the hardness of a food item, rather than the total consumption percent, contributes to differences in arch shape.

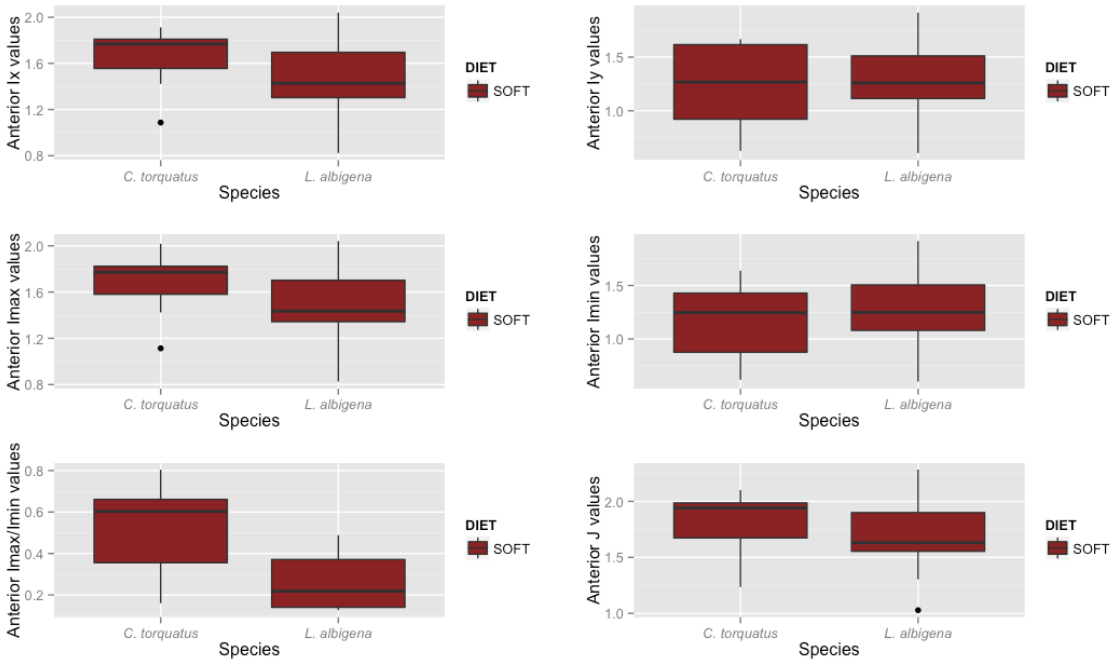

Figure 28k. Boxplots of pairwise comparisons between *C. torquatus* and *L. albigena* for each biomechanical variable.

Comparisons between hard-object consumer *Macaca fuscata* and tough consumer *Macaca mulatta* found significant results in I_{max} and I_x indicating that maximum bending resistance differences may be significantly different in some tough versus hard-object consumers. If consistent, then this suggests that hard-object feeding versus tough food consumption resorts in differential bone response.

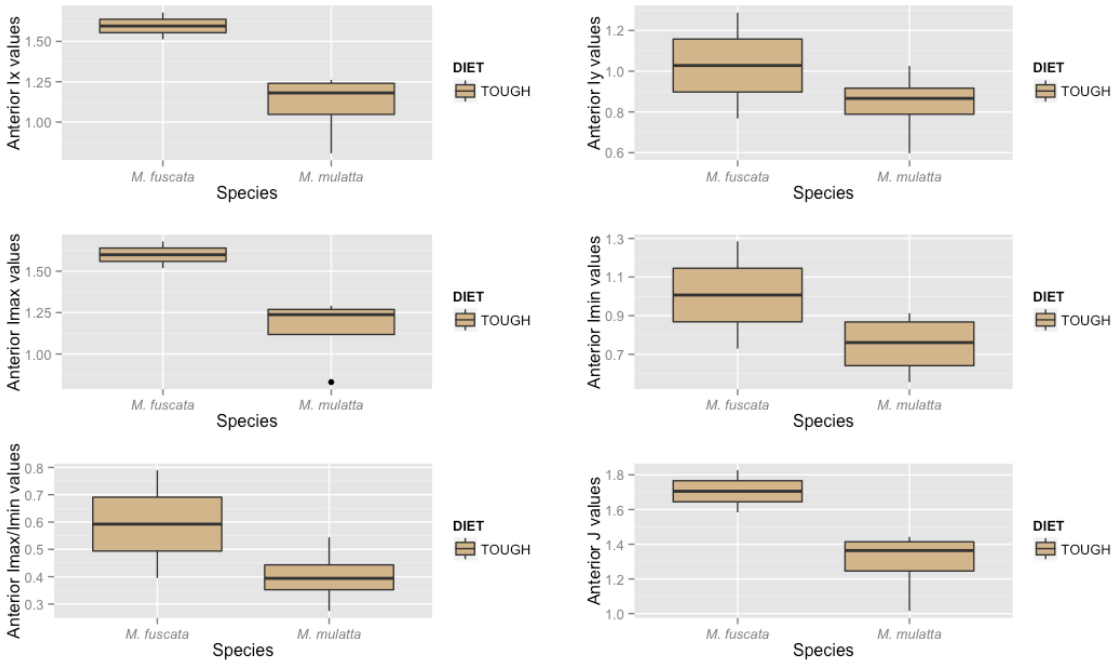

Figure 28l. Boxplots of pairwise comparisons between *M. fuscata* and *M. mulatta* for each biomechanical variable.

To investigate the effect of hard-object consumption, intradietary comparisons were conducted on three sets of taxa (*M. fuscata* & *M. mulatta*, *C. torquatus* & *L. albigena*, *P. badius* & *C. polykomos*) with the same primary diet type but different hard-object consumption amounts.

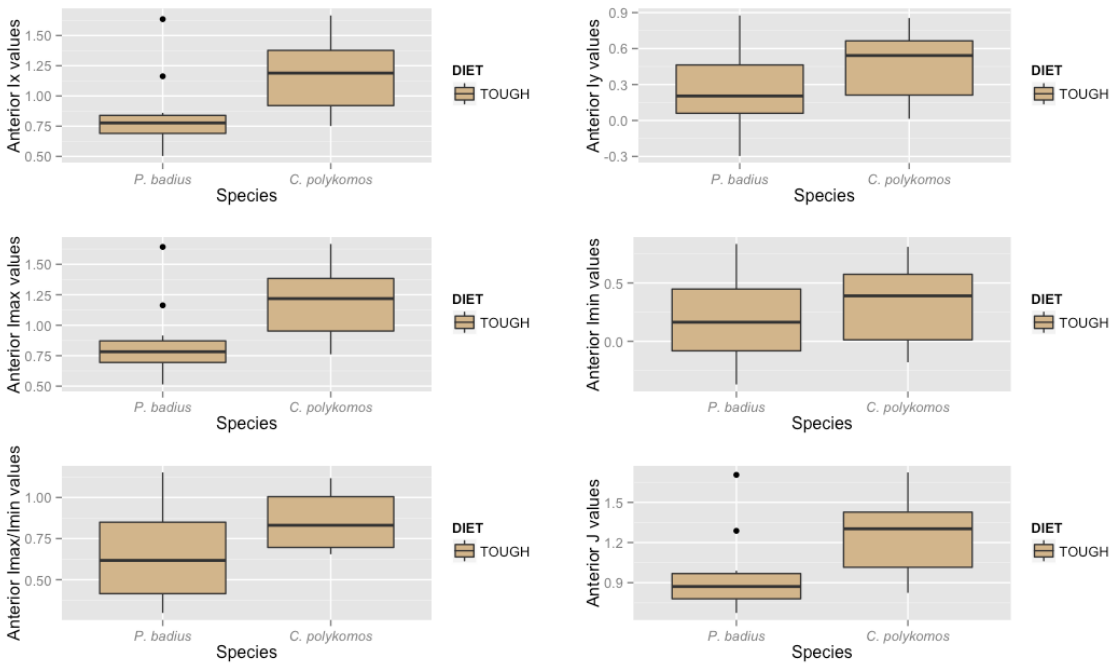

Figure 28m. Boxplots of pairwise comparisons between *P. badius* and *C. polykomos* for each biomechanical variable.

Welch's two-sample *t*-tests found significant differences in the following: for I_{max} in *M. fuscata* and *M. mulatta* (t=3.351, p=0.031), for I_{max} and J in *P. badius* and *C. polykomos* (t=-2.642, p= 0.016; t=-2.384, p=0.027 respectively), and for no comparisons in *C. torquatus* and *L. albigena* (Fig. 28). Notably, when the values for I_{max}, I_{min}, and J are plotted for each species, the species with the greater hard-object consumption percent consistently possessed higher values on average for all three variables. While the relationships were significant in three cases (noted previously), this suggests that hard-object consumption may contribute to greater maximum, minimum, and torsional resistance values, even if the primary dietary type is the same in the both taxa.

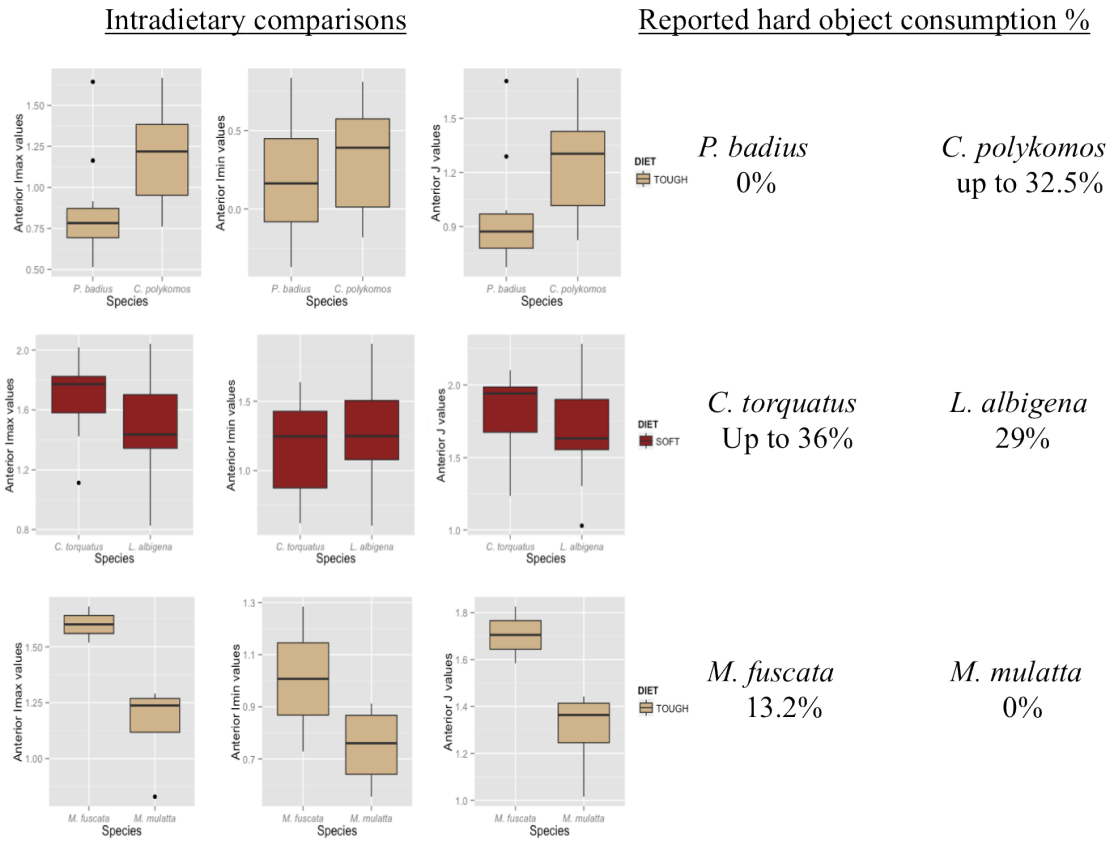

Figure 29. Box plots for intrasietary comparisons conducted on closely related taxa with similar primary diet types. Hard-object consumption percent values are reported for each species in the pairwise comparison.

5.4.8 *FMPs and cross-sectional geometry*

The cross-sectional geometric properties (I_{max}, I_{min}, I_x, I_y, J, I_{max}/I_{min}) for anterior arch sections in the sub-sample of the study taxa (*n*=9 species), for which food materials properties data were available, were compared using Phylogenetic Generalized Least Squares (PGLS) multiple regressions to determine whether there was an effect of phylogeny on the data and to account for size in the cross-sectional variables. In these models, FMPs data on mean toughness (*R*) and mean Young's modulus (*E*) were regressed with measures of cross-sectional geometry to determine whether significant

relationships occurred. This same set of comparisons was also performed between cross-sectional variables and stress-limited ($[E*R]^{0.5}$) and displacement-limited indices ($[R/E]^{0.5}$). These results are presented in Appendix D, Tables SM7.

Results for both Young's modulus measures and toughness measures found no significant relationships between these FMP measures and cross-sectional variables. In addition, the PGLS models found a lambda value approximating 1.0, indicating the presence of a strong phylogenetic signal in the residuals of these data. Results for displacement-limited and indices also found no significant correlations with cross-sectional variables. No models were significant, and the lambda values obtained also approximate 1.0, indicating a phylogenetic effect on the data. In sum, these findings do not provide evidence that FMP or other indices of *E* and *R* are good predictors for cross-sectional variables. Given the small sample size for this set of analyses, a lack of statistical power is a likely contributor.

Finally, Pearson product-moment correlations (Pearson's *r*) between anterior I_{max}/I_{min} measures and average food material properties measures of toughness (*R*) and Young's modulus were conducted to determine the dependence of one variable on the other. Results of these comparisons found no correlation between anterior I_{max}/I_{min} ratios and toughness (Pearson r=0.394, p=0.293), or between anterior I_{max}/I_{min} and Young's modulus (Pearson r=-1.146, p=0.303). A pearson product moment correlations between anterior I_{max}/I_{min} values and dietary categories based on total consumption percent found no relationship between dietary category and I_{max}/I_{min} shape ratios.

5.5 Discussion

Questions concerning the developmental, biomechanical, and adaptive value of the zygomatic arch and zygoma have seen a renaissance with the recent publication of two special issues dedicated to the topic. The zygomatic arch is but one of the series of diverse, overlapping, and competing craniofacial features arranged in a relatively small area and subjected to varying amounts of masticatory strain. Given the complexity of this region, the variation in the constituent features, and their contributions to masticatory load resistance (Vinyard and Ryan, 2006), it is not surprising that comparative analyses of zygomatic arch mechanics sometimes fail to discern a clear signal in terms of bone behavior under specific types of loading. Case in point, the traditional approach to modeling the zygomatic arch as a beam is problematic because while it looks like a beam, the arch does not behave as one (Herring et al., 1996; Teng et al., 1997; Rafferty et al, 2000; Smith and Grosse, 2016). This, however, does not preclude the continued study of this feature, but instead challenges morphologists to consider form in relation to load type and load resistance exhibited by bone, and consider alternative mechanical models that incorporate the differential strain profile observed in the arch.

One of the most pertinent observations from the first *in vivo* studies on macaques (e.g., Hylander and Johnson, 1997) was the presence of an anteroposterior strain gradient which matches cortical bone distributions as well as section moduli (strength) measures throughout higher order primates (Edmonds, 2016). Given the consistency of this gradient, the expectation was that bone form would also follow a similar pattern. Thus, the analyses in this study were undertaken in large part to examine the cross-sectional geometry of the arch – an approach not yet used to examine arch form in relation to

dietary function –to examine the consequences of masticatory loading on bone form.

Unlike direct measures of bending and torsion resistance, cross-sectional shape did not adhere to the same anteroposterior gradient. In general, arch form was elliptical across the majority of regions in all species, which supports the hypothesis that parasagittal bending is the primary load type. Despite the lack of consistency regarding cross-sectional shape, the results for maximum bending resistance and resistance to torsion provide compelling evidence that zygomatic arch loading is similar at a species level, and potentially at the family level, with few exceptions. While *in vivo* strain data are available for only a few primate taxa, the data gathered in this study provide biomechanically meaningful measures of bending and torsion resistance across a wide primate sample that demonstrates a regular pattern of bone resistance along the zygomatic arch. In concert with the results of strain, cortical bone, and section moduli measures, the findings of this study reinforce the presence of mechanical gradient along the zygomatic arch and as such calls for the formulation of a heterogeneous beam model that incorporates these aspects.

One of the means by which these models can be tested is through the use of visualization techniques, such as Finite Element Modeling (FEM). Recent FEM work published by Smith and Grosse (2016) investigated zygomatic arch cross-sectional shape in the context of strain pattern differences in relation to hypothetical cross-sectional arch shapes. Smith and Grosse (2016) concluded that few consistent strain patterns emerged with respect to manipulations of cross-sectional shape in a chimpanzee model. In the present study though, cross-sectional properties within chimpanzees were found to vary – specifically that measures of I_x were significantly different in anterior versus posterior

suture sections meaning that the bending resistance about the x-axis was relatively increased, and that presumably there wouldn't be as much deformation in these regions. In addition, measures of I_{max}/I_{min} within chimpanzees were different in anterior versus posterior and anterior suture versus posterior regions, showing that anterior sections were more elliptically shaped compared to posterior regions, which indicates that bending loads were relatively higher anteriorly. This suggests that shape differences exist along the arch and that they confer specific load resistance capabilities, and that the construction of an FEM model meant to replicate *in vivo* conditions would be best done by modeling the zygomatic arch according to these regional differences rather than modeling it as a uniformly similar structure. Great strides in model improvement have been made through the inclusion of data on bone material composition in addition to landmark data as well as *in vivo* strain data, however, when modeling the zygomatic arch, this study argues that an accounting for the differences in bone behavior and shape variation would provide a more accurate basis upon which to construct an FEM model and enhance the strength of the conclusions drawn from such models in the pursuit of answers concerning evolutionary questions about masticatory adaptation in primates.

5.5.1 *Dietary groups and cross-sectional geometric properties*

Grouping taxa together on the basis of dietary type is a common method for understanding the interface of dietary quality and morphological features. Recent work investigating the utility of traditional dietary categories (e.g., frugivore, folivore, faunivore) found that these designations do not correspond to food material properties (Coiner-Collier et al., 2016) and thus may not be the most meaningful or appropriate

groupings to use for analyses. Criticisms of the use of traditional dietary categories cite the disproportionate reliance on different criteria, the difficulty in how to account for the degree of seasonal and/or population variation in primates, and the challenge of defining categories that are biologically, ecologically, and ultimately evolutionarily meaningful. The separation of taxa into more mechanically relevant categories (e.g., tough consumer, hard consumer, soft consumer) in this study was meant to match biomechanical variables with biomechanically relevant dietary groupings. While this study finds that mechanical dietary designations are informative about certain morphological characteristics related to diet, the best approach for future wok would be the inclusion of food material properties data in conjunction ecological data. The use of food material properties data in this study was limited due to the availability of these measures within the literature for the taxa included here. Though limited, these results indicate that food material properties may be a more appropriate means by which to quantify primate diet given the direct relationship between the mechanical needs of a food (measured as toughness or Young's Modulus) and the response of the bone to these loads. This point is discussed more extensively in the following sections.

Within this study, examining the entire series of biomechanical variables by dietary group (on the basis of total consumption percent) found that the most significant differences occurred in tough versus exudate consumers and that the significant differences between these groups extended to all regions of the zygomatic arch. Body size is likely a contributing factor to the differences observed in this group given the taxa subsumed under tough feeding included some of the largest bodied taxa in the sample (e.g., *G. gorilla* and *T. gelada*) whereas exudate consumers contained some of the

smallest bodied taxa (e.g., *C. jacchus*). It is well known that primate diet and body size are intricately linked, and that primates of relatively greater body size consume large quantities of low-quality food (e.g., leaves) while smaller bodied individuals consume higher quality (e.g., insects) (Kay, 1984; Fleagle, 1998) and thus it is to be expected that some effect of body size is present in these comparisons.

The shape ratio I_{max}/I_{min} was not significantly different between dietary groups for any arch region indicating that, while tough and exudate consumers differ with respect to bending and torsional resistance, they did not differ in cross-sectional shape. Because I_{max}/I_{min} is corrected for body size, the lack of difference between the dietary groups may also further indicate an effect of body size is present. Intra-dietary comparisons found that tough and soft food consumers possessed significant differences in shape ratios across the zygomatic arch, whereas hard and exudate consumers did not. The significant degree of variation observed in these groups may indicate that shape differences exist because of the taxonomic diversity rather than as a result of the differences in masticatory loading.

The consumption of soft foods is found in most primate taxa to some degree, and the primary reliance on such foods varies in conjunction with seasonal and regional availability. Of the dietary categories included here, soft food consuming encompasses the most generality in terms of food type as well as the largest number of species. Intra-dietary group comparisons of soft consumers found significant differences in the variance for each biomechanical variable at each zygomatic arch region ($p<0.001$) with regard to bone bending resistance about the x- and y- axes (I_x, I_y), maximum bending resistance (I_{max}), and resistance to torsion (J). This amount if variation is not unexpected given the

wide taxonomic breadth included under this dietary category. Because of this extensive variation, it does not appear that the consumption of soft foods leads to any specific patterning that with respect to zygomatic arch architecture.

In contrast to a mechanically soft diet, the nature of a hard diet is relatively more specialized and often involves the consumption of fruits as well. To process hard objects, such as seeds or nuts, requires relatively high, but infrequent, bite forces generated by specific craniofacial configurations. For example, within cebids the relative positioning of the temporalis and masseter muscles in *Sapajus apella* and *Cebus olivaceus* were more anterior compared to other species of platyrhine, which allows for greater force production on the anterior teeth (Wright, 2005). This is also reflected in the cross-sectional variables for *S. apella*, which reveal that anterior arch sections are significantly different in bending and torsional resistance from all other regions, indicating that the relative anterior shift of the muscles places greater loading in this region of the arch. Niche broadening characteristics, such as the increased leverage at the anterior teeth afforded by the masticatory muscle placement, is advantageous in that it permits the consumption of foods of varying toughness (Wright, 2005) as well as hardness. While this pattern is exaggerated in *S. apella*, the key element in these primates is that the craniodental complex permits the regular processing of soft food items as well as the ability to use increased bite forces on the anterior teeth to breach hard food items (Wright, 2005; Wright et al., 2009).

In terms of adaptation, the ability to access more resistant foods items, even if the food item is not a staple in the individual's diet, confers an important fitness benefit particularly in times of food scarcity. In a 2008 study by Taylor and colleagues, food

material properties in relation to loading in the mandible were compared in hominoids to determine relative load resistance abilities. The results found that mandibular load resistance is linked with the maximum toughness of a food material, rather than the total average consumption. In other words, the food with greatest toughness, even if consumed less often, determines the load capacity of the bone (Taylor et al., 2008). Given the variation within tough (and soft consumers) with respect to cross-sectional variables, it is likely that differences in relative toughness of the foods likely vary across these species as well. For instance, toughness values recorded for *Pongo pygmaeus (*classified as a soft food consumer in this study) actually surpass values for *Alouatta palliata* and *Theropithecus gelada*, both of which are classified as tough food consumers (Coiner-Collier et al., 2014). When maximum bending resistance and polar moment of inertia values for *P. pygmaeus* and *T. gelada* are compared, *P. pygmaeus* was found to have greater bending and torsional resistance measures in all arch regions except posterior portions. While tough foods on average do not constitute the general quality of the foods consumed by *P. pygmaeus*, it suggests that the zygomatic arch of this species is fortified to resist higher masticatory loads even if those loads are infrequent.

Compared to both tough consumers and soft consumers, hard-object consumers demonstrated significant differences in all cross-sectional variables except I_{max}/I_{min} ratios. Because of the more specific mechanical demands of a hard diet, the relative lack of variation among hard-object consumers indicates that the zygomatic arch is more uniform in bending and torsion resistance. While hard-object consumers constituted a relatively smaller group within this study, the manner in which bone is oriented in each cross-section appears to be relatively similar, generating an overall cross-sectional shape that is

uniform throughout. Despite the similarity in overall cross-sectional shape, bending and torsional values across all arch locations vary throughout this dietary group suggesting that while overall shape is similar, the bone regions which bear the highest loads vary.

Exudate consumers performed similarly in this regard, as no significant variation was found in their shape ratios. However, unlike the other dietary groups, exudate consumers possessed relatively uniform measures of I_y and I_{min} in anterior and anterior suture regions. Given this region expressed the highest I_{max} and J measures of all arch regions, the lack of variation in I_y and I_{min} in this region suggests that these taxa experience relatively similar transverse loads. The marmosets (*Callithrix jacchus*, *Mico argentata*, *Mico humeralifera*) included in this exudate group are known to rely on exudate consumption to a greater degree as compared to closely related tamarins (*Leontopithecus* and *Saguinas*) and use their lower teeth and wide gapes (Hogg et al., 2011) to gouge holes into tree back to stimulate exudate flow (Kinzey et al., 1975; Sussman and Kinzey, 1984). While this strategy is effective for obtaining exudates, it does not provide increased load resistance capabilities (Hogg et al., 2011). Furthermore, comparative analysis of fiber architecture in the masseter and temporalis muscles of marmosets suggests they are capable of relatively increased excursion but possess reduced force-producing potential compared to tamarins (Taylor and Vinyard, 2004). When the I_{max} and J measures for the marmoset and tamarin (*Saguinas oedipus*) species are compared, both *M. argentata* and *M. humeralifera* were found to possess relatively lower values, not only in comparison to *S. oedipus*, but compared to the study taxa as a whole, suggesting that these taxa possess relatively reduced maximum bending and torsional resistance potential compared to all other taxa. Despite having the lowest

values observed in the sample, all exudate consumers (i.e., species of marmosets) adhered to the predicted pattern of possessing their highest bending and torsional resistance values in anterior sections.

Several taxa appeared to be outliers with respect to variation in each cross-sectional variable for each dietary group. In tough consumers, *A. palliata, G. gorilla,* and *C. polykomos* were consistently different in their comparisons with other tough consumers with regard to I_x, I_{max}, and J measures across all zygomatic arch regions. With regard to maximum bending resistance measures, both *A. palliata* and *G. gorilla* possessed the relatively highest measures of I_{max} in the sample. Both of these taxa consume diets high in toughness, and while *Alouatta* does not grow to the size of a gorilla, they have relatively large teeth for their body size, high crowns and long shearing crests compared to other platyrrhines of equal body size (Rosenberger et al., 2011; Terhune et al., 2015) that aid in processing large quantities of structural carbohydrates (Terhune et al., 2015). The zygomatic arches of *A. palliata* appear to be relatively robust compared other platyrrhines given that cross-sections are generally taller and maintain a uniform shape at both superior and inferior edges, and lack a curve along the medial. Other platyrrhines by comparison have relatively short arches that are relatively constricted mediolaterally and whose inferior margins taper to render a "teardrop" shape, such as in *Aotus,* or can have a curved mesial margin, as in *Saimiri*. Importantly, masseter and temporalis muscle physiological cross-sectional areas (PCSA) are known to scale with negative allometry in platyrrhines (Taylor et al., 2015) which contrasts with the positively allometric relationships observed in Old World monkeys (Anapol et al., 2008;

Taylor et al., 2013) and further reinforces functionally distinct differences in the crania and masticatory morphology between these two groups.

If masseter muscle PCSA is negatively allometric with respect to body size, then what explains the high I_{max} values observed in *A. palliata*? It appears that *A. palliata* is an exception to the pattern observed in other platyrrhines in that it deviates considerably above the RMA slopes for comparisons of masseter muscle size in relation to jaw length and condyle-to-first mandibular molar length (see Fig. 3A in Taylor et al., 2015) indicating the presence of a relatively large masseter PCSA for both load arm lengths (Taylor et al., 2015). Upon activation, relatively larger masseter muscles likely induce relatively higher parasagittal bending moments on the zygomatic arch, requiring that the arch be able to resist such loads to avoid failure. In humans, temporalis PCSA and anteroposterior length of the zygomatic arch was weakly correlated (Antón, 1994) but it is not clear if that relationship is upheld across non-human primates. To better answer this question, scaling relationships between the masticatory muscles and zygomatic arch would provide a better understanding of the effect of muscle PCSA in relation to arch form and its mechanical behavior.

Within soft consumers, no single species was found to be consistently different from other soft feeders with respect to bending resistance indicating high variance among species in the group as well as between species, but no predictable patterns overall. Within hard-object consumers, maximum and minimum bending resistance differences were primarily observed between *Macaca fuscata* and other hard object consumers. The diet of *Macaca fuscata* is highly variable both seasonally and regionally (Aoki et al., 2015) and their consumption of hard seeds can vary from 13.2 % (Hill, 1997) to 44% or

more (Agestsuma and Nakagawa, 1998). Hard-object consumption in other taxa in this group such as *Macaca sylvanus* (26.7-32.2%, see Menard and Vallet, 1996) is more consistent and less variable which may influence the regularity with which higher magnitude loading is experienced in the zygomatic arch. Additionally, the average maximum bending resistance in *M. sylvanus* is greater than that of *M. fuscata* which may relate to the relatively higher and more consistent hard-object consumption found in the former.

In exudate consumers significant differences were found across arch locations for each variable with the exception of I_y, I_{min}, indicating relatively uniform measures of transverse bending resistance throughout the zygomatic arch, and I_{max}/I_{min} indicating similar cross-sectional shapes throughout the arch. Within this group, *C. jacchus* and *C. argentata* cross-sectional shape was not found to differ, but aspects of bending tendencies do differ markedly between this pair. Though both primarily consume exudates, *C. argentata* appeared to possess relatively higher bending and torsional resistance measures as compared to *C. jacchus* even though *C. jacchus* is reported to consume more tough foods (up to 18.1%, Smith and Smith, 2013) than *C. argentata*. For this reason, it is also important to consider the effect of local dietary shifts that may have occurred in the primates' habitat. For example, populations of *C. jacchus* in Pontes and Soares' (2005) study were reported to consume upwards of 61.5% fruits and 28.7% of exudates. However a similar study in the same geographical region in 2010 found *C. jacchus*'*s* diet included 61.99% for exudates and 2.9% fruit (Silva et al., 2010). A shift from a low exudate, high fruit to a high exudate, low fruit strategy likely imparts a shift in masticatory loading as well, such as a concomitant increase in bending moments,

particularly if the high fruit consumption included fruits comprised of varying measures of toughness and stiffness. Compared to *C. jacchus*, *C. argentata* also incorporates more fruit on average (up to 36%, Smith and Smith, 2013). The difference in food restrictions is likely due to human intervention and changes to the local ecology (Silva et al., 2010) and further emphasizes the difficulty is assigning taxa to specific dietary groupings when populations of the same species can vary over relatively short time spans.

Comparisons between arch regions for bending and torsional resistance in *C. argentata* more closely echo those observed in soft consumers than in other exudate consumers, particularly because *C. argentata* possesses significantly different I_x and I_{max} measures in comparisons of anterior regions to more posterior regions; a common trend in soft consumers that is absent in both *C. jacchus* and *C. humeralifera*. Thus, morphologically *C. argentata* appears to align more closely to other primates that are more dietarily similar in fruit consumption, rather than with more closely related species of marmosets.

The findings of this study do not strongly support total consumption percent as a means of comparing diet in relation to mechanical variables measured on the primate zygomatic arch. While the differences between tough consumers and exudate consumers speak to some level of dietary differentiation, this approach alone is not sufficient to predict patterns in dietary categorization because the criteria upon which groupings are made are to a degree subjective. With the amount of seasonal variation present in many primate species, it is difficult to set criteria for assigning a taxon to a particular dietary category that truly represents their average dietary intake throughout the year. Moving forward, relying on more empirical standards of categorization (i.e., food material

properties) may provide the necessary resolution by way of comparisons along a continuous scale rather than binning taxa into discrete groups.

5.5.2 *Resistance to bending and torsion*

The tendency for a bone to bend about the x- and y-axes (I_x, I_y) as measured in cross-sections of the zygomatic arch was found, in general to be greatest in anterior regions as compared to any other region across the study taxa which supports this study's second hypothesis. Larger values of I indicate that a shape has an area at a greater distance away from an axis through its centroid. Within the zygomatic arch it appears that the increased distance of the bone border from the centroid effectively increases the stiffness because it places more bone farther from the neutral axis of the structure. Given that stresses are highest moving away from the neutral axis, the addition of bone material would strengthen the cross-sectional shape. Operating under the model that strain is highest anteriorly due to the positioning of the masseter; it stands to reason that the masticatory loads experienced are also concentrated anteriorly. Because parasagittal bending appears to be the dominant loading regime overall (especially in anterior sections), it follows that bending resistance would also be greatest in the portions of the arch subjected to the highest loads.

The expectation was that this pattern would be exaggerated in taxa consuming more mechanically challenging diets (tough and/or hard) in that they would possess relatively higher I_{max} and J measures compared to taxa who primarily consumed less mechanically challenging foods (soft or exudate). When average values of maximum bending tendencies were compared across dietary groups, tough consumers possessed the

highest average I_{max} and J measures, followed by soft consumers, hard consumers, and exudate consumers. While this result may be linked to the mechanically challenging nature of a tough diet, these results may be more influenced by body size given the largest bodied taxa (*Gorilla*) in the study were generally tough consumers, followed by other large bodied taxa (*Pan* and *Pongo*) in the soft consumer group. When overall dietary group averages were compared by region, anterior measures of bending and torsional resistance were greatest overall in all dietary groups regardless of diet type.

Of the 43 species included in this study, only *Macaca sylvanus*, *Pithecia pithecia, Pithecia monachus, Theropithecus gelada*, *Mandrillus leucophaeus*, and *Chiropotes albinansus* did not possess their greatest second moments of area, maximum bending resistance, and polar moments of inertia in anterior or anterior suture regions. Potential explanations to account for the differences in these taxa are discussed in the following sections. The findings for the remaining taxa however, strongly support the hypothesis that anterior zygomatic arch regions routinely experience higher bending loads as compared to posterior regions, and thus exhibit greater bone structural response to combat these loads. These findings also agree with the documented strain distribution described by Hylander and Johnson (1997) and suggest that the presence of an anteroposterior strain gradient in the zygomatic arch reflects a pattern that exists regardless of diet type, and that may represent a general primate pattern.

In hard-object consumers, all taxa except *Macaca sylvanus*, *Pithecia pithecia,* and *Presbytis rubicunda* (highest posteriorly only in I_y) exhibited their highest I_x, I_y, I_{max}, and J measures in anterior regions. In *P. rubicunda* though, posterior measures of I_y were not significantly different than those in anterior sections. Interestingly, *Macaca sylvanus* was

the only species within the entire study to possess its greatest measures of bending resistance at the midsuture region followed by the posterior suture regions. However, this species is represented by a single individual, which limits the statistical power of this observation. While *M. sylvanus* in designated as a hard-object consumer in this study on the basis of the food item of which it consumes the most, this species also consumes leaves (up to 13%, see Menard and Vallet, 1996; 1997) and insects (10.5% see Menard and Vallet, 1996; 1997). It is unexpected that the highest I_{max} values occurred at the midsuture region given that suture sites are seen as locations of strain dispersion and potential structural weakness under high loading (Kupczik et al., 2007; Wang et al., 2010; 2012). I am cautious in drawing the conclusion that the highest bending resistance values regularly occur in midsuture sections in *M. sylvanus* in the absence of a larger sample size for this species. Further study on this point is necessary to tease out whether *M. sylvanus* exemplifies a pattern that is different not only from other macaque, but from haplorhine primates in general.

Chiropotes albinasus was found to have its greatest measures in posterior regions, however issues associated with the small sample size of this species do not provide adequate statistical power to conclude that posterior regions are consistently highest in this taxon. Therefore, future work with larger sample sizes is necessary to render a more confident result. The *P. pithecia* and *P. monachus* samples were sufficient for statistical analysis, and they had absolutely higher I_x, I_y, I_{max}, and J values in posterior suture regions when compared to all other arch locations intraspecifically, though these differences are not statistically significant. One explanation is that the apparent shift in strain may be due to a change in masseter placement and/or activation. Without *in vivo*

strain data to compare to the cross-sectional geometry or detailed soft tissue measurements of these pithecids, this conclusion remains speculative at best. As hard-object specialists, pithecids face two functional challenges: the size of the object to be fractured, and the material properties of the food item contained therein. Pithecids are known to possess specific craniodental features that aid in the processing and consumption of hard seeds, which include increased occlusal area on the postcanine teeth, large splayed canines, and tall appressed incisors (Kinzey, 1992). These dental tools function to breach or masticate one or multiple plant tissue layers in order to access the nutrient rich pulp or endosperm (Wright, 2004). Pithecids also place hard seeds on their molarized premolars, a characteristic associated with hard-object consumption in primates (Kay, 1990), which enables efficient trituration of the seed tissues (Kinzey, 1992; Rosenberger, 1992).

Within the realm of ingestible foods, some plant tissues are more easily processed (i.e., are easily torn or comminuted) while other layers are more mechanically resistant (i.e., more difficult to breach, tear, or comminute) meaning that within a single food item, a primate may encounter a series of plant layers with markedly different processing requirements (Wright, 2004). For instance, the *Inga* fruit consumed by *P. pithecia* varies in toughness from the endosperm (measuring about 182.1 J m^{-2}) to much higher measures in the external woody tissues (4382.9 J m^{-2}) (See Table 5.3 in Wright, 2004). Thus, the tissues in these fruits fall within the range of many types of leaves, and place increased mechanical demands on the masticatory complex. It is on this point that the mechanical demands imposed by the processing of specific plant tissues, rather than the demands of

processing specific food types, impact the form and muscular components of the masticatory system in primates.

In humans, small vertical changes in jaw height (obtained from subjects biting on a pad) were found to significantly affect the nature of motor unit recruitment in distinct portions of the masseter muscle and that recruitment was greater in the deep masseter as compared to the superficial masseter (Terebesi et al., 2015). This study observed that masseteric activity decreased as vertical distance increases even while maintain a constant bite force (Terebesi et al., 2015). In the case of the pithecids, placing an object on the posterior teeth would require a larger vertical distance in jaw height (i.e., gape), which would conceivably reduce masseter muscle activation compared to biting on a smaller object and possibly displace the locations of strain as well. It may be that the activation of different masseter motor units in relation to the size of the food object results in more posteriorly concentrated strains on the zygomatic arch in this species. Spencer (1995) found that the mechanical advantage of the masticatory muscles in *P. pithecia* was substantially lower than in other hard-object consumers (*Chiropotes* and *Cacajao*). However, masseter muscle PCSA size in *P. pithecia* is relatively larger compared to other pithecids (Taylor et al., 2015) which may be necessary to provide increased power as a tradeoff to counteract the lack of mechanical advantage. In addition, placing the food item closer to the TMJ, would also function to reduce the magnitude of the masseter muscle during a bite. The fact that this pattern of bending and torsional resistance is observed in both taxa, this may indicate the presence of a species-specific pattern. Future work examining this pattern in *P. pithecia* and *P. monachus* in relation to other pithecids would be necessary to confirm this. Further investigation into

the multiple factors (e.g., muscle architecture, fiber length, insertion location etc) that are undoubtedly contributing to this phenomenon would also be valuable for future work.

Similar to the pithecids, *Theropithecus gelada,* a committed gramnivore with a diet high in toughness, exhibited their greatest bending resistance in posterior regions. It is interesting that *P. pithecia, P. monachus,* and *T. gelada* yield high measures in posterior regions given they are architecturally and dietarily distinct; *Pithecia* is relatively short faced and consumes hard seeds while *T. gelada* is more prognathaic and consumes grasses. As previously discussed, differential motor unit recruitment may vary in *T. gelada* to the extent that high strain concentrate posteriorly. The consumption of grasses does not require a particularly large gape, but the presence of large, dimorphic canines does. Like pitheicids, geladas possess unique dental characteristics that reflect their grazing habit; these include large, thickly enameled, high-crowned molars, that wear to become curved enamel crests upon which tough foods are effectively comminuted and ingested (Jolly, 1970; Jablonski, 1993, 1994; Venkataraman et al., 2014).

The soft tissue emanating from the zygomatic arch in *T. gelada* includes the origin of the *pars superficialis*, a thick aponeurosis that originates from the anterior two-thirds of the inferior surface of the zygomatic arch (Jablonsky, 1981, p. 72), the second internal aponeurosis which takes its origin from the inferior aspect of the central portion of the zygomatic arch (Jablonsky, 1981, p. 73), and the *pars profunda* which has its more muscular attachment in at the posterior third of the arch and extends the entire inferior and a large portion of the inferomedial aspect of the arch (Jablonsky, 1981, p. 77). Upon activation, these soft tissue structures may induce greater loading in posterior regions, particularly if temporalis activation is diminished in comparison to masseter activation in

this species. However, more data on in vivo strain patterns in this species are necessary to determine if strains do concentrate posteriorly, and if so, is that accomplished in a different way than is observed in *Pithecia*.

Mandrillus leucophaeus was also characterized as having its largest measures of I_x, I_y, I_{max}, and J in posterior regions and also possesses a relatively prognathaic facial structure. Unlike geladas, this species of mandrill generally consumes soft foods (58%, see Gonzalez-Kirchner and Sainz de la Maza, 1996) and some leaves (16%, see Gonzalez-Kirchner and Sainz de la Maza, 1996). One explanation for the similarity in these arch measures across these taxa could derive from the similarity in the toughness of the foods consumed. *Sensu* Taylor et al., 2008, the maximum toughness of the foods consumed by mandrills may approximate that of geladas even if the frequency with which the tough foods are consumed varies. Without material properties data on mandrill diets though, this remains unclear. Alternatively, the similarity in the bending moments of these taxa may relate to relative positioning of the arch on the cranium given both *Mandrillus* and *Theropithecus* possess relatively high degrees of snout prognathism and large gapes. While zygomatic arch position was outside the purview of this study, the architectural similarities between these taxa may explain the presumed posterior shift of high zygomatic arch strain.

While the presence of higher posterior bending loads may be derived in these taxa relative to other primates, the presence of relatively high instances of bending in posterior zygomatic arch sections is not unheard-of in other mammals. In herbivorous marsupials, high posterior zygomatic arch strains have been observed in the common wallaby (*Vombatus ursinus*), a known grazer. The zygomatic arch was the most highly strained

part of the skull during molar biting overall among all models and the results suggest that variation in the performance of the masticatory system in marsupials is tied to diet. The highly grazing wombat exhibited the highest mechanical efficiency indicating the cranium (and zygomatic arch) is strong and efficient for transmitting masticatory muscle loads to the teeth and is thus optimized to combat high bite forces (Sharp, 2015). Wombats consume diets high in toughness (e.g., Tussock grasses) and possess adaptions to aid in combatting the resulting functional loads. While wombats are morphologically different than geladas in key ways (e.g., the teeth), the high instances of posterior bending may induce a shift in strain such that the highest strain loads are concentrated posteriorly.

Similarly, pigs (*Sus scrofa*) have also been found to experience high loads on posterior arch (on the squamosal bone) portions. Strain in the zygomatic arch derives primarily, but likely not exclusively, from the masseter muscle (Herring et al., 1996) but also from the soft tissue aponeuroses that envelop this area of the cranium. In both pigs and primates, the zygomatic arch is composed of two bones: the zygomatic and squamosal in pigs, and the zygomatic and temporal bone in primates. In primates, Hylander and Johnson (1992) noted the presence of an anteroposterior strain gradient that traversed the full length of the arch, whereas pigs have distinct strain patterns unique to each constituent part of the arch. In the zygomatic arch of pigs, Herring et al. (1996) noted the presence of bending on both arch portions but that the direction of bending was opposite in each portion; namely that the zygomatic portion experiences in plane bending while the squamosal portion experiences out-of-plane bending. It appears a transition happens at the zygomaticosquamosal suture in which a load transmitted from the zygomatic bone to the squamosal bone is transferred posteriorly as well as ventrally

(Herring et al., 1996). This transfer results in relatively higher strain values in squamosal sections compared to those in the zygomatic bone.

The out-of-plane bending in the squamosal bone is the reverse of what is expected given the masseter attaches anteriorly and functions as the sole muscle that pulls directly on the bone. If the out-of-plane bending derives from the medial muscle pull of the masseter, why is the strain greatest in the squamosal region? These assumptions operate on the premise that the arch is a homogenous bony structure composed of isotropic bony tissue. However, the microstructure of the squamosal and zygomatic bones reveals that the squamosal portion contains osseous tissue arranged mediolaterally, which stiffens the arch in the transverse plane (but less stiff along the plane of measurement) whereas the zygomatic is buttressed against loading in all three directions (Herring et al., 1996). In these primates, the posteriorly higher bending resistances may be derived from a similar circumstance. Rafferty et al. (2000) noted that upon contraction, the masseter muscle in pigs pulls the zygomatic bone medially, posteriorly, and inferiorly while the squamosal portion remains fixed posteriorly to the cranium. Under this condition the vertical componenet of the zygomatico-squamosal suture experiences compression (Herring and Mucci, 1991). At the suture, the zygomatic bone is lateral to the squamosal bone and the contraction of the masseter must cause the zygomatic bone to push inferiorly and posteriorly on the squamosal bone, causing it to bend medially and experience out-of-plane bending (Rafferty et al., 2000). In the studies of macaques, Hylander and Johnson (1997) noted that the high anterior strains on the arch derive from the in-plane bending induced by the anteriorly concerntrated masseter muscle. Thus, the role of in-plane versus out-of-plane bending differs between macaques (and likely other primates) and

pigs. Unlike pigs which have dorsoventrally tall arches well suited to resist in-plane bending (Rafferty et al., 2000), *M. leucophaeus* appears to possess relatively robust and round arch sections while *T. gelada* appears to have more "teardrop"shaped arches; neither of which appear to be suited to resist in-plane bending. Based on the results presented here it would be intriguing to compare the osseous tissues of these taxa to determine whether they adhere to the pig or primate pattern.

5.5.3 *Shape ratio differences: I_{max}/I_{min}*

The application of a biomechanical shape ratio (I_{max}/I_{min}) has not been used in previous studies of zygomatic arch morphology but provides a shape index for which to assess the relative ability of a cross-section to resist bending or twisting loads. While typically used to assess long bone or mandibular shape and loading, this study is the first to apply this technique to the zygomatic arch to investigate the cross-sectional shape consequences of different masticatory loads. I predicted that cross-sectional shape, as indexed by I_{max}/I_{min}, would predict whether the masseter line of action was more vertical (indicating high bending loads and lower BZBR ratios) or more oblique (indicating high torsional loads and greater BZBR ratios). Elliptically shaped zygomatic arch cross-sections were predicted to occur in taxa with more vertical masseter insertions as compared whereas more circular cross-sections should occur in taxa with more obliquely oriented masseter muscles. Unlike strict measures of bending and torsion, I_{max}/I_{min} ratios did not follow a predictable pattern across arch regions. In a general sense, all taxa possessed arches that were generally elliptical (to some degree) in each arch region regardless of the predicted masseteric line of action.

Under the initial prediction, more flared zygomatic arches should result in a higher bizygomatic-biramus ratio (BZBR), I_{max}/I_{min} ratio approximating 1.0, greater torsional moments, and thus more circular cross-sections. The taxa with the lowest BZBR ratio are expected to experience the highest torsional moments. *T. gelada, A. caraya*, and *P. paniscus* possessed some of the lowest bizygomatic-biramus width ratios and their associated I_{max}/I_{min} values did not approximate 1.0 more than most other taxa. Furthermore, when the site-specific I_{max}/I_{min} ratios for these taxa are compared, they are not markedly circular in shape. In *T. gelada*, midsuture sections were relatively circular, but anterior and posterior sections were quite elliptical by comparison. Notably, the most elliptical arch sections for geladas appear in their posterior regions, which corresponds to their sites of highest I_{max} measures. While polar moment of inertia measures were also highest posteriorly in this species, it is likely that the magnitude of parasagittal bending exceeds that of torsion, requiring that the arch's cross-sectional shape be more elliptical, rather than circular, to combat the primary load type.

In contrast, taxa with the highest BZBR ratios, and thus presumably most vertical masseters, were predicted to have more elliptical cross-sections. Of the entire sample, *H. lar*, *C. jacchus*, and *C. humeralifera* possessed bizygomatic-biramus width ratios closest to 1.0, however their I_{max}/I_{min} ratios were relatively low and thus are predicted to possess more circular arch cross-sections. Within these three taxa, the sites found to be most elliptically shaped, (posterior in *H. lar*, midsuture in *C. humeralifer*, and anterior suture in *C. jacchus*) did not correspond to regions where I_{max} measures were highest.

From the perspective of strict I_{max}/I_{min} ratio patterns by arch region, the species whose arch sections were relatively more circular compared to others was soft consumer

P. rubicunda (I_{max}/I_{min} ratios 0.91-1.06), followed by tough consumer *Nasalis larvatus* (I_{max}/I_{min} ratios 0.82-1.06). Based on this result, one would expect that *P. rubicunda* and *N. larvatus* would possess more flared arches compared to other taxa. These taxa had relatively similar bizygomatic-biramus width ratios (0.82 and 0.85 respectively). However, these ratios do not indicate that these taxa have particularly flared arches in comparison to other taxa, which suggests that bizygomatic-biramus width ratios do not clearly determine I_{max}/I_{min} ratios. Despite the lack of consistent patterning with respect to arch shape, it is notable that the taxa with relatively more flared arches were tough or hard-object consumers in comparison to taxa with relatively less flared arches, which were generally soft or exudate consumers. Compared to the other biomechanical variables quantified in this study, I_{max}/I_{min} measures were relatively consistent across arch locations among all taxa. This suggests that unlike measures of bending or torsion, I_{max}/I_{min} ratios are not simply mirroring where masticatory strain is most concentrated. In the majority of primate taxa examined here, I_{max}/I_{min} measures indicate that parasagittal bending, rather than transverse bending, are the primary bending loads experienced. There is also likely an effect of where the masseter attaches on the zygomatic arch; an attachment superior to the central axis would counteract some torsional loading and generate a medial bending load instead. Furthermore, an elliptical shape may enhance the surface area of attachment for the masseter in addition to indicating a parasagittal bending load. However, *in vivo* data demonstrating the load pattern are required to verify this prediction.

In circular cross-sections, the presumption is that there is a more equitable arrangement of cortical bone about the axis, and thus the cross-section is best suited to

resisting a combination of transverse bending and torsional loads. The polar moment of inertia (J) can overestimate torsional rigidity in non-cylindrical sections (Daegling, 2002b). However, Daegling (2002) determined that departures of approximately 20% or less result in negligible errors while departures up to 50% produce modest errors of 5%. When I_{max}/I_{min} ratios exceed 1.5 though, the results enter into significant error and thus generate erroneous results (Daegling, 2002b). A cross-section with large J measures is generally interpreted to be more resistant to torsional loads; however this interpretation is most robust when cross-sections are (physically) nearly circular (I_{max}/I_{max} <1.5) (Marelli and Simons, 2014). In the taxa examined here, species averages were less than 1.5 and thus I argue that measures of J and the ways they pattern in the zygomatic arch are reflective of true biological form. In future, it would be prudent to calculate alternative measures of torsional rigidity (K or an "effective J", see Daegling, 2002b) to compare the results of both variables.

5.5.4 *Pairwise comparisons*

The strongest contrasts between taxa occurred in the comparisons between soft consumer *A. geoffroyi* and tough consumer *A. palliata*, followed by soft consumer *P. troglodytes* and tough consumer *G. gorilla.* In both of these pairs, significant differences between I_x, I_y, I_{max}, and J measures were observed. In comparisons of *Ateles/Alouatta*, *Alouatta* consistently possessed higher values for each variable, indicating greater resistance to bending and torsion in all measures. In *Pan/Gorilla* comparisons, *Gorilla* was also possessed higher values, but to a lesser degree than was observed in *Aloutta/Ateles*. This relationship was also observed in soft consumer *M. fasciularis* and

tough consumer *M. fuscata*, *G. gorilla* and *P. pygmaeus* (though these differences were not significant). The strength of these differences, suggests that tough and soft food consumers vary in their ability to resist bending and torsional loads, and that tough consumers on average possess higher resistance potentials. The only comparison that did not follow this pattern was between *P. anubis* and *T. gelada*. Because these comparisons were restricted to anterior measures, it is not surprising that *T. gelada*, despite being a tough food consumer, had relatively lower values for a given cross-sectional measure given its highest values occurred in posterior and not anterior regions. However, when the highest values for bending and torsional resistance in *P. anubis* are compared to the highest values of *T. gelada, T. gelada* is surprisingly found to be absolutely lower given their highly tough diet. This result is likely due to the differences in sample size between these two species. Because of the small size of the *T. gelada* sample, there is limited statistical power for this result. Thus, I am cautious in drawing the conclusion that geladas are consistently lower in cross-sectional geometry measures as compared to baboons. Future comparisons conducted with a larger sample size would better speak to this point. With the exception of the *Papio/Theropithecus* pairing, the results of these comparisons suggest that tough food consumers consistently possess relatively greater bending and torsion resistance potentials as compared to soft consumers further supporting the prediction that the more mechanically challenging nature of a tough diet exerts greater bone response relative to a less challenging diet.

The findings for pairwise comparisons between hard-object consumers and soft consumers are less clear however. Analogous to the predictions for soft and tough consumers, hard-object consumers were expected to exceed soft consumers in each

measure. Comparisons between hard-object consumer *P. pithecia* and soft consumer *P. monachus* found that *P. pithecia* exceeded *P. monachus* in all variables. In contrast, the comparison of *S. apella* and *C. capucinus* revealed no significant differences between the pair, and found soft consumer *C. capucinus* exceeded *S. apella* on average in all measures. The contrasting results from these two pairings make it unclear whether hard-object feeding results in greater measures of bending and resistance. The lack of differences observed in the *Sapajus/Cebus* comparison likely stem from the degree of pre-oral preparation (e.g., smashing nut with a rock) used by *Sapajus* to breach a hard object rather than solely relying on bite force to propogate a crack. Tufted capuchins (*S. apella*) and non-tufted capuchins (*C. capucinus*) are clearly demarcated by their cranial and dental morphology in that tufted or 'robust' capuchins possess clear adaptations (e.g., thickened corpora, larger ascending rami, and shorter mandibles) for a durophageous diet that are absent in 'gracile' capuchins (Bouvier, 1986; Daegling, 1992; Silva, 2001; Wright et al., 2009). Notably, robust capuchins were described as having larger zygomatic arches with greater flare (Bouvier, 1986; G. Jones in Fragaszy et al., 2004a; Fig. 2 in Alfaro et al., 2012) relative to gracile capuchins.

In this study though, relative zygomatic arch flare was very similar in both *C. capucinus* and *S. apella* (BZBR ratios of 0.85 and 0.83 respectively), which is counter to the observations made in previous studies. In addition, under the assumption that *Sapajus* possess relatively more robust zygomatic arches than *C. capucinus*, the expectation is that maximum bending resistance and/or torsional resistance should also exceed that of *C. capucinus*. Contrary to expectation, this study found that *C. capucinus* possessed greater average I_x, I_y, I_{max}, and J measures than *S. apella*. In this regard, gracile capuchin *C.*

capucinus appears to possess zygomatic arches that are better strengthened to withstand loads compared to robust capuchin *S. apella*.

One explanation for this may derive from the diet profiles of these two taxa. *S. apella* consumes hard seeds (up to 16%) on a seasonal basis, as well as varying portions of flowers (11.1%), leaves (6.3%), and even corn (13.9%) when in close proximity to agricultural fields (Galetti and Pedroni, 1994). However, the bulk of the capuchin diet stems from fruit pulp consumption (53.9%) and include a wide spectrum of fruit type ranging from small drupes like *Urera baccifera* to large pods of *Inga spp.* (Galetti and Pedroni, 1994). As noted previously, *Inga* pods contain plant tissues of significant toughness and processing such a food would require significant masticatory force. As a commonly available food in regions where *S.apella* feeds, regular consumption of such a tough food would presumably induce relative high masticatory loads. The apparent increase in cross-sectional geometry in *C. capucinus* may be due to the consumption of some other mechanically challenging foods in spite of the absence of load resisting adaptations in other portions of the cranium.

Chapman and Fedigan (1990) found neighboring groups of *C. capucinus* yielded very different dietary profiles in terms of fruit consumption ranging from 53-81.2% depending on the capuchin group. Without the specific food material properties data for each fruit consumed, it is difficult to compare the mechanical nature of these diets, however, this raises an important point about variance in food range ecology as well as behavioral practices such as food selection based on learned group tradition (Chapman and Fedigan, 1990) rather than strict food availability. It would be interesting to compare food material properties data between these two groups to determine whether *C.*

capucinus consumes plants of similar toughness to *S. apella* and if that may explain the differences in zygomatic arch cross-sectional geometry.

Other primate taxa, such as *Cercocebus torquatus* and *Lophocebus albigena*, consume hard objects, though generally to a lesser degree compared to durophagy specialists. Though categorized as soft consumers based on consumption percent, both taxa consume hard objects as well. Pairwise comparisons between these two species found that *C. torquatus*, whose diet contains up 36% hard objects, consistently possessed greater bending and torsional resistance measures as compared to *L. albigena* (whose hard-object consumption can be up to 29%). These taxa also make a compelling comparison because they are reported to subsist on similar levels of relatively soft, fruits (60% and 59% respectively, see Table 2). Holding this portion of their diet constant, the marked differences in their cross-sectional geometry suggest that hard-object consumption induces greater bone response in the zygomatic arch even if it does not constitute the majority of the primate's diet.

To test this further, intra-dietary pairwise comparisons contrasting tough consumers *Piliocolobus badius* and *Colobus polykomos* revealed that despite the similarity in tough food consumption in these species (47% and 52.2% respectively), *C. polykomos* persisted in possessing greater values for each cross-sectional measure. This result may to due to the relatively greater consumption of hard objects by *C. polykomos* (up to 32.5%) as compared to the lack of hard objects consumed in *P. badius*. Similarly, the pairing between tough consumers *Macaca fuscata* and *Macaca mulatta* found that *M. fuscata* consistently exceeded *M. mulatta* in all cross-sectional variables. The presence of hard-object feeding in *M. fuscata* (up to 13.2%) compared to the lack of hard-object

feeding in *M. mulatta* (and other taxa mentioned previously) suggests that the differences in bending and torsional resistance may stem from the supplementary consumption of hard objects.

While these comparisons are albeit limited, these results suggest that the effects of hard-object consumption may be detectable in cases where primary food type consumption is equivalent, but hard-object consumption varies. Even if the hard objects consumed are done so as a result of a fallback food strategy, this finding suggests that even infrequent bouts of hard-object feeding may be sufficient to induce strengthened zygomatic arches.

5.5.5 *Food material properties (FMPs) and cross-sectional geometry*

On the smaller subsample of study taxa for which published food material properties data were available, PGLS multiple regressions found no relationships between FMPs data, stress-limited and displacement-limited indices, and cross-sectional variables in the zygomatic arch. One of the limiting factors in this particular study was the low sample size for this test group. In addition, both size and phylogenetic relatedness among the taxa are also likely responsible for the non-significant findings. Young's modulus measures have been observed to be inversely correlated with body mass while no relationship occurs between toughness and body mass (Coiner-Collier et al., 2016). In the former, a sampling bias may be responsible given not all foods a primate consumes were measured (Coiner-Collier et al., 2016) and some of the most challenging foods could not be included due to limitation of the mechanical tester (e.g., as described in Vogel et al., 2008; 2014). This species sample may be too constrained, both

phylogenetically and with regard to measures of FMPs, to adequately assess whether any relationships pertaining to load resistance manifest in the zygomatic arch. In addition, the use of weighted measures of toughness (Venkataraman et al., 2014) and Young's modulus may serve as better predictors of diet type in relation to bone morphology because they take both consumption frequency and FMPs measures into account. Given the observed findings in the inter- and intradietary pairwise comparisons in this study as well as the large experimental literature on facial morphology and diet type, it would seem plausible that foods of higher stiffness should compel some form of bone adaptation to resist the higher magnitude forces. However, bending and torsional resistance capabilities along the zygomatic arch may not be as plastic, necessitating that the morphology remain relatively unchaged regardless of the magnitudes of the forces experienced. It may be that smaller-scale changes in bone mineralization (Franks et al., 2016) and/or isotrophy may accomodate differences in FMPs. Without further testing though, these explanations are conjectural at best.

The extent and scale to which FMPs affect bone form has been examined in macaques (e.g., Iwasaki, 1989) but the magnitude to which these relationships exist across primates still remains unclear. The effects of a hard versus soft diet have been tested extensively within the experimental literature though many gaps in our understanding of the functional links among chewing patterns, FMPs, and craniofacial form remain. One of the foundational assumptions concerning diet consistency and masticatory form and function is that infrequent, high-magnitude masticatory force production and low-magnitude, cyclical loading are expected to prompt the same physiological and evolutionarily adaptive responses (Bouvier and Hylander, 1981;

Lanyon and Rubin, 1985; Biewener, 1993). For this reason, tough and hard (stiff) foods are often grouped categorically as "mechanically challenging". One issue pertaining to this assumption is an incomplete understanding of the influence of FMPs on chewing behaviors that likely underlie load-related variation in masticatory morphology (Ravosa et al., 2015), such as the zygomatic arch.

Examinations of the effects of chewing frequency and chewing investment (as they pertain to chewing duration) in relation to FMPs in rabbits determined that elastic modulus measures are the primary influence on chewing investment, and that increases in the rate of force production, rather than increases in chewing duration are related to dietary properties (Ravosa et al., 2015). It is well established that a positive association between bite force magnitudes and food stiffness exists among mammals (e.g., Weijs and De Jongh, 1977; Hylander, 1986; Hylander et al., 1998; Ross et al., 2007; Ravosa et al., 2010; Rafferty et al., 2012), and thus it is reasonable to interpret the robusticity in parts of the masticatory complex, such as the mandible and (potentially) the zygomatic arch, as plastic responses to high-magnitude loading.

Previous studies which mapped principal strain distributions on the zygomatic arches of pigs (Herring et al., 1996; Herring, 2005) and macaques (Iwasaki, 1989), found that the mastication of hard foods (in both adults and juveniles/infants) yielded differences in strain magnitude as well as between the two constituent bones comprising the zygomatic arch; namely the zygomatic and squamosal in pigs, and the zygomatic and temporal bones in primates. Iwasaki (1989) examined the effects of hard versus soft foods on the dynamic nature of the cranium noting that the zygomatic arch bears relatively high strains because it serves as the attachment for the masseter but that the

arch also serves as an important stress dissipater. In this work, Iwasaki described the "buffer effect" in which cranial bones dispersed stresses of muscles on the non-masticatory side as stresses are transmitted from the working side (Iwasaki, 1989). In the study's sample of adult macaques, the balancing side temporal bone, TMJ, and posterior zygomatic arch serve this purpose as each bone individually acts as a stress buffer using elements of the their shape and position on the cranium (Iwasaki, 1989). Furthermore, Iwasaki (1989) argues that these strains are "ingeniously dispersed" (Iwasaki, 1989, page 89) using the nature of the dual bone construction of the zygomatic arch.

The proposed mechanism for this is as follows: the division of the arch into, on the one hand, an anterior zygomatic portion, and on the other hand, a posterior temporal portion changes the nature of strain orientation. Anterior regions exhibit compressive strains in the anteroposterior direction while tensile strains are oriented along the vertical axis. The posterior region is oriented in the exact opposite way in that tensile strains are oriented anteroposteriorly, and compressive strains are oriented vertically (see Table 10 in Iwasaki, 1989). During mastication, the directions of the principal strains did not change in anterior and posterior regions, but there was considerable variation on the non-masticating (balancing) side.

Recall that pigs and macaques have opposite strain spectrums along their zygomatic arches. Herring et al. (2005) noted that infant piglets exhibit twisting and or shearing moments in their squamosal region; the same pattern that is reported for the posterior zygomatic arch in macaques (Iwasaki, 1989; Hylander and Johnson, 1997). Thus, despite their differences, infant pigs and macaques converge on this pattern, suggesting that infant piglets more closely resemble higher order primates like macaques

than adult pigs in this respect (Herring, 2005). These similarities extend to juvenile pigs as well in that tensile strain is directed anteriorly and dorsally as opposed to anteriorly and ventral like in infants (Herring, 2005).

In macaque experiments using soft food, the strain magnitude of the posterior arch on the balancing side exceeded that of the anterior principal strain magnitudes on the balancing side zygomatic arch (see Table 4 in Iwasaki, 1989). In contrast to these results for adult macaques, the results for infant macaques indicate that the magnitude of the balancing side zygomatic arch strains are relatively low compared to adults, and that the parts of the cranium have to work collectively to buffer stress from the working side. There may be a selective advantage to consuming hard foods sooner in order to prime the bones (especially the zygomatic arch) to act as a buffer for masticatory loads. To test this fully, more food materials properties data on the foods regularly consumed by primates are needed. While this is a tall order given the scale and variation of foods in primate diets, straightforward measures of toughness and Young's modulus would provide mechanically relevant and quantifiable data that would bolster work on the craniofacial complex in primates.

5.5.6 *Implications for future work on zygomatic arch morphology*

The basis of this study was centered in an investigation of cross-sectional shape and the mechanical nature of bone resistance to loading. While this region of masticatory complex is receiving increased attention by researchers, much is still unknown about zygomatic arch morphology. Studies on bone biology note that there are multiple osteogenic factors that influence bone remodeling, and that attempts to minimize strain

are not the primary catalysts for bone response (Rubin et al., 2001; Demes, 2007). Among post-cranial studies there is disagreement as to whether bone deposition is driven by strain magnitudes (Ruff et al., 2006) or not (Judex et al., 1997). Yet, in studies of the craniofacial complex, changes in diet and the concomitant increases in masticatory strain do appear to precipitate an adaptive osteogenic response in key masticatory features (Franks et al., 2016). Future questions that would elaborate on these effects would include an account of the ontogenetic changes in bone shape and curvature once a primate is weaned and begins an adult diet. Herring et al. (2005) noted that infant piglet zygomatic arches were relatively rounded in cross-section and straighter than that of adult pigs. This concomitant increase in dorsoventral arch height and decrease in the mediolateral thickness of the squamosal bone indicates that adult individuals adapt to an adult diet during growth. As such, strain patterns are more predictable in adults; once weaned, piglets appear to assume this adult strain pattern following the adoption of a fully adult diet. These results suggest that the pig facial skeleton is not pre-adapted to functional loads but rather its response is contingent on the nature of the loads experienced. At the point of feeding transition (from suckling to adult diet) there is a presumably radical change in the both the magnitude and pattern of masticatory loading. If this model were tested across primates, it would be intriguing to see whether differences in strain patterns and/or bone architecture tracked with the shift to an adult diet.

The question of whether relative zygomatic arch curvature or lateral flare changes in response to muscle maintenance is also unclear. In humans, differences in the curvature of the zygomatic arch have been attributed to age, such that older individuals

experienced changes in bone curvature presumably as a result of masticatory muscle atrophy, and deterioration (Williams and Slice, 2010). Reductions in muscle quality have been found to correlate with age (Williams and Slice, 2010), meaning diminished muscle functionality impacts the mechanical stimulus on the bone by effectively minimizing the process of bone formation and maintenance (Borkan et al., 1983; Porter et al., 1995; Gallagher et al., 1997; Peyron et al., 2004; Rubin et al., 2006; Judex et al., 2007). As primates senesce, does the functional capacity of the masticatory muscles become reduced, and does that then impart changes on the zygomatic arch? In humans, observed masticatory muscle activity is generally partitioned into the energy needed to power the mandible, and the energy needed to overcome the food items being processed (Ottenhoff et al., 1992a,b). Regardless of whether a food item is hard or soft, human masseter muscles have been found to show an increase in excitatory drive in two distinct phases within the chew cycle: one at the beginning, and one at the end (Grigoriadis et al., 2014). These phases appear to correspond to the points when the mandible is adducted and comes into contact with the food items. Unsurprisingly, hard foods generated relatively greater EMG readings than soft foods during these phases. The underlying muscle commands operate such that the early phase loading relies on signals from the muscle spindles to generate enough bite force to fracture the food item while the later excitation phase relies on inputs form both the masseter muscle spindles and periodontal mechanoreceptors (Grigoriadis et al., 2014). If the muscles are comprised however, they may be able to generate an initial response during the first phase but may not be able to recruit adequate power for the latter phase. Thus reduced functionality would presumably lead to decreased muscle performance, lower bite force potentials, and smaller magnitude

masticatory strains overall. While the relative contribution of masticatory muscles in relation to zygomatic arch morphology was not quantified in this study, it would be compelling to conduct a study comparing the relative contribution of different masticatory muscles in relation to arch robusticity to determine if the differences in activation equate to changes in strain patterns and the underlying bone morphology.

Furthermore, an important next step in the analyses presented here would be an investigation into the size adjustments and scaling relationships between zygomatic arch morphology, body size, and masticatory musculature. Because of the variation in primate body sizes it is critical to account for these differences during biomechical analyses to tease out the adaptive mechanical implications of specific morphologies from those that are simply attributable to size.

5.5.7 *Implications for hominin craniofacial adaptation*

As a distinctive feature in African Plio-Plesitocene hominins, particularly in *Paranthropus*, the zygomatic arch persists as a source of insight relating to the adaptive significance of efficient masticatory force dispersion through bone. In recent times, questions related to early hominin diets and dietary adaptation have benefitted from a combination of improved methodological innovations and access to previously unavailable specimens (Strait et al., 2013). At the crux of many questions regarding craniofacial adaption is how do the effects of processing different foods translate to differences in bone morphology and in what ways are those differences experimentally detectable. One of the archetypal debates within paleoanthropology centers on the dietary reconstruction for robust australopiths and whether their derived craniodental features are representative adaptions for consuming hard or tough foods. Recent work

done on the crania and teeth in australopiths (Lucas et al., 2008b; Strait et al., 2009, 2010; Lawn and Lee, 2009; Constantino et al., 2010) determined that specific craniodental traits present in these taxa were adaptations for consuming hard foods (e.g., seeds or nuts). In contrast to this finding, dental texture analyses (Scott et al., 2005; Ungar et al., 2008, 2010) did not detect evidence of hard-object consumption in most australopiths. The robust morphological complexes in *Paranthropus robustus* and *Paranthropus boisei* are hypothesized to serve similar dietary purposes and yet the dental microwear signals indicate the presence of hard-object consumption in *P. robustus*, but not in *P. boisei* despite the similarity in their craniodental features. The results of stable isotope analyses supports the findings for microwear in that *P. robustus* indicates the consumption of C3 plants (which includes most plants the generate nuts) while *P. boisei* has high levels of C4 plants, which are generally highly tough (Cerling et al., 2011). This apparent dietary dichotomization between such morphologically similar taxa continues to fuel debates within paleoanthropology concerning how to most effectively reconstruct diet in the face of so many varying lines of evidence. While the explicit testing of stable isotopes and dental microwear are beyond the purview of this study, this work offers an opportunity to comment on the utility of morphological and biomechanical analyses of the zygomatic arch with respect to the hominin craniofacial form.

While no single line of evidence or method of analysis can fully answer the questions regarding dietary differences in *Paranthropus*, the inclusion of additional information gleaned from the zygomatic arch would bolster our current understanding of these highly derived facial morphologies. Strain and bite force results from FEM models created for OH5 (*P. boisei*) found that the cranium for this individual possessed

considerable mechanical capability for producing relatively high bite forces without inducing distractive forces on the working side TMJ (Smith et al., 2014). The robust facial skeleton and chewing muscles possessed by OH5 suggest that the consumption of mechanically resistant foods requiring highly repetitive feeding loads (Van der Merwe et al., 2008) must have been primary components of the diet in order to maintain such high levels of bone mass. While tough foods have been proposed as the most likely candidate food given the presence of C4 rather than C3 stable isotope signals, the fact that OH5 possesses relatively blunt occlusal morphology, rather than teeth with increased shearing ability, does not seem probable (Strait et al., 2013). In the case of *P. boisei*, the consumption of hard foods (as well as the relative hardness/stiffness of a food overall) exercises greater selective importance in terms of masticatory features and their ability to process such a diet. Thus, the evolution of the feeding apparatus of *P. boisei*, as well as other hominins, may stem from the consumption of hard objects, regardless of how frequently they are consumed. If this is the case, then microwear analyses, which capture dietary signals only in the last weeks, may fail to detect hard-object feeding that falls outside that timeframe. Thus, I propose that the application of a comprehensive comparison of the cross-sectional geometry of *P. boisei* compared to other robust australopiths would potentially reveal new understanding concerning the nature of their diet.

Paleoanthropologists generally agree that *P. robustus* subsisted on the consumption of hard objects (e.g., Grine and Kay, 1988; Teaford and Ungar, 2000; Ungar et al., 2008; Strait et al., 2013) for at least part of the time as they may have served as critical fallback foods during periods where preferred foods were less plentiful (Scott et

al., 2005). If the robust functional morphology observed in both *P. boisei* and *P. robustus* are indicative of at least partial consumption of hard objects during life, there are two potential scenarios to explain this: First, similar selection pressures for the consumption of hard objects caused both taxa to evolve convergently, or alternatively the robust morphology in both taxa evolved at the base of the *Paranthropus* clade and represents an adaptation for consuming hard objects (Smith et al., 2014). If instead the robust morphology of *P. boisei* is an adaption for consuming tough foods, then *P. robustus* and *P. boisei* independently converged on a similar morphological set of traits as a response to feeding on different diets (Strait et al., 2013; Smith et al., 2014). It is difficult to disentangle this scenario without the (obvious) benefit of truly observing what foods these taxa selected; however the lack of known examples of this in living primates makes it difficult to test this phenomenon (Smith et al., 2014).

While this study does not argue that zygomatic arch morphology, or any single morphological feature for that matter, can diagnose the diet of a species, the dietary insight the zygomatic arch provides in terms of cross-sectional geometry may lend credence to one of the evolutionary scenarios posed above. Within the intra-dietary comparisons performed on extant primates in this study, the consumption of hard objects appears to catalyze a relative increase in bending and torsional resistance in the zygomatic arch to offset the higher loading conditions that accompany this food type. It would be intriguing to compare *P. boisei* and *P. robustus* in this regard to determine whether significant differences in bending and/ or torsional resistance exist between their zygomatic arches. If the zygomatic arch strain pattern observed in extant primates is a suitable proxy for the strain pattern that existed in robust australopiths, then we can

surmise that anterior measures of the zygomatic arch would presumably be greater than posterior portions, reflecting a shared pattern of strain dispersion in living and fossil taxa. Comparative studies on mandibular cross-sectional geometry of *Australopithecus*, *Paranthropus*, and living hominoids revealed fundamental shape differences that confer greater strength in resisting torsional and bending loads in fossil taxa than in living taxa (Daegling, 1989, 1990). In these studies, Daegling surmised that the qualitative differences in mandibular form and robusticity are ostensibly due to qualitative differences in diet. It is plausible perhaps, that similar relationships exist with regard to the zygomatic arch, because it is functionally connected to the mandible via the masseter, and bears relatively high masticatory strains.

To my knowledge, no comprehensive comparisons of zygomatic arch cross-sectional morphology in hominins exists, despite the numerous studies that have identified the zygomatic arch as a key masticatory feature. Furthermore, the zygomatic arch provides a 'fresh' feature upon which to test hypotheses about dietary loading and masticatory muscle recruitment. While such studies on fossil zygomatic arches would be constrained due to issues concerning the relative preservation of the zygomatic arch in fossil crania, the potential insight such a comparison would afford our current understanding of fossil hominin diets would be undeniably valuable.

5.6 Conclusions

This study found support for the hypothesis that highest measures of bending (I_{max}) and torsional (J) resistance appear in anterior sections as compared to posterior sections in accordance with experimentally determined strain patterns along the

zygomatic arch. With respect to differential loading in relation to specific diet types, this study found that on average, tough consumers exhibited the greatest average I_{max} and J values, followed by soft consumers, hard-object consumers, and finally by exudate consumers. The relative degree of lateral flare of the zygomatic arch was also predicted to dictate the angle of the masseter to be either more angled (inducing greater torsional loads), or more vertical (inducing greater bending loads). In general, this study found that the degree of arch flare did not predict the resulting arch cross-sectional shape. In the study sample overall, arch cross-sections were primarily elliptical in shape rather than round, indicating parasagittal bending is the dominant load type. Unlike direct measures of load resistance (I_{max}, I_x, J) an index of cross-sectional shape (I_{max}/I_{min}) is not as predicable along the zygomatic arch. It is probable that the influences on cross-sectional shape are more variable and may be tied to the effects of soft tissue (e.g., aponeurosis, masseter activation patterns and attachment sites).

Within the fossil record, zygomatic arches are continually upheld as key evidence of dietary specialization (particularly in cases of mechanically challenging diets), however the dearth of information available on bone morphology, mechanical resistance, and whether patterning is related to diet in the zygomatic arch leaves researchers without the necessary evidence from which to draw conclusions. This project bridges that gap by conducting a comprehensive, comparative study using living primates in accordance with two different dietary data sets to test hypotheses centered on masticatory loading in relation to diet type. Of the diet schemes employed here, the utilization of FMPs rather than traditional dietary categories may be more appropriate when testing biomechanically based questions because these measures are more objectively quantifiable. The finding

that measures of Young's modulus and toughness were not significantly correlated with bone cross-sectional variables but that consumption of hard foods may result in differential load resisitance potentials raises the question of how to generate better estimates of diet moving forward. This work provides evidence that supports the presence of the zygomatic arch strain gradient and cites key functional aspects of bone cross-sectional form which will inform current and future work conducted with FEM and other visualization techniques.

At the crux of understanding the biomechanics of the zygomatic arch, and the continuation of its study, is the formulation of a model that is applicable across taxa. The dilemma encountered by many studying the arch is that in a comparative context, no single model has yet explained the variation in its morphology. Because morphological variation, particularly in this region, appears so diverse, the possibility looms that a single biomechanical model may not adequately characterize the observed variation with the desired accuracy (Daegling, 2002b). It is also important to note that the morphology alone only shows the amount and distribution of bone material present to resist a load across varying locations but does not show what the load types experienced are or to what magnitude they occue. Thus, *in vivo* data are a critical complement to morphological studies for understanding precisely what load types are present.

The morphology and development of the primate zygoma and zygomatic arch are becoming burgeoning fields of research with the potential to provide previously untapped insight into primate feeding adaption in the skull. Studies on the biomechanics of the zygomatic arch are critical components of the masticatory system and possess insight to make compelling observations about the nature feeding, masticatory forces, and bone

adaptation. With the addition of *in vivo* data, food material properties and high-resolution ecological data, morphologists can conduct comprehensive studies on the craniofacial complex and draw more informed conclusions about the interface of diet and bone morphology within an evolutionary context.

CHAPTER 6: CONCLUSIONS

The goal of the current study was to assess the morphological variation concerning the internal architecture and cross-sectional shape of the arch in conjunction with the experimentally obtained strain values measured in previous studies. Furthermore, this study also quantified the complexity of the zygomaticotemporal suture to determine whether differences in dietary loading are detectable in sutural complexity and to examine the mechanical relevance of the suture to the zygomatic arch. In addition to the comparative, qualitative analyses concerning bone morphology and mechanical behavior, this study examined the relationship between arch morphology and dietary type to determine whether different diet types, and therefore different dietary loading scenarios, influence arch morphology. To assess these relationships between zygomatic arch morphology and diet, it was necessary to procure data on arch morphology from individuals that could then be compared at a variety of scales including intraspecifically, interspecifically, and by diet type. In order to access the internal bone morphology and cross-sectional shape of the arch, and to obtain the greatest image resolution, μCT scans were used to generate three-dimensional skull models, which were an integral part of the data collection for this study. The arch cross-sectional images captured and analyzed in this study represent the largest and most taxonomically diverse examination of primate zygomatic arch morphology currently available.

In Chapter 3, cortical area (CA) distributions were compared across arch regions to determine whether the largest concentrations of cortical area occurred in anterior regions as compared to posterior regions. Bone remodeling, which maintains cortical bone structure and properties, is altered by mechanical stimuli (Ascenzi, 1988, Burr et al.,

1989b; Dechow et al., 2010) and thus the expectation is that differential masticatory loading results in varying amounts of cortical bone in the zygomatic arch. Across the entire sample, cortical area measures appear to track with known strain magnitudes.

When dietary groups were compared, tough consumers in general possessed relatively uniform amounts of cortical bone area throughout the arch as compared to other dietary groups. The highest absolute measures of cortical bone appeared anteriorly in all taxa with the exception of *G. gorilla*, whose highest values occurred in posterior regions. In contrast, soft consumers possessed significantly different cortical bone distributions primarily in anterior versus midsuture and anterior versus posterior suture and posterior arch sections. These findings support the hypothesis that cortical area tracks with portions of the arch subjected to the highest masticatory strains in soft consumers, and while the relationships across tough consumers were not statistically significant, the pattern of absolute cortical bone measures does adhere to the expected pattern with the exception of gorillas.

However, the trends in hard-object consumers are not as clear. For instance, hard-object consumer *Sapajus apella* possessed significant differences in all anterior comparisons indicating that the amount of cortical bone varies throughout arch regions and thus aligns with the patterns observed in soft consumers. Given that that *S. apella* supplements its diet with varying amounts of fruit, which can reach levels of up to 82.5% of the diet (Teborgh, 1983), it is not surprising that their cortical bone distributions fall within the pattern observed in other frugivorous primates. In contrast, *Pithecia pithecia*, a hard-object specialist, was found to have no significant differences in cortical bone distributions across arch regions, which is more similar to the patterning found in tough

food consumers. Compared to *S. apella*, *P. pithecia* consumes relatively more hard seeds (up to ~60%, Kinzey and Norconk, 1993) and slightly more leaves than *S. apella,* which may account for their biomechanical affinity with tough consumers. Exudate consumer *Callithrix jacchus* was found to have significant differences in anterior and anterior suture comparisons but not between any other regions along the arch. The absolutely highest measures of cortical bone appear in anterior regions of this diet group as well. Taken together, these results suggest that the majority of primate taxa possess cortical area concentrations that track with the portions of the arch subjected to the highest masticatory strains. Importantly, the differences in the deployment of cortical bone suggests that loading in this region is sufficient to elicit bone remodeling and maintenance events throughout the life of the individual. In addition, the presence of significant differences in the intermediate areas (anterior suture and posterior suture measures) between the traditional arch measurement locations (anterior, midsuture, and posterior measures) suggests that strain variation is mutable in adjacent regions, and that the strain gradient that exists along zygomatic arch may be more complex that previously thought. If cortical bone geometry is sensitive to load history (Daegling and Hotzman, 2003), then the consistent presence of relatively higher cortical bone distributions in anterior versus posterior arch sections may serve as evidence that zygomatic arch loading patterns are conservative across, at the very least, haplorhines.

Comparisons of cortical area to total area ratios (CA/TA) across arch regions were also performed to determine whether anterior regions possessed a relatively greater proportion of cortical bone compared to other arch regions. If CA distributions are absolutely greatest anteriorly, then the expectation is that these distributions should also

be relatively greater with respect to total arch area in anterior sections as well. In the majority of the study taxa this hypothesis was supported; CA/TA ratios were generally highest anteriorly and decreased posteriorly across dietary groups. However, several taxa did not follow this model. For instance, both hard-object consumer *S. apella* and soft consumer *Cebus capucinus* yielded their highest CA/TA ratios in posterior portions as compared to anterior portions despite possessing their absolutely largest cortical area measures in anterior regions. The reasons for this trend are not immediately clear, however there are several potential explanations. Jaw kinematics in relation to FMPs in *Cebus* observed a regularized gape cycle but a temporal and spatial variability within the phases of a gape cycle (Reed and Ross, 2010). Primates are known to exhibit higher variance in the durations of the constituent phases that compose a gape cycle, than in overall chewing duration as a whole (Reed and Ross, 2010). In the case of capuchins, the adaptions for a generalized diet and hard-object consumption may make the feeding sequence durations less sensitive to changes in FMPs (Wright, 2005) and consequently may not translate to differences in cortical area amounts. Exploring these relationships further would provide greater resolution to these findings.

Section moduli measures (Z_x and Z_y) quantify the bending tendency of a cross-section about both the transverse and sagittal planes. In every species included in this study, the highest measures of Z_x (strength about the transverse axis) occurred in anterior sections. This result suggests that measures of cross-sectional strength occur in anterior arch regions relatively more consistently than do the highest concentrations of cortical bone area. In other words, the relatively large amounts of cortical bone do not necessarily correspond to regions with the largest bone strength measures. This result is supported

by the recent work by Franks et al. (2016) which found that biomineralization levels, rather than cortical distributions, were more responsive to masticatory loads on the zygomatic arch in pigs and rabbits. While cortical bone distributions and section moduli measures appear to correspond in most cases, the assumption that cortical bone always accumulates in the areas of greatest loading may not always be true across all taxa.

The measures of axial strength about the superoinferior axis, Z_y, were greatest anteriorly in all species except *G. gorilla*, whose largest value appeared posteriorly and thus corresponded to the portions with the highest cortical bone. In cross-section, gorillas appear to have very tall and narrow arches well suited to the resistance of parasagittal loading. The finding that their highest cortical values and Z_y measures occur posteriorly is presumably due to higher loading experienced posteriorly as compared to anteriorly. Thus, the increased strength about the superoinferior axis coupled with the cortical bone distributions in posterior regions suggests significant parasagittal loading is experienced in that region. Strength measures about the transverse axis in this species are highest anteriorly and thus follow the predicted pattern. Across the species sample as a whole, areas of the highest cortical area and those with the highest measures of strength appear to correspond, suggesting that both bone internal architecture and relative strength are reliably connected. In instances when section moduli measures are highest in different arch sections, the suggestion is that the overall cross-sectional shape requires increased strength about one axis (either in the coronal or transverse plane), rather than both. This occurred primarily in taxa with relatively more exaggerated cross-sectional shapes.

Pairwise comparisons conducted on closely related taxa of different diets determined that cortical area and section moduli measures varied between taxa in anterior

sections and that the relationships by in large were significant. Interestingly, comparisons between hard-object consumer *S. apella* and tough consumers *P. badius* and *A. caraya* were also significant indicating that differences between mechanically resistant diets are also potentially detectable. Often, the terms "hard" and "tough" are subsumed under the single term of "mechanically challenging". However, the results of this study suggest that important differences between tough and hard-object consumption exist and should be considered separately to provide greater resolution to questions of dietary loading and bone response in primates. This is particularly relevant to comparisons between *P. boisei* and *P. robustus* as the debate concerning their dietary strategies (i.e., hard-object feeding versus tough food consumption) remains contentious within paleoanthropology. In sum, this study provides provisional support for the hypothesis that masticatory induced bone loading produces a large strain gradient from anterior to posterior along the zygomatic arch and that local variation in cortical bone mass and strength measures are associated with these gradients.

Chapter 4 investigated zygomaticotemporal sutural complexity, and tested the predictions that (1) sutural complexity is relatively increased in taxa consuming tough and/or hard diets and (2) that primates with diets consisting of high toughness (*R)* or high Young's modulus (*E*) possess more complex sutures compared to taxa with lower values of toughness and Young's modulus. The influence of differential dietary loading has been observed in other species of *Cebus* and *Sapajus* primates in which increased sagittal sutural complexity occurred in *S. apella*, a hard-object consumer, compared to other closely related species of *Cebus* that did not routinely consume hard objects (Byron, 2009). Reduced Major Axis (RMA) regressions of skull size with zygomatic arch size

found a significant, positively allometric relationship indicating zygomatic archs are relatively larger than would be expected under an isometric relationship. One means of explaining this could include the need for more robust arches in order to support relatively larger masticatory muscles. It is known that masticatory muscle size is relatively isometric in relation to body size in primates (Cachel, 1984), however it is currently unknown how masseter muscle size scales with zygomatic arch size in primates. In canids, masticatory muscles also scale isometrically, but endocranial volume is found to scale with negative allometry. In these taxa, masseter muscle size has been found to scale isometrically with zygomatic arch width (Penrose et al., 2016), and primate zygomatic arches may scale to masticatory muscles in a similar way.

Within canid taxa, skull shape changes in the zygomatic arch (namely the relatively wide arches and large sagittal crests) found in species with greater body masses allows the skull to accommodate the relative enlargement of the jaw adductors compared with the endocranium. Interestingly, primates have been shown to have isometrically scaling masticatory muscles (Cachel, 1984), as well as negatively scaling endocrania (Rilling, 2006). In addition, large-bodied primates also possess sagittal crests (Ankel-Simons, 2007) and relatively wide zygomatic arches (Frost et al., 2003). This suggests that the need for muscle accommodation is more universal than previously thought (Penrose et al., 2016) and is an arrangement shared among, at the very least, primates and canids.

Ordinary Least Squares (OLS) regression results for skull size and sutural complexity measures found a positive relationship, indicating that individuals with relatively larger skulls have more complex sutures. This result does not indicate that skull

size accounts for the majority of the variation observed in sutural complexity across the study taxa. The same result was also found in comparisons of sutural complexity and zygomatic arch size. In addition, associated measures of lacunarity and prefactor lacunarity (heterogeneity and overall fractal texture) do not appear to have any relationship to skull size. Suture length was correlated with both skull and arch size, but the relationships were relatively weak, indicating that size does not explain the majority of the variation with respect to relative length.

In the context of the dietary groupings used in this study, neither total consumption percent categories nor food material properties (FMPs) data are good predictors for sutural complexity in these species of primates. The hypothesis that increased sutural complexity would occur in taxa with more resistant diets was supported in that taxa that primarily consumed hard or tough foods on average possessed relatively greater complexity values. However, these findings were not statistically significant and the findings that both size and dietary category are not good predictors for complexity suggests other factors are responsible for the amount of variation observed. Within dietary groups both tough and soft consumers possessed differences among taxa in each respective group, indicating high variance in sutural values. These results contrast with the relatively low variance observed in exudate and hard consumers. The differences in the variance found in tough and soft consumers is likely attributable to the relatively larger sample sizes available compared to those for hard and exudate consumption. In other words, the high variance found in soft and tough consumers may result from the fact that more primate taxa fall into those categories than into hard or exudate consumers, which had much fewer taxa. In addition, the taxonomic breadth found in the tough and

soft consumption groups is greater than that observed in exudate or hard-object consumption groups. Because of this, the variation in complexity within groups may be due to differences in sampling.

When raw complexity values alone are compared across dietary groups, hard-object consumers generally possessed the highest complexity values compared to all dietary groups despite the fact that hard-object feeders included fewer individuals than tough or soft consumers. According to the Byron (2009) study, the sutural complexity measures in the sagittal sutures were significantly different between *C. capucinus* and *S. apella*, in which *S. apella* had relatively greater sutural values in this region. In the current study, the same comparison was conducted comparing zygomaticotemporal sutural complexity finding that *S. apella* had only slightly greater complexity values than *C. capucinus*, but these results were not significant. If hard-object feeding indeed induces relatively greater sutural complexity then the expectation for all pairwise comparisons would be that hard-object consumers would consistently possess relatively greater complexity values. With the exception of the *Sapajus*/*Cebus* comparison, no other closely related taxa pairs yielded higher complexity measures in the taxon that consumed hard objects. In all pairwise comparisons, no significant differences were found except in the comparison of soft consumer *P. anubis* and tough consumer *T. gelada*. Surprisingly, complexity values were greater in *P. anubis* than in *T. gelada* despite the fact that geladas are specialized gramnivores with highly tough diets (Venkataraman et al., 2014). There are several potential explanations for these findings. First, the zygomaticotemporal suture's relative interdigitation may be highly constrained because it must maintain some safety factor that guard against bone failure given the region is habitually bombarded by

high masticatory strains. In addition, the surface area of the connection between the zygomatic and temporal bones is relatively small compared to the relatively long cranial sutures that traverse along the skull. Secondly, there may not be sufficient differences in masticatory loading to in induce greater sutural complexity in mechanically challenging diets as compared to those that are less mechanically challenging. Like the sutural complexity in the midpalatal sutures of *P. badius* and *C. polykomos*, there may be no dietary differentiation because the transfer of strains to the sutures may be hampered by the presence of other bone structures (Daegling and Hotzman, 2004). The more mechanically meaningful aspect of sutural morphology on the zygomatic arch may relate to the degree of overlap of the sutures as a means of strengthening the sutural joint rather than just measures of interdigitation alone. Thus, future work investigating this further is necessary.

In Chapter 5 cross-sectional geometric variables relating to maximum and minimum bending resistance, torsion, and cross-sectional shape were quantified and compared to determine whether different diet types elicited unique bone responses. Typical investigations of bone cross-sectional geometry have applied measures of bone mechanical behavior to long bones (e.g., Ruff and Hayes, 1983; Ruff et al., 1984; Ruff, 2000; Patel et al., 2013) and the mandible (e.g., Daegling, 1989; 1990; 1992; 1993; 2002) in primates to deduce the effects of form on function. This study applied similar methodologies to investigate mechanical resistance and bone form in the zygomatic arch by conducting comparisons on a taxonomically broad primate sample.

Cross-sectional shape measures of I_{max}/I_{min} varied throughout the zygomatic arch in all primates, with the majority of sections indicating the presence of an elliptically-

shaped section suited to resisting high parasagittal bending loads. Comparisons of arch shape by region generally found no significant differences in cross-sectional form along the arch, which indicates that significant shape change is not present even if significant differences in strain exist. Significant variation was found within tough and soft consumer dietary groups, likely as a result of the greater species abundance included in these categories as compared to the hard-object consumer or exudate groups. Overall, these results do not suggest I_{max}/I_{min} ratios adhere to any predictable patterns within this sample of primates.

To further examine cross-sectional shape, bi-zygomatic to bi-ramus width ratios (BZBR) were calculated as proxies for the relative degree of zygomatic arch flare and to approximate the angle of the masseter to estimate whether parasagittal bending (vertical masseter) or torsion (angled masseter) concurred with the observed I_{max}/I_{min} values obtained. Taxa with BZBR ratios indicating highly elliptical arches were found to have elliptically shaped cross-sections, but not to a greater degree than other taxa. The taxa with the highest I_{max}/I_{min} ratios did not possess BZBR ratios indicating highly elliptical cross-sections. The same was also true for measures of how circular arch sections were in relation to I_{max}/I_{min} ratios. These results indicate that BZBR ratios do not predict cross-sectional shape when used in conjunction with I_{max}/I_{min} ratios. The utility of cross-sectional indices may be restricted in the zygomatic as compared to the postcrania because the nature of loading is markedly different in each region. For instance, masticatory loading and locomotor loading have different force magnitudes and directions, and the loading episodes themselves differ in intensity and duration. In addition the orientation of the bones and muscles relative to the direction of gravity, the

muscle force, and load differs in these two regions as well, which affects how the results can be interpreted biologically.

Cross-sectional variables quantifying bending resistance about the x- and y- axes (I_x, I_y), as well as maximum and minimum bending resistance (I_{max}, I_{min}), and torsional resistance (J) were compared intraspecifically, interspecifically, and by diet group with the expectation that these measures would reflect the same gradient observed via experimentally obtained strain values. In 37 of the 43 species examined, this hypothesis was supported; leaving six species that did not. Two of these six taxa (*M. sylvanus, C. albinasus*) had low sample sizes and extensive statistical comparisons were therefore not possible; thus, some caution in the conclusion that they do not follow the expected morphological patterning is warranted. Future work with larger samples is necessary to confirm this pattern in these species. The remaining four taxa (*T. gelada, M. leuchophaeus, P. pithecia, P. monachus*) possess unique craniodental and craniofacial architectural features that may account for their divergence from the expected pattern. For instance, both *T. gelada* and *M. leuchophaeus* possess relatively prognathaic facial skeletons with the capacity to exercise large gapes while both *P. pithecia* and *P. monachus* are specialized hard-object consumers.

Comparisons between dietary groups found significant differences between tough and exudate consumers for all variables, which are likely attributable to differences in size. Significant variability within dietary groups was also observed, though no single taxon appeared to drive the differences in any particular group. Instead there appears to be substantial variation for each cross-sectional variable regardless of dietary category. Intraspecific comparisons reveal that there are significant changes in bending and

torsional resistance throughout the arch. In particular, closely adjacent areas were frequently and significantly different in this regard, citing that increased capacities to resist loading are not relegated to only the anterior-most or posterior-most portions of the arch. By combining intermediate arch locations with the primary locations measured by Hylander and Johnson (1997), this study was able to determine that loading along the arch is more complex and varied than originally thought.

Finally, FMPs and indices of stress-limited and displacement-limited foods were compared with cross-sectional variables to determine whether a relationship was present. The results found no predictive value in these FMPs measures with regard to arch form, however the small sample size and effect of phylogeny clearly impacted these results. Confounding these findings are the observations that closely related taxa that consume different diets were found to have significant differences in mechanical resistance. Furthermore, intra-dietary pairwise comparisons found taxa that consume relatively more hard objects generally had greater measures of load resistance. While these results were not all significant, they allude to a pattern that may exist in relation to hard-object consumption. Two potential alternative hypotheses to address this further could include: 1) hard-object consumption elicits greater bending and torsional differences in the zygomatic arch or 2) presumed dietary differences among haplorhine primates are not accompanied by important differences in masticatory loads given the dietary breadth found across primates in general. While the findings for this study did not support the prediction that FMPs measures correlate with bone mechanical resistance in the arch, there is a wide comparative literature where bone response to differential dietary loading

has been demonstrated. Thus, more work with a larger and more phylogenetically restricted sample is necessary to probe these research questions more fully.

Taken together, the results obtained on the internal bone architecture, external shape, and sutural complexity indicate that the zygomatic arch is a dynamic and complex portion of the craniofacial complex. The relationship between masticatory loading and bone response observed in this study has important implications for understanding how masticatory strain in distributed and resisted in the zygomatic arch. The observable variation in its morphology, both in living and extinct taxa, and its consistent role as a bearer of high masticatory strain make it a critical area for continued study, particularly in terms of dietary adaptation in primates.

REFERENCES

Adams, L.A. (1918). "A memoir on the phylogeny of the jaw muscles in recent and fossil vertebrates." *Annals of the New York Academy of Sciences,* 28:51-166.

Agestsuma, N., & Nakagwa, N. (1998). "Effects of habitat differences on feeding behaviors of Japanese monkeys: comparison between Yakushima and Kinkazan." *Primates*, 39:275-289.

Agrawal, K.R., Lucas, P.W., Prinz, J.F., & Bruce, I.C. (1998). "Mechanical properties of foods responsible for resisting food breakdown in the human mouth." *Archives of Oral Biology,* 42: 1–9.

Alaqeel, S. M., Hinton, R. J., & Opperman, L.A. (2006). "Cellular response to force application at craniofacial sutures." *Orthodontic and Craniofacial Research,* 9: 111–122.

Alfaro, J. W. L., Silva, J. de S. E., & Rylands, A. B. (2012). "How Different Are Robust and Gracile Capuchin Monkeys? An Argument for the Use of Sapajus and Cebus." *American Journal of Primatology*, 74(4): 273–286.

Anapol, F., & Barry, K. (1996). "Fiber architecture of the extensors of the hindlimb in semiterestrail and arboreal guenons." *American Journal of Physical Anthropology,* 99:429-447.

Anapol, F., & Lee, S. (1994). "Morphological adaptation to diet in platyrrhine primates." *American Journal of Physical Anthropology,* 94: 239-261.

Anapol, F., Shahnoor, N., & Ross, C.F. (2008). "Scaling of reduced physiologic cross-sectional area in primate muscles of mastication." In: Vinyard CJ, Ravosa MJ, Wall CE, editors. *Primate craniofacial function and biology*. New York: Springer. p 201– 215.

Ankel-Simons F. (2007). "Skull." In: *Primate anatomy*: an introduction. Third ed. London: Elsevier, p161–197.

Antón, S.C. (1994). "Mechanical and other perspectives on Neandertal craniofacial morphology." In (R. S. Corruccini & R. L. Ciochion, Eds) *Integrative Paths to the Past: Paleoanthropological Advances in Honor of F. Clark Howell*, pp. 677–695. Englewood Cliffs, NJ: Prentice Hall.

Antón, S.C. (1999). "Macaque masseter muscle: internal architecture, fiber length, and cross- sectional area." *International Journal of Primatology,* 20:441-462.

Antón, S.C. (2009). "Framing the question: diet and evolution in early *Homo*." In: Vinyard CJ, Ravosa MJ, Wall CE, editors. *Primate craniofacial function and biology. Developments in primatology series.* New York: Springer, p 443-482.

Aoki, K., Mitsutsuka, S., Yamazaki, A., Nagai, K., Tezuka, A., & Tsuji, Y. (2015). "Effects of seasonal changes in dietary energy on body weight of captive Japanese macaques (Macaca fuscata)." *Zoo Biology*, 34: 255–261.

Arnold, C., Matthews, L.J., & Nunn, C.L., (2010). "The 10kTrees website: A new online resource for primate phylogeny." *Evolutionary Anthropology*, 19: 114-118.

Ascenzi, A. (1988). "The micromechanics versus the macromechanics of cortical bone—a comprehensive presentation." *Journal of Biomechanics and Engineering*, 110:357–363.

Ayres, J.M. (1981). "Observacoes sobre a ecologica e o comparmento dos cuxius (*Chiropotes albinasus*, *Chiropotes satanas*, *Cebidae*: Primates)." Fundacao Universidade do Amazonas, Manuas, Brazil.

Ayres, J.M. (1989). "Comparative feeding ecology of the ukari and bearded saki, Cacajao and Chiropotes." *Journal of Human Evolution*, 18:697-716.

Bakke, M., & Michler, L. (1991). "Temporalis and masseter muscle activity in patients with anterior open bite and craniomandibular disorder." *Scandanavian Journal of Dental Research,* 99:219-228.

Balter, V., Braa, J., Telouk, P., & Thackery, J.F. (2012). "Evidence for dietary change but not landscape use in South African early hominins." *Nature,* 489: 558-560.

Barnett, A. A., Boyle, S. A., Pinto, L. P., Lourenço, W. C., Almedia, T., Sousa Silva, W., Ronchi-Teles, B., Ross, C., MacLarnon, A., & Spironello W. R. (2012). "Primary seed dispersal by three Neotropical seed-predating primates (*Cacajao melanocephalus oukary*, *Chiropotes chiropotes* and *Chiropotes albinasus*)." *Journal of Tropical Ecology,* 28:543-555.

Bartlett, T.Q. (1999). "Feeding and ranging behavior of the white-handed gibbon (Hylobates lar) in Khao Yai National Parl, Thailand." [*PhD diss.*]. Washington University, St. Louis.

Barton, R.A., Whiten, A., Byrne, R.W., & English, M. (1993). "Chemical composition of baboon plant foods: implications for the interpretation of intra-interspecific differences in diet." *Folia Primatologica*, 61:1-20.

Beecher, R.M., & Corruccini, R.S. (1981). "Effects of dietary consistency on craniofacial and occlusal development in the rat." *Angle Orthodontist,* 51:61–69.

Beecher, R.M., Corruccini, R.S., & Freeman, M. (1983). "Craniofacial correlates of dietary consistency in a nonhuman primate." *Journal Craniofacial Genetics and Developmental Biology*, 3: 193–202.

Behrents, R. G., Carlson, D. S., & Abdelnour, T. (1978). "In vivo analysis of bone strain about the sagittal suture in Macaca mulatta during masticatory movements." *Journal of Dental Research,* 57:904–908.

Bennett, E.L. & Sebastian, A.C. (1988). "Social organization and ecology of proboscis monkeys (*Nasalis larvatus*) in mixed coastal forest in Sarawak." *International Journal of Primatology,* 9: 233-255

Benninghoff, A. (1925). "Spaltlinien am Knochen, Eine Methode zur Ermttlung der Architektur platter Knochen." *Anatomischer Anzeiger,* 60: 189-206.

Bicca-Marques, J.C. (1993). "Padrao de ativades diarias do bugio-preto Alouatta caraya (Primates: Cebidae): uma analise temporal e bioenergetica." *Primatology Brasil,* 4:35-49.

Biegert, J. (1963). "The evaluation of characteristics of the skull, hands, and feet for primate taxonomy." In: Washburn SL, editor. *Classification and human evolution*, New York: Wenner-Gren Foundation for Anthropological Research, p 116–145.

Biewener, A. A. (1993). "Safety factors in bone strength." *Calcified Tissue International*, 53:568–574.

Bluntschli, H. (1926). "Ruckwirkung des Kieferapparates auf den Gesamtschadel. *Z." Zahnarztl Orthodpädie*, 18: 57-79.

Boesch, C., and Boesch, H. (1982). "Optimization of nut-cracking with natural hammers by wild chimpanzees." *Behaviour,* 83: 265-286

Boonratana R. (1994). "The ecology and behavior of the proboscis monkey (Nasalis larvatus) in the Lower Kinabatangan, Sabah." [*PhD diss.*]. Mahidol University, Bangkok.

Borkan, G., Hults, D., Gerzof, D., Robbins, A., & Silbert, C. (1983). "Age changes in body composition revealed by computed tomography." *The Journals of Gerontology. Series A, Biological Sciences and Medical Sciences,* 38:673–677.

Boubli, J. P. (1999). "Feeding ecology of black-headed uacaris (*Cacajao melanocephalus melanocephalus*) in Pico da Neblina National Park, Brazil." *International Journal of Primatology,* 20:719–749.

Bouvier, M. (1986). "Biomechanical scaling of mandibular dimensions in New World monkeys." *International Journal of Primatology,* 7:551– 567.

Bouvier, M., & Hylander, W.L. (1981). "Effect of bone strain on cortical bone structure in macaques (*Macaca mulatta*)." *Journal of Morpholology*, 167:1–12.

Bouvier, M., & Hylander, W.L. (1982). "The effect of dietary consistency on morphology of the mandibular condylar cartilage in young macaques (*Macaca mulatta*)." In: Dixon AD, and Sarnat BG, editors. *Factors and Mechanisms Influencing Bone Growth.* New York: Alan R. Liss, Inc, p 569-579.

Bouvier, M., & Hylander, W.L. (1984). "The effect of dietary consistency on gross histologic morphology in the craniofacial region of young rats." *American Journal of Physical Anthropology,* 170:117-126.

Bouvier, M., & Hylander, W.L. (1996). "Strain gradients, age, and levels of modeling and remodeling in the facial bones of *Macaca fascicularis*." In: Davidovitch Z, and Norton LA, editors. Boston: Harvard Society for the Advancement of Orthodontics, p 407-412.

Bouvier, M., & Tsang, S.M. (1990). "Comparison of muscle mass and force ratios in New and Old World monkeys." *American Journal of Physical Anthropology,* 69:474-482.

Bouxsein, M. L., Boyd, S. K., Christiansen, B. A., Guldberg, R. E., Jepsen, K. J., & Müller, R. (2010). "Guidelines for assessment of bone microstructure in rodents using micro-computed tomography." *Journal of Bone and Mineral Research*, *25*:1468–1486.

Bright J.A., & Gröning, F. (2011). "Strain accommodation in the zygomatic arch of the pig: A validation study using digital speckle pattern interferometry and finite element analysis." *Journal of Morphology,* 272:1388-1398.

Broom, R., & Schepers, G.W.H. (1946). "The South African fossil ape man, the Australopithecinae." *Transvaal museum Memoir No.2*, Pretoria.

Broom, R., Robinson, R.J.T., & Schepers, G.W.H. (1950). "Sterkfontein ape-man Plesianthropus." *Transvaal museum Memoir No.4*, Pretoria.

Buckland-Wright, J.C. (1978). "Bone Structure and the patterns of force transmission in the cat skull (*Felis catus*)." *Journal of Morphology,* 155:35-61.

Buikstra, J. E., & Ubelaker, D. (1994). "Standards for data collection from human skeletal remains*." Research series no. 44*. Fayetteville, Arkansas: Arkansas archeological survey research series no 44.

Burn, A. K., Herring, S. W., Hubbard, R., Zink, K., Rafferty, K., & Lieberman, D. E. (2010). "Dietary consistency and the midline suture in growing pigs." *Orthodontic and Craniofac Research,* 13: 106-113.

Burr, D.B., Ruff, C.B., & Johnson, C. (1989a). "Structural adaptations of the femur and humerus to arboreal and terrestrial environments in three species of macaques." *American Journal of Physical Anthropology,* 79:357–368.

Burr, D.B., Schaffler, M.B., Yang, K.H., Wu, D.D., Lukoschek, M., Kandzari, D., Sivaneri, N., Blaha, J.D., & Radin, E.L. (1989b). "The effects of altered strain environments on bone tissue kinetics." *Bone,* 10:215–221.

Byron, C.D. (2005). "The mechanobiology of cranial sutures." [*PhD diss*.]. Medical College of Georgia, Augusta, Georgia p 1-168.

Byron, C. D. (2006). "Role of the osteoclast in cranial suture waveform patterning." *Anatomical Record,* 288A: 552–563.

Byron, C.D. (2009). "Cranial suture morphology and its relationship to diet in Cebus." *Journal of Human Evolution,* 57:649-655.

Byron, C.D., Borke, J., Yu, J, Pashley, D. Wingard, C.J, & Hamrick, M., (2004a). "Effects of increased muscle mass on mouse sagittal suture morphology and mechanics." *Anatomical Record,* 279A:676–684.

Byron, C. D., Hamrick, M. W., Borke, J, & Yu J. (2004b). "The mechanobiology of cranial sutures." *American Journal of Physical Anthropology Supplement,* 38:72.

Byron, C., Maness, H., & Yu, J. (2008) "Enlargement of the temporalis muscle and alterations in the lateral cranial vault." *International Computational Biology,* 48: 338–344.

Cachel, S.M. (1979). "A functional analysis of the primate masticatory system and the origin of the anthropoid post-orbital septum." *American Journal of Physical Anthropology,* 50:1–18.

Cachel, S. (1984). "Growth and allometry in primate masticatory muscles." *Archives of Oral Biology,* 29:287-293.

Carlson, K.J. (2002). "Shape and material properties of African pongid femora and humeri: their relationship to observed positional behaviors." [*PhD diss*.]. Indiana University, Bloomington.

Carlson, K.J. (2005). "Investigating the form-function interface in African apes: relationships between principal moments of area and positional behaviors in femoral and humeral diaphysis." *American Journal of Physical Anthropology*, 127:312–334.

Cartmill, M. (1970). "The orbits of arboreal mammals: a reassessment of the arboreal theory of primate evolution." [*PhD diss*], University of Chicago, Chicago, IL.

Cartmill, M. (1972). "Arboreal adaptations and the origin of the order Primates." In R.H. Tuttle (Ed.) *The Functional and Evolutionary Biology of Primates*. Aldine de Gruyter: New York p 97–122.

Cartmill, M. (1980). "Morphology, function and evolution of the anthropoid postorbital septum." In R.L. Ciochon and A.B. Chiarelli (eds.). *Evolutionary Biology of the New World Monkeys and Continental Drif*t. Plenum: New York, p 243-274.

Cerling, T.E., Mbua, E., Kirera, F.M., Manthi, F.K., Grine, F.E., Leakey, M.G., Sponheimer M, & Uno, K.T. (2011). "Diet of Paranthropus boisei in the early Pleistocene of East Africa." *Proceedings of the National Academy of Sciemces USA,* 108:9337–9341.

Chalk, J., Richmond, B.G., Ross, C.F., Strait, D.S., Wright, B.W., Spencer, M.A., Wang, Q., & Dechow, P.C. (2011). "A finite element analysis of masticatory stress hypotheses." *American Journal of Physical Anthropology,* 145: 1-10.

Chamay, A., & Tschantz, P. (1972). "Mechanical influences in bone remodeling. Experimental research on Wolff's Law." *Journal of Biomechanics,* 5:173-180.

Chapman, C. (1987). "Flexibility in diets of three species of Costa Rican primates." *Folia Primatologica,* 49:90-105.

Chapman, C. (1988). "Patterns of foraging and range use by three species of neotropical primates." *Primates,* 29:177-194.

Chapman, C.A., & Fedigan, L.M. (1990). "Dietary differences between neighboring Cebus capucinus groups: local traditions, food availability or responses to food profitability?" *Folia Primatologica,* 54: 177-186.

Chapman, C.A., Wrangham, R.W., & Chapman, L.J. (1995). "Ecological constraints on group sizes: an analysis of spider monkey and chimpanzee subgroups." *Behavior, Ecology and Sociobiology*, 36:59-70.

Chivers, D.J. (1974). "The siamang in Malaya: a field study of a primate in tropical rain forest." *Contributions to Primatology,* 4:1-335.

Christiansen, P., & Wroe, S. (2007). "Bite forces and evolutionary adaptations to feeding ecology in carnivores." *Ecology,* 88:347-358.

Clausen, P., Wroe, S., McHenry, C., Moreno, K., & Bourke, J. (2008). "The vector of jaw muscle force as determined by computer-generated three dimensional simulation: A test of Greaves' model." *Journal of Biomechanics,* 41:3184-3188.

Coiner-Collier, S., Scott, R. S., Chalk-Wilayto, J., Cheyne, S. M., Constantino, P., Dominy, N. J., Elgart, A.A., Glowacka, H., Loyola, L.C., Ossi-Lupo, K., Raguet-Schofield, M., Talebi, M.G., Sala, E.A., Sieradzy, P., Taylor, A.B., Vinyard, C.J., Wright, B.W., Yamashita, N., Lucas, P.W.,& Vogel, E. R. (2016). "Primate dietary ecology in the context of food mechanical properties." *Journal of Human Evolution,* 98: 103–118

Cole, T. M. (1992). "Postnatal heterochrony of the masticatory apparatus in *Cebus apella* and *Cebus albifrons." Journal of Human Evolution*, 23:253–282

Conklin-Brittai, N.L., Knott, C.D., & Wrangham, R.W. (2006). "Energy intake by wild chimpanzees and orangutans: methodological considerations and a preliminary comparison". In: Hohmann G., Robbins, M.M., and Boesche, C. (eds), *Feeding ecology in apes and other primates: Eological, physiological, and behavioural aspects*. Cambridge University Press, Cambridge. p 445-472.

Constantino, P. (2007). "Primate masticatory adaptations to fracture-resistant foods." [*PhD. diss*], George Washington University, Washington D.C.

Constantino P.J., Lee, J.J.-W., Chai, H., Zipfel, B., Ziscovici, C., Lawn BR, & Lucas PW. (2010). "Tooth chipping can reveal the diet and bite forces of fossil hominins." *Biology Letters,* 6:826–829

Constantino, P. J., Lee, J. J. W., Gerbig, Y., Hartstone-Rose, A., Talebi, M., Lawn, B. R., & Lucas, P. W. (2012). "The role of tooth enamel mechanical properties in primate dietary adaptation." *American Journal of Physical Anthropology*, 148: 171–177.

Cooke, C.A. (2012). "The feeding, ranging, and positional behaviors of Cercocebus torquatus, the red capped mangabey, in sette cama Gabon: A phylogenetic perspective". [*PhD diss*]. The Ohio State University, Ohio.

Cordeiro, M. S., Backes, A. R., Durighetto Junior A. F., Goncalves, E. H. G., de Oliverira. (2016). "Fibrous dysplasia characterization using lacunarity analysis. *Journal of Digital Imaging* 29:134-140.

Cords, M. (1986). "Interspecific and intraspecific variation in diet of two forest guenons, Cercopithecus ascanius and C. mitis." *Journal of Animal Ecology,* 55:811-827

Correa, H., Coutinho, P. E. G., Ferrari, & S. F. (2000). "Between-year differences in the feeding ecology of highland marmosets (Callithrix aurita and Callithrix flaviceps) in south-eastern Brazil." *Journal of Zoology,* 252, 421e427

Corruccini, R.S., & Beecher, R.M. (1982). "Occlusal variation related to soft diet in a nonhuman primate." *Science*, 218:74-76.

Corruccini, R.S., & Beecher, R.M. (1984). "Occlusofacial morphological integration lowered in baboons raised on soft diet." *Journal of Craniofacial Genetetics and Developmental Biology*, 4:135-142.

Cray Jr, J., Meindl, R. S., Sherwood, C. C., & Lovejoy, C. O. (2008) "Ectocranial suture closure in *Pan troglodytes* and *Gorilla gorilla*: pattern and phylogeny." *American Journal of Physical Anthropology,* 136: 394–399.

Cray Jr, J., Mooney, M. P., Siegel, & M. I. (2010) "Timing of ectocranial suture activity in *Pan troglodytes* as related to cranial volume and dental eruption." *Anatomical Record*, 293: 1289–1296.

Cray Jr, J., Cooper, G. M., Mooney, M.P., Siege, M.I. (2011). "Timing of ectocranial suture activity in *Gorilla gorilla* as related to cranial volume and dental eruption." *Journal of Anatomy,* 218:471-479.

Currey, J.D. (2002). *Bones: structure and mechanics*. Princeton: Princeton University Press.

Curtis, N. (2011). "Craniofacial biomechanics: an overview of recent multibody modelling studies." *Journal of Anatomy,* 218:16-25

Curtis, N., Jones, M. E. H., Evans, S. E., O'Higgins, P, & Fagan, M. J. (2013). "Cranial sutures work collectively to distribute strain throughout the reptile skull." *Journal of the Royal Society,* 10:1-8.

Curtis, N., Witzel, U., & Fagan, M. J. (2014). "Development and three-dimensional morphology of the zygomaticotemporal suture in primate skulls." *Folia Primatologica,* 85:77-87.

Curtis, N., Witzel, U., Fitton, L., O'Higgins, P. & Fagan, M. (2011). "The mechanical significance of the temporal fasciae in Macaca fascicularis: an investigation using finite element analysis." *Anatomical Record,* 294:1178-1190.

Daegling, D.J. (1989). "Biomechanics of cross-sectional size and shape in the hominoid mandibular corpus." *American Journal of Physical Anthropology,* 80:91-106.

Daegling, D.J. (1990). "Geometry and biomechanics of hominoid mandibles". [*PhD diss.*]. State University of New York at Stony Brook, New York.

Daegling, D. J. (1992). "Mandibular morphology and diet in the genus *Cebus." International Journal of Primatology,* 13: 545–570.

Daegling, D. J. (1993). "The relationship of in vivo bone strain to mandibular corpus morphology in *Macaca fascicularis." Journal of Human Evolution,* 25: 247–269.

Daegling, D.J. (2002). “Bone geometry in cercopithecoid mandibles.” *Archives of Oral Biology,* 47:315-325.

Daegling, D.J., & Grine F.E. (1991). “Compact bone distribution and biomechanics of early hominid mandibles.” *American Journal of Physical Anthropology*, 86:321–339.

Daegling, D. J., & Hotzman, J. L. (2003). “Functional Significance of Cortical Bone Distribution in Anthropoid Mandibles : An In Vitro Assessment of Bone Strain Under Combined Loads.” *American Journal of Physical Anthropology,* 50:38–50.

Daegling, D.J., & Grine, F.E. (2007). “Mandibular biomechanics and the paleontological evidence for the evolution of human diet.” In: Ungar PS, editor. *The evolution of human diet: the known, the unknown, and the unknowable*. Oxford: Oxford University Press. p 77–105.

Daegling, D.J., Granatosky, M.C., McGraw, W.S., & Rapoff, A.J. (2011). “Reduced stiffness of alveolar bone in the colobine mandible.” *American Journal of Physical Anthropology,* 144:421-431.

Daegling, D.J., McGraw, W.S., Ungar, P.S., Pamposh J.D., Vick A.E., & Bitty, E.A. (2011). “Hard-Object Feeding in Sooty Mangabeys (*Cercocebus atys*) and Interpretation of Early Hominin Feeding Ecology.” *PLoS one,* 6: e23095.

Daegling, D.J., Judex, S., Ozcivici, E., Ravosa, M.J., Taylor, A.B., Grine, F.E., Teaford, M.F., & Ungar, P.S. (2013). “Viewpoints: Feeding mechanics, diet, and dietary adaptations in early hominins.” *American Journal of Physical Anthropology,* 151:356-371.

Daniels, D.W., Tian, Z., & Barton, E.R. (2008). “Sexual dimorphism of murine masticatory muscle function.” *Archives of Oral Biology,* 53:187-192.

Davies, A.G. (1984). “An ecological study of the red leaf monkey (Presbtis rubicunda) in the dipterocarp forest of northern Borneo.” [*PhD diss.]*. Cambridge University, Cambridge.

Davies, A.G., Oates, J.F., & Dasilva, G.L. (1999). “Patterns of frugivory in three west African Colobine Monkeys.” *International Journal of Primatology,* 20:327-357.

Dechow, P.C., & Hylander, W.L. (2000). “Elastic properties and masticatory bone stress in the macaque mandible.” *American Journal of Physical Anthropology,* 112:553-574.

Dechow, P. C., Wang, Q., & Peterson, J. (2010). “Edentulation Alters Material Properties of Cortical Bone in the Human Craniofacial Skeleton : Functional Implications for Craniofacial Structure in Primate Evolution.” *Anatomical Record,* 629: 618–629.

DeGusta, D., Everett, M.A., & Milton, K. (2003). "Natural selection on molar size in a wild population of howler monkeys (Alouatta palliata)." *Proceedings of the Royal Society of London B Biological Sciences (Suppl.),* 270: 15-17.

Demes, B. (2007). "In vivo bone strain and bone functional adaptation." *American Journal of Physical Anthropology*, 133:717-722.

Demes, B., & Creel, N.(1988). "Bite force, diet, and cranial morphology of fossil hominids." *Journal of Human Evolution,* 17:657-670.

Demes, B., Jungers, W.L., & Walker, C. (2000). "Cortical bone distribution in the femoral neck of strepsirrhine primates." *Journal of Human Evolution,* 39:367-379.

Demes, B., Creel, N., & Preuschoft, H. (1986). "Functional significance of allometric trends in the hominoid masticatory apparatus." In: Else JG., Lee PC, editors. *Primate Evolution*. Cambridge: Cambridge University Press p 229-237.

Di Ieva, A., Bruner, E., Davidson, J., Pisano, P., Haider, T., Stone, S. S., Cusimano, M. D, Tschabitscher, & Grizzi, F. (2013). "Cranial sutures: a multidisciplinary review." *Childs Nervous System,* 29:893- 905.

Ding, M., Odgaard, A., & Hvid, I. (1999). "Accuracy of cancellous bone volume fraction measured by micro-CT scanning." *Journal of Biomechanics*, 32: 323–326

Dominy, N.J., Vogel, E.R., Yeakel, J.D., Constantino, P., & Lucas, P.W. (2008). "Mechanical properties of plant underground storage organs and implications for dietary models of early hominins." *Evolutionary Biology,* 35:159-175.

Doran-Sheehy, D., Mongo, P., Lodwick, J., & Conklin-Brittain, N.L. (2009). "Male and female western gorilla diet: Preferred foods, use of fallback resources, and implications for ape versus old world monkey foraging strategies." *American Journal of Physical Anthropology,* 140:727-738.

DuBrul, E.L. (1977). "Early hominid feeding mechanisms." *American Journal of Physical Anthropology,* 47:305-320.

Dumont, E.R. (1995). "Enamel thickness and dietary adaptation among extant primates and Chiropterans." *Journal of Mammalology,* 76:1127-1136.

Dumont, E.R., Piccirillo, J., & Grosse, I.R. (2005). "Finite-element analysis of biting behavior and bone stress in the facial skeletons of bats." *Anatomical Record Part A*., 283A: 319-330.

Dunbar, R.I.M. (1977). "Feeding ecology of the gelada baboons: a preliminary report." In: Clutton-Brock, T.H. (ed.), *Primate Ecology: Studies in Feeding and Ranging Behaviour in Lemurs, Monkeys, and Apes*. Academic Press, London p 251-273.

Dunbar, R.I.M., & Dunbar, E.P. (1974). "Ecological relations and niche separation between sympatric terrestrial primates in Ethiopia." *Folia Primatologica,* 21:36-60.

Dzialo, C., Wood, S. A., Berthuame, M., Smith, A., Dumont, E. R., Benazzi, S., Weber, G. W., Strait D. S., & Grosse I. R. (2014)."Functional implications of squamosal suture size in *Paranthropus boisei*." *American Journal of Physical Anthropology,* 153:260-268.

Eaglen, R. H. (1984). "Incisor size and diet revisited: the view from a platyrrhine perspective." *American Journal of Physical Anthropology*, 64:263–275

Edmonds, H.M. (2015). "Bent out of shape: A preliminary analysis of the cross-sectional geometric properties of the primate zygomatic arch." *American Journal of Physical Anthropology,* 156 (Suppl 60): 127.

Edmonds, H.M. (2016). "Zygomatic Arch Cortical Area and Diet in Haplorhines." *Anatomical Record*, 299, 1789–1800.

Eisenberg, N. A., & Brodie, A. G. (1965). "Antagonism of temporal fascia to masseteric contraction." *Anatomical Record*, 294:1178-1190.

Ellefson, J. (1974). "A natural history of white-handed gibbons in the Malayan Peninsula." In: Rumbaugh, D.M. (ed.), *Gibbon and Simang*, vol 3. Karger, Basel p 1-136.

Endo, B. (1965). "Distribution of stress and strain produced in the human facial skeleton by the masticatory force." *Journal of Anthropological Society Nippon,* 73:123-136.

Endo, B. (1966). "Experimental studies on the mechanical significance of the form of the human facial skeleton." *Journal of Facial Sciences University Tokyo Section* V, 3:1-106.

Endo, B. (1967). "Mechanical analysis of the form of the human facial skeleton." VII *Congress International Sciences Anthropolology et Ethnology,* 2:346-353.

Endo, B. (1970). "Analysis of stresses around the orbit due to masseter and temporalis muscles respectively." *Journal of Anthropological Society Nippon,* 78:251-265.

Endo, B. (1973). “Stress analysis on the facial skeleton of gorilla by means of the wire strain gauge method.” *Primates,* 14:37-45.

Eng, C.M., Lieberman, D.E., Zink, K.D., & Peters, M.A. (2013). “Bite force and occlusal stress production in hominin evolution.” *American Journal of Physical Anthropology,* 151:544-557.

Enlow, D., & Hans, M. (1996). *Essentials of Facial Growth*. Ann Arbor: Needham Press.

Evans, A., Wilson, G., Fortelius, M., & Jernvall, J. (2007). “High-level similarity of dentitionsin carnivorans and rodents.” *Nature,* 445:78–81.

Farke, A. A. (2008). “Frontal sinuses and head-butting in goats: a finite element analysis.” *Journal of Experimental Biology,* 211:3085–3094.

Finstermeier, K., Zinner, D., Brameier, M., Meyer, M., Kreuz, E., Hofreiter, M., & Roos, C. (2013). “A Mitogenomic Phylogeny of Living Primates.” *PLoS ONE*, 8:1–10.

Fitton, L.C., Kupczik, K., Milne, N., Fagan, M.J., & O’Higgins, P. (2009). “The role of sutures in modulating strain distribution within the skull of Macaca fascicularis.” *American Journal of Physical Anthropology Supplement,* 48:189.

Fleagle, J.G. (2008). *Primate Adaptation and Evolution*. Academic Press, Massachusetts.

Foley, J.D., van Dam, A., Hughes, J.F., & Feiner, S.K. (1990). "Spatial-partitioning representations; Surface detail." Computer Graphics: Principles and Practice. *The Systems Programming Series*. Addison-Wesley. ISBN 0-201-12110-7.

Fong, K. D., Nacamuli, R. P., Loboa, E. G., Henderson, J. H., Fang, T. D., Song, H. M., Cowan, C. M., Warren, S. M., Carter, D. R., & Longaker, M. T. (2003) “Equibiaxial tensile strain affects calvarial osteoblast biology.” *Journal of Craniofacial Surgery,* 14:348–355.

Franks, E. M., Holton, N. E., Scott, J. E., McAbee, K. R., Rink, J. T., Pax, K. C., Pasquinelly, A.C., Scollan, J.P., Eastman, M.M., & Ravosa, M. J. (2016). “Betwixt and Between: Intracranial Perspective on Zygomatic Arch Plasticity and Function in Mammals.” *Anatomical Record*, 299: 1646–1660.

Freeland, W.J. (1979). “Mangabey (Cercocebus albigena) social organization and population density in relation to food use and availability.” *Folia Primatologica,* 32:108-124.

Freeman, J.A., Teng, S., & Herring, S.W. (1997). "Rigid fixation and strain patterns in the pig zygomatic arch and suture." *Journal of Oral and Maxillofacial Surgery,* 55:496-504.

Galetti, M., & Pedroni, F. (1994). "Seasonal diet of capuchin monkeys (Cebus apella) in a semi-deciduous forest in couth-east Brazil." *Journal of Tropical Ecology,* 10:27-39.

Galetti, M., Pedroni, F., & Pashoal, M. (1994). "Infanticide in the brown howloer monkey, Alouatta fusca." *Neotropical Primates,* 2:6-7.

Gallagher, D., Visser, M., & De Meersman, R. (1997). "Appendicular skeletal muscle mass: effects of age, gender, and ethnicity." *Journal of Applied Physiology*, 83:229–239.

Gautier-Hion, A. (1988). "Diet and dietary habits of forest guenons." In: Gautier-Hion, A., Bourliere, F., Gautier, J.P., and Kingdon, J. (eds.), *A Primate Radiation: Evolutionary Biology of the African Guenons*. Cambridge University Press, New York p 257-283.

Glander, K.E. (1978). "Howling monkey feeding behavior and plant secondary compounds: a study of strategies." In: Montgomery, G.G (ed.), *The ecology of Arboreal Folivores*. Smithsonian Institution Press, Washington DC p 561-573.

Goldstein, S.J., & Richard, A.F. (1989). "Ecology of rhesus macaques (Macaca mulatta) in northwest Pakistan." *International Journal of Primatology*, 10:531-567.

Gonzalez-Kirchner, J.P., & Sainz de la Mazxa, M. (1996). "Preliminary notes on the ecology of the drill (*Mandrillus leucophageus*) on Bioko Island, Rep. Equitorial Guinea." *Garcia Orta Ser Zool Lisboa,* 21:1-5.

Gordon, J. (1978). *Structures, or, Why Things Don't Fall Down*. Penguin, London.

Górski, A. J., & Skrzat, J. (2006). "Error estimation of the fractal dimension measurements of cranial sutures." *Journal of Anatomy,* 208: 353-359.

Gosman, J.H., Hubbell, Z.H., Shaw, C.N., & Ryan, T.M. (2013). "Development of cortical bone geometry in the human femoral and tibial diaphysis". *Anatomical Record*, 296:774-787.

Greaves, W.S. (1978). "The jaw lever system in ungulates: a new model." *Journal of Zoology,* 184:271–285.

Greaves, W.S. (1985). "The mammalian postorbital bar as a torsion-resisting helical strut." *Journal of Zoology,* 207:125–136.

Greaves, W.S. (1995). “Functional predictions from theoretical models of the skull and jaws in reptiles and mammals.” In: Thomason JJ, editor. *Functional morphology in vertebrate paleontology*. Cambridge: Cambridge University Press p 99–105.

Grigoriadis, A., Johansson, R. S., & Trulsson, M. (2014). “Temporal profile and amplitude of human masseter muscle activity is adapted to food properties during individual chewing cycles.” *Journal of Oral Rehabilitation,* 41:367-373.

Grine, F.E. (1981). “Trophic differences between “gracile” and “robust” Australopithecines: a scanning electron microscope analysis of occlusal events.” *South African Journal of Science,* 77: 203–230.

Grine, F.E. (1986). “Dental evidence for dietary differences in *Australopithecus* and *Paranthropus*: A quantitative analysis of permanent molar microwear.” *Journal of Human Evolution,* 15:783-822.

Grine, F.E., & Kay, R.F. (1988). “Early hominid diets from quantitative image analysis of dental microwear.” *Nature,* 333:765–768.

Grine, F.E., & Martin, L.B. (1988) “Enamel thickness and development in Australopithecus and Paranthropus.” In: Grine FE, ed. *Evolutionary History of the ‘‘Robust’’ Australopithecines*. New York: Aldine de Gruyter p 3–42.

Grine, F.E., Judex, S., Daegling, D.J., Ozcivici, Ungar, P.S., Teaford, M.F., Sponheimer, M., Scott, J., Scott, R.S., & Walker, A. (2010). “Craniofacial biomechanics and functional and dietary inferences in hominin paleontology.” *Journal of Human Evolution,* 58:293-308.

Gysi, S. (1921). “Studies on the leverage problem of the mandible.” *Dental Digest.* 27:74-84, 144-150, 203-308.

Habib, M.B., & Ruff, C.B. (2008). “The effects of locomotion on the structural characteristics of avian limb bones.” *Zoological Journal of the Linnean Society*, 153:601–624.

Ham, R. (1994). “Behaviour and ecology of gray-cheeked mangabeys (*Cercocebus albigena*) in the Lope Reserve, Gabon.” [*PhD diss.*]. University of Stirling, Stirling.

Hannam, A.G. (1976). “The regulation of the jaw bite force in man.” *Archives of Oral Biology,* 21:641-644.

Hanya, G. and Bernard, H. (2015). “Different roles of seeds and young leaves in the diet of red leaf monkeys (Presbytis rubicunda): Comparisons of avilability, nutritional properties, and associated feeding behavior.” *International Journal of Primatology,* 36:177-193.

Happel, R.E. (1982). “Ecology of Pithecia hirsuta in Peru.” *Journal of Human Evolution*, 11:581–590.

Hartwig, W.C. (1991). “Fractal analysis of sagittal suture morphology.” *Journal of Morphology,* 210:289–298.

Hayes, V.J., Freedman, L., & Oxnard, C.E. (1996). “Dental sexual dimorphism and morphology in African colobus monkeys as related to diet.” *International Journal of Primatology*, 17:725-757.

He, T., and Kiliaridis, S. (2003). “Effects of masticatory muscle function on craniofacial morphology in growing ferrets (*Mustela putorius furo*).” *European Journal of Oral Sciences*, 11:510–517.

Hendee, W. (1983). *The physical principles of computed tomography*. Boston: Little, Brown, and Co.

Herring, S.W. (1972). “Sutures–a tool in functional cranial analysis.” *Acta Anatomica (Basel),* 83: 222–247.

Herring, S.W. (1993). “Epigenetic and functional influences on skull growth.” In: *The Skull,* (eds Hanken J, Hall B) p 153–206. Chicago: University of Chicago Press.

Herring, S. W. (2005). “Ontogeny of bone strain: the zygomatic arch in pigs.” *Journal of Experimental Biology*, 208:4509–4521.

Herring, S.W. (2008). “Mechanical influences on suture development and patency.” *Frontiers in Oral Biology,* 12:41–56.

Herring, S.W., & Herring S.E. (1974). “The superficial masseter and gape in mammals.” *American Naturalist,* 108:561–576.

Herring, S.W., & Mucci R.J. (1991). “In vivo strain in cranial sutures: the zygomatic arch.” *Journal of Morphology,* 207:225–239.

Herring, S.W., & Scapino, R.P. (1973). “Physiology of feeding in miniature pigs”. *Journal of Morpholo*gy, 141:427–460.

Herring, S. W., & Teng, S. (2000). “Strain in the braincase and its suture during function.” *American Journal of Physical Anthropology,* 112: 575–593.

Herring, S.W., Grimm A.F., & Grimm B.R. (1979).”Functional heterogeneity in a multipinnate muscle.” *American Jounral of Anatomy,* 154:563-576.

Herring, S.W., Pedersen S.C., & Huang X. (2005). “Ontogeny of bone strain: the zygomatic arch in pigs.” *Journal of Experimental Biology,* 208:4509-4521.

Herring, S. W., Rafferty, K. L., Liu, Z. J., & Marshall, C. D. (2001). "Jaw muscles and the skull in mammals: the biomechanics of mastication." *Computation Biochemical Physiology*, 131:207-219.

Herring, S.W., Rafferty, K.L., Liu, Z..J, & Sun, Z. (2009). "A non-primate model for the fused symphysis: In vivo studies of the pig." In: Vinyard CJ, Ravosa MJ, Wall CE, editors. *Primate craniofacial function and biology*. Developments in primatology series. New York: Springer. p 19-38.

Herring, S.W., Teng, S., Huang, X., Mucci, R.J., & Freeman, J. (1996). "Patterns of bone strain in the zygomatic arch." *Anatomical Record*, 246:446-457.

Hill, D.A. (1997). "Seasonal variation in the feeding behavior and diet of Japanese macaques (*Macaca fuscata yakui*) in lowland forest of Yakushima." *American Journal of Primatology*, 43:305-322.

Hogg, R. T., Ravosa, M. J., Ryan, T. M., & Vinyard, C. J. (2011). "The functional morphology of the anterior masticatory apparatus in tree-gouging marmosets (cebidae, primates)." *Journal of Morphology*, 272(7): 833–849.

Hohmann, G. (2009). "The diets of non-human primates: frugivory, food processing, and food sharing." In: Hublin JJ, Richards MP, editors. *The Evolution of Hominin Diets*. Springer Netherlands p 1-14.

Hollister, N. (1917). "Some effects of environment and habit on captive lions." *Proceedings of the US National Museum*, 53:177–193.

Holm, S. (1979). "A simple sequential rejective multiple test procedure." *Scandanavian Journal of Statistics*, 6: 65–70.

Holmes, M.A., & Ruff, C.B. (2011). "Dietary effects on development of the human mandibular corpus." *American Journal of Physical Anthropology*, 145:615-628.

Homburg, I. (1997). "Okologie and sozialverhalten einer gruppe von weibgesicht-sakis (Pithecia pithecia pithecia Linneaus 1766) Im estado Bolivar, Venezuela." [*PhD diss*.]. Universitat Bielefeld, Bielefeld.

Hoshino, J. (1984). "Feeding ecology of mandrills (Mandrillus sphinx) in Campo Animal Reserve, Cameroon." *Primates,* 26:248-273.

Hubbard, R. P., Melvin, J.W., & Barodawala, I.T. (1971) "Flexure of cranial sutures." *Journal of Biomechanics,* 4:491-492.

Hylander, W.L. (1975). "The human mandible: lever or link?" *American Journal of Physical Anthropology,* 43:227–242.

Hylander, W.L. (1979a). "The functional significance of primate mandibular form." *Journal of Morphology,* 160:223-240.

Hylander, W.L. (1979b). "Mandibular function in *Galago crassicaudatus* and *Macaca fascicularis*: an *in vivo* approach to stress analysis of the mandible." *Journal of Morphology,* 159: 253–296.

Hylander, W.L. (1981). "Patterns of stress and strain in the macaque mandible." In: Carlson C.S., (ed.). *Craniofacial biology*. Monograph #10, Craniofacial Growth Series, Center for Human Growth and Development. University of Michigan: Ann Arbor p 1–37.

Hylander, W.L. (1984). "Stress and strain in the mandibular symphysis of primates: A test of competing hypotheses." *American Journal of Physical Anthropology*, 64:1–46.

Hylander, W.L. (1985). "Mandibular function and biomechanical stress and scaling." *American Zoology,* 25:315–330.

Hylander, W. L. (1986). "*In vivo* bone strain as an indicator of masticatory bite force in *Macaca fascicularis." Archives of Oral Biology*. 31:149–157.

Hylander, W.L. (1988). "Implications of in vivo experiments for interpreting the functional significance of "robust" australopithecine jaws." In: Grine F, editor. *Evolutionary History of the "Robust" Australopithecines.* Aldine De Gruyter: New York p 55–83.

Hylander W.L. (2009). The functional significance of canine height reduction in early hominins. *American Journal of Physical Anthropology,* 48S:154.

Hylander, W.L., & Johnson, K.R. (1992). "Strain gradients in the craniofacial region of primates." In Z Davidovitch (ed.): *The Biological Mechanisms of Tooth Movement and Craniofacial Adaptation*. Columbus, Ohio, U.S.A.: Ohio State University College of Dentistry p 559–569.

Hylander, W.L., & Johnson, K.R. (1994). "Jaw muscle function and wishboning of the mandible during mastication in macaques and baboons." *American Journal of Physical Anthropology,* 94:523-547.

Hylander, W.L., & Johnson, K.R. (1997). "*In vivo* bone strain patterns in the zygomatic arch of macaques and the significance of these patterns for functional patterns of craniofacial form." *American Journal of Physical Anthropology,* 102:203-232.

Hylander, W.L., & Ravosa, M.J. (1992). "An analysis of the supraorbital region of primates: a morphometric and experimental approach." P Smith, E Tchernov (Eds.), *Structure, Function, and Evolution of Teeth*, Freund, Tel Aviv p 233–255

Hylander, W.L., Johnson, K.R., & Crompton, A.W. (1987). "Loading patterns and jaw movements during mastication in Macaca fascicularis: A bone-strain, electromyographic, and cineradiographic analysis." *American Journal of Physical Anthropology,* 72:287-314.

Hylander, W.L., Picq, P.G., & Johnson, K.R. (1991a). "Masticatory stress hypotheses and the supraorbital region of primates." *American Journal of Physical Anthropology,* 86:1-36.

Hylander W.L., Picq P.G., & Johnson K.R. (1991b). "Function of the supraorbital region in primates." *Archivess of Oral Biology,* 36:273-281.

Hylander, W.L., Johnson, K.R., & Crompton, A.W. (1992). "Muscle force recruitment and biomechanical modeling: an analysis of masseter muscle function during mastication in *Macaca fascicularis*." *American Journal of Physical Anthropology,* 88:365–387.

Hylander, W.L., Ravosa, M.J., Ross, C.F., & Johnson, K. R. (1998). "Mandibular corpus strain in primates: further evidence for a functional link between symphyseal fusion and jaw-adductor muscle force." *American Journal of Physical Anthropology,* 107:257–271.

Hylander, W.L., Wall, C.E., Vinyard, C.J., Ross, C.F., Ravosa, M.J., Williams, S.H., & Johnson K.R. (2005). "Temporalis function in anthropoids and strepsirrhines: and EMG study." *American Journal of Physical Anthropology,* 128:35–56.

Ikai, M., & Fukunaga, T. (1968). "Calculation of muscle strength unit cross-sectional area of human muscle by means of ultrasonic measurement." *International Zetischrift fur Angewandte Physiologie Einschliesslich,* 2:26-32.

Isbell, L.A. (1998). "Diet for a small primate: insectivory and gummivory in the (large) patas monkey (Erythrocebus patas pyrrhonotus)." *American Journal of Primatology,* 45:381-389.

Iwasaki, K. (1989) "Dynamic responses in adult and infant monkey craniums during occlusion and mastication." *Journal Osaka Dental University*, 23:77-97.

Jablonski, N.G. (1981). "Functional analysis of the masticatory apparatus of Theropithecus gelada (Primates: Cercopithecidae)". [*PhD diss.*]. University of Washington.

Jablonski, N.G., editor. (1993). *Theropithecus: the rise and fall of a primate genus*. Cambridge: Cambridge University Press, p 536.

Jablonski, N.G. (1994). "Convergent evolution in the dentitions of grazing macropodine marsupials and the grass-eating cercopithecine primate Theropithecus gelada," *Journal of the Royal Society of West Australia,* 77: 37–43.

Jaffe, E.K., & Isbell, L. (2011)."The Guenons." In C. Campbell, A. Fuentes, K. C. MacKinnon, S. K. Bearder, & R.M. Stumpf (Eds.), *Primates in Perspective (2nd ed.)*. Oxford: Oxford University Press, p 277-300.

Janzen, D.H. (1971). "Seed predation by animals." *Annual Review of Ecological System*, 2:465–492

Jasinoski, S. C., Rayfield, E. J., & Chinsamy, A. (2010). "Functional implications of dicynodont cranial suture morphology." *Journal of Morphology,* 271:705–728.

Jasinoski, S. C., Reddy, B. D. (2012). "Mechanics of cranial sutures during simulated cyclic loading." *Journal of Biomechanics,* 45:2050-2054.

Jaslow, C. R. (1989). "Sexual dimorphism of cranial suture complexity in wild sheep (*Ovis orientalis*)." *Zoolological Journal of the Linnean Society-London,* 95:273-284.

Jaslow, C.R. (1990). "Mechanical properties of cranial sutures." *Journal of Biomechanics,* 23:313-321.

Jaslow, C.R., & Biewener, A. A. (1995). "Strain patterns in the horncores, cranial bones and sutures of goats (Capra hircus) during impact loading." *Journal of Zoology,* 235:193–210.

Johansen, V. A., & Hall, S. H. (1982) "Morphogenesis of the mouse coronal suture." *Acla Anatomica,* 114:58-67.

Jolly, C.J. (1970). "The seed-eaters: a new model of hominid differentiation based on a baboon analogy." *Man,* 5:5–26

Judex, S., Gross, T.S., & Zernicke, R.F. (1997). "Strain gradients corre- late with sites of exercise-induced bone-forming surfaces in the adult skeleton." *Journal of Bone Mineral Research,* 12:1737–1745

Judex, S., Lei, X., Han, D., & Rubin, C. (2007). "Low-magnitude mechanical signals that stimulate bone formation in the ovariectomized rat are dependent on the applied frequency but not on the strain magnitude." *Journal of Biomechanics*, 40:1333–1339

Karperien, A. (1999-2013) FracLac for ImageJ. http://rsb.info.nih.gov/ij/plugins/fraclac/FLHelp/Introduction.htm.

Kay, R. F. (1973).” Mastication, molar tooth structure and diet in primates.” [*PhD diss.*]. Yale University, New Haven, Connecticut.

Kay, R.F. (1975). “The functional adaptations of primate molar teeth.” *American Journal of Physical Anthropology,* 42:327-352.

Kay, R.F. (1981). “The nut-crackers: a new theory of the adaptations of the Ramapithecines.” *American Journal of Physical Anthropology,* 55:141-151.

Kay, R. F. (1984). “On the use of anatomical features to infer foraging behavior in extinct primates.” In: PS Rodman and JGH Cant (eds.): *Adaptations for Foraging in Nonhuman Primates: Contributions to an Organismal Biology of Prosimians, Monkeys, and Ape*s. New York: Columbia University Press, p 21-53.

Kay, R. F. (1985). “Dental evidence for the diet of Australopithecus.” *Annual Review of Anthropology,* 14: 315–341.

Kay, R. F. (1990). “The phyletic relationships of extant and fossil Pitheciinae (Platyrrhini, Anthropoidea).” *Journal of Human Evolution,* 19:175-208.

Kiliaridis, S. (1989). “Muscle function as a determinant of mandibular growth in normal and hypocalcaemic rat.” *European Journal of Orthodontics*, 11:298–308.

Kiliaridis, S., Engstron, C., & Thilander, B. (1986). “The relationship between masticatory function and craniofacial morphology: A cephalometric longitudinal analysis in the growing rat fed a soft diet.” *European Journal of Orthodontics,* 7:273–283.

Kiliaridis, S., Engström, C., & Chavez, L.M.E. (1992). “Influence of masticatory muscle function on craniofacial growth in hypocalcemic rats.” *Scandanavian Journal of Dental Research,* 100: 330–336.

Kinzey, W.G. (1992) “Dietary and dental adaptations in the Pitheciinae.” *American Journal of Physical Anthropology*, 53:499-514.

Kinzey, W.G., & Norconk, M.A. (1990). “Hardness as a basis of fruit choice in two sympatric primates.” *American Journal of Physical Anthropology,* 81:5-15.

Kinzey, W.G. & Norconk, M.A. (1993). “Physical and chemical properties of fruit and seeds eaten by Pithecia and Chiropotes in Suriname and Venezuela.” *International Journal of Primatology,* 14:207-227.

Kinzey, W.G., Rosenberger, A.L., & Ramirez M. (1975). “Vertical clinging and leaping in a neotropical anthropoid.” *Nature,* 225:327– 328.

Kirk, E.C., & Simons ,E.L. (2001). "Diets of fossil primates from the Fayum Depression of Egypt: a quantitative analysis of molar shearing." *Journal of Human Evolution,* 40:203-229.

Kokich, V. G. (1986) "The biology of sutures. Craniosynostsis: Diaynosis*." Evaluation, and Manayemrnr* (Edited by Cohen, M. M., Jr.). Raven Press, New York, p 81-103.

Kokich, V.G. (1992). "Sutural response to orthopedic forces." In: Carlson DS, Goldstein SA, editors. *Bone biodynamics in orthodontic and orthopedic treatment*. Ann Arbor, MI: University of Michigan, p 173–188.

Koskinen. L., Isotupa, K. & Koski. K. (1976) "A note on craniofacial sutural growth." *American Journal of Physical Anthropology*, 45, 511-516.

Kopher, R.A., & Mao, J. J. (2003). "Suture growth modulated by the oscillatory component of micromechanical strain." *Journal of Bone Mineral Research,* 18:521-528.

Koyabu, D.B., & Endo, H. (2009). "Craniofacial variation and dietary adaptations of African colobines," *Journal of Human Evolution,* 56:525-536.

Koyabu D.B., Oshida T, Dang N.X., Can D.N., Kimura J, Sasaki M, Motokawa M, Son N.T., Hayashida A, Shintaku Y, & Endo B. (2009). "Craniodental mechanics and the feedingecology of two sympatric callosciurine squirrels in Vietnam*." Journal of Zoolology,* 372- 380

Kunz, B.K., & Lisenmair, K.E. (2008). "The disregarded west: diet and behavioural ecology of olive baboons in the Ivory Coast." *Folia Primatologica,* 79:31-51.

Kupczik, K., Dobson, C.A., Crompton, R.H., Phillips, R., Oxnard, C.E., Fagan, M.J., & O'Higgins, P., (2009). "Masticatory loading and bone adaptation in the supraorbital torus of developing macaques." *American Journal of Physical Anthropology,* 139, 193–203.

Kupczik, K., Dobson, C.A., Fagan, M.J., Crompton, R.H., Oxnard, C.E., & O'Higgins, P. (2007). "Assessing mechanical function of the zygomatic region in macaques: validation and sensitivity testing of finite element models." *Journal of Anatomy*, 210: 41-53.

Laib, A., Barou, O., Vico, L., Lafage-Proust, M. H., Alexandre, C., & Rügsegger, P. (2000). "3D micro-computed tomography of trabecular and cortical bone architecture with application to a rat model of immobilisation osteoporosis." *Medical & Biological Engineering and Computing*, 38:326–332.

Lambert, J. E. (2010). "Primate nutritional ecology: Feeding biology and diet at

ecological and evolutionary scales." In C. Campbell, A. Fuentes, K. C. MacKinnon, S. K. Bearder, & R.M. Stumpf (Eds.), *Primates in Perspective* (2nd ed.). Oxford: Oxford University Press.

Lambert, J. E., Chapman, C. A., Wrangham, R. W., & Conklin-Brittain, N. L. (2004). "Hardness of cercopithecine foods: Implications for the critical function of enamel thickness in exploiting fallback foods." *American Journal of Physical Anthropology*, 125:363-368.

Lanyon, L.E., & Baggott, D.G. (1976). "Mechanical function as an influence on the structure and form of bone." *Journal of Bone and Joint Surgery-British Volume*, 58:436-443.

Lanyon, L.E., & Rubin, C.T. (1984). "Static vs dynamic loads as an influence on bone remodeling." *Journal of Biomechanics,* 12:897-905.

Lawn B, & Lee JJ-W. (2009). "Analysis of fracture and deformation modes in teeth subjected to occlusal loading." *Acta Biomateralia,* 5: 2213–2221.

Ledogar, J. A., Winchester, J. M., St. Clair, E. M., & Boyer, D. M. (2013). "Diet and dental topography in pitheciine seed predators." *American Journal of Physical Anthropology,* 150: 107–121.

Lee-Thorp J.A., Sponheimer M, Passey B.H., de Ruiter D.J., & Cerling T.E. (2010). "Stable isotopes in fossil hominin tooth enamel suggest a fundamental dietary shift in the Pliocene." *Proceedings of the Royal Society B,* 365: 3389–3396

Li, J., Du, Q., & Sun, C. (2009). "An improved box-counting method for image fractal dimension estimation." *Pattern Recognition,* 42:2460-2469.

Lieber, R.L., & Friden, J. (2000). "Functional and clinical significance of skeletal muscle architecture." *Muscle Nerve,* 23:1647-1666.

Lieberman, D.E., Krovitz, G.E., Yates, F.W., Devlin, M., & St Claire, M. (2004a) "Effects of food processing on masticatory strain and craniofacial growth in a retrognathic face." *Journal of Human Evolution*, 46:655–677.

Lieberman, D.E., Polk, J.D., & Demes, B. (2004b). "Predicting long bone loading from cross-sectional geometry." *American Journal of Physical Anthropology*, 123:156-171.

Liu, Z.J., & Herring, S.W. (2000). "Bone surface strains and internal bony pressures at the jaw joint of the miniature pig during masticatory muscle contraction." *Archives in Oral Biology,* 45:95-112.

Long, C. A. (1985). “Intricate sutures as fractal curves.” *Journal of Morphology,* 185: 285–295.

Long, C. A., & Long, J. E. (1992). “Fractal dimensions of cranial sutures and waveforms.” *Acta Anatomica (Basel),* 145:201–206.

Lovejoy, C.O., & Burstein, A.H. (1977). “Geometrical properties of bone sections determine by laminography and physical section.” *Journal of Biomechanics*, 10:527-528.

Lucas, P.W. (1989). “Significance of Mezzettia leptopoda fruits eaten by orang-utans for dental microwear analysis.” *Folia Primatologica*, 52:185–190.

Lucas, P. W. (2004). *Dental functional morphology: how teeth work.* Cambridge: Cambridge University Press

Lucas, L. (2012). “Variation in dental morphology and bite force along the tooth row in anthropoids”. [*PhD diss*.]. Arizona State University, Arizona.

Lucas, P.W., & Luke, D.A. (1984). “Chewing it over: basic principles of food acquisition.” In: D.J. Chivers, B.A. Wood, A. Bilsborough (Eds.), *Food Acquisition and Processing in Primates,* Plenum Press, New York, p 283–301

Lucas, P.W., & Pereira, B. (1990). “Estimation of the fracture toughness of leaves.” *Functional Ecology*, 4:819–822

Lucas, P.W., Lowrey, T.K., Pereira, B.P., Sarafis, V., & Kuhn, W. (1991). “The ecology of Mezzettia leptopoda (Hk. f. et Thoms.) Oliv. (Annona- ceae) seeds as viewed from a mechanical perspective.” *Functional Ecology*, 5:545–553.

Lucas, P. W., Beta, T., Darvell, B. W., Dominy, N. J., Essackjee, H. C., Lee, P. K. D., Osorio, D., Ramsden, L., Yamashita, N., Yuen, T. D. (2001). “Field kit to characterize physical, chemical and spatial aspects of potential primate foods.” *Folia Primatologica,* 72:11-25.

Lucas, P. W., Constantino, P. J., & Wood, B. A. (2008a). “Inferences regarding the diet of extinct hominins: Structural and functional trends in dental and mandibular morphology within the hominin clade.” *Journal of Anatomy*, 212:486–500.

Lucas, P.W., Constantino, P., Wood, B., & Lawn B. (2008b). “Dental enamel as a dietary indicator in mammals.” *BioEssays,* 30: 374–385.

Lucas, P.W., Copes, L, Constantino, P.J., Vogel, E.R., Chalk, J, Talebi, M, Landis, M, & Wagner, M. (2012). “Measuring the toughness of primate foods and its ecological value.” *International Journal of Primatology,* 33:598-610.

Lucas, P.W., Corlett, R.T., & D.A. Luke. (1985) "Plio-Pleistocene hominid diets: An approach combining masticatory and ecological analysis." *Journal of Human Evolution,* 14:187- 202.

Lucas, P.W., Corlett R.T., & Luke D.A. (1986a). "Sexual dimorphism of tooth size in Anthropoids." *Journal of Human Evolution,* 1:23-39.

Lucas, P.W., Corlett R.T., & Luke D.A. (1986b). "Postcanine tooth size and diet in anthropoid primates*." Zeritschrift fur Morphologie und,* 76:253-276.

Lucas, P. W., Prinz, J. F., Agrawal, K. R., & Bruce, I. C. (2002). "Food physics and oral physiology." *Food Quality and Preference*, 13: 203–213.

Lucas, P. W., Turner, I. M., Dominy, N. J., & Yamashita, N. (2000)."Mechanical defences to herbivory." *Annals of Botany*, 86:913–920.

Lund, J. P., & Lamarre, Y. (1974). "Activity of neurones in the lower precentral cortex during voluntary and rhythmical jaw movements in the monkey." *Experimental Brain Reearch,* 19:282-299.

Luschei, E.S., & Goodwin, G.M. (1974). "Patterns of mandibular movement and jaw muscle activity during mastication in monkeys." *Journal of Neurophysiology,* 37:954–966.

Lynnerup, N., & Jacobsen, J. C. (2003). "Brief communication: age and fractal dimensions of human sagittal and coronal sutures." *American Journal of Physical Anthropology,* 121:332–336.

Macho, G.A., Shimizu, D., Jiang, Y., & Spears, L.R., (2005). "Australopithecus anamensis: a finite element approach to studying the functional adaptations of extinct hominins." *Anatomical Record,* 283A: 310–318.

MacKinnon, J.R. & Mackinnon, K.S. (1980). "Niche differentiation in a primate community." In: Chivers, D.J. (ed.), *Malayan Forest Primates: Ten years study in tropical rain forest.*

Mandelbrot, B. (1967). "How long is the coast of Britain? Statistical self-similarity and fractional dimension." *Science,* 156:636–638.

Mandelbrot, B. (1977). *Fractals: form, chance, and dimension*. San Francisco: W.H. Freeman and Company

Mandelbrot, B. (1983). *The Fractal Geometry of Nature*. New York, NY: W.H. Freeman.

Mantila Roosa, S.M., Turner, C.H., & Liu, Y. (2012). "Regulatory mechanisms in bone following mechanical loading." *Gene Regulation and Systems Biology,* 6:43-53.

Mao, J.J. (2002).”Mechanobiology of sutures.” *Journal of Dental Research,* 12:810-812

Mao, J.J., Wang, X., & Kopher, R.A. (2003). “Biomechanics of craniofacial sutures: orthopedic implications.” *Angle Orthodontist,* 73:128–135.

Maloul, A., Fialkov, J., & Whyne, C. M. (2013). “Characterization of the bending strength of craniofacial sutures.” *Journal of Biomechanics,* 46:912-917.

Marelli, C. A., & Simons, E. L. R. (2014). “Microstructure and cross-sectional shape of limb bones in great horned owls and red-tailed hawks: How do these features relate to differences in flight and hunting behavior?” *PLoS ONE*, 9(8).

Marks, L., Teng, S., Årtun, J., & Herring, S. (1997). “Reaction strains on the condylar neck during mastication and maximum muscle stimulation in different condylar positions: an experimental study in the miniature pig.” *Journal of Dental Research*, 76:1412–1420.

Martin R.B., & Burr D.B. (1989). *Structure, function, and adaptation of compact bone.* New York: Raven Press.

Martin, R.B., Burr, D.B., & Sharkey, N.A. (1998). *Skeletal tissue mechanic*s. New York: Springer-Verlag.

Martin L.B., Olejniczak A.J., Maas M.C. (2003). “Enamel thickness and microstructure in pitheciinae primates, with comments on dietary adaptations of the middle Miocene hominoid, Kenyapithecus.” *Journal of Human Evolution,* 45:351-367.

Massler, M., & Schour, I. (1951). “The growth pattern of the cranial vault in the albino rat as measured by vital staining with alizarine red ‘s’.” *Anatomical Record,* I: 83-101.

Masterson, T. (1996). “Cranial form in *Cebus*: an ontogenetic analysis of cranial form and sexual dimorphism.” [*PhD diss.*]. University of Wisconsin, USA.

McGraw, W.S., Vick, A.E., Daegling, D.J. (2012). “Sex and age differences in the diet and ingestive behaviors of sooty mangabeys in the Tai Forest, Ivory Coast.” *American Journal of Physical Anthropology,* 144: 140–153.

McCollum M.A. (1994). “Mechanical and spatial determinants of *Paranthropus* facial form.” *American Journal of Physical Anthropology,* 93:259-273.

Meindl, R.S., & Lovejoy, C.O. (1985) “Ectocranial suture closure: a revised method for the determination of skeletal age at death based on the lateral-anterior sutures.” *American Journal of Physical Anthropology,* 68:57–66.

Menard, N., & Vallet, D. (1996). "Demography and ecology of Barbary macaques (*Macaca sylvanus*) in two different habitats." In: Fa, J. E., and Lindburg, D.G., (eds.), *Evolution and Ecology of Macaque Societies*. Cambridge University Press, Cambridge, p 106-131.

Menard, N., & Vallet, D. (1997). "Behavioral responses of Barbary macaques (*Macaca sylvanus*) to variations in environmental conditions in Algeria." *American Journal of Physical Anthropology*, 43:285-304.

Menegaz, R.A., Sublett, S.V., Figueroa, S.D., Hoffman, T.J., & Ravosa, M.J. (2009). "Phenotypic plasticity and function of the hard palate in growing rabbits." *Anatomical Record*, 292:277–284.

Menegaz, R.A., Sublett, S.V., Figueroa, S.D., Hoffman, T.J., Ravosa, M.J., & Aldridge, K. (2010). "Evidence for the influence of diet on cranial form and robusticity." *Anatomical Record*, 293:630–641.

Miloševi, N.T., & Ristanovi, D. (2006). "Fractality of dendritic arborization of spinal cord neurons." *Neuroscience Letters,* 396:172-176.

Mitani, J.C. (1989). "Orangutan activity budgets: monthly variation and the effects of body size, partuition, and sociality." *American Journal of Primatology*, 18:87-100.

Mitchell, A. H. (1994). "Ecology of Hose's langur, Presbytis hosei, in mixed logged and unlogged dipterocarp forest of north Borneo." [*PhD diss.*]. Yale University.

Mittra, E., Rubin, C., Gruber, B., & Qin, Y. X. (2008). "Evaluation of trabecular mechanical and microstructural properties in human calcaneal bone of advanced age using mechanical testing, μCT, and DXA." *Journal of Biomechanics,* 41(2): 368–375.

Monteiro, L.R., & Lessa, L.G. (2000). "Comparative analysis of cranial suture complexity in the genus Caiman (Crocodylia, Alligatoridae)." *Brazilian Journal of Biology,* 60:689–694.

Mooney, M., Siegel, M., & Smith, T. (2002). "Evolutionary changes in the cranial vault and base: establishing the primate form." In: *Understanding Craniofacial Anomalies: the Etiopathogenesis of Craniosynostosis and Facial Clefting* (eds. Mooney M, Siegel M), p 275–293. New York: John Wiley.

Moore ,W.J. (1965). "Masticatory function and skull growth." *Journal of Zoology. London,* 146:123–131

Morrogh-Bernard, H.C., Husson, S.J., Knott, C.D., Wich, S.A., vanSchaik, C.P., van Noordwijk, M., Lackman-Ancrenaz, I., Marshall, A.J., Kanamori, T., Kuze, N.,

& bin Sakong, R. (2009). "Orangutan activity budgets and diet." In: Wich, S.A., Utami, S.S., Mitra Setia, T., and van Schaik, C. (eds.), *Orangutans: Geographic Variation in Behavioral Ecology and Conservation*. Oxford University Press, Oxford. PP.119-134

Moss, M. L. (1957) "Experimental alteration of sutural area morphology." *Anatomical Record,* 127:569-590.

Moss, M. L., & Young, R. W. (1960) "A functional approach to craniology." *American Journal of Physical Anthropology,* 18, 281–292.

Moss, M. L. (1962). *The functional matrix*. In: Kraus, B., Reidel, R. (Eds.), Vistas in Orthodontics. Lea & Febiger, Philadelphia, p 85–98.

Moss, M.L. (1969) "The differential roles of periosteal and capsular functional matrices in orofacial growth." *Report of the Congress of European Orthodontic Society*, 193–205.

Moss, M.L., & Salentijn, L. (1969). "The capsular matrix." *American Journal of Orthodontics,* 56: 474–490.

Muchlinski, M.N. (2010). "Ecological correlates of infraorbital foramen area in primates." *American Journal of Physical Anthropology*, 141:131-141.

Mulder L, van Ruijven L.J., Koolstra J.H., & van Eijden T.M.G.J, (2007). "The Influence of Mineralization on Intratrabecular Stress and Strain Distribution in Developing Trabecular Bone." *Annals Biomedical Engineering,* 35:1608-1677.

Müller, K-H. (1996) "Diet and feeding ecology of masked titis (Callicebus personatus)." In: Norconk, M.A., Rosenberger, A.L., and Garber,P.A., (eds.), *Adaptive Radiations of Neotropical Primates.* Plenum Press, New York, p 383-401.

Mundry, R. (2014). "Statistical issues and assumptions of phylogenetic generalized least squares." In: Garamszegi, L.Z. (ed.) *Modern Phylogenetic Comparative Methods and their Application in Evolutionary Biology: Concepts and Practice.* Springer: New York, p 131-156.

Murphy, R.A., & Beardsley A.C. (1974). "Mechanical properties of the cat soleus muscle in situ." *American Journal of Physiology,* 227:1008-1013.

Nakagawa, N. (2000). "Seasonal, Sex, and Interspecific Differences in Activity Time Budgets and Diets of Patas Monkeys (Erythrocebus patas) and Tantalus Monkeys (Cercopithecus aethiops tantalus), Living Sympatrically in Northern Cameroon." *Primates,* 41:161-174.

Nicolay, C. W., & Vaders, M. J. (2008). "Cranial suture complexity in White-Tailed deer

(Odocoileus virginianus)." *Journal of Morphology* 267:841–849

Norconk, M.A. (1996). "Seasonal vairation in the diets of white-faced and bearded sakis (Pithecia pithecia and Chiropotes satanas) in Guri Lake, Venezuela." In: Norconk, MA, Rosenberger AL, and Garber PA (eds.), *Adaptive Radiations of Neotropical Primates*. Plenum Press, New York, p 403-423.

Norconk, M. A, Grafton, B. W., Conklin-Brittain, N. L. (2008). "Seed dispersal by neotropical seed predators." *American Journal of Primatology*, 45:103–126.

Norconk, M.A., Wright, B.W., Conklin-Brittain, N.L., & Vinyard, C.J. (2009). "Mechanical and nutritional properties of foods as factors in platyrrhine dietary adaptations." In P.A. Garber et al. (eds.), *South American Primates, Developments in Primatology: 279 Progress and Prospects*. Springer: New York, p 279-319.

Nordin, M., & Frankel, V.H.. (2012). *Basic biomechanics of the musculoskeletal system.* Lippincott Williams & Wilkins: Baltimore, MD.

Nowell, A. A., & Fletcher, A. W. (2008). "The development of feeding behavior in wild western lowland gorillas (Gorilla gorilla gorilla)." *Behaviour Nowell,* 145:171-193.

Nunn, C. L. (2011). *The comparative approach in evolutionary anthropology and biology*. University of Chicago Press, Chicago, Illinois.

Oberheim, M.C., Mao, J.J., (2002). "Bone strain patterns of the zygomatic complex in response to simulated orthopedic forces." *Journal of Dental Research,* 8:608-612.

Ohman, J.C. (1993). "Cross-sectional geometric properties from biplanar radiographs and computed tomography: functional application to the humerus and femur in hominoids". *Ph.D. dissertation,* Kent State University, Kent, OH.

Ohman, J.C., Krochta, T.J., Lovejoy, C.O., Mensforth, R.P., & Latimer, B. (1997). "Cortical bone distribution in the femoral neck of hominoids: Implications for the locomotion of Australopithecus afarensis." *American Journal of Physical Anthropology,* 104:117-131.

Oketcha, A., & Newton-Fisher, N. (2006). "The diet of olive baboons (Papio anubis) in the Budongo Forest Reserve, Uganda." In: Newton-Fisher, N., Notham, H., Paterson, J.D., and Reynolds, V. (eds.), *Primates of Western Uganda.* Springer, New York, p 61-73.

Olupot, W., Waser, P.M., & Chapman, C.A. (1998). “Fruit finding by mangabeys (Lophcebus albigena): are monitoring of fig trees and use of sympatric frugivore calls possible strategies?” *International Journal of Primatology*, 19:339-353.

O’Neill, M.C., & Ruff, C.B. (2004). “Estimating human long bone cross-sectional geometric properties: a comparison of noninvasive methods.*” Journal of Human Evolution,* 47:221-235.

Orme, D., Freckleton, R., Thomas, G., Petzoldt, T., Fritz, S., Isaac, N., & Pearse, W. (2013). “The caper package: Comparative analysis of phylogenetics and evolution in R.” R package version 0.5, p 1-36.

Ottenhoff, F.A., van der Bilt, A., van der Glas, H.W., & Bosman, F. (1992a). “Peripherally induced and anticipating elevator muscle activity during simulated chewing in humans.” *Journal of Neoruphysiology,* 67:75–83.

Ottenhoff, F.A., van der Bilt, A., van der Glas, H.W., & Bosman, F. (1992b). “Control of elevator muscle activity during simulated chewing with varying food resistance in humans.” *Journal of Neurophysiology,* 68:933–944.

Oudhof, H. A. J. (1982). “Sutural growth.” *Actu Anarchiste,* 112:58-68.

Palombit, R.A. (1997). “Inter-intraspecific variation in the diets of the siamang (Hylobates syndactylus) and lar gibbons (Hylobates lar).” *Folia Primatologica,* 68:321-337.

Paradis, E., Claude, J., & Strimmer, K. (2004). “APE: Analyses of Phylogenetics and Evolution in R language.” *Bioinformatics,* 20:289-290.

Patel, B.A., Ruff, C.B., Simons, E.L.R., & Organ, J.M. (2013). “Humeral cross-sectional shape in suspensory primates and sloths.” *Anatomical Record*, 296:545-556.

Penrose, F., Kemp, G.J., & Jeffrey, N. (2016). “Scaling and accommodation of jaw adductor muscles in canidae.” *Anatomical Record,* 299:951-966.

Peptan, A. I., Lopez, A., Kopher R. A., & Mao, J. J. (2008). “Responses of intramembranous bone and sutures upon in vivo cyclic tensile and compressive loading.” *Bone,* 42:432-438.

Peres, C.A. (1991). "Seed predation of *Cariniana micrantha*(Lecythidaceae) by brown capuchin monkeys in central Amazonia.” *Biotropica*, 23:262–270.

Perry, J.M.G., & Hartstone-Rose, A. (2010). “Maximum Ingested Food Size in Captive Strepsirrhine Primates: Scaling and the Effects of Diet.” *American Journal of Physical Anthropology,* 142:625-635.

Perry, J.M.G., & Wall, C.E. (2009). “Scaling of the chewing muscles in prosimians”. In: Vinyard CJ, Ravosa MJ, Wall CE, editors. *Primate craniofacial function and biology. Developments in primatology series*. New York: Springer, p 217-240.

Persson, M. (1983). “The role of movements in the development of sutural and diarthrodial joints tested in longterm paralysis of chick embryos.” *Journal of Anatomy,* 137:591–599.

Peters, C.R. (1987). “Nut-like oil seeds: food for monkeys, chimpanzees, humans, and probably ape-men.” *American Journal of Physical Anthropology,* 73:333–363.

Peterson J, & Dechow P.C. (2003). “Material properties of the human cranial vault and zygoma.” *Anatomical Record,* 274A: 785-797.

Peyrin, E., Salome, M., Cloetens, A. M., Laval-Jeantet, A. M., Ritman, E., & Rijgsegger, R. (1998). “Micro-CT examinations of trabeculax bone samples at different esolutions: 14, 7 and 2 micron level.” *Technology Health Care,* 6:391-401.

Peyron, M., Blanc, O., Lund, J., & Woda, A. (2004). “Influence of age on adaptability of human mastication.” *Journal of Neurophysiology,* 92:773– 779

Pickett, S.B., Bergey, C.M., & DiFiore, A. (2012). “A Metagenomic Study of Primate Insect Diet Diversity.” *American Journal of Primatology,* 74:622-631.

Picq, P.G., Hylander, W.L. (1989). “Endo’s stress analysis of the primate skull and the functional significance of the supraorbital region.” *American Journal of Physical Anthropology,* 79:393–398.

Plotnick, R., Gardner, R., & O' Neill, R. (1993). “Lacunarity indices as measures of l andscape texture.” *Landscape Ecology*, 8:201−211.

Polk, J.D., Demes, B., Jungers, W.L., Biknevicius, A.R., Heinrich, R.E., & Runestad, J.A. (2000). “A comparison of primate, carnivoran and rodent limb bone cross-sectional properties: are primates really unique?” *Journal of Human Evolution,* 39:297-325.

Polk, J.D., Lieberman, D.E., & Demes, B. (2002). “Predicting long bone loading from cross-sectional geometry.” *Integrative and Comparative Biology*, 42:1296-1296.

Pontes, A.R.M. & Soares, M.L. (2005). “Sleeping sites of common marmosets (*Callithrix jacchus*) in defaunated urban forest fragments: a strategy to maximize food intake.” *Journal of Zoology*, 266:55–63.

Porter, M., Vandervoort, A., & Lexell, J. (1995). “Aging of human muscle: structure, function and adaptability.” *Scandanavian Journal of Medice and Science in Sports*, 5:129–142.

Poulsen, J.R., Clark, C.J., & Smith, T.B. (2001). "Seasonal variation in the feeding ecology of the grey-cheeked mangabey (*Lophcebus albigena*) in Cameroon." *American Journal of Physical Anthropology*, 54:91-105.

Powell P.L., Roy R.R., Kanim P, Bello M.A., & Edgerton V.R. (1984). "Predictability of skeletal muscle tension from architectural determinations in guinea pig hindlimbs." *Journal of Applied Physiology,* 57:1715–1721.

Prahl-Andersen, B. (1968). "Sutural growth." Unpubl. [*PhD diss.*]. Univ. of Nijmegen; The Netherlands.

Preuschoft, H., & Witzel, U. (2005). "Functional shape of the skull in vertebrates: which forces determine skull morphology in lower primates and ancestral synapsids?" *Anatomical Record,* 283A:402-413.

Pritchard, J. J., Scott, J. H., Girgis, F. G., (1956). "The structure and development of cranial and facial sutures." *Journal of Anatomy,* 90:73–86.

Pryor McIntosh, L., Strait, D. S., Ledogar, J. A., Smith, A. L., Ross, C. F., Wang, Q., & Dechow, P. C. (2016). "Internal Bone Architecture in the Zygoma of Human and Pan." *Anatomical Record*, 299: 1704–1717.

R Development Core Team. (2014). "R: A language and environment for statistical computing." R Foundation for Statistical Computing, Vienna, Austria. ISBN 3-900051-07-0.

Raemaekers, J.J. (1979). "Ecology of sympatric gibbons." *Folia Primatologica,* 31:227-245.

Rafferty, K.L., Herring, S.W., (1999). "Craniofacial sutures: morphology, growth, and in vivo masticatory strains." *Journal of Morphology*, 242:167–179.

Rafferty, K.L., Herring, S.W., & Artese F. (2000). "Three-dimensional loading and growth of the zygomatic arch." *Journal of Experimeantal Biology*, 203:2093-3004.

Rafferty, K. L., Herring, S. W., & Marshall, C. D. (2003). "Biomechanics of the rostrum and the role of facial sutures." *Journal of Morphology*, 257: 33–44.

Rafferty, K. L., Liu, Z. J., Ye, W., Navarrete, A. L., Nguyen, T. T., Salamati, A., & Herring, S. W. (2012). "Botulinum toxin in masticatory muscles: short- and long-term effects on muscle, bone, and craniofacial function in adult rabbits." *Bone*, 50:651–662.

Rafferty, K. L., Teaford, M. F., & Jungers, W. L. (2003)" Molar microwear of subfossil lemurs: improving the resolution of dietary inferences." *Journal of Human Evolution,* 43: 645– 657.

Rak, Y. (1978). "The functional significance of the squamosal suture in Australopithecus boisei." *American Journal of Physical Anthropology,* 49: 71–78.

Rak, Y. (1983). *The Australopithecine Face*. New York: The Academic Press.

Rantalainen, T., Nikander, R., Daly, R.M., Heinonen, A., & Sievanen, H. (2011). "Exercise loading and cortical bone distribution at the tibial shaft." *Bone,* 48:786-791.

Ravosa, M.J. (1990). "Functional assessment of subfamily variation in maxillomandibular morphology among Old World monkeys." *American Journal of Physical Anthropology,* 82:199-212.

Ravosa, M.J. (1991). "Stuctural allometry of the mandibular corpus and symphysis in prosimian primates." *Journal of Human Evolution,* 20:3-20.

Ravosa M.J. (2000). "Stressed out: Masticatory forces and primate circumorbital form." *Anatomical Record,* 261:173-175.

Ravosa, M.J., & Hylander, W.L. (1994). "Function and fusion of the mandibular symphysis in primates: stiffness or strength?" In (J. G. Fleagle & R. F. Kay, (Eds) *Anthropoid Origins*. Plenum Press: New York, p 447–468.

Ravosa, M.J., Johnson, K.R., & Hylander ,W.L. (2000a). "Strain in the galago facial skull." *Journal of Morphology,* 244:51–66.

Ravosa, M.J., Noble, V.E., Hylander, W.L., Johnson, K.R., & Kowalski, E.M. (2000b). "Masticatory stress, orbital orientation and the evolution of the primate postorbital bar." *Journal of Human Evolution,* 38:667-693.

Ravosa, M.J., Kunwar, R., Stock, S.R., & Stack, M.S. (2007). "Pushing the limit: masticatory stress and adaptive plasticity in mammalian craniomandibular joints" *Journal of Experimental Biology*, 210:628–641.

Ravosa, M.J., Lopez, E.K., Menegaz, R.A., Stock, S.R., Stack, M.S., & Hamrick, M.W. (2009). "Adaptive plasticity in the mammaliam masticatory complex: you are what, and how, you eat." In: Vinyard CJ, Ravosa MJ, Wall CE, editors. *Primate craniofacial function and biology. Developments in primatology series*. New York: Springer. p 293-328.

Ravosa, M.J., Ning, J., Costley, D.B., Daniel, A.N., & Stack, M.S. (2010). "Masticatory biomechanics and masseter fiber-type plasticity." *Journal of Musculoskeletal and*

Neuronal Interactions, 10:46–55.

Ravosa, M.J., Noble, V.E., Hylander, W.L., Johnson, K.R., Kowalski, E.M. (2000). "Masticatory stress, orbital orientation and the evolution of the primate postorbital bar." *Journal of Human Evolution,* 38:667-693.

Ravosa, M. J., Ross, C.F., Williams, S.H, & Costley, D.B. (2010). "Allometry of masticatory loading parameters in mammals." *Anatomical Record*, 29:557–571.

Ravosa, M. J., Scott, J. E., McAbee, K. R., Veit, A. J., & Fling, A. L. (2015). "Chewed out: an experimental link between food material properties and repetitive loading of the masticatory apparatus in mammals." *PeerJ*, *3*:e1345.

Rayfield, E. J., (2004). "Cranial mechanics and feeding in Tyrannosaurus rex." *Proceedings of the Royal Society B: Biological Sciences* 271:1451–1459.

Rayfield, E.J. (2005). "Using Finite Element Analysis to investigate suture morphology: a case study using large, carnivorous dinosaurs." *Anatomical Record,* 283A, 349–365.

Rayfield, E.J. (2007)."Finite element analysis and understanding the biomechanics and evolution of living and fossil organisms." *Annual Review of Earth and Planetary Sciences,* 35:541–576.

Rayfield, E.J. (2011). "Strain in the ostrich mandible during simulated pecking and validation of specimen-specific finite element models." *Journal of Anatomy,* 218:47-58.

Reed, D.A., & Ross, C.F. (2010). "The influence of food material properties on jaw kinematics in the primate, *Cebus." Archives of Oral Biology,* 55:946-962.

Rentes, A.M., Gaviao, M.B.D., & Amaral, J.R., (2002). "Bite force determination in children with primary dentition." *Journal of Oral Rehabilitation,* 29:1174–1180.

Remis, M.J. (1997)."Western lowland gorillas (Gorilla gorilla gorilla) as seasonal frugivores: use of variable resources." *American Journal of Physical Anthropology,* 43:87-109.

Rice, D. P., (2008). "Developmental anatomy of craniofacial sutures." *Frontiers of Oral Biology*, 12:1–21.

Richter, W. (1920). "Der Obergesichtsschadel des Menschen als gebissturm, ein statisches Kunstwerk." *Arch D Mschr Zahnhlkd*, 2:49-68.

Richtsmeier, J.T., Aldridge K, DeLeon VB, Panchal, J., Kane, A. A., Marsh, J. L., Yan, P., & Cole, T. M. (2006) "Phenotypic integration of neurocranium and brain".

Journal of Experimental Zoology Part B- Molecular and Developmental Evolution, 306:360–378.

Rilling, J.K. (2006). "Human and nonhuman primate brains: Are they allometrically scaled versions of the same design?" *Evolutionary Anthropology,* 15:65–77.

Ristanovic, D., Milosevic, N. T., Jelinek, H. F., & Stefanovic, I.B. (2009). "The mathematical modeling of neuronal dendritic branching patterns in two dimensions: application to retinal ganglion cells in the cat and the rat." *Biological Cybernetics,* 100:97-108.

Roberts, D., & Tattersall, I. (1974). "Skull form and the mechanics of mandibular elevation in mammals." *American Museum Novitates* No. 2536.

Robinson, J.T. (1954a). "The genera and species of the Australopithecinae." *American Journal of Physical Anthropology,* 12:181-200.

Robinson, J.T. (1954b). "Prehominid dentition and hominid evolution." *Evolution,* 8:324-334.

Robinson, J. T. (1956). "The dentition of the Australopithecinae." *Transvaal Museum Mern*, 9:1-179.

Rodriguez-Vegas, J. M., & Casado-Perez, C. (2004). "Inexpensive custom-made external splint for isolated closed zygomatic arch fractures." *Plastic and Reconstructive Surgery,* 113:1517-1518.

Rosenberger, A. L. (1992). "The evolution of feeding niches in New World monkeys." *American Journal of Physical Anthropology,* 88:525–562.

Rosenberger, A. L., Halenar, L., Cooke, & S. B. (2011). "The making of platyrrhine semi-folivores: models of the evolution of folivory in primates." *Anatomical Record,* 294: 2112–2130.

Ross, C.F. (1995). "Muscular and osseous anatomy of the primate anterior temporal fossa and the function of the postorbital septum." *American Journal of Physical Anthropology,* 98:275–306.

Ross, C.F. (2001). "In vivo function of the craniofacial haft: the interorbital 'pillar'." *American Journal of Physical Anthropology,* 116:108–139.

Ross, C.F. (2009). "Does the primate face torque?" In: Vinyard CJ, Ravosa MJ, Wall CE, editors. *Primate craniofacial function and biology. Developments in primatology series*. New York: Springer, p 63-82.

Ross, C.F., & Hylander, W.L. (1996). "*In vivo* and *in vitro* strain in the owl monkey circumorbital region and the function of the postorbital septum." *American Journal of Physical Anthropology,* 101:183-215.

Ross, C.F., & Hylander,W.L. (2000). "Electromyography of the anterior temporalis and the masseter muscles of owl monkeys (*Aotus trivirigatus*) and the function of the postorbital septum." *American Journal of Physical Anthropology,* 112:455-468.

Ross, C.F., & Metzger, K.A. (2004). "Bone strain gradients an optimization in vertebrate skulls." *Annals of Anatomy,* 186:387–396.

Ross, C, Berthaume, M.A., Dechow, P.C., Iriarte-Diaz, J., Porro, L.B., Richmond, B.G., Spencer, M.A., & Strait, D. (2011). "*In vivo* bone strain and finite-element modeling of the craniofacial haft in catarrhine primates." *Journal of Anatomy,* 281:112-141.

Ross, C.F., Dharia, R., Herring, S.W., Hylander, W.L., Liu, Z. J., Rafferty, K. L., Ravosa, M. J., &Williams, S. H. (2007). "Modulation of mandibular loading and bite force in mammals during mastication." *Journal of Experimental Biology*, 210:1046–1063.

Ross, C.F., Patel, B.A., & Slice, D.E. (2005). "Modeling masticatory muscle force in finite element analysis: sensitivity analysis using principal coordinates analysis." *Anatomical Record,* 283A:288–299.

Ross, C.F., Reed, D.A., Washington, R.L., Eckhardt, A, Anapol, F., & Shahnoor, N. (2009a). "Scaling of chewing cycle duration in primates." *American Journal of Physical Anthropology,* 138:30–44.

Rothman, J.M., Plumptre, A.J., Dierenfeld, E.S., & Pell, A.N. (2007). "Nutritional composition of the diet of the gorilla (*Gorilla beringei*): a comparison between two montane habitats." *Journal of Tropical Ecology,* 23:673-682.

Rubin, C.T., & Lanyon, L.E. (1984). "Regulation of bone formation by applied dynamic loads." *Journal of Bone and Joint Surgery,* 66-A: 397-402.

Rubin, C.T., Judex, S., McLeod, K.J., & Qin, Y-X. (2001). "Inhibition of osteopenia by biophysical intervention." In: Marcus R, Feldman D, Kelsey J, editors. *Osteoporosis*, 2nd ed. San Diego: Academic Press, p 489–507.

Rubin, C.T., Judex, S., & Qin, Y.X. (2006). "Low-level mechanical signals and their potential as a non-pharmacological intervention for osteoporosis." *Age and Ageing,* 35:ii32–ii36.

Ruff, C.B. (2000). "Body size, body shape, and long bone strength in modern humans." *Journal of Human Evolution,* 38:269-290.

Ruff, C.B. (2002). "Long bone articular and diaphyseal structure in Old World monkeys and apes. I: locomotor effects." *American Journal of Physical Anthropology*, 119:305–342.

Ruff, C.B. (2006). Moment macro for NIH Image and Image J. Available at http://www.hopkinsmedicine.org/FAE/mmacro.htm.

Ruff, C.B. (2008). "Femoral/humeral strength in early African *Homo erectus." Journal of Human Evolution,* 54:382-390.

Ruff, C.B., & Hayes, W.C. (1983). "Cross-sectional geometry of Pecos Pueblo femora and tibiae—a biomechanical investigation: I. Method and general patterns of variation." *American Journal of Physical Anthropology*, 60:359–381.

Ruff, C.B., Holt, B., & Trinkaus, E. (2006). "Who's afraid of the big bad Wolff?: "Wolff's law" and bone functional adaptation." *American Journal of Physical Anthropology*, 129:484–498.

Ruff, C.B., Larsen, C.S., & Hayes, W.C. (1984). "Structural changes in the femur with the transition to agriculture on the Georgia coast." *American Journal of Physical Anthropology*, 64:125–136.

Ruff, C.B., & Runestad, J.A. (1992). "Primate limb bone structural adaptations." *Annual Review of Anthropology*, 21:407–433.

Sardi, M. L., Ventrice, F., & Ramirez Rozzi, F. (2007). "Allometries throughout the late prenatal and early postnatal human craniofacial ontogeny*." Anatomical Record, (Hoboken)* 290:1112–1120.

Schaffler, M.B., Burr, D., Jungers, W.L., & Ruff, C.B. (1985)."Structural and mechanical indicators of limb specialization in primates." *Folia Primatologica,* 45:61–75.

Schneider, C. A., Rasband, W. S., & Eliceiri, K. W. (2012), "NIH Image to ImageJ: 25 years of image analysis." *Nature Methods,* 9(7): 671-675.

Sciote, J.J., Horton, M.J., Rowlerson, A.M., & Link, J. (2003). "Specialized cranial muscles: how different are they from limb and abdominal muscles?" *Cells Tissues Organs,* 174:73-86.

Scott, J.R., Godfrey L.R., Jungers W.L., Scott R.S., Simons E.L., Teaford M.F., Ungar P.S.,& Walker A. (2009) "Dental microwear texture analysis of two families of subfossil lemurs from Madagascar." *Journal of Human Evolution,* 56:405–416.

Scott, J.E., McAbee, K.R., Eastman, M.M., & Ravosa, M.J. (2014). "Teaching an old jaw new tricks: diet-induced plasticity in a model organism from weaning to adulthood." *Journal of Experimental Biology*, 217:4099–4107.

Scott, R.S., Ungar, P.S., Bergstrom, T.S., & Brown, C.A. (2005). "Dental microwear texture analysis shows within-species diet variability in fossil hominins." *Nature*, 436:693–695.

Serra, C.M., & Manns A.E. (2013). "Bite force measurements with hard and soft bite urfaces." *Journal of Oral Rehabilitation,* 40:563-568.

Shaw, C.N., & Ryan, T.M. (2012). "Does skeletal anatomy reflect adaptation to locomotor patterns? Cortical and trabecular architecture in human and nonhuman anthropoids." *American Journal of Physical Anthropology*, 147:187–200.

Sharp, A. C. (2015). "Comparative finite element analysis of the cranial performance of four herbivorous marsupials." *Journal of Morphology*, 276:1230–1243.

Shea, B.T. (1983) "Size and diet in the evolution of African ape craniodental form." *Folia Primatologica (Basel),* 40:32–68.

Shea, B.T. (1985) "On aspects of skull form in African apes and orangutans, with implications for hominoid evolution." *American Journal of Physical Anthropology,* 68:329–342.

Shibazaki, R., Dechow, P. C., Maki, K., & Opperman, L. A. (2007). "Biomechanical strain and morphologic changes with age in rat calvarial bone and sutures." *Plastic and Reconstructive Surgery,* 119:2167–2178.

Silva, J.S., Jr. (2001). "Especiac¸ao nos macacos-prego e caiararas, ˜ genero ˆ Cebus Erxleben, 1777 (Primates, Cebidae)". [*PhD diss.*]. Universidade Federal do Rio de Janeiro, Rio de Janeiro.

Silva, J.M., Albuquerque, J.R., & Borstelmann, M.A. (2010). "Consumo de itens de origem vegetal por um grupo de Callithrix jacchus habitantes do Parque Estadual Dois Irmaos," in ˜ *Proceedings of the 10th Jornada de Ensino, Pesquisa e Extensao (JEPEX '10)*, p 18–20, Universidade Federal Rural de Pernambuco, Recife, Brazil.

Singleton M. (2004) "Geometric morphometric analysis of functional divergence in mangabey facial form." *Journal of Anthropological Sciences,* 82: 27–44.

Skrzat, J., & Walocha, J.. (2003a). "Application of fractal dimension in evaluation of cranial suture complexity." *Harmonic Fractal Image Annals,* 1:39–41.

Skrzat, J., & Walocha, J. (2003b). "Fractal dimensions of the sagittal (interparietal)

sutures in humans." *Folia Morphologica* (Warsz), 62: 119–122.

Smith, R.J. (1978). "Mandibular biomechanics and temporomandibular joint function in primates." *American Journal of Physical Anthropology,* 49:341-350.

Smith, R. J. (2009). "Use and misuse of the reduced major axis line fitting." *American Journal of Physical Anthropology,* 140:476-486.

Smith, A. L., & Grosse, I. R. (2016). "The Biomechanics of Zygomatic Arch Shape." *Anatomical Record*, 299: 1734–1752.

Smith, K. K., & Hylander, W. L. (1985). "Strain gauge measurement of mesokinetic movement in the lizard *Varanus exanthematicus." Journal of Experimental Biology,* 114:53–70.

Smith, J.M., & Smith, A.C. (2013). "An investigation of ecological correlates with had and foot morphology in callitrichid primates." *American Journal of Physical Anthropology,* 152:447-458.

Smith, A.L., Benazzi, S., Ledogar, J.A., Tamvada, K., Smith, L.C., Weber, G.W., Spencer, M.A., Dechow, P.C., Grosse, I.R., Ross, C.F., Richmond, B.G., Wright, B.W., Wang. Q., Byron, C., Slice, D.E., Strait, D.S. (2014). "Biomechanical implications of intraspecific shape variation in chimpanzee crania: moving towards an integration of geometric morphometrics and finite element analysis." *Anatomical Record*, 298:122–144.

Smith Jr, T. G., Lange, G. D., & Marks, W. B. (1996). "Fractal methods and results in cellular morphology - dimensions, lacunarity and multifractals." *Journal of Neuroscience Methods,* 69:123-136.

Soini, P. (1986). "A synecological study of a primate community inPacaya-Samiria National Reserve, Peru." *Primate Conservation,* 7:63–71.

Spears, I.R., Crompton, R.H. (1996). "The mechanical significance of the occlusal geometry of great ape molars in food breakdown." *Journal of Human Evolution,* 31:517–535.

Spencer, M.A. (1995). "Masticatory system configuration and diet in anthropoid primates." [*PhD diss*.]. State University of New York, Stony Brook.

Spencer, M.A. (1998). "Force production in the primate masticatory system: electromyographic tests of biomechanical hypotheses." *Journal of Human Evolution,* 34:25– 54.

Spencer, M.A. (1999). "Constraints on masticatory system evolution in anthropoid Primates." *American Journal of Physical Anthropology,* 108:450–483.

Spencer, M.A. (2003). "Tooth-root form and function in platyrrhine seed-eaters." *American Journal of Physical Anthropology,* 122:325–335.

Spencer M.A., & Demes, B. (1993). "Biomechanical analysis of masticatory function: configuration in Neandertals and Inuits." *American Journal of Physical Anthropology,* 91:1–20.

Sponheimer, M., Lee-Thorp, J., de Ruiter, D., Codron, D., Codron, J., Baugh, A.T., & Thackeray, F. (2005). "Hominins, sedges, and termites: new carbon isotope data from the Sterkfonetin valley and Kruger National Park." *Journal of Human Evolution,* 48:301-312.

Spoor, F., Jeffery, N., & Zonneveld, F. (2000). "Using diagnostic radiology in human evolutionary studies." *Journal of Anatomy,* 197:61–76.

Starin, E.D. (1991). "Socioecology of the red colobus monkey in the Gambia with particular reference to female-male differences and transfer patterns". [*PhD diss.*]. City University of New York, New York.

Stock, J.T., & Shaw, C.N. (2007). "Which measures of diaphyseal robusticity are robust? A comparison of external methods of quantifying the strength of long bone diaphysis to cross-sectional geometric properties." *American Journal of Physical Anthropology*, 134:412-423.

Stoner, K.A. (1996). "Habitat selection and seasonal patterns of activity and foraging in mantled howling monkeys (Alouatta palliata) in northeastern Costa Rica." *International Journal of Primatology,* 17:1-30.

Strait, D.S., Constantino, P., Lucas, P.W., Richmond, B.G., Spencer, M.A., Dechow, P.C., Ross, C.F., Grosse, I.R., Wright, B.W., Wood, B.A., Weber, G.W., Wang, Q., Byron, C., Slice, D.E., Chalk, J., Smith, A.L., Smith, L.C., Wood, S., Berthaume, M., Benazzi, S., Dzialo, C., Tamvada, K., & Ledogar, J.A. (2013). "Diet and dietary adaptations in early hominins: the hard food perspective." *American Journal of Physical Anthropology*, 151:339–355.

Strait, D.S., Grosse, I.R., Dechow, P.C., Smith, A.L., Wang, Q., Weber, G.W., Neubauer, S., Slice, D.E., Chalk, J., Richmond, B.G., Lucas, P.W., Spencer, M.A., Schrein, C., Wright, B.W., & Byron, C. (2010). "The structural rigidity of the cranium of Australopithecus africanus: implications for the allometry of feeding biomechanics." *Anatomical Record,* 293:583–593.

Strait, D.S., Weber, G.W., Neubauer, S., Chalk, J., Richmond, B.G., Lucas, P.W., Spencer, M.A., Schrein, C., Wright, B.W., Ross, C.F., Dechow, P.C., Wang, Q., Grosse, I., Byron, C., Wood, B.A., Lawn, B., Constantino, P., Slice, D.E., & Smith, A.L. (2009). "The feeding biomechanics and dietary ecology of

Australopithecus africanus." *Proceedings of the Nationl Academy of Sciences, USA,* 106:2124–2129.

Strait D.S., Wright B.W., Richmond B.G., Ross C.F., Dechow P.C., Spencer M.A., & Wang Q. (2008). "Craniofacial strain patterns during premolar loading: implications for human evolution". In: Vinyard CJ, Ravosa MJ, Wall CE, editors. *Primate craniofacial function and biology*. New York: Springer, p 173–198.

Sun, Z.Y., Lee, E., & Herring, S. W. (2004) "Cranial sutures and bones: growth and fusion in relation to masticatory strain." *Anatomical Record Part A,* 276A, 150–161.

Sussman, RW, & Kinzey, W.G. (1984). "The ecological role of the callitrichidae: A review." *American Journal of Physical Anthropology,* 64:419–449.

Taylor, A. B. (2002) "Masticatory form and function in the African apes." *American Journal of Physical Anthropology,* 117:133–156.

Taylor, A. B. (2006). "Diet and mandibular morphology in African Apes." *International Journal of Primatology,* 27:181-201.

Taylor, A.B., & Vinyard, C.J. (2004). "Comparative analysis of masseter fiber architecture in tree-gouging (*Callithrix jacchus*) and nongouging (*Saguinas oedipus*) callitrichids." *Journal of Morphology,* 261:276-285.

Taylor, A.B., & Vinyard, C.J. (2008). "The relationship between jaw-muscle architecture and feeding behavior in primates: tree-gouging and nongouging gummivorous callitrichids as a natural experiment." In: Vinyard CJ, Ravosa MJ, Wall CE, editors. *Primate craniofacial function and biology*. New York: Springer, p 241-264.

Taylor A.B., & Vinyard C.J. (2009). "Jaw-muscle fiber architecture in tufted capuchins favors generating relatively large muscle forces without compromising jaw gape." *Journal of Human Evolution,* 57:710-720.

Taylor A.B., Vogel E.R., Dominy N.J. (2008). "Food material properties and mandibular load resistance abilities in large-bodied hominoids." *Journal of Human Evolution,* 55:604-616.

Taylor A.B., Yuan, T., Ross, C.F., & Vinyard, C.J. (2013). "The scaling of jaw-muscle fiber architecture in anthropoid primates." *American Journal of Physical Anthropology,* 150:269.

Taylor, A. B., Yuan, T., Ross, C. F., & Vinyard, C. J. (2015). "Jaw-muscle force and excursion scale with negative allometry in platyrrhine primates." *American Journal of Physical Anthropology,* 158: 242-256.

Teaford, M.F. (1994) "Dental microwear and dental function." *Evolutionary Anthropology,* 3:17-30.

Teaford, M.F., & Ungar, P.F. (2000). "Diet and the evolution of the earliest human ancestors". *Proceedings of the National Academy of Sciences* USA. 97:13506–13511.

Terborgh, J. (1983). *Five New World Primates*. Princeton University Press, Princeton, New Jersey.

Teng, S., Choi, I.W., Herring, S.W., & Rensberger, J.M. (1997). "Sterological analysis of bone architecture in the pig zygomatic arch." *Anatomical Record,* 248: 205-213.

Terebesi, S., Giannakopoulos, N. N., Brustle, F., Hellman, D., Turp, J. C., & Schindler, H. J. (2015). "Small vertical changes in jaw relation affect motor unit recruitment in the masseter." *Journal of Oral Rehabilitation,* 43:259-268.

Terhune, C.E. (2011). "Dietary correclates of temporomandibular joint morphology in New World primates." *Journal of Human Evolution,* 61:583-596.

Throckmorton, G.S., Throckmorton, L.S. (1985). "Quantitative calculations of temporomandibular joint reaction forces – I. The importance of the magnitude of the jaw muscle forces." *Journal of Biomechanics,* 18:445–452.

Trinkaus, E., Churchill, S.E., Villemeur, I., Riley, K.G., Heller, J.A., & Ruff, C.B. (1991). "Robusticity versus shape: the functional interpretation of Neandertal appendicular morphology." *Journal of Anthropological Society Nippon*, 99:257–278.

Trinkaus, E.R., Churchill, S.E., & Ruff, C.B. (1994). "Postcranial robusticity in Homo, II: Humeral bilateral asymmetry and bone plasticity." *American Journal of Physical Anthropology,* l93:1–34.

Ungar, P. S. (1994). "Patterns of ingestive behavior and anterior tooth use differences in sympatric anthropoid primates." *American Journal of Physical Anthropology,* 95:197–219

Ungar, P.S. (2011). "Dental evidence for the diets of Plio-Pleistocene hominins." *Yearbook of Physical Anthropology,* 146:47–62.

Ungar, P. S., and Grine, F. (1991). "Incisor size and wear in *Australopithecus africanus* and *Paranthropus robustus"*. *Journal of Human Evolution,* 20:313–340.

Ungar, P.S., & Sponheimer, M. (2011). "The diets of early hominins." *Science,* 334:190-193.

Ungar, P.S., Grine, F.E., & Teaford, M.F. (2008). "Dental microwear and diet of the Plio-Pleistocene hominin Paranthropus boisei." *PLOS One,* 3:e2044

Ungar, P.S., Scott, R.S., Grine, F.E., & Teaford, M.F. (2010). "Molar microwear textures and the diets of Australopithecus anamensis and Australopithecus afarensis." *Philosophical Transactions of the Royal Society of Biology,* 365: 3345–3354.

Van Eijden, T.M.G.J. (1990). "Jaw muscle activity in relation to the direction and point of application of bite force." *Journal of Dental Research,* 69:901–905.

van Eijden, T.M.G.J. (1991). "Three-dimensional analyses of human bite-force magnitude and moment." *Archives of Oral Biology,* 36: 535-539.

Van Eijden, T. M., Brugman, P., Weijs, W. A., & Oosting, J. (1990). "Coactivation of jaw muscles: recruitment order and level as a function of bite force direction and magnitude." *Journal of Biomechanics,* 23:475–485.

Van der Merwe, N.J., Masao, F.T., & Bamford, M.K. (2008). "Isotopic evidence for contrasting diets of early hominins *Homo habilis* and *Australopithecus boisei* of Tanzania*." South African Journal of Science*, 104:153–155.

Venkataraman, V. V., Glowacka, H., Fritz, J., Clauss, M., Seyoum, C., Nguyen, N., & Fashing, P. J. (2014). "Effects of dietary fracture toughness and dental wear on chewing efficiency in geladas (*Theropithecus gelada*)." *American Journal of Physical Anthropology,* 155: 17–32.

Veiga, L. (2006). "A ecologia e o comparmento do cuxiu-preto (Chiropotes satanas) na paisagem fragmentada da Amazonia Oriental". [*PhD diss*.]. Univesidade Federal do Para, Belem, Brazil.

Veiga, L.M. & Ferrari, S.F. (2006). "Predation of arthropods by southern bearded sakis (Chiropotes satanas) in Eastern Brazilian Amazonia." *American Journal of Physical Anthropology,* 68:209-215.

Vinyard, C.J. (2007). "An interspecific analysis of covariance structure in the masticatory apparatus of galagos." *Americal Journal of Primatology,* 69:46-58.

Vinyard, C.J. (2009). "Putting shape to work: making functional interpretations of masticatory apparatus shapes in primates." In: Vinyard CJ, Ravosa MJ, Wall CE, editors. *Primate craniofacial function and biology. Developments in primatology series*. New York: Springer, p 357-386.

Vinyard, C. J., & Ryan, T. M. (2006). "Cross-sectional bone distribution in the mandibles of gouging and non-gouging platyrrhini." *International Journal of Primatology*, 27: 1461–1490.

Vinyard, C.J., Williams, S.H., Wall, C.E., Johnson, K.R. & Hylander, W.L. (2005). "Jaw- muscle electromyography during chewing in Belanger's Treeshrews (Tupaia belangeri)." *American Journal of Physical Anthropology,* 127:26-45.

Vinyard C.J., Wall C.E., Williams S.H., Johnson K.R., & Hyander W.L. (2006). "Masseter electromyography during chewing in ring-tailed lemurs (*Lemur catta*)." *American Journal of Physical Anthropology,* 130:85-95.

Vinyard, C.J., Wall, C.E., Williams, S.H., & Hylander, W.L. (2003). "Comparative function of skull morphology of tree-gouging primates." *American Journal of Physical Anthropology,* 120:153-170.

Vinyard, C.J., & Taylor, A.B. (2010). "A preliminary analysis of the relationship between jaw-muscle architecture and jaw-muscle electromyography during chewing across primates." *Anatomical Record,* 293:572–582.

Vinyard, C.J., Taylor, A.B., Teaford, M.F., Glander, K.E., Ravosa, M.J., Rossie, J.B., Ryan, T.M., & Williams, S.H. (2011). "Are we looking for loads in all the right places? New research directions for studying the masticatory apparatus of New World Monkeys." *Anatomical Record,* 294:2140-2157.

Vogel, E. R., van Woerden, J. T., Lucas, P. W., Utami Atmoko, S. S., van Schaik, C. P., & Dominy, N. J. (2008). "Functional ecology and evolution of hominoid molar enamel thickness: Pan troglodytes schweinfurthii and Pongo pygmaeus wurmbii." *Journal of Human Evolution*, 55: 60–74.

Vogel, E.R., Zulfa, A., Hardus, M.E., Wich, S.A., Dominy, N.J., & Taylor, A.B. (2014). "Food mechanical properties, feeding ecology, and the mandibular morphology of wild orangutans." *Journal of Human Evolution,* 75:110-124.

Wainwright, S.A., Biggs, W.D., Currey, J.D., & Gosline, J.M. (1976). *Mechanical design in organisms*. Princeton: Princeton University Press.

Walker, A.C. (1981). "Dietary hypotheses and human evolution." *Philosophical Transactions of the Royal Society of London B,* 292:57–64.

Wall, C.E., Perry, J.G.M., Briggs, M, & Schachat, F. (2007). "Mechanical correlates of sexual dimorphism in the jaw muscles and bones of baboons." *American Journal of Physical Anthropology,* 242.

Wall, C.E., Vinyard, C.J., Johnson, K.R., William, S.H., & Hylander, W.L. (2006). "Phase II Jaw Movements and Masseter Muscle Activity During Chewing in Papio Anubis." *American Journal of Physical Anthropology,* 129:215-224.

Wall, C.E., Vinyard, C.J., Williams, S.H., & Hylander, W.L. (2009). "Analysis of variation in masseter and temporalis EMGs during mastication in primates and treeshrews." *American Journal of Physical Anthropology,* 293: 265 – 266.

Wall, C.E., Vinyard, C.J., William, S.H., Johnson, K.R., & Hylander, W.L. (2008). "Specialization of the superficial anterior temporalis in baboons for mastication of hard foods." In: Vinyard CJ, Ravosa MJ, Wall CE, editors. *Primate craniofacial function and biology. Developments in primatology series*. New York: Springer, p 84-113.

Wang, Q, & Dechow, P.C. (2006). "Elastic properties of external cortical bone in the craniofacial skeleton of the rhesus macaque." *American Journal of Physical Anthropology,* 131:402–415.

Wang, Q, Dechow, P.C., Wright, B.W., Ross, C.F., Strait, D.S., Richmond, B.G., Spencer, M.A., & Byron, C.D. (2008)."Surface strain on bone and sutures in a monkey facial skeleton: an in vitro method and its relevance to finite element analysis." In: Vinyard CJ, Ravosa MJ, Wall CE, editors. *Primate craniofacial function and biology. Developments in primatology series*. New York: Springer, p 149–172.

Wang, Q., Smith, A. L., Strait, D. S., Wright, B. W., Richmond, B. G., Grosse, I. R. Byron C, & Zapata, U. (2010). "The global impact of sutures assessed in a finite element model of a macaque cranium." *Anatomical Record*, 293: 1477–1491.

Wang, Q., Strait, D.S., & Dechow, P.C. (2006). "A comparison of cortical elastic properties in the craniofacial skeletons of three primate species and its relevance to the study of human evolution." *Journal of Human Evolution,* 51:375:382.

Wang, Q., Strait, D. S., Smith, A.L., Chalk, J., Wright, B. W., Dechow, P. C., Richmond, B. G., Ross, C. F., & Spencer, M. A. (2007). "Crossing the lines: suture biomechanics in the primate craniofacial skeleton examined using finite element analysis." *American Journal of Physical Anthropology Supplement,* 44:243.

Wang, Q., Wood, S. A., Grosse, I. R., Ross, C. F., Zapata, U., Byron, C. D. Wright, B.W., & Strait, D. S. (2012). "The Role of the Sutures in Biomechanical Dynamic Simulation of a Macaque Cranial Finite Element Model: Implications for the Evolution of Craniofacial Form." *Anatomical Record*, 295:278–288.

Warton, D. I., Wright, I. J., Falster, D. S., & Westoby, M. (2006). "Bivariate line-fitting methods for allometry." *Biological Reviews,* 81:259–291.

Weidenreich, F. (1941). "The brain and its role in the phylogenetic transformation of the human skull." *Translations of the American Philosophical Society,* 31:321– 442.

Weijs, W.A., & Hillen, B. (1985). "Cross-sectional areas and estimated instrinsic strength of the human jaw muscle muscles." *Acta morphologica Neerlando-Scandinavica,* 23:267-274.

Weijs, W.A., Brugman, P., & Grimbergen, C.A. (1989). "Jaw movements and muscle activity during mastication in growing rabbits." *Anatomical Record,* 224:407–416.

Weijs, W. A., De Jongh, H. J. (1977). "Strain in mandibular alveolar bone during mastication in the rabbit." *Archives of Oral Biology*, 22:667–675.

Wheatley, B.P. (1980). "Feeding and ranging of east Bornean Macaca fasicularis." In: Lindburg, D.G. (ed.), *The Macaques: Studies in ecology, behavior, and evolution*. Van Nostrand Reinhold, New York, p 215-246.

Williams, P.E., & Goldspink, G. (1978). "Changes in sarcomere length and physiological properties in immobilized muscle." *Journal of Anatomy,* 127: 459–468.

Williams, S.H., Wall, C.E., Vinyard, C.J., & Hylander, W.L. (2002). A biomechanical analysis of skull form in gum-harvesting galagids." *Folia Primatologica*, 73:197–209.

Williams, S. E., & Slice, D. E. (2010). "Regional shape change in adult facial bone curvature with age." *American Journal of Physical Anthropology*, 143: 437–447.

Williams, S.H., Wright, B.W., Truong, V., Daubert, C.R., & Vinyard, C.J. (2005). "Mechanical properties of foods used in experimental studies of primate masticatory function." *American Journal of Primatology*, 67:329-346.

Willoughby, D. P. (1978) *All About Gorillas*. South Brunswick, NJ: A.S. Barnes.

Witzel U, Preuschoft H, & Sick H. (2004). "The role of the zygomatic arch in the statics of the skull and its adaptive shape." *Folia Primatologica,* 75:202-218.

Wood, J.L. (1971). "Dynamic response of human cranial bone." *Journal of Biomechanics,* 4:1-12.

Wood B.A, & Constantino P. (2007). "Paranthropus boisei: Fifty years of evidence and analysis". *American Journal of Physical Anthropology* 134(Suppl 45):106–132.

Wood B.A., & Lieberman D.E. (2001). "Craniodental Variation in *Paranthropus boisei*: A Developmental and Functional Perspective." *American Journal of Physical Anthropology*, 116:13-25.

Wood, B. & Schroer, K. (2012). "Reconstructing the diet of an extinct hominin taxon: the role of extant primate models." *International Journal of Primatology,* 33:716-742.

Wood B.A., & Strait D. (2004). "Patterns of resource use in early *Homo* and *Paranthropus." Journal of Human Evolution,* 46:119-162.

Wrangham, R.W. (1977). "Feeding behaviorof chimpanzees in Gombe National Park, Tanzania". In: Clutton-Brock, T.H.(ed.), *Primate Ecology*. London: Academic Press, p 504-538.

Wrangham, R.W. (1976)."Aspects of feeding and social behaviour in gelada baboons." In: *A resport to the Science Research Council of the U.K*, p 1-60

Wright, B.W. (2004). "Ecological distinctions in diet, food toughness, and masticatory anatomy in a community of six neotropical primates in Guyana, South America." [*PhD diss.*]. Univerisity of Indiana, Urbana-Champagne. Urbana-Champagne

Wright, B.W. (2005). "Craniodental biomechanics and dietary toughness in the genus Cebus." *Journal of Human Evolution*, 48: 473–492.

Wright, P.C. (1985). "The costs and benefits of nocturnality for *Aotus trivirgatus* (the night monkey)." *[PhD diss*.]. City University of New York, New York.

Wright, B.W., Wright, K. A., Chalk, J., Verderane, M. P., Fragaszy, D., Visalberghi, E., Izar, P., Ottoni, E.B., Constantino, P., & Vinyard, C. (2009). "Fallback foraging as a way of life: Using dietary toughness to compare the fallback signal among capuchins and implications for interpreting morphological variation." *American Journal of Physical Anthropology*, 140: 687–699.

Wroe, S., Moreno, K., Clausen, P., McHenry, C., & Curnoe, D. (2007). "High-resolution three-dimensional computer simulation of cranial mechanics." *Anatomical Record,* 290:1248-1255.

Wu, Y. D., Chien, C. H., Chao, Y. J., Yu, J. C., & Williamson, M. A. (2007). "Fourier analysis of human sagittal sutures." *Cleft Palate Craniofacial Journal,* 44:482–493.

Yamada, K., & Kimmel, D.B. (1991)."The effect of dietary consistency on bone mass and turnover in the growing rat mandible." *Archives of Oral Biology,* 36:129–138

Yamashita, N. (2008a). "Chemical properties of the diets of two lemurs species in southwestern Madagascar." *International Journal of Primatology,* 29:339-364.

Yamashita, N. (2008b). "Food physical properties and their relationship to morphology: the curious cases of *kily".* In: Vinyard CJ, Ravosa MJ, Wall CE, editors. *Primate*

craniofacial function and biology. Developments in primatology series. New York: Springer, p 387-406.

Yamashita, N., Vinyard, C.J., & Tan, C.L. (2009). "Food mechanical properties in three sympatric species of *Hapalemur* in Ranomafana National Park, Madagascar." *American Journal of Physical Anthropology,* 139:368–381.

Yeager, C. P. (1989). "Feeding ecology of the proboscis monkey (*Nasalis larvatus*)." *International Journal of Primatology,* 10: 497-530.

Yeager, C. P. (1990). "Proboscis monkey (*Nasalis larvatus*) social organization: group structure." *American Journal of Primatology*, 20:95–106.

Yeager, C.P. (1996). "Feeding ecology of the long-tailed macaque (Macaca fasicularis) in Kalimantan Tengah, Indonesia." *International Journal of Primatology*, 17:51-62

Yu, J. C., Wright, R. L., Williamson, M. A., Braselton, J. P., & Abell, M. L. (2003). "A fractal analysis of human cranial sutures." *Cleft Palate Craniofacial Journal,* 40:409–415.

Yu, J. C., Chen, J. R., & Lin, C. H. (2009) "Tensile strain-induced Ets-2 phosphorylation by CaMKII and the homeostasis of cranial sutures." *Plastic and Reconstructive Surgery,* 123, 83S–93S.

Zoller, R. M., & Laskin, D. M. (1968)." Growth of the zygomaticomaxillary suture in pigs after sectioning the zygomatic arch." *Journal of Dental Research,* 48:573-378.

Zollikofer, C. P. E., & Weissman, J. D. (2011). "A bidirectional interface growth model for cranial interosseous suture morphogenesis." *Journal of Anatomy,* 219:100-114.

Zunino, G.E., & Rumiz, D.I. (1986). "Observaciones sobre el comportamiento territorial del mono aullador negro (*Alouatta caraya*)." *Bolivian Primatology Argentina,* 4:36-52.

APPENDIX A

SUPPLEMENTARY TABLES FOR CHAPTER 3 (SM1 TO SM2)

Consult Attached Files using Microsoft Excel

APPENDIX B

SUPPLEMENTARY TABLES FOR CHAPTER 3 (SM1 TO SM3)

Consult Attached Files using Microsoft Excel

317

APPENDIX C

DESCRIPTIVE STATISTICS FOR ALL SPECIES IN CHAPTER 5

TABLE SM1 Descriptive Statistics Mean (standard deviations) for all study species

SPECIES	REGION	$logI_x$	$logI_y$	$logI_{max}$	$logI_{min}$	logJ	I_{max}/I_{min}
Alouatta caraya	Anterior	1.758 (1.381)	0.711 (1.228)	1.775 (1.359)	0.489 (1.467)	1.798 (1.364)	1.285 (0.173)
	Anterior suture	1.569 (1.391)	0.485 (1.231)	1.589 (1.374)	0.141 (1.449)	1.606 (1.377)	1.447 (0.229)
	Midsuture	1.455 (1.322)	0.373 (1.213)	1.473 (1.285)	0.132 (1.285)	1.493 (1.309)	1.341 (0.130)
	Posterior suture	1.424 (1.384)	0.382 (1.147)	1.438 (1.360)	0.294 (1.224)	1.472 (1.346)	1.143 (0.249)
	Posterior	1.310 (1.270)	0.599 (1.301)	1.331 (1.301)	0.480 (1.352)	1.389 (1.274)	0.851 (0.116)
Alouatta palliata	Anterior	2.297 (0.271)	1.028 (0.409)	2.301 (0.272)	0.938 (0.425)	2.323 (0.277)	1.363 (0.252)
	Anterior suture	2.233 (0.223)	0.863 (0.304)	2.240 (0.224)	0.648 (0.302)	2.252 (0.224)	1.594 (0.179)
	Midsuture	1.970 (0.258)	0.617 (0.293)	1.982 (0.253)	0.370 (0.213)	1.994 (0.249)	1.601 (0.238)
	Posterior suture	1.877 (0.211)	0.664 (0.278)	1.885 (0.213)	0.540 (0.234)	1.905 (0.211)	1.344 (0.169)
	Posterior	1.768 (0.188)	0.899 (0.264)	1.785 (0.188)	0.766 (0.225)	1.828 (0.184)	1.019 (0.196)
Colobus polykomos	Anterior	1.172 (0.301)	0.468 (0.310)	1.199 (0.285)	0.338 (0.351)	1.258 (0.288)	0.860 (0.177)
	Anterior suture	0.875 (0.408)	0.167 (0.402)	0.893 (0.405)	0.078 (0.392)	0.960 (0.395)	0.814 (0.210)
	Midsuture	0.467 (0.230)	-0.302 (0.279)	0.478 (0.223)	-0.357 (0.294)	0.544 (0.216)	0.836 (0.254)
	Posterior suture	0.121 (0.307)	-0.648 (0.314)	0.130 (0.301)	-0.706 (0.344)	0.197 (0.295)	0.837 (0.248)
	Posterior	0.010 (0.381)	-0.435 (0.254)	0.065 (0.352)	-0.605 (0.281)	0.161 (0.324)	0.670 (0.290)
Gorilla gorilla	Anterior	2.170 (0.938)	1.056 (1.065)	2.181 (0.938)	0.850 (1.195)	2.205 (0.946)	1.330 (0.342)
	Anterior suture	2.041 (0.040)	0.935 (0.870)	2.054 (0.837)	0.830 (0.853)	2.085 (0.834)	1.274 (0.417)
	Midsuture	2.058 (0.830)	1.213 (0.741)	2.091 (0.810)	1.042 (0.824)	2.134 (0.809)	1.048 (0.279)
	Posterior suture	1.984 (0.903)	1.110 (0.975)	1.996 (0.909)	1.034 (0.937)	2.048 (0.912)	0.961 (0.278)
	Posterior	1.966 (0.885)	1.438 (0.974)	2.017 (0.886)	1.248 (1.001)	2.091 (0.899)	0.769 (0.208)
Macaca mulatta	Anterior	1.107 (0.208)	0.838 (0.178)	1.149 (0.214)	0.747 (0.164)	1.296 (0.193)	0.401 (0.111)
	Anterior suture	1.155 (0.344)	0.755 (0.285)	1.199 (0.337)	0.611 (0.330)	1.305 (0.324)	0.588 (0.205)
	Midsuture	1.007 (0.463)	0.688 (0.517)	1.078 (0.489)	0.459 (0.478)	0.999 (0.478)	0.618 (0.246)
	Posterior suture	0.780 (0.625)	0.422 (0.625)	0.830 (0.614)	0.286 (0.541)	0.944 (0.594)	0.544 (0.164)

	Posterior	0.729 (0.579)	0.537 (0.579)	0.852 (0.530)	0.256 (0.672)	0.954 (0.557)	0.596 (0.172)
Nasalis larvatus	Anterior	1.124 (0.319)	0.140 (0.295)	1.131 (0.316)	0.071 (0.336)	1.169 (0.315)	1.060 (0.152)
	Anterior suture	1.030 (0.331)	0.147 (0.331)	1.037 (0.329)	0.071 (0.368)	1.084 (0.330)	0.966 (0.170)
	Midsuture	0.745 (0.301)	-0.205 (0.363)	0.753 (0.300)	-0.294 (0.394)	0.792 (0.305)	1.047 (0.178)
	Posterior suture	0.493 (0.366)	-0.652 (0.395)	0.499 (0.362)	-0.760 (0.476)	0.524 (0.366)	1.259 (0.198)
	Posterior	0.012 (0.400)	-0.619 (0.426)	0.043 (0.388)	-0.77 (0.496)	0.110 (0.399)	0.821 (0.215)
Piliocolobus badius	Anterior	0.839 (0.315)	0.262 (0.341)	0.855 (0.311)	0.182 (0.381)	0.951 (0.301)	0.672 (0.301)
	Anterior suture	0.864 (0.259)	0.233 (0.314)	0.877 (0.261)	0.152 (0.347)	0.964 (0.252)	0.724 (0.303)
	Midsuture	0.821 (0.274)	0.066 (0.235)	0.834 (0.269)	-0.016 (0.280)	0.895 (0.262)	0.850 (0.208)
	Posterior suture	0.614 (0.469)	-0.182 (0.511)	0.628 (0.467)	-0.280 (0.548)	0.689 (0.461)	0.908 (0.332)
	Posterior	0.673 (0.399)	0.241 (0.354)	0.723 (0.383)	0.090 (0.373)	0.822 (0.369)	0.632 (0.215)
Presbytis hosei	Anterior	0.387 (0.316)	-0.093 (0.266)	0.447 (0.272)	-0.315 (0.414)	0.521 (0.284)	0.762 (0.214)
	Anterior suture	0.382 (0.104)	-0.066 (0.170)	0.428 (0.089)	-0.213 (0.176)	0.519 (0.105)	0.642 (0.107)
	Midsuture	0.176 (0.180)	-0.315 (0.175)	0.200 (0.174)	-0.401 (0.209)	0.299 (0.174)	0.601 (0.118)
	Posterior suture	-0.018 (0.154)	-0.597 (0.229)	-0.008 (0.152)	-0.634 (0.224)	0.090 (0.142)	0.626 (0.211)
	Posterior	-0.055 (0.147)	-0.441 (0.395)	0.071 (0.119)	-0.755 (0.161)	0.132(0.120)	0.827 (0.104)
Theropithecus gelada	Anterior	1.383 (0.663)	0.683 (0.947)	1.385 (0.667)	0.675 (0.936)	1.468 (0.712)	0.709 (0.268)
	Anterior suture	1.244 (0.843)	0.491 (0.956)	1.246 (0.844)	0.482 (0.956)	1.316 (0.860)	0.764 (0.112)
	Midsuture	1.208 (0.544)	0.241 (0.800)	1.214 (0.542)	0.174 (0.852)	1.256 (0.569)	1.040 (0.309)
	Posterior suture	1.337 (0.822)	0.765 (1.081)	1.359 (0.851)	0.697 (1.000)	1.446 (0.878)	0.662 (0.149)
	Posterior	1.504 (0.708)	0.973 (0.926)	1.529 (0.743)	0.899 (0.823)	1.621 (0.758)	0.630 (0.079)
Trachypithecus cristatus	Anterior	0.105 (0.322)	-0.229 (0.356)	0.153 (0.316)	0.502 (0.366)	0.274 (0.327)	0.274 (0.093)
	Anterior suture	0.044 (0.365)	-0.359 (0.420)	0.073 (0.364)	0.507 (0.424)	0.193 (0.375)	0.193 (0.115)
	Midsuture	-0.084 (0.355)	-0.470 (0.405)	-0.071 (0.362)	0.428 (0.391)	0.067 (0.369)	0.067 (0.079)
	Posterior suture	-0.525 (0.364)	-0.758 (0.389)	-0.487 (0.356)	0.333 (0.393)	-0.319 (0.366)	-0.319 (0.101)
	Posterior	-0.348 (0.348)	-0.655 (0.344)	-0.320 (0.346)	0.394 (0.350)	-0.169 (0.339)	-0.169 (0.143)

Aotus trivirgatus	Anterior	-0.307 (0.435)	-0.859 (0.403)	-0.220 (0.416)	-1.416 (0.424)	-0.189 (0.411)	1.195 (0.266)
	Anterior suture	-0.519 (0.438)	-1.168 (0.336)	-0.455 (0.426)	-1.651 (0.261)	-0.422 (0.408)	1.195 (0.335)
	Midsuture	-0.653 (0.273)	-1.298 (0.352)	-0.587 (0.286)	-1.835 (0.295)	-0.558 (0.277)	1.248 (0.314)
	Posterior suture	-0.718 (0.343)	-1.075 (0.395)	-0.604 (0.334)	-1.533 (0.447)	-0.541 (0.324)	0.929 (0.391)
	Posterior	-0.840 (0.404)	-0.978 (0.279)	-0.671 (0.360)	-1.423 (0.321)	-0.589 (0.336)	0.751 (0.294)
Ateles geoffroyi	Anterior	0.612 (0.537)	0.116 (0.655)	0.672 (0.547)	-0.125 (0.612)	0.745 (0.553)	0.797 (0.235)
	Anterior suture	0.443 (0.615)	-0.073 (0.720)	0.514 (0.626)	-0.399 (0.691)	0.570 (0.630)	0.913 (0.238)
	Midsuture	0.414 (0.590)	-0.422 (0.715)	0.459 (0.597)	-0.820 (0.667)	0.488 (0.598)	1.279 (0.383)
	Posterior suture	0.487 (0.586)	-0.554 (0.659)	0.513 (0.588)	-0.908 (0.623)	0.534 (0.585)	1.422 (0.323)
	Posterior	0.343 (0.663)	-0.196 (0.693)	0.396 (0.673)	-0.582 (0.639)	0.469 (0.656)	0.822 (0.303)
Callicebus moloch	Anterior	0.597 (0.304)	-0.154 (0.342)	0.659 (0.298)	-0.816 (0.415)	0.674 (0.301)	1.476 (0.192)
	Anterior suture	-0.332 (1.939)	-1.000 (1.875)	-0.262 (1.949)	-1.803 (1.591)	-0.244 (1.928)	1.540 (0.388)
	Midsuture	-0.320 (0.801)	-1.076 (0.792)	-0.257 (0.801)	-1.988 (0.716)	-0.247 (0.799)	1.731 (0.239)
	Posterior suture	-0.565 (0.893)	-1.029 (0.764)	-0.461 (0.871)	-1.681 (0.741)	-0.429 (0.852)	1.220 (0.336)
	Posterior	-0.818 (0.852)	-0.912 (0.774)	-0.615 (0.823)	-1.501 (0.786)	-0.557 (0.814)	0.886 (0.216)
Cebus capucinus	Anterior	0.622 (0.269)	0.306 (0.261)	0.700 (0.273)	0.056 (0.246)	0.797 (0.258)	0.644 (0.230)
	Anterior suture	0.510 (0.363)	-0.063 (0.349)	0.560 (0.358)	-0.299 (0.343)	0.623 (0.347)	0.860 (0.237)
	Midsuture	0.438 (0.280)	-0.354 (0.293)	0.480 (0.265)	-0.745 (0.391)	0.511 (0.269)	1.225 (0.288)
	Posterior suture	0.371 (0.240)	-0.381 (0.172)	0.413 (0.225)	-0.720 (0.240)	0.447 (0.220)	1.133 (0.212)
	Posterior	0.032 (0.198)	-0.189 (0.219)	0.194 (0.187)	-0.744 (0.287)	0.244 (0.196)	0.938 (0.166)
Cercocebus torquatus	Anterior	1.642 (0.290)	1.233 (0.437)	1.673 (0.304)	1.158 (0.403)	1.799 (0.317)	0.514 (0.240)
	Anterior suture	1.463 (0.369)	0.785 (0.428)	1.475 (0.363)	0.722 (0.466)	1.550 (0.375)	0.752 (0.187)
	Midsuture	1.277 (0.378)	0.563 (0.428)	1.287 (0.376)	0.503 (0.462)	1.360 (0.382)	0.784 (0.230)
	Posterior suture	1.015 (0.472)	0.328 (0.509)	1.020 (0.473)	0.307 (0.507)	1.101 (0.475)	0.713 (0.159)
	Posterior	0.901 (0.451)	0.430 (0.463)	0.924 (0.456)	0.357 (0.444)	1.031 (0.451)	0.567 (0.451)
Cercopithecus mitis	Anterior	1.104 (0.258)	0.501 (0.295)	1.135 (0.255)	0.358 (0.309)	1.206 (0.258)	1.206 (0.157)
	Anterior suture	0.867 (0.187)	0.224 (0.154)	0.904 (0.170)	0.047 (0.128)	0.963 (0.158)	0.963 (0.128)
	Midsuture	0.489 (0.182)	-0.064 (0.194)	0.534 (0.173)	-0.241 (0.135)	0.605 (0.154)	0.605 (0.180)

	Posterior suture	0.332 (0.184)	-0.259 (0.206)	0.358 (0.183)	-0.382 (0.217)	0.438 (0.165)	0.438 (0.237)
	Posterior	0.112 (0.271)	-0.171 (0.290)	0.212 (0.257)	-0.441 (0.314)	0.301 (0.266)	0.301 (0.266)
Chiropotes albinasus	Anterior	-0.383 (NA)	-1.075 (NA)	-0.369 (NA)	-1.150 (NA)	-0.303 (NA)	0.781 (NA)
	Anterior suture	-0.634 (NA)	-1.451 (NA)	-0.627 (NA)	-1.499 (NA)	-0.572 (NA)	0.871 (NA)
	Midsuture	-0.717 (NA)	-1.753 (NA)	-0.711 (NA)	-1.818 (NA)	-0.679 (NA)	1.106 (NA)
	Posterior suture	-0.484 (NA)	-1.311 (NA)	-0.466 (NA)	-1.451 (NA)	-0.423 (NA)	0.985 (NA)
	Posterior	-0.410 (NA)	-0.737 (NA)	-0.318 (NA)	-1.039 (NA)	-0.242 (NA)	0.721 (NA)
Erythrocebus patas	Anterior	1.029 (0.182)	0.650 (0.256)	1.069 (0.193)	0.537 (0.237)	1.182 (0.202)	0.531 (0.069)
	Anterior suture	0.475 (0.337)	0.475 (0.421)	0.942 (0.346)	0.303 (0.388)	1.033 (0.353)	0.639 (0.084)
	Midsuture	0.968 (0.383)	0.432 (0.455)	1.026 (0.455)	0.148 (0.457)	1.081 (0.396)	0.877 (0.124)
	Posterior suture	0.915 (0.375)	0.392 (0.427)	0.972 (0.427)	0.144 (0.459)	1.033 (0.382)	0.828 (0.103)
	Posterior	0.772 (0.349)	0.437 (0.409)	0.865 (0.409)	0.130 (0.452)	0.941 (0.362)	0.735 (0.362)
Hylobates lar	Anterior	0.563 (0.364)	-0.230 (0.412)	0.599 (0.364)	-0.521 (0.458)	0.636 (0.363)	1.121 (0.363)
	Anterior suture	0.334 (0.329)	-0.645 (0.384)	0.358 (0.329)	-0.942 (0.384)	0.383 (0.327)	1.301 (0.327)
	Midsuture	0.050 (1.063)	-0.803 (0.882)	0.081 (1.049)	-1.084 (0.831)	0.120 (1.005)	1.165 (1.005)
	Posterior suture	-0.000 (0.366)	-0.799 (0.454)	0.036 (0.374)	-1.074 (0.381)	0.071 (0.371)	1.111 (0.371)
	Posterior	-0.698 (0.356)	-1.108 (0.389)	-0.647 (0.347)	-1.261 (0.418)	-0.544 (0.350)	0.614 (0.350)
Lophocebus albigena	Anterior	1.483 (0.386)	1.276 (0.366)	1.502 (0.374)	1.244 (0.389)	1.697 (0.376)	0.258 (0.133)
	Anterior suture	1.418 (0.410)	0.854 (0.493)	1.425 (0.411)	0.825 (0.492)	1.529 (0.427)	0.599 (0.193)
	Midsuture	1.169 (0.351)	0.539 (0.524)	1.183 (0.465)	0.481 (0.510)	1.265 (0.468)	0.701 (0.170)
	Posterior suture	0.865 (0.351)	0.334 (0.495)	0.882 (0.363)	0.287 (0.474)	0.985 (0.383)	0.595 (0.169)
	Posterior	0.760 (0.436)	0.427 (0.429)	0.817 (0.425)	0.281 (0.443)	0.930 (0.103)	0.536 (0.103)
Macaca fascicularis	Anterior	0.771 (0.333)	0.439 (0.276)	0.823 (0.313)	0.345 (0.265)	0.951 (0.295)	0.477 (0.131)
	Anterior suture	0.710 (0.411)	0.177 (0.347)	0.741 (0.410)	0.078 (0.316)	0.832 (0.390)	0.662 (0.189)
	Midsuture	0.581 (0.403)	-0.049 (0.386)	0.601 (0.403)	-0.125 (0.372)	0.683 (0.387)	0.726 (0.230)
	Posterior suture	0.425 (0.415)	-0.189 (0.378)	0.438 (0.414)	-0.234 (0.361)	0.531 (0.388)	0.672 (0.249)

	Posterior	0.323 (0.475)	-0.061 (0.387)	0.373 (0.441)	-0.151 (0.383)	0.496 (0.414)	0.525 (0.232)
Mandrillus leucophaeus	Anterior	2.355 (0.101)	2.194 (0.055)	2.359 (0.100)	2.188 (0.059)	2.585 (0.072)	0.170 (0.097)
	Anterior suture	2.262 (0.100)	2.044 (0.056)	2.270 (0.093)	2.033 (0.056)	2.470 (0.070)	0.236 (0.087)
	Midsuture	2.171 (0.145)	1.963 (0.196)	2.191 (0.152)	1.933 (0.180)	2.383 (0.162)	0.257 (0.162)
	Posterior suture	2.251 (0.247)	2.174 (0.237)	2.347 (0.279)	2.014 (0.163)	2.515 (0.242)	0.333 (0.242)
	Posterior	2.403 (0.269)	2.301 (0.189)	2.552 (0.247)	1.989 (0.175)	2.659 (0.229)	0.562 (0.229)
Mandrillus sphinx	Anterior	1.811 (0.774)	1.213 (0.947)	1.814 (0.776)	1.201 (0.946)	1.913 (0.812)	0.613 (0.172)
	Anterior suture	1.771 (0.838)	1.141 (0.984)	1.777 (0.844)	1.124 (0.971)	1.866 (0.868)	0.653 (0.134)
	Midsuture	1.581 (0.759)	0.982 (1.044)	1.607 (0.797)	0.930 (0.971)	1.694 (0.830)	0.677 (0.183)
	Posterior suture	1.369 (0.840)	0.913 (1.156)	1.432 (0.930)	0.797 (0.995)	1.523 (0.942)	0.635 (0.085)
	Posterior	1.344 (0.873)	1.008 (1.113)	1.414 (0.961)	0.870 (0.970)	1.523 (0.963)	0.543 (0.056)
Miopithecus talapoin	Anterior	-0.507 (0.069)	-0.997 (0.159)	-0.459 (0.075)	-1.207 (0.248)	-0.382 (0.465)	0.747 (0.220)
	Anterior suture	-0.896 (0.223)	-1.306 (0.207)	-0.840 (0.221)	-1.485 (0.230)	-0.748 (1.474)	0.644 (0.149)
	Midsuture	-1.573 (0.369)	-1.573 (0.315)	-1.015 (0.352)	-1.707 (0.335)	-0.933 (0.505)	0.692 (0.348)
	Posterior suture	-1.646 (0.375)	-1.646 (0.221)	-1.056 (0.351)	-1.863 (0.241)	-0.991 (0.475)	0.807 (0.334)
	Posterior	-1.493 (0.409)	-1.493 (0.434)	-1.091 (0.419)	-1.982 (0.391)	-1.038 (0.594)	0.890 (0.414)
Pan paniscus	Anterior	1.430 (0.220)	0.147 (0.084)	1.432 (0.218)	0.109 (0.112)	1.453 (0.212)	1.323 (0.134)
	Anterior suture	1.157 (0.359)	-0.088 (0.282)	1.172 (0.336)	-0.213 (0.214)	1.198 (0.309)	1.386 (0.502)
	Midsuture	0.913 (0.252)	0.065 (0.222)	0.951 (0.196)	-0.100 (0.090)	0.990 (0.184)	1.052 (0.159)
	Posterior suture	0.890 (0.418)	0.528 (0.620)	1.000 (0.473)	0.139 (0.436)	1.057 (0.468)	0.861 (0.073)
	Posterior	0.775 (0.252)	0.605 (0.385)	0.952 (0.312)	0.042 (0.258)	1.003 (0.305)	0.909 (0.090)
Pan troglodytes	Anterior	1.189 (0.478)	0.136 (0.463)	1.202 (0.484)	0.946 (0.351)	1.234 (0.465)	0.172 (0.259)
	Anterior suture	0.743 (1.524)	-0.297 (1.262)	0.764 (1.492)	0.971 (1.329)	0.802 (1.474)	0.134 (0.386)
	Midsuture	1.070 (0.512)	0.011 (0.483)	1.083 (0.518)	0.971 (0.388)	1.109 (0.505)	0.183 (0.309)
	Posterior suture	0.782 (0.484)	0.044 (0.564)	0.836 (0.490)	0.995 (0.436)	0.886 (0.475)	0.085 (0.434)
	Posterior	0.646 (0.629)	0.188 (0.634)	0.743 (0.627)	0.970 (0.508)	0.819 (0.594)	0.056 (0.361)

Papio anubis	Anterior	2.094 (0.425)	1.763 (0.563)	2.132 (0.438)	1.679 (0.530)	2.270 (0.185)	0.453 (0.453)
	Anterior suture	2.126 (0.444)	1.735 (0.566)	2.183 (0.452)	1.628 (0.510)	2.294 (0.510)	0.554 (0.461)
	Midsuture	2.059 (0.638)	1.607 (0.804)	2.120 (0.652)	1.494 (0.741)	2.216 (0.741)	0.625 (0.697)
	Posterior suture	1.946 (0.672)	1.590 (0.853)	1.995 (0.689)	1.484 (0.815)	2.116 (0.815)	0.510 (0.714)
	Posterior	1.904 (0.740)	1.646 (0.847)	1.976 (0.756)	1.490 (0.824)	2.103 (0.824)	0.486 (0.769)
Pithecia monachus	Anterior	-0.315 (0.351)	-0.991 (0.331)	-0.271 (0.332)	-1.049 (0.296)	-0.185 (0.288)	-0.168 (0.275)
	Anterior suture	-0.437 (0.197)	-0.954 (0.193)	-0.389 (0.151)	-1.157 (0.361)	-0.307 (0.152)	-0.148 (0.191)
	Midsuture	-0.196 (0.287)	-1.019 (0.298)	-0.170 (0.290)	-1.227 (0.272)	-0.131 (0.285)	0.018 (0.079)
	Posterior suture	-0.112 (0.154)	-0.620 (0.349)	-0.042 (0.199)	-0.947 (0.296)	0.018 (0.182)	-0.067 (0.164)
	Posterior	-0.217 (0.229)	-0.411 (0.386)	-0.068 (0.285)	-0.779 (0.292)	0.014 (0.278)	-0.166 (0.278)
Pongo pygmaeus	Anterior	1.842 (0.450)	0.842 (0.276)	1.854 (0.441)	0.717 (0.292)	1.886 (0.429)	1.137 (0.169)
	Anterior suture	1.808 (0.440)	1.004 (0.111)	1.866 (0.355)	0.762 (0.166)	1.901 (0.340)	1.104 (0.189)
	Midsuture	1.853 (0.037)	0.915 (0.007)	1.862 (0.038)	0.823 (0.079)	1.900 (0.033)	1.039 (0.097)
	Posterior suture	1.725 (0.206)	0.662 (0.095)	1.728 (0.205)	0.641 (0.071)	1.765 (0.188)	1.093 (0.259)
	Posterior	1.414 (0.218)	0.752 (0.171)	1.465 (0.151)	0.523 (0.053)	1.512 (0.146)	0.882 (0.053)
Saguinus oedipus	Anterior	-0.776 (0.968)	-1.450 (1.072)	-0.740 (0.980)	-1.629 (1.007)	-0.686 (0.983)	0.889 (0.095)
	Anterior suture	-1.144 (0.987)	-1.788 (0.984)	-1.104 (0.986)	-1.981 (0.970)	-1.047 (0.983)	0.877 (0.160)
	Midsuture	-1.437 (1.092)	-2.037 (1.121)	-1.407 (1.100)	-2.168 (1.083)	-1.330 (1.089)	0.760 (0.237)
	Posterior suture	-1.602 (1.015)	-2.169 (1.037)	-1.549 (1.025)	-2.384 (1.013)	-1.480 (1.016)	0.834 (0.290)
	Posterior	-1.708 (1.068)	-2.059 (1.090)	-1.599 (1.073)	-2.385 (1.061)	-1.527 (1.069)	0.786 (0.212)
Saimiri oerstedii	Anterior	-0.461 (0.387)	-0.788 (0.280)	-0.312 (0.335)	-1.410 (0.402)	-0.271 (0.326)	1.098 (0.306)
	Anterior suture	-1.107 (0.334)	-1.290 (0.369)	-0.988 (0.346)	-1.617 (0.424)	-0.883 (0.341)	0.628 (0.301)
	Midsuture	-1.205 (0.362)	-1.577 (0.361)	-1.149 (0.365)	-1.764 (0.402)	-1.044 (0.352)	0.615 (0.269)
	Posterior suture	-1.195 (0.330)	-1.301 (0.367)	-1.041 (0.330)	-1.612 (0.382)	-0.931 (0.329)	0.571 (0.199)
	Posterior	-1.284 (0.409)	-1.253 (0.442)	-1.067 (0.435)	-1.627 (0.392)	-0.953 (0.410)	0.559 (0.224)

Saimiri sciureus	Anterior	-0.714 (0.345)	-0.943 (0.183)	-0.561 (0.292)	-1.430 (0.235)	-0.500 (0.274)	0.868 (0.260)
	Anterior suture	-1.221 (0.353)	-1.410 (0.361)	-1.144 (0.356)	-1.556 (0.347)	-1.002 (0.353)	0.412 (0.262)
	Midsuture	-1.334 (0.321)	-1.675 (0.314)	-1.300 (0.360)	-1.769 (0.182)	-1.169 (0.314)	0.468 (0.267)
	Posterior suture	-1.405 (0.263)	-1.465 (0.360)	-1.249 (0.296)	-1.746 (0.312)	-1.127 (0.295)	0.497 (0.107)
	Posterior	-1.371 (0.504)	-1.381 (0.558)	-1.193 (0.568)	-1.709 (0.411)	-1.075 (0.531)	0.516 (0.156)
Symphalangus syndactylus	Anterior	0.076 (NA)	-0.222 (NA)	0.202 (NA)	0.687 (NA)	0.253 (NA)	0.485 (NA)
	Anterior suture	-0.032 (NA)	-0.523 (NA)	0.060 (NA)	0.831 (NA)	0.088 (NA)	0.760 (NA)
	Midsuture	-0.031 (NA)	-0.701 (NA)	0.007 (NA)	1.069 (NA)	0.052 (NA)	0.646 (NA)
	Posterior suture	0.002 (NA)	-0.904 (NA)	0.027 (NA)	1.028 (NA)	0.053 (NA)	0.609 (NA)
	Posterior	-0.581 (NA)	-0.572 (NA)	-0.369 (NA)	0.675 (NA)	-0.276 (NA)	0.484 (NA)
Cacajao rubicunda	Anterior	0.407 (0.471)	-0.091 (0.508)	0.451 (0.512)	-0.287 (0.306)	0.527 (0.480)	0.738 (0.206)
	Anterior suture	-0.066 (0.325)	-0.591 (0.142)	-0.048 (0.323)	-0.676 (0.217)	0.069 (0.214)	0.628 (0.540)
	Midsuture	-0.073 (0.035)	-0.724 (0.120)	-0.063 (0.028)	-0.762 (0.092)	0.016 (0.008)	0.698 (0.121)
	Posterior suture	-0.098 (0.351)	-0.834 (0.284)	-0.088 (0.338)	-0.896 (0.355)	-0.025 (0.340)	0.808 (0.016)
	Posterior	-0.086 (0.136)	-0.333 (0.057)	0.057 (0.117)	-0.842 (0.031)	0.109 (0.107)	0.899 (0.086)
Chiropotes satanas	Anterior	-0.483 (NA)	-0.673 (NA)	-0.394 (NA)	-0.862 (NA)	-0.267 (NA)	0.467 (NA)
	Anterior suture	-1.041 (NA)	-1.226 (NA)	-1.030 (NA)	-1.243 (NA)	-0.823 (NA)	0.212 (NA)
	Midsuture	-0.921 (NA)	-1.267 (NA)	-0.918 (NA)	-1.275 (NA)	-0.760 (NA)	0.357 (NA)
	Posterior suture	-1.017 (NA)	-1.682 (NA)	-1.010 (NA)	-1.711 (NA)	-0.932 (NA)	0.701 (NA)
	Posterior	-1.022 (NA)	-1.808 (NA)	-1.022 (NA)	-1.808 (NA)	-0.957 (NA)	0.785 (NA)
Macaca fuscata	Anterior		1.027 (0.367)	1.599 (0.113)	1.006 (0.393)	1.705 (0.171)	0.592 (0.279)

	Anterior suture	1.551 (NA)	1.012 (NA)	1.591 (NA)	0.831 (NA)	1.661 (NA)	0.760 (NA)
	Midsuture	1.681 (NA)	1.197 (NA)	1.716 (NA)	1.069 (NA)	1.804 (NA)	0.646 (NA)
	Posterior suture	1.609 (NA)	1.125 (NA)	1.637 (NA)	1.028 (NA)	1.733 (NA)	0.609 (NA)
	Posterior	1.086 (NA)	0.844 (NA)	1.160 (NA)	0.675 (NA)	1.283 (NA)	0.484 (NA)
Pithecia pithecia	Anterior	0.167 (0.219)	-0.602 (0.552)	0.211 (0.248)	-0.908 (0.434)	0.251 (0.252)	1.120 (0.398)
	Anterior suture	0.122 (0.325)	-0.728 (0.771)	0.171 (0.346)	-1.047 (0.565)	0.204 (0.348)	1.218 (0.393)
	Midsuture	0.128 (0.292)	-0.436 (0.376)	0.209 (0.312)	-1.041 (0.255)	0.233 (0.309)	1.251 (0.095)
	Posterior suture	0.355 (0.324)	0.138 (0.386)	0.519 (0.348)	-0.436 (0.347)	0.568 (0.342)	0.955 (0.241)
	Posterior	0.210 (0.273)	0.081 (0.359)	0.390 (0.311)	-0.407 (0.296)	0.454 (0.309)	0.797 (0.037)
Presbytis rubicunda	Anterior	0.276 (0.179)	-0.380 (0.255)	0.316 (0.183)	-0.607 (0.239)	0.368 (0.179)	0.923 (0.195)
	Anterior suture	0.156 (0.400)	-0.372 (0.269)	0.233 (0.354)	-0.725 (0.359)	0.280 (0.351)	0.958 (0.158)
	Midsuture	0.067 (0.317)	-0.415 (0.269)	0.147 (0.293)	-0.768 (0.305)	0.202 (0.283)	0.915 (0.232)
	Posterior suture	0.099 (0.309)	-0.509 (0.336)	0.172 (0.320)	-0.875 (0.228)	0.222 (0.277)	1.048 (0.331)
	Posterior	0.054 (0.390)	-0.366 (0.343)	0.199 (0.273)	-0.868 (0.349)	0.236 (0.276)	1.067 (0.156)
Sapajus apella	Anterior	0.494 (0.205)	0.257 (0.224)	0.606 (0.187)	-0.027 (0.258)	0.705 (0.180)	0.633 (0.210)
	Anterior suture	-0.113 (0.312)	-0.609 (0.322)	-0.078 (0.312)	-0.738 (0.324)	0.013 (0.304)	0.659 (0.195)
	Midsuture	-0.136 (0.277)	-0.834 (0.396)	-0.105 (0.275)	-0.977 (0.374)	-0.042 (0.274)	0.871 (0.275)
	Posterior suture	-0.078 (0.320)	-0.734 (0.393)	-0.030 (0.321)	-1.008 (0.377)	0.019 (0.320)	0.977 (0.245)
	Posterior	-0.154 (0.332)	-0.536 (0.371)	-0.058 (0.335)	-0.906 (0.367)	0.006 (0.333)	0.847 (0.247)
Callithrix (Mico) argentata	Anterior	-0.340 (0.184)	-0.937 (0.239)	-0.279 (0.192)	-1.325 (0.233)	-0.240 (0.192)	1.046 (0.144)
	Anterior suture	-0.814 (0.186)	-1.315 (0.234)	-0.773 (0.195)	-1.488 (0.260)	-0.690 (0.185)	0.715 (0.223)
	Midsuture	-0.718 (0.134)	-1.198 (0.189)	-0.695 (0.144)	274 (0.165)	-0.588 (0.125)	0.578 (0.193)
	Posterior suture	-0.877 (0.169)	-1.370 (0.187)	-0.845 (0.187)	-1.507 (0.180)	-0.751 (0.155)	0.661 (0.227)
	Posterior	-1.097 (0.161)	-1.280 (0.205)	-0.973 (0.152)	-1.581 (0.236)	-0.873 (0.160)	0.608 (0.160)
Callithrix jacchus	Anterior	-0.882 (0.381)	-1.231 (0.330)	-0.789 (0.361)	-1.447 (0.213)	-0.692 (0.323)	0.657 (0.324)
	Anterior suture	-1.272 (0.202)	-1.489 (0.256)	-1.232 (0.209)	-1.550 (0.209)	-1.060 (0.205)	0.317 (0.090)
	Midsuture	-1.298 (0.124)	-1.695 (0.209)	-1.281 (0.149)	-1.736 (0.149)	-1.151 (0.149)	0.455 (0.002)

	Posterior suture	-1.875 (0.579)	-2.129 (0.615)	-1.839 (0.637)	-2.219 (0.469)	-1.679 (0.584)	0.380 (0.234)
	Posterior	-1.633 (0.191)	-1.805 (0.155)	-1.546 (0.222)	-1.994 (0.083)	-1.409 (0.175)	0.447 (0.176)
Callithrix (Mico) humeralifera	Anterior	-0.404 (0.069)	-0.571 (0.410)	-0.351 (0.167)	-1.227 (0.116)	-0.293 (0.148)	0.875 (0.202)
	Anterior suture	-0.846 (0.280)	-1.566 (0.322)	-0.821 (0.309)	-1.719 (0.281)	-0.987 (0.279)	0.623 (0.368)
	Midsuture	-0.665 (0.199)	-1.350 (0.232)	-0.644 (0.193)	-1.424 (0.222)	-0.752 (0.193)	0.565 (0.135)
	Posterior suture	-0.819 (0.094)	-1.409 (0.054)	-0.763 (0.062)	-1.614 (0.091)	-0.920 (0.068)	0.595 (0.032)
	Posterior	-0.935 (0.204)	-1.493 (0.219)	-0.843 (0.176)	-1.822 (0.225)	-0.783 (0.183)	0.697 (0.067)

APPENDIX D

SUPPLEMENTARY TABLES FOR CHAPTER 5 (SM1 TO SM7)

Consult Attached Files using Microsoft Excel